Ferrocenylated Buckybowls

Inaugural-Dissertation towards the academic degree
Doctor rerum naturalium (Dr. rer. nat.)

Submitted to the Department of Biology, Chemistry and Pharmacy,
Freie Universität Berlin

Berit Annafrid Topolinski

January 2014

The present work was carried out under the supervision of Prof. Dr. Dieter Lentz from April 2011 to January 2014 at the Institute of Chemistry and Biochemistry, at the Freie Universität Berlin.

First Referee: Prof. Dr. Dieter Lentz

Second Referee: Prof. Dr. Biprajit Sarkar

Date of Defense: 26.03.2014

“*Whatever it is you're seeking won't come in the form you're expecting*.”

Haruki Murakami (Kafka On The Shore)

Acknowledgements

Foremost I would like to express my gratitude to Professor Dr. Dieter Lentz for the possibility to carry out research in his group, for his supervision and advice. I thank Prof. Dr. Biprajit Sarkar for reviewing this thesis.

I am very grateful and in deepest debt to Professor Dr. Hidehiro Sakurai for his outstanding support, good advises, his trust and his hospitality and to Dr. Shuhei Higashibayashi for all the same reasons.

I am in debt to all members of Lentz group (former and present): Dr. Blazej Duda, Dr. Stefanie Fritz, Darina Heinrich, Dr. Thomas Huegle, Juliane Krüger, Dr. Moritz Kühnel, Annika Meyer, Dr. Max Roemer, Dr. Bernd Schmidt and to all students who contributed to my project: Sebastian Czarnecki, Sergej Schwagerus and especially Michael Kathan and Antti Senf and much gratitude goes to all members and part-time members of Sakurai group who were always friendly and supportive: Dr. Nasir Baig, Dr. Raghu Nath Dhital, Setsiri Haesuwannakij, Yuka Ishida, Patcharin Kaewmati, Noriko Kai, Keita Kataoka, Jinyoung Koo, Dr. Yuki Morita, Sachiko Nakano, Yuki Okabe, Satoru Onogi, Prof. Dr. Gautam Panda, Dr. Patcharee Preedasuriyachai, Dr. Qitao Tan, Dr. Ryoji Tsuruoka, Dr. Tsuyuka Sugiishi and Dr. Sal Prima Yudha. Thanks to Dr. Mihoko Yamada, a former fellow corannulene-chemist.

Thanks to Prof. Dr. Sergej Troyanov (HU Berlin) for synchrotron measurements at BESSI.

Many thanks to Sarkar group for helping me with electrochemical problems and measurements, especially to Naina Deibl, Stephan Hohloch and Fritz Weißer.

I am very grateful to Doreen and Christiane Niether and Sandra Mierschink who suffered through over a decade of chemistry alongside with me.

Further, thank you all of my not-chemist-friends for just being there and all the good time we spent together and will hopefully keep spending.

I am very grateful to my family and of course to Bernd Schmidt who supported and encouraged me beyond all measure.

I thank the DFG (Deutsche Forschungsgemeinschaft) for funding in 2013/14.

2. Publications

Parts of this work have been published prior to submission of this manuscript:

Papers:

B. Topolinski, B. M. Schmidt, S. Higashibayashi, S. Sakurai, D. Lentz, Sumanenylferrocenes and their Solid State Self-assembly, *Dalton Transactions* **2013**, 42, 13809-13812.

B. Topolinski, B. M. Schmidt, M. Kathan, S. I. Troyanov, D. Lentz, Corannulenylferrocenes: Towards a 1D, Non-covalent Metal-organic Nanowire. *Chemical Communications* **2012**, *48*, 6298-6300.

Conference lectures:

B. Topolinski, B. M. Schmidt, M. Kathan, H. Sakurai and D. Lentz "Ferrocenylated Buckybowls" 20th European Conference on Organometallic Chemistry, June 2013, St. Andrews (Scotland).

B. Topolinski, B. M. Schmidt, M. Kathan, H. Sakurai and D. Lentz "Ferrocenylated Buckybowls" 11th Ferrocene Colloqium, February 2013, Hannover (Germany).

Posters:

B. Topolinski, B. M. Schmidt, M. Kathan and D. Lentz, "Ferrocenylcorannulenes" 10th Ferrocene Colloqium, February 2012, Braunschweig (Germany).

Contents

1. Introduction

1.1 Buckybowls

Buckybowls are a subgroup of the large family of polycyclic aromatic hydrocarbons (PAHs). In contrast to most PAHs these compounds are not planar or twisted but bowl-shaped and can be seen as subunits of the spherical, all-carbon fullerenes. The properties of these molecules are to some extent similar to those of fullerenes, but they offer more possibilities in modification[1] of their CH-aromatic positions, superior solubility in common organic solvents and can be accessed by organic synthesis in solution or by flash-vacuum-pyrolysis.

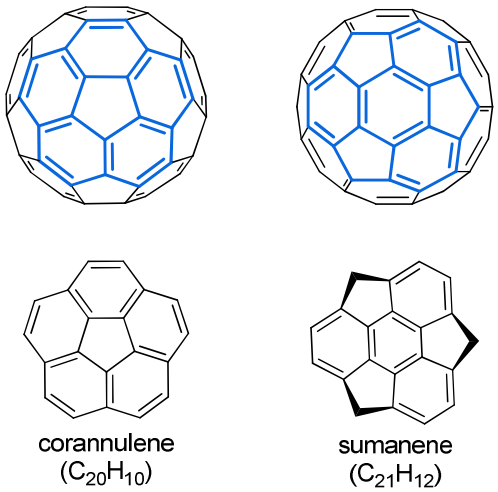

Figure 1.1.1 Corannulene and sumanene, the two best known buckybowls, presented as subunit of the C_{60} Buckminster Fullerene.

Unlike planar aromatic systems, these non-planar hydrocarbons are not rigid in solution but undergo a bowl-to-bowl inversion *via* a planar[2] (or S-shaped[3] in case of larger derivatives) transition state, while the barrier of this inversion is strongly depending on the size and curvature of the buckybowl.

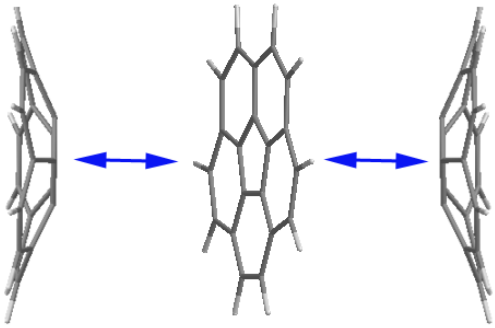

Figure 1.1.2 Schematic bowl-to-bowl inversion of corannulene *via* a planar transition state depicted with chemdraw 3D.

Since the discovery of buckybowls in 1966[4] a variety of differently shaped and sized compounds was synthesized, testing the boundaries of synthetic methods. In 2011 the group of Scott created the so far deepest buckybowl, $C_{50}H_{10}$.[5]
This work focuses on the two smallest buckybowls, corannulene and sumanene.

1.2 Synthesis of Buckybowls

The C_{5v}-symmetrical corannulene ($C_{20}H_{10}$) (Figure 1.2.1) was the first buckybowl to be discovered, even before the discovery of fullerenes in 1985. [4,6] Until today its synthesis has been improved considerably. The first synthetic route towards corannulene ($C_{20}H_{10}$) was reported by Barth and Lawton.[4, 7] A multistep organic synthesis, in 16 steps starting from 1,2-dihydroacenaphthylene was applied and the desired compound was formed in a very low overall yield. A few decades later in 1991 the group of Scott presented a convenient new synthetic route.[8]

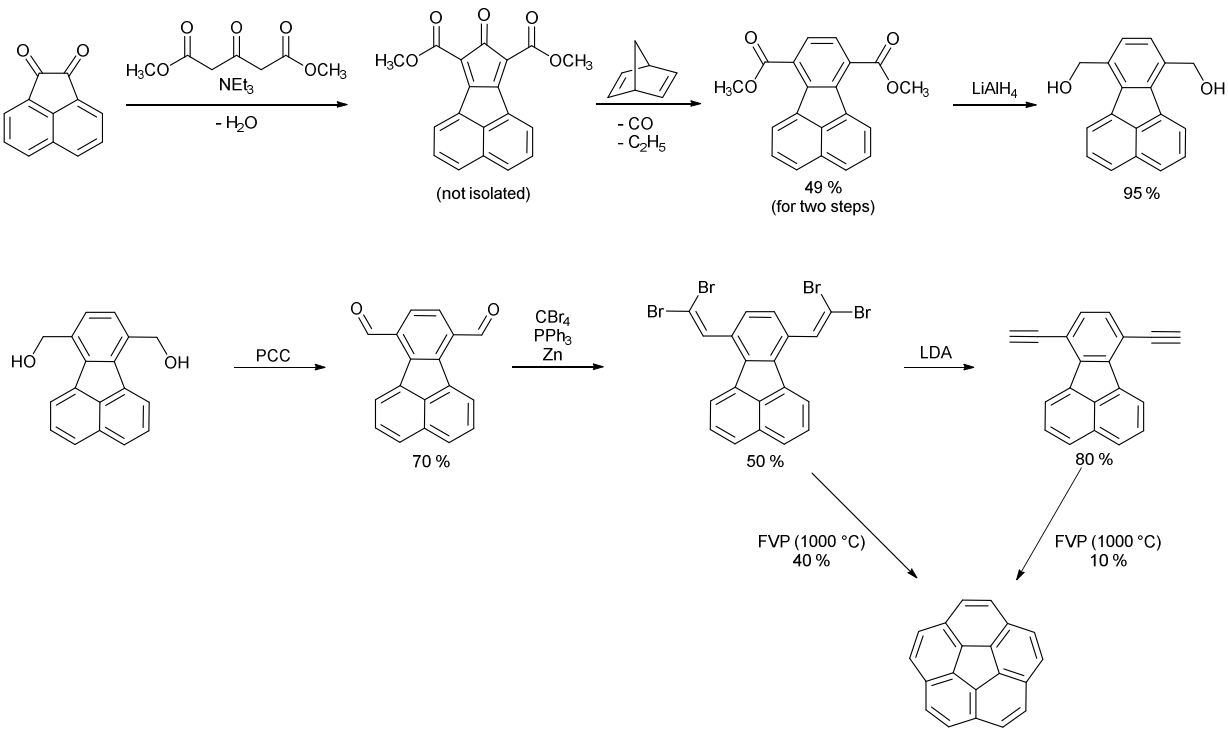

Scheme 1.2.1 First published preparation of corannulene with a final flash-vacuum-pyrolysis step, as published by Scott *et al.*[8]

Corannulene was prepared starting from acenaphthoquinone which was reacted under Knoevenagel conditions, followed by a Diels-Alder and retro-Diels-Alder cycloaddition which provided a 7,10-fluoranthenedicarboxylic ester. The ester groups were reduced to diols and subsequently oxidized to the aldehyde. Applying Corey-Fuchs conditions[9] aldehyde groups were converted to 2,2-dibromovinyl groups. The last step of synthesis was a pyrolysis at 1000 °C. After the purification of crude material a maximum of 10 % corannulene was obtained. The pyrolysis could also be applied to the tetrabromide substrate which provided higher yields of up to 40 % for the last step. This reaction was later modified by using a chlorovinyl pyrolysis precursor.[10] Although yields improved, it was not possible to conduct the pyrolysis reaction on a large scale and the high temperature does not tolerate functional groups.

Parallel, the groups of Sygula,[11] Rabideau[12] and also Siegel[13] worked on improving the milder liquid phase preparation of corannulene and in 2012 the group of Siegel finally reported a large scale, liquid phase synthesis for corannulene.

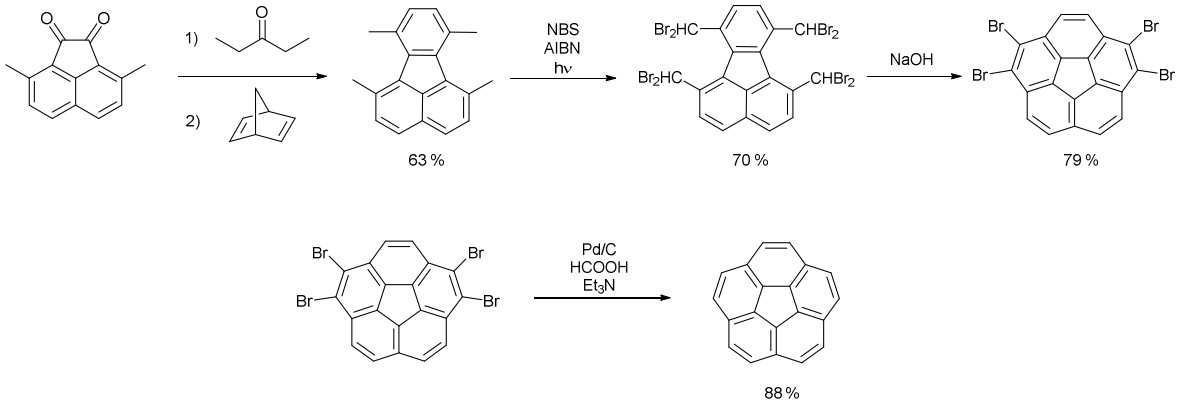

Scheme 1.2.2 Corannulene kilogram-synthesis according to Siegel *et al*. Yields are HPLC corrected yields.[13c]

In this synthesis dimethylacenaphtenechinone is reacted, similar to previous approaches, under Knovenagel and Diels-Alder conditions to construct 1,6,7,10-tetramethylfluoranthene, which then is brominated in its benzylic positions. The brominated fluroanthene derivative later undergoes a ring-closing reaction to yield 1,2,4,5-tetrabromocorannulene. After dehalogenation with palladium on carbon, corannulene can be obtained in up to a kilogram scale. This synthesis enabled corannulene to be prepared industrially and to be commercially available for the first time since its discovery 47 years ago.

Sumanene ($C_{21}H_{12}$), named after the Hindi word for “flower”, although already envisioned by Mehta in 1993,[14] was not successfully synthesized until 2003.[15]

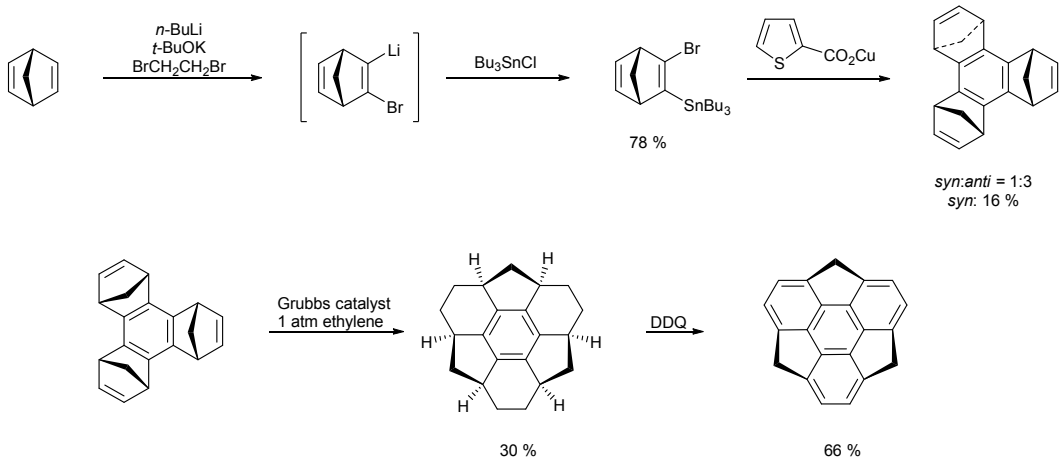

Scheme 1.2.3 Synthetic pathway towards sumanene as reported by Sakurai *et al*.[15]

Preparation started with the functionalization of norbornadiene. The stannylated derivative underwent a trimerization and yielded *syn*- and *anti*-benzotris(norbornadiene) in a ratio of 1:3. Only the *syn*-compound, which was formed in 16 % isolated yield, could undergo the ring-opening and ring-closing metathesis and after dehydrogenation sumanene was obtained.

1.3 Properties of Buckybowls

Corannulene is the smallest existing buckbowl. It exhibits a rather low inversion barrier of 42.7 kJ*mol^{-1} at -64 °C in solution[2a] while showing a bowl depth of 0.87 Å.[16] Corannulene's solid state crystal structure is dominated by CH···π interactions but can strongly be influenced by the substitution of its CH-aromatic rim.[1b,17] Introduction of suitable substituents leads to a variety of packing motifs, including highly charge-conductive columnar structures dominated by π···π interactions.[17c] A noteworthy property of corannulene is its electron acceptor ability, similar to fullerenes. Corannulene can be chemically reduced in one-electron steps to the tetraanion using alkali metals, if the reduction is carried out in dry aprotic solvents and under inert conditions.[18] Odd-numbered reduction states are paramagnetic species while even numbered states are diamagnetic.[19] After prediction of the solid state structure of the tetraanion ($C_{20}H_{10}^{4-}$) as an octaanionic dimer in 1994,[20] the group of Petrukhina presented the first crystal structure of a corannulene tetraanion with lithium cations in 2012,[21] confirming the previously predicted sandwich-like structure. Electrochemically corannulene can be reduced reversibly up to three times under certain conditions.[22]

Besides being a fellow buckybowl, sumanene's properties are drastically different from corannulene's properties. Sumanene possesses three benzylic positions, a slightly larger surface area than corannulene, deeper bowl depth of 1.11 Å and a much higher inversion barrier of 82 kJ/mol at 140 °C.[23] In contrast to corannulene the crystal structure of unsubstituted sumanene already shows a dense columnar arrangement.[23a,24] Sumanene displays a lower ability to exchange electrons than corannulene and only shows quasi-reversible (DMF) or irreversible (MeCN) reduction processes at very negative potentials.[25]

1.4 Ferrocenylated Aromatics

Ferrocene was discovered in 1951 by Kelay and Pauson who tried to synthesize fulvalene by reaction of iron(III) chloride with cyclopentadiene magnesium bromide and was the first η^5-bond complex to be discovered.[26] Today, already known for more than six decades, it is the most investigated sandwich complex. Because of its favorable properties like reversible redox behavior, its chemical modification possibilities and its stability under aerobic conditions it is not only used widely in catalysis[27] and pharmaceutics[28] but also frequently applied as a substituent in macromolecular assemblies,[29] polymers[30] and redox-systems.[31]

Ferrocene reliably undergoes oxidation to ferrocinium which is only modestly stable in aerobic solutions. Nevertheless, the ferrocene/ferrocinium redox couple is often used as a reference to compare the electronic properties of many different organic and organometallic compounds.
Star shaped oligoferrocenes are promising materials as multi-redox systems and in molecular electronics. Ridgid star-shaped perferrocenyl molecules with a benzene core have been reported and in 2006 hexaferrocenylbenzene, a molecule that previously had been regarded as impossible to synthesize, was presented.[32] The compound was prepared by treatment of hexaiodobenzene with six equivalents of diferrocenylzinc. The resulting *per*ferrocenylated molecule is highly crowded which leads to a distortion of the central benzene ring (as depicted in Figure 1.4.1).

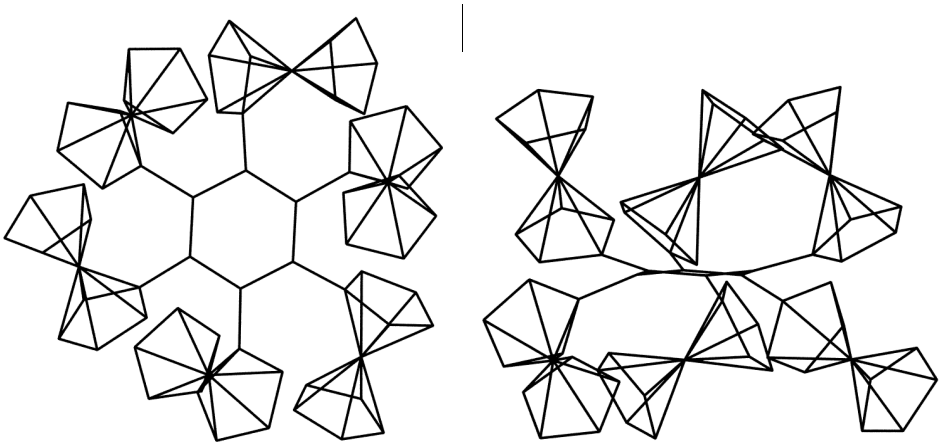

Figure 1.4.1 Crystal structure of hexaferrocenylbenzene as a wireframe model visualized with Mercury. The benzene ring is slightly distorted (left side).[32]

The compound was reported to be sensitive to air, especially in solution. The ferrocene substituents show electronic communication which can be determined by the bathochromic shifts relative to ferrocene in the UV-spectrum and the cyclic voltammogram shows three separated redox waves ($E_{1/2}$ = 163 mV (one-electron wave), 232 mV (two-electron wave), and 222 mV (three-electron wave) in dichloromethane versus ferrocene/ferrocinium).[32]

Further crowded ferrocenylated aromatic compounds were presented by the groups of Astruc and Lang. The group of Astruc created rigid redox stars, also prepared under Negishi-type reaction conditions.[31,33] The ferrocene substituents are connected by ethynyl spacers to the benzene core. Due to the low solubility of the compounds with ethynylferrocene substituents, methylated ethynylferrocenes were also prepared.

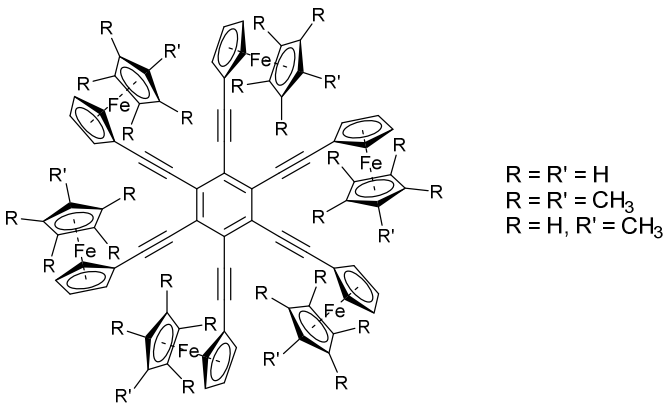

Scheme 1.4.2 Hexa(ferrocenylethynyl)benzenes synthesized by Negishi-type *C,C* cross-coupling reactions of hexabromobenzene with the corresponding zincated ferrocenylethynylferrocene.

Electrochemically, the ethynyl spacers prevent significant electronical interactions between the ferrocene substituents, nevertheless frustration effects and electrostatic interactions were observed by using a fluorinated bulky non-coordinating conducting salt (*n*-$NBu_4BAr^F{}_4$), to prevent ion-pairing.[31,34] In contrast to hexaferrocenylbenzene, these ethynyl bridged compounds are stable in solution and under aerobic conditions. Chemical oxidation yields stable iron(III) compounds which can be reversibly reduced to iron(II) species. Within their studies the group of Astruc investigated the influence of the substitution pattern on the observation of electronic and electrostatic interaction on ethynyl substituted benzene compounds.

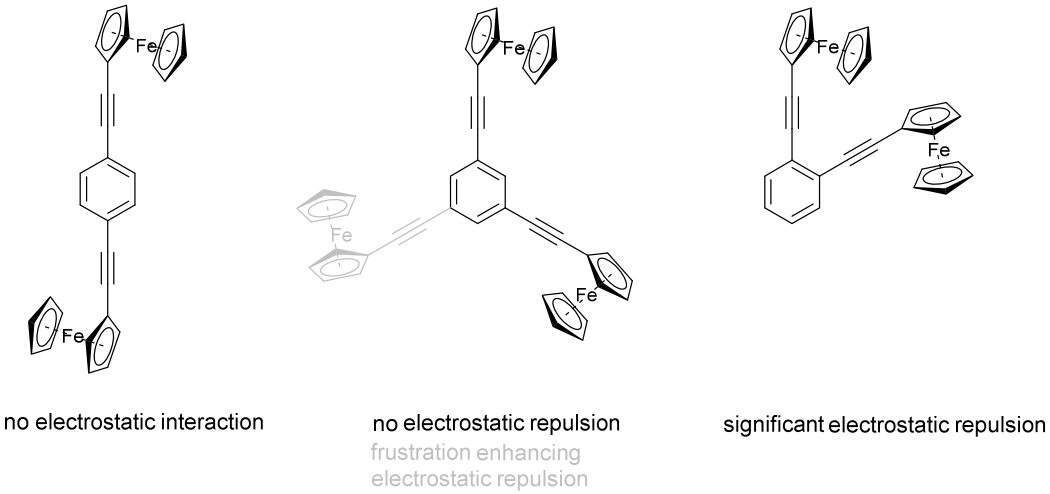

Scheme 1.4.3 While ethynyl bridged ferrocene substituents do not show electronic communication on a benzene core, depending on the substitution pattern other electrochemical interactions can be observed.

A broad variety of heterocycles with sandwich termini is established.[35] The group of Lang focused on studying five- and six-membered heterocyclic aromatic systems including thiophenes,[36] pyrroles,[37] furanes[36c] and phospholes[38] with directly bonded ferrocenyl substituents. These compounds were examined by cyclic voltammetry and spectro-electrochemical measurements to verify intramolecular interactions of the ferrocene substituents.

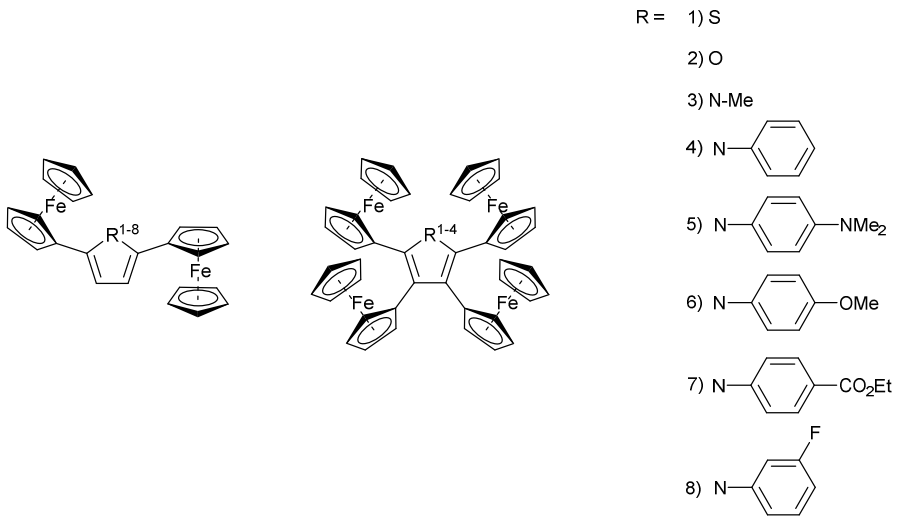

Scheme 1.4.4 A selection of di- and tetrasubstituted heteroaromatics synthesized by the group of Lang.[35b]

All compounds were prepared by Negishi-type *C,C* cross-coupling reactions and were air stable, even in solution. Electrochemical measurements of these diferrocenylthiophenes showed a different grade in interaction between the ferrocenyl moieties depending on the incorporated heteroatom in the five membered ring and their position at the heteroaromatic thiophene core (molecules not included in figure 1.4.3).[36b]

The disubstituted 2,5-diferrocenyl-1-phenyl-1H-pyrrole exhibits the largest separation of oxidation potentials among ferrocenyl aromatics reported so far, due to the decreased energy gap between the ferrocenyl moieties and the heterocyclic core accompanied by an increased delocalization in the heterocyclic core.[36c,37] For all diferrocenylated molecules intervalence charge transfer (IVCT) absorptions of different intensities were visible in the UV-spectra deriving from spectroelectrochemical measurements, indicating different grades of charge transfer.

IVCT bands were also visible for the tetrasubstituted compounds, the only exception being 2,3,4,5-tetraferrocenylthiophene which showed separated redox waves but no intervalence charge transfer (IVCT) absorptions in the near IR region when stepwise oxidized, thus only electrostatical but no electronical communication of the ferrocenyl substituents was observed.

In 2009 the group of Hirao synthesized the first cyclopentadienyl iron complexes of sumanene being also the first $CpFe^+$ complex of π-bowls in general.[25,39] Three different derivatives were prepared (see Figure 1.4.5).

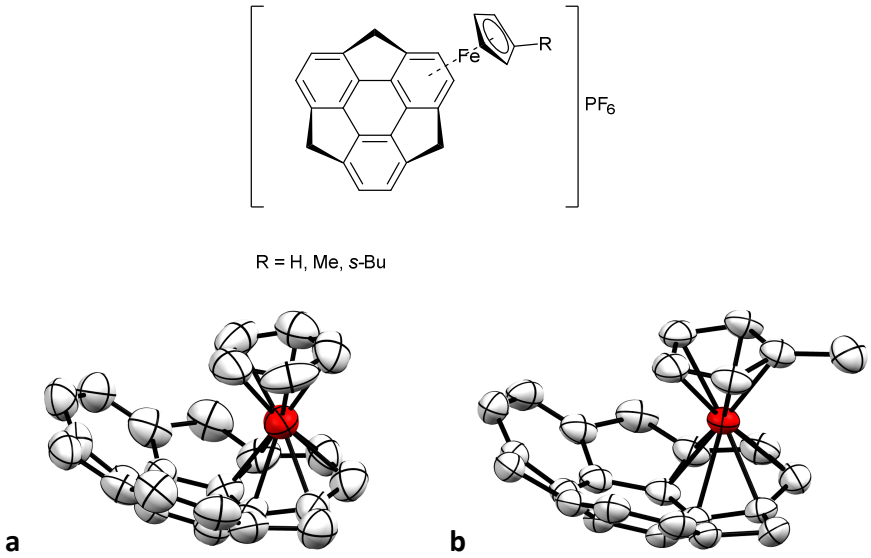

Figure 1.4.5 Cyclopentadienyl iron complexes of sumanene prepared by the group of Hirao. Crystal structures **a** and **b** in Mercury representation, ellipsoids drawn at 50 % probability, hydrogen atoms, counter anions and residual solvent molecules were omitted for clarity.[39a, 40]

In these compounds the $CpFe^+$ substituent is η^6-bound to a benzene unit in the concave side of the sumanene bowl. The bowl-inversion of these compounds is prevented or very slow as observed by ^1H NMR.

At the beginning of this work no other ferrocenylated buckybowl compounds were known but other organometallic derivatives were prepared, for example the groups of Rabideau and Sygula presented a mono- and a dimetalated compound where one Cp^*Ru^+ unit is coordinated on the convex surface or on each side, convex and concave, on benzene units of the corannulene bowl.[41] This coordination led to a decrease of bowl-depth (0.74 for the mono- and 0.42 Å for the dimetalated compound) and thus a much smaller inversion barrier.[42] A preference for *exo*-metal binding was later described by the group of Scott[43] and η^6-bound metal complexes with ruthenium and osmium were reported.[44] Rim-metalation was the target of several groups and a variety of metals can be used for this coordination including nickel, platinum, palladium and silver.[45] Corannulene's ten CH-aromatic positions are not only suitable for η^2-coordination of metals but also for halogenation and subsequent reactions.

2. Synthesis

Synthesis of the ferrocenylated buckybowls presented herein was achieved by metal mediated *C,C* cross-coupling reactions with the corresponding halogenated buckybowls, as described in detail below. Though some η^5-coordinated cyclopentadienyl iron[39,40] and ruthenium[41,46] complexes of buckybowls are known, until 2012 no buckybowl substituted ferrocene compounds were reported.

2. 1 Ferrocene Derivatives

Ferrocene (**1**) itself is broadly used in redox active systems, sometimes modifications are needed to adjust the properties of the synthesized materials. Therefore different ferrocene derivatives were prepared in order to gain insight into a variety of differently substituted corannulene based systems. The effect of spacers such as ethynyl, vinyl, butadienyl and phenyl on the properties of the ferrocenylated buckybowls will be discussed. It was found to be important to increase the solubility of higher ferrocenylated buckybowls and to lower the oxidation potential of the ferrocenyl unit.

Vinyl spacers offer the possibility for electronic interaction between two redox-active species to some extent. Vinylferrocene (**2**) is commercially available. A *trans*-butadienyl spacer on the other hand had to be prepared[47] for comparison of properties between vinyl and butadienyl bridged corannulenylferrocenes and is the longest spacer used in this work.

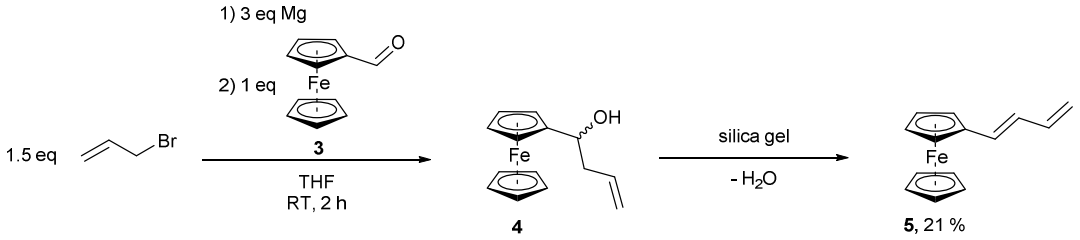

Scheme 2.1.1 (*E*)-Buta-1,3-dien-1-ylferrocene (**5**) prepared by Grignard reaction and elimination.[47]

The synthesis started with alkylation of ferrocenecarboxaldehyde (**3**) by a Grignard reaction with *in situ* prepared allylmagnesium bromide. The secondary alcohol **4** resulting from that reaction eliminated water after addition of silica gel and **5** was obtained after filtration in a 21 % yield (Scheme 2.1.1).

In literature "mixed" ferrocenes like 1-ethenyl-1',2',3',4',5'-pentametylferrocene were reported to increase the solubility of higher ferrocenylated aromatic systems, while having much lower oxidation values.[48,49] The preparation of such compounds was found to be described poorly in literature and already the separation of 1,2,3,4,5-pentamethylferrocene from the crude material was unsuccessful. A mixture of decamethylferrocene, 1,2,3,4,5-pentamethylferrocene and **1** was obtained. This problem was suggestively evoked by "ligand scrambling". These compounds were not separable by recrystallization or column chromatography. Subsequent oxidative purification lead to an enrichment of 1,2,3,4,5-pentamethylferrocene but no pure compound could be obtained. Thus 1-ethylene-1',2,2',3,3',4,4',5-octamethylferrocene (**6**) was prepared (Scheme 2.1.2),[50] expected to combine improved solubility of higher substituted ferrocenylated corannulenes with an oxidation value of the ferrocenyl unit similar to that of decamethylferrocene. The first step of this synthesis was the introduction of an acetyl function by a Friedel-Crafts acylation to 1,1',2,2'3,3'4,4'-octamethylferrocene (**7**). An electrophilic iminium cation was formed by a Vilsmeyer-Haag reaction between phosphoryl chloride and *N,N*-dimethylformamide (DMF), which then reacted with the acetyl function to form **9**. Elimination and decarboxylation proceeded under basic conditions and after acidic work-up the ethynyl compound **6** could be isolated with sufficient purity by column chromatography.

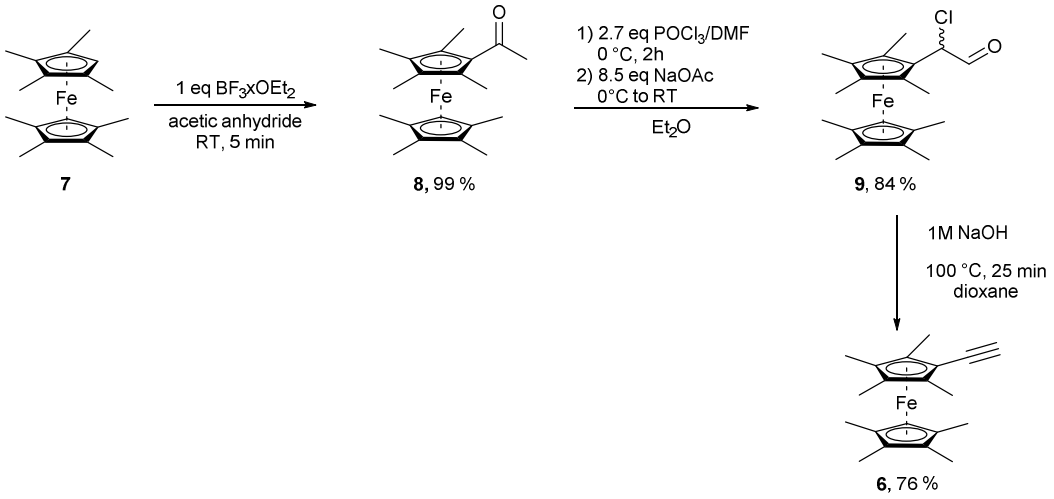

Figure 2.1.2 4-Step synthesis of ethynyl substituted ferrocene **6**.[50]

Introduction of alkyl groups to the cyclopentadienyl rings is known to improve the solubility of ferrocenylated compounds[51] and these groups were expected to not having a strong influence on the electrochemical properties of the corresponding ferrocene. This improved solubility is beneficial when ferrocenyl substituents are introduced to larger molecules or perferrocenylation is targeted. For this, *n*-alkyl groups can be used. Inconveniently, most of these groups show complex sets of overlapping signals in the resulting ^{1}H NMR spectra, making the analysis of conversion and purity of subsequent compounds *via* NMR spectroscopy a challenging task. The neopentyl group on the other hand only shows two singlets, one including all resonances of the three methyl groups and one for two protons of the benzylic positions in the ^{1}H-NMR spectrum. Consequently, it combines a rather simple NMR spectrum with the desired improved solubility.

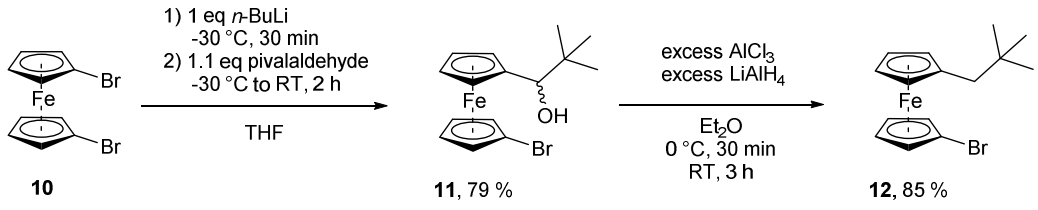

Scheme 2.1.3 Synthesis of **12** by metalation followed by addition of an aldehyde and reduction.[52]

The synthesis of **12** started from 1,1'-dibromoferrocene (**10**)[53] analogous to ref. 52 (Scheme 2.1.3). After monolithiation, the addition of pivalaldehyde furnishes the secondary alcohol **11**. Reduction of the alcohol with a large excess of aluminum(III) chloride and lithium aluminum hydride gives **12** in a 67 % yield (for two steps).

As an aromatic spacer, a phenyl group was introduced with the intention to not only influence the electrochemical properties of the resulting corannulenylferrocenes but also of the solid-state packing structure, by extending the aromatic π-surface hence giving new possibilities for CH···π- and π···π-interactions. 1-Iodo-4-ferrocenylbenzene (**13**) was prepared by an aryl-aryl coupling reaction of a 4-iodobenzenediazonium ion (**14**) with **1**.[54] Gomberg-Bachmann reactions are known for their possible side reaction and consequently low yields, due to the reactive character of diazonium salts. For this reaction the major side product detected was the 1,1'-substituted ferrocene derivative as well as residual **1**. Yet, the one-step procedure and readily available starting materials made this synthesis lucrative.

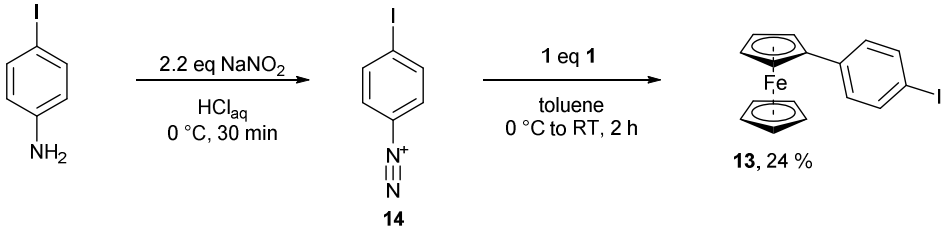

Scheme 2.1.4 Synthesis of **13** by a Gomberg-Bachmann reaction.[54]

In comparison to ferrocene-based compounds biferrocene compounds are more readily oxidized and the resulting cation is a more robust oxidation product than the ferrocenium ion. Biferrocene possesses a richer electrochemistry and is often used for generating organometallic mixed-valence species.[55] 1',1'''-Dibromobiferrocene (**15**) is a suitable reactant for palladium-catalyzed cross-coupling reactions and was prepared by a homocoupling reaction of 1,1'-brominated ferrocene **10** (Scheme 2.1.5).[56]

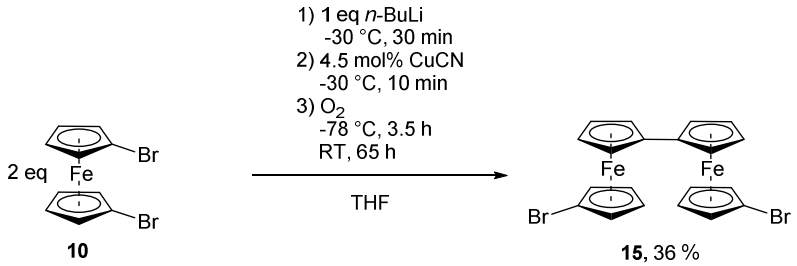

Scheme 2.1.5 Preparation of **15**.[56]

After monolithiation, catalytic amounts of copper(I) cyanide were added to the reaction mixture under oxygen atmosphere. The reaction conditions applied were similar to the Glaser or Eglington reaction which is using copper catalysts, a strong base and oxygen for the oxidative dimerization of alkynes.

2.2 Monosubstituted Corannulene and Sumanene Derivatives

2. 2. 1 Monoiodation of Buckybowls

Corannulene (**16**) was prepared according to the procedure reported by Siegel *et al*.[13c] Sumanene (**17**) was synthesized according to the protocol of Sakurai *et al*.[15] Applying the gold(III) catalyzed reaction conditions of Wang *et al*.[57] with adjusted reaction temperatures and reaction times, monoiodocorannulene (**18**)[58] and monoioidosumanene (**19**)[59] could be prepared in good to excellent yields. Reactions were typically run in a 100 mg scale under inert conditions. **16** or **17** were added to a suspension of NIS and gold(III) chloride in 1,2-dichloroethane. As Sakurai *et al.* showed **17** already reacted at room temperature with a high conversion within 22 h,[59] **16** seemed slightly less reactive and a higher reaction temperature was needed.

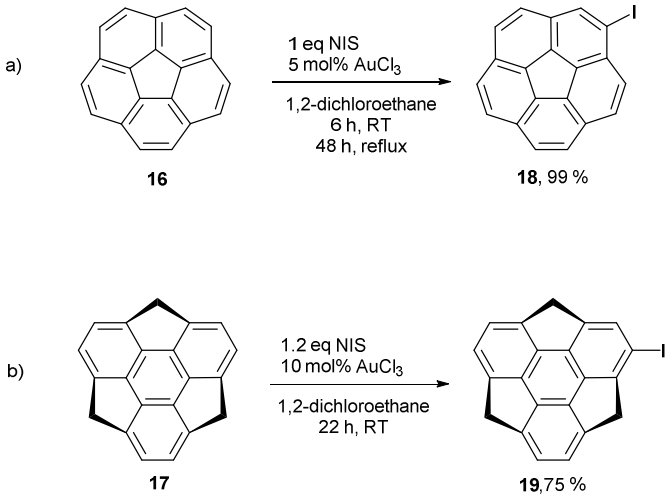

Scheme 2.2.1.1 Gold(III) catalyzed halogenation of a) **16** and b) **17**.[58-59]

In both cases purification was carried out by filtration through a plug of silica gel with a 20:1 mixture of *n*-pentane and ethyl acetate. If the conversion towards the halogenated compound was not complete, the residual **16** and **17** could not be removed from the product by common purification techniques but would not undergo the following reactions and could be removed in the next steps in all cases. Equivalents of reactants and reagents and as well as the yields were always calculated to the absolute amounts of **18** and **19**. Both compounds are colorless air stable amorphous powders that slightly darken when kept for several days at ambient temperature and in light. These iododated buckybowls are versatile building blocks for cross-coupling reactions.[58-59]

2.2.2 Monoferrocenylated Buckybowls

A variety of monoferrocenylated buckybowl compounds was prepared by *C,C* cross-coupling reactions. According to the literature and in our experience ferrocene is most effectively introduced to an aromatic moiety by Negishi *C,C* cross-coupling (NCC) conditions.[31-33,38,58] For these kind of reaction ferrocenylzinc chloride (**20**), a very reactive and hence sensitive species, had to be prepared.

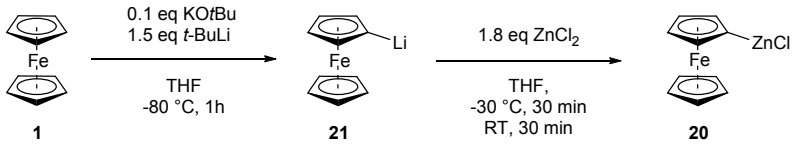

Scheme 2.2.2.1 Lithiation and zincation of **1**.

1 can be monolithiated at low temperatures using the strong base *tert*-butyllithium in THF or diethyl ether. Yields of monolithioferrocene (**21**) increase under "super-basic" conditions, when potassium *tert*-butoxide is added, through the formation of the Lochmann-Schlosser-Base or LICKOR-Base.[53,60] The lithiated species **21** is remotely stable at -80 °C and precipitates partially as a red powder in THF. Metathesis with anhydrous zinc(II) chloride yields ferrocenylzinc chloride (**20**), which is stable at room temperature under inert conditions for several days. **20** was never isolated and always used *in situ* within less than two hours for further reactions. During the preparation of ferrocenylzinc chloride compounds it was generally crucial to be strict about adherence of the different temperatures. The reactions were run in THF which is a suitable solvent for dissolving both buckybowls and hence for the following cross-coupling reactions. Its higher boiling point compared to diethyl ether was also beneficial.

To a solution of **20** in THF usually palladium(II) acetate, triphenylphosphane and the corresponding iodobuckybowl (**18** or **19**) were added (Scheme 2.2.2.2). Surprisingly, the NCC reaction of **20** and iodated buckybowls did not require expensive sterically demanding ligands or palladium(0) sources. Changing palladium(II) acetate to tris(dibenzylidene-acetone)dipalladium(0) did not increase the yields. Upon heating, the reaction mixtures turned deep red immediately. After the given reaction time purification was done by column chromatography on silica gel. The C_1-symmetric compounds corannulenylferrocene (**22**)[58,61] and sumanenylferrocene (**23**)[62] were synthesized according to this procedure. Both compounds are stable towards air and moisture, even in solution.

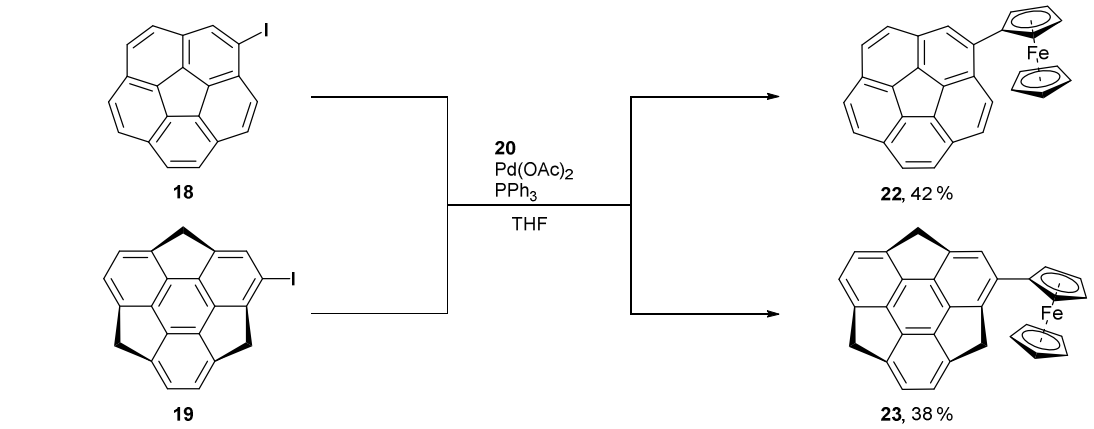

Scheme 2.2.2.2 NCC reaction between **20** and iodated buckybowls **18** and **19**. **22**: 2 eq **20**, 1 mol% palladium(II) acetate, 2 mol% triphenylphosphane, 60 °C, 48 h; **23**: 4 eq **20**, 3 mol% palladium(II) acetate, 6 mol% triphenylphosphane, 70 °C, 3 d.[58, 61-62]

A corannulenylferrocene bearing a neopentyl group in 1'-position was also prepared by NCC conditions similar to the conditions described above. Halogen-lithium-exchange (-30 °C, *n*-butyllithium) yielded the monozincated ferrocene **24**.

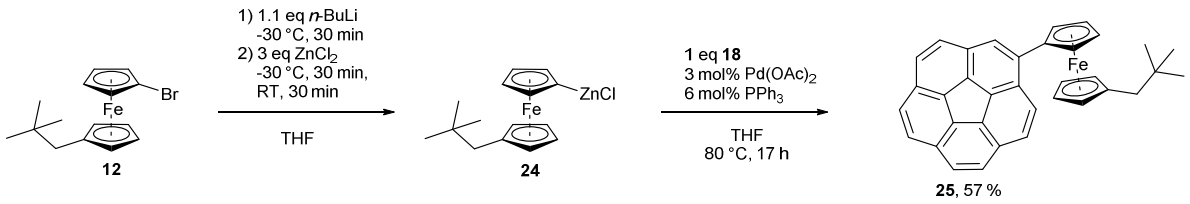

Scheme 2.2.2.3 Synthesis of **25** by metalation of **12** and subsequent NCC.

The compound is deep red and has a very low melting point of 61 °C. The introduction of a neopentyl group to the ferrocene moiety increases the solubility; **25** is soluble in most organic solvents even including *n*-pentane.

2.2.3 Ferrocenylcorannulenes with Spacers

Several molecules with ferrocene substituents connected *via* spacers to the corannulene moiety were synthesized in order to study the influence of the various spacers. Phenylferrocene **13** can be linked to the corannulene moiety by again applying NCC conditions.[63] **26** was isolated

after column chromatography in 56 % yield, the major side product was the homocoupling product of **13**, 4,4'-diferrocenyl-1,1'-biphenyl.

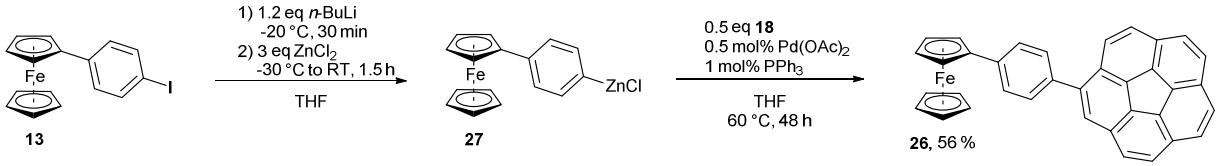

Scheme 2.2.3.1 Synthetic route to phenyl-bridged **26** by halogen-lithium exchange, metathesis with anhydrous zinc(II) chloride, followed by NCC reaction with **18**.[63]

Ethynyl derivatives of corannulene are known and have shown to be an efficient fluorophores while also showing a columnar structure in the solid state.[64] Copper free Sonogashira-type reaction of ethynylferrocene (**28**) and 1-ethylene-1',2,2',3,3',4,4',5-octamethylferrocene (**6**) with the iodated buckybowl **18** resulted in compounds **29** and **30**. For this reaction a palladium(0) species was used as precatalyst.

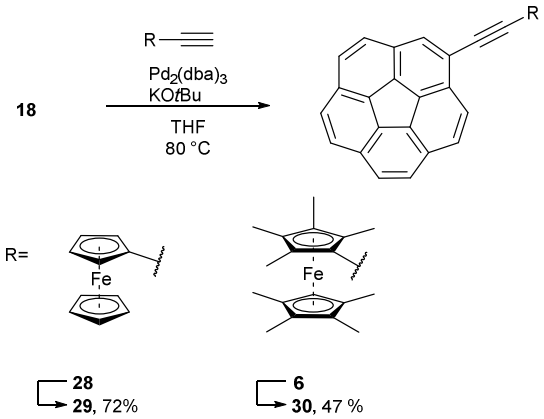

Figure 2.2.3.2 Sonogashira-type reactions of **18** with ethynylferrocenes **6** and **28. 29**: 1.2 eq **28** 2 eq potassium *tert*-butoxide, 1 mol% tris(dibenzylideneacetone)dipalladium(0), 4 h; **30**: 2 eq **6** 3.6 eq potassium *tert*-butoxide, 3.5 mol% tris(di-benzylideneacetone)dipalladium(0), 5 h.

29 is a dark red solid. Crystals of this compound were described in a previous work and showed severe disorders in the solid state.[61] **30** is deep red in solution and dark purple as a solid. Crystals could be grown by slow evaporation of dichloromethane or toluene or by slow evaporation of chloroform but were not suitable for X-ray analysis. The lower yield of **30** is explained by its sensitivity toward oxidative conditions. During column chromatography,

decomposition could be observed, producing a grey insoluble solid, which could not be eluted from the column.

Heck-type reactions of **18** with vinylferrocene (**2**) or butadienylferrocene (**5**) yielded the compounds **31** and **32** as bright red solids in satisfying yields.

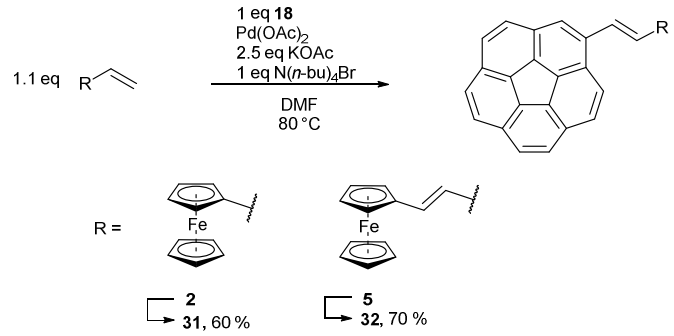

Figure 2.2.3.3 Heck reactions of **18**. **31**: 10 mol% palladium(II) acetate 15 h; **32**: 5 mol% palladium(II) acetate, 24 h.[61]

Crystals of **31** were the subject of earlier work[61] and also showed disorders in the solid state while no crystals of **32** suitable for X-ray analysis were obtained.

2.3 Dibuckybowlferrocenes

C. M. Lui *et al*. reported high yields in the synthesis of heteroarylferrocenes using Stille-type reaction conditions.[65] Nevertheless, attempts to synthesize 1,1'-dicorannulenylferrocene (**33**) by cross-coupling of 1,1'-bis(tri-*n*-butylstannyl)ferrocene with **18** failed and only the starting materials were isolated from the reaction mixture. Suzuki-reaction of 1,1'-ferrocenediboronic acid pinacol ester with **18** modifying the conditions of R. Knapp and M. Rehahn[66] did not lead to the targeted product. Instead 1-boronicacid-1'-corannulenylferrocene could be isolated in 31 % yield.[67] Finally, NCC reaction conditions were applied. 1,1'-Dilithioferrocene can be easily synthesized by addition of *n*-butyllithium and TMEDA to ferrocene in ether at room temperature. These conditions revealed another problem: TMEDA is a strongly coordinating base that competes with other ligands in palladium-catalyzed cross-coupling reactions and thus

inhibits the reaction by blocking the transmetalation step. Hence “free” 1,1’-dilithioferrocene had to be prepared. Bromine-lithium exchange on dibromo compound **10** followed by metathesis with anhydrous zinc chloride gives access to 1,1’-dizincated ferrocenes. Subsequent reaction with iodated buckybowls **18** of **19** lead to the 1,1’-buckbowl substituted ferrocene derivatives for **33**[58,67] and 1,1’-disumanenylferrocene (**34**)[62] in 40 % and 11 % yield, respectively. The isolated yield of **34** is comparatively low, even when considering the high sensitivity of unstabilized 1,1’-dilithioferrocene and might be also attributed to the very poor solubility of **34** in common organic solvents. No other compound bearing two sumanene units was present in the reaction mixture of **34**; however, significant amounts of **34** and starting materials were isolated. A prolonged reaction time or a higher catalyst loading did not increase the yield.

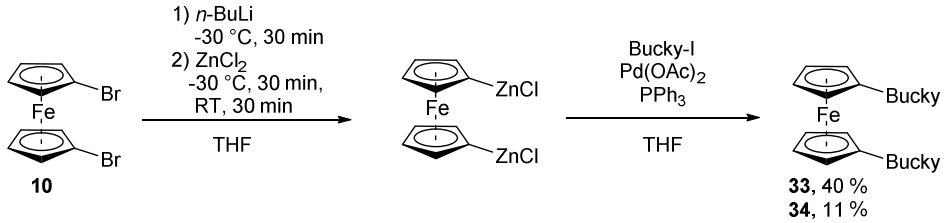

Figure 2.3.1 Synthesis of 1,1’-buckybowl substituted ferrocenes by NCC reactions**. 33**: 1. 3 eq *n*-butyllithium, 3.5 eq zinc(II) chloride; 2. 2.2 eq **18**, 2.5 mol% palladium(II) acetate, 5 mol% triphenylphosphane, 70 °C, 12 h; **34**: 1. 2.5 eq *n*-butyllithium, 3 eq zinc(II) chloride, 2. 5 mol% palladium(II) acetate, 10 mol% triphenylphosphane, 2.2 eq **19** 70 °C, 24 h.

2.4 1,2-Dicorannulenylferrocene (35)

The idea of synthesizing 1,2-dicorannulenylferrocene (**35**) had its origin in the following: Whereas the corannulene 1,1’-substitution on ferrocene brought both corannulenyl substituents in close proximity while retaining a certain flexibility of the system in one plane by the rotation of the cyclopentadienyl rings, another motif was chosen, where both corannulenyl substituents would be fixed in 1,2-positon on one cyclopentadienyl ring of ferrocene forcing both substituents to interact. An extension of this idea would lead to an inverting molecular paddlewheel if a *per*corannulation of one cyclopentadienyl ring would be possible. 1,2-

Dibromoferrocene (**36**) was synthesized according to literature procedure.[68] NCC conditions showed to be the most effective method to introduce corannulenyl substituents and in a first approach similar conditions as for the preparation of the 1,1'-substituted derivative **33** were applied and a reaction temperature of -78 °C for the lithiation was used. After work-up *via* column chromatography starting materials, **1** and **16** were observed in the ^{1}H NMR spectrum. Further, 1-bromo-2-corannulenylferrocene (**37**) and the monosubstituted, dehalogenated **22** identified by NMR and EI-Mass measurements, were obtained as a mixture in a 5:1 ratio. No traces of the desired **35** were observed. **22** and **37** showed similar R_f values and an isolation of analytically pure **37** could not be achieved by column chromatography or recrystallization.

Similar reaction conditions with a lithiation temperature of -30 °C as well as the usage of *tert*-butyllithium, as a stronger base, showed similar results which lead to the assumption that 1,2-dilithioferrocene might not be stable under the given conditions, due to the close proximity of the two lithium atoms and the strongly polarized C-Li bond. A successive lithiation and corannulenyl substitution was not possible since **16**, also as a substituent, undergoes an addition reaction when treated with organolithium bases.[18e] To circumvent the problematic heterogenic charge distribution, Suzuki-reactions were applied. The synthesis of 2-(corannulenyl)-4,4,5,5-tetramethyl-1,3,2-dioxaborolane is reported in literature[17d] and 1,1'-bis(diphenylphosphino)ferrocene was assumed to be a suitable ligand for substitution reactions on this borolane. Recently, SPhos was used as a suitable ligand for sterically demanding reactants. Under both conditions only **36** and monobromoferrocene (**38**) were recovered after filtration through silica gel.

Since a synthesis of **35** was not successful, a selective synthesis of **37** was attempted under NCC conditions using only one equivalent of **18** and *n*-butyllithium as base. Nevertheless, dehalogenation occurred and this reaction yielded again an inseparable mixture of **22** and **37**.

2.5 1,1'''-Dicorannulenylbiferrocene (39)

As discussed previously, biferrocene units offer an interesting electrochemistry combined with a good stability of the oxidized species. For 1',1'''-(dicorannulenyl)biferrocene (**39**), **10** was lithiated, then zincated with anhydrous zinc(II) chloride. Under similar NCC reaction conditions as described earlier **39** was formed in 28 % yield with 13 % of biferrocenylcorannulene (**40**) as side product (Scheme 2.5.1).[69]

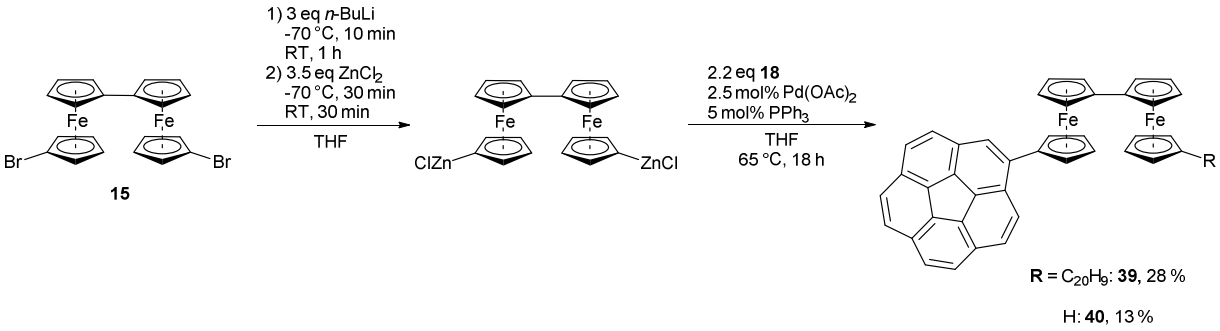

Scheme 2.5.1 Synthesis of **39**.

39 is a deep red solid which is soluble in THF, toluene and dichloromethane but is very sensitive towards acidic conditions while **40** possesses a superior solubility and showed a wax like consistency in the solid. Contrary to expectations **39** decomposes slowly in solution.

2.6 (R)-(+)-*N*,*N*-Dimethyl-1-ferrocenylethylaminecorannulene (41)

The ferrocene used for the preparation of (R)-(+)-*N*,*N*-Dimethyl-1-ferrocenylethylaminecorannulene (**41**) is named after its developer I. K. Ugi: "Ugi's amine" (**42**).[70] It is a chiral ferrocene containing a tertiary amine. **41** and its derivatives are widely used as ligands in asymmetric catalysis.[27c,71] The lithiation on Ugi's amine only occurs in *ortho*-position with an enantiomeric excess of 96 % after deprotonation with *n*-butyllithium and quenching with an electrophile.

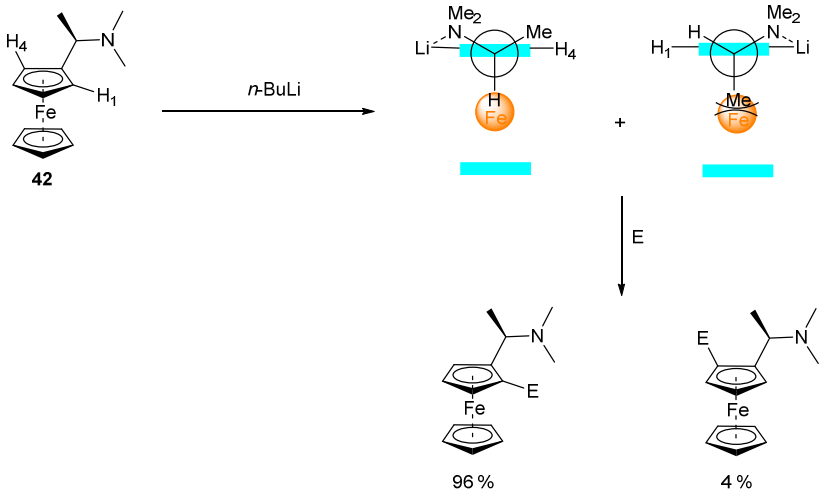

Scheme 2.6.1 *Ortho*-metalation of **42**.

The reason for the enantiomerically clean *ortho*-lithiation is shown in Scheme 2.2.7.1. Due to the favorable Li-N interaction only the substituted cyclopentadienylring in one of the two *ortho*-positions neighboring the amine function is attacked. In case that the metalation occurs in the position of H_4 (Figure 2.6.1), a sterically unfavorable interaction between the methyl group of the amine function and the iron atom occurs. Thus metalation occurs favorably in the position of H_1.

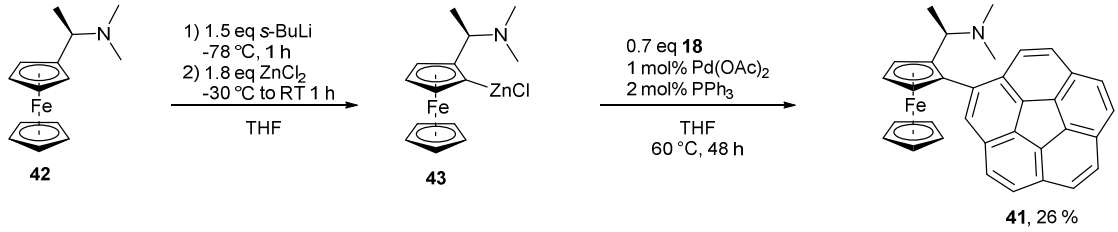

Scheme 2.6.2 Synthesis of **41** by NCC.[72]

In this work the slightly more reactive base *sec*-butyllithium was used for the metalation which was again followed by metathesis with anhydrous zinc chloride. After palladium-catalyzed cross-coupling with **18** the desired product **41** was formed in 26 % yield.[72] **41** is an orange solid that is not very stable at ambient temperature. It decomposes slowly in solution, resulting in an insoluble precipitate.

To prove the retention of the chiral information of **41** a circular dichroism spectrum was recorded. The minimum at 275 nm can be found for both compounds, **42** and **41** and confirmed the retention of the steric information. **41** further showed a minimum at 343 nm and 482 nm that can be assigned to the corannulene substituent.

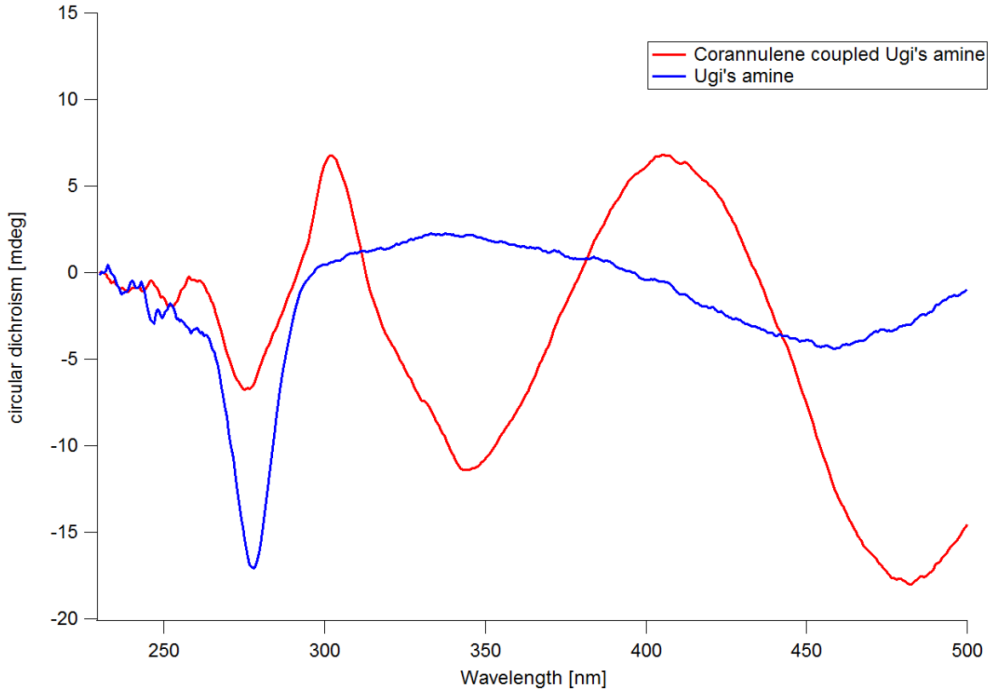

Figure 2.6.1 CD-spectrum of **41** and **42** measured in dichloromethane solution.

2.7 Diferrocenylated Corannulenes

Diferrocenylated corannulenes were prepared starting from previously reported 1,6-dibromo-2,5-dimethylcorannulene (**44**) which can be prepared analogues to corannulene itself by using diethylketone instead of dimethylketone in the Knoevenagel condensation step.[64]

Yields of **44** were lower than described in literature. An explanation was found in the incomplete bromination during the bromination step. A prolonged reaction time and the usage of a larger amount of *N*-bromosuccinimide both resulted in an insoluble solid and only traces of **44** were detected after the ring closing reaction. Yet, **44** is a suitable precursor for diferrocenylated corannulene derivatives. In a first attempt ferrocenyl substituents were introduced by the established NCC reaction. The yield of 1,6-diferrocenyl-2,5-

dimethylcorannulene (**45**) of 7 % was comparable low and can be explained by the low solubility of the compound which complicates the purification process by column chromatography and lead to only a small amount of analytically pure compound although the yield of the crude product was satisfying.

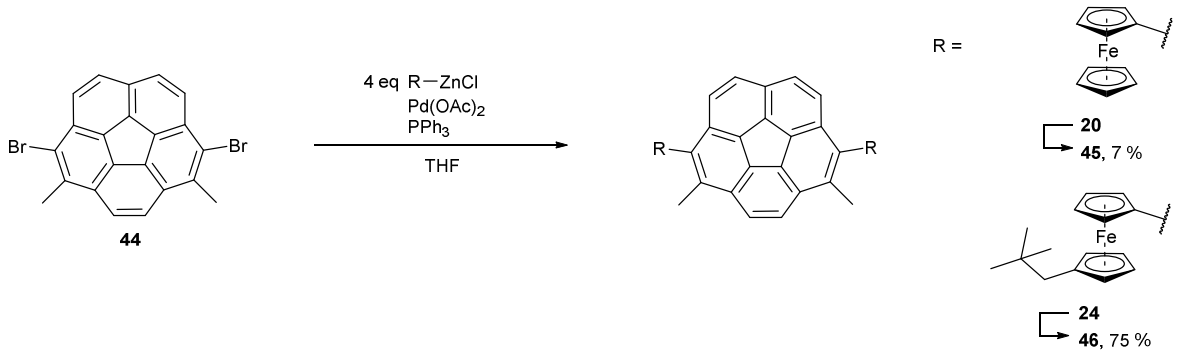

Scheme 2.7.1 Synthesis of **45** and **46**. **45**: 4 mol% palladium(II) acetate, 8 mol% triphenylphosphane, 70 °C, 18 h; **46**: 2 mol% palladium(II) acetate, 4 mol% triphenylphosphane, 65 °C, 19 h.

Using the brominated ferrocene with the solubilizing group **12** as reactant gave a satisfying yield of 75 % due to the increased solubility. Both compounds possess C_s-symmetry in solution.

Sonogashira-type coupling with **28** gave 2,5-dimethyl-1,6-bis(ethynylferrocenyl)corannulene (**47**). Again moderate yields were achieved. The reaction to the mono-coupled product and homocoupling reactions of **28** were competing with the reaction to the targeted product. If slightly less than two equivalents of **28** were used of the monoferrocenylated derivative could be obtained in 88 % yield. Thus it seems that after the first coupling reaction, reactivity of the residual bromine substituent is diminished and the use of a more effective catalyst or different ligand would be advisable.

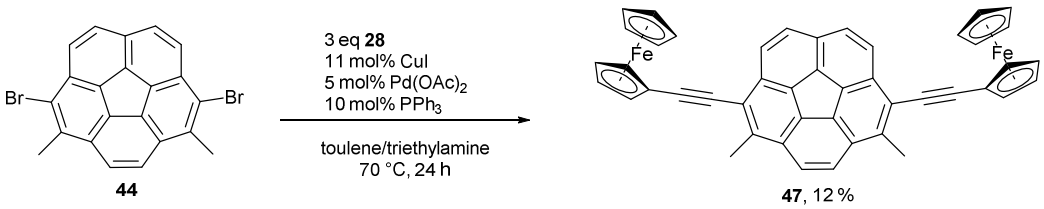

Scheme 2.7.2 Sonogashira reaction between **28** and **44**.[73]

The purification of **47** by column chromatography gave only small amounts of analytically pure product. Larger mixed fractions were obtained containing **47** with 1,4-diferrocenylbuta-1,3-diyne and with the monoferrocenylated derivative. Yet, 12 % of pure product could be isolated.[73]

1,6-Dibromo-3,4-bis(trifluoromethyl)corannulene (**48**) could be synthesized like described by Schmidt *et al*.[17b] Due to the bulkiness of the trifluoromethyl groups, the methyl groups of the fluoroanthene neighbouring these groups only undergo a monobromination, hence after a ring closing reaction the dibrominated corannulene **49** is formed exclusively. Only two bromine substituents remain after the ring closing step. Trifluoromethyl groups inherit a strong -I-effect, facilitating the reduction of the corannulene moiety.

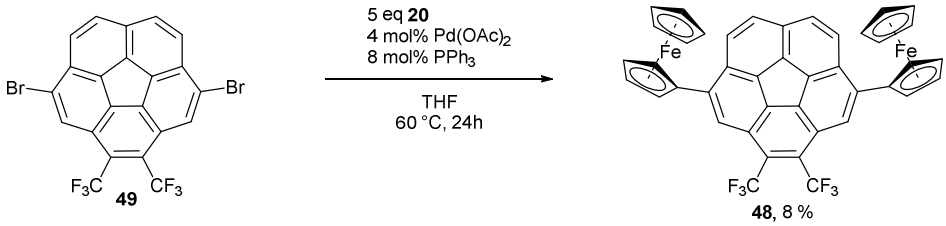

Scheme 2.7.3 Synthesis of a diferrocenylated corannulene with electron withdrawing trifluoromethyl groups.[67]

The crude product contained a large amount of biferrocene, which possesses a very similar R_f value to that of **48**. After a two-step column chromatography with different mixtures of *n*-pentane and dichloromethane (5:1 and 10:1) the pure product could be isolated in a moderate yield of 8 %.[67] The solubility of the wine red **48** compound is rather low in common organic solvents.

2.8 Tetraferrocenylated Corannulenes

The penultimate step of the corannulene synthesis is the ring-closing reaction of the brominated fluoranthene precursor. From this reaction pure 1,2,5,6-tetrabromocorannulene (**50**) can be obtained.[13c] Although it possesses very low solubility in common organic solvents,

it is nevertheless a suitable reactant for a variety of cross-coupling reactions as for some derivatives shown previously.[61] Coupling reactions with nearly all ferrocene derivatives presented for the monoferrocenylated buckybowls are possible and were conducted.

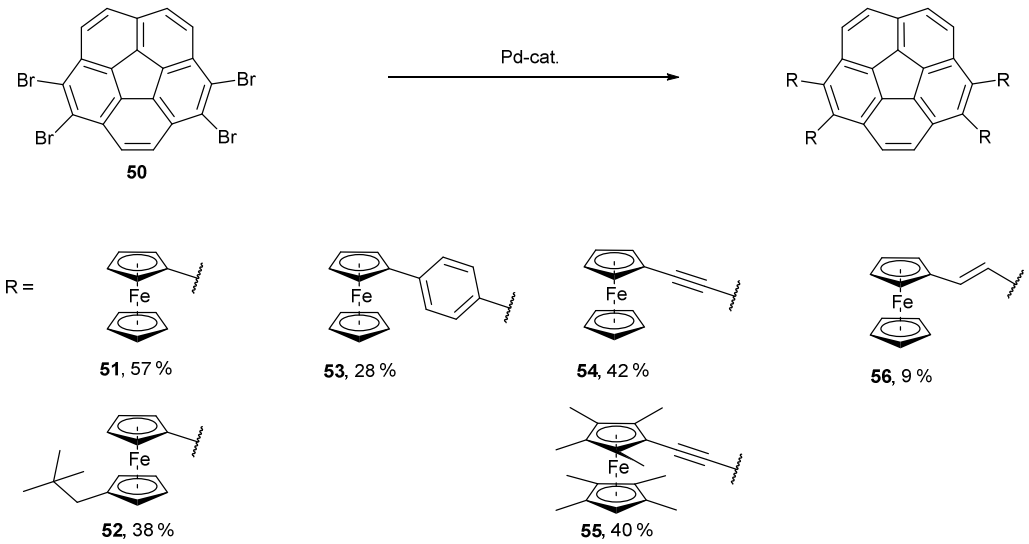

Scheme 2.8.1 Tetraferrocenylated corannulenes. **51**: 8 eq **20**, 4 mol% palladium(II) acetate, 8 mol% triphenylphosphane, THF, 60 °C, 48 h; **52**: 8 eq **24**, 4 mol% palladium(II) acetate, 8 mol% triphenylphosphane, THF, 62 °C, 48 h; **53**: 8 eq **27**, 4 mol% palladium(II) acetate, 8 mol% triphenylphosphane, THF, 70 °C, 24 h; **54**: 4.4 eq **28**, 0.2 eq copper(I) iodide, 10 mol% palladium(II) acetate, 20 mol% triphenylphosphane, toluene, triethylamine, 70 °C, 20 h; **55**: 4.4 eq **6**, 5 mol% palladium(II) acetate, 10 mol% triphenylphosphane, 5 mol% copper(I) iodide, diisopropylamine, 80 °C, 56 h; **56**: 1. 4.5 eq **2**, 45 eq potassium carbonate, 18 eq tetra-*n*-butylammonium bromide, 10 mol% palladium(II) acetate, DMF, 80 °C, 48 h, 2. 4.5 eq **2**, 10 mol% palladium(II) acetate, 80 °C, 24 h.

Reaction conditions were similar to the conditions described previously in this work. Yields of the tetrasubstituted compounds are satisfying. The colours of the pure solids of compounds **51**-**56** range from orange (**53**) over red (**51**, **52**) and dark red (**55**) to very dark purple (**55**) All compounds are stable towards air and moisture and moderately stable in solution. The low yield of **56** was due to the very low solubility of this compound and the consequential difficulty in purification by column chromatography. **52** benefits again from the additional neopentyl groups whereby it possesses a much higher solubility than **51** in common organic solvents.

2.9 Attempts to Synthesize 1,2,5,6-Tetrakis((*R*)-(+)-*N*,*N*-dimethyl-1-ferrocenylethylamine) corannulene (57)

After successful synthesis of **41** and retention of the ferrocenes stereochemistry, the next goal was to prepare a four times Ugi amine substituted corannulene (**57**). Several attempts were made to synthesize described in Table 2.9.1.[72]

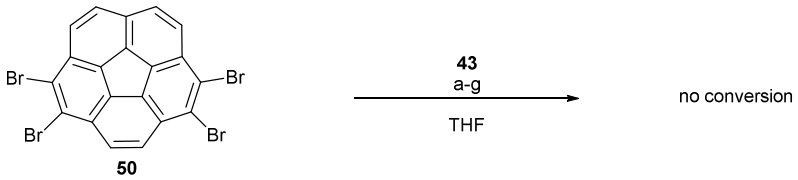

Table 2.9.1 Attempts to synthesize **57**.

System	Catalyst	%	Ligand	%	Temperature [°C]	Time [h]
a*	$Pd(OAc)_2$	1	PPh_3	2	60	48
b*	$Pd(OAc)_2$	10	iPr·HCl	10	110	72
c	$Pd_2(dba)_3$	2	-	-	60	72
d	$Pd_2(dba)_3$	2	XPhos	4	60	72
e	$Pd_2(dba)_3$	2	SPhos	4	60	72
f	$Pd_2(dba)_3$	2	dppf	4	60	72
g	$Ni(dppp)Cl_2$	30	-	-	60	72

Reactions were run on a 100 mg scale (*) or 4 mg scale based on **50**. Reaction progresses were checked by TLC. After the given time the reaction mixture was quenched with water and extracted with dichloromethane. The crude material was analyzed by ^{1}H NMR measurements.

The previously successful system using palladium(II) acetate and triphenylphosphane did not yield the targeted tetraferrocenylated product thus different catalytic systems were screened. Even when using more drastic reaction conditions (entry b) or a palladium(0) species no conversion towards a substituted product could be detected. Reactions were examined by TLC and ^{1}H NMR. Under the conditions described in entry f) some minor lower substituted

compounds could be detected. However all other reaction conditions resulted in the observation of the starting materials only.

1.10 *Sym*-pentaferrocenylated Corannulenes

After tetrasubstitution, pentasubstitution of **16** was approached. Two symmetrically substituted corannulene derivatives were reported in literature, which were considered as suitable starting molecules for symmetrically (*sym*)-ferrocenylated corannulenes, 1,3,5,7,9-pentakis(4,4,5,5-tetramethyl-1,3,2-dioxaborolan-2-yl)corannulene (**58**)[74] and 1,3,5,7,9-pentachlorocorannulene (**59**).[75]

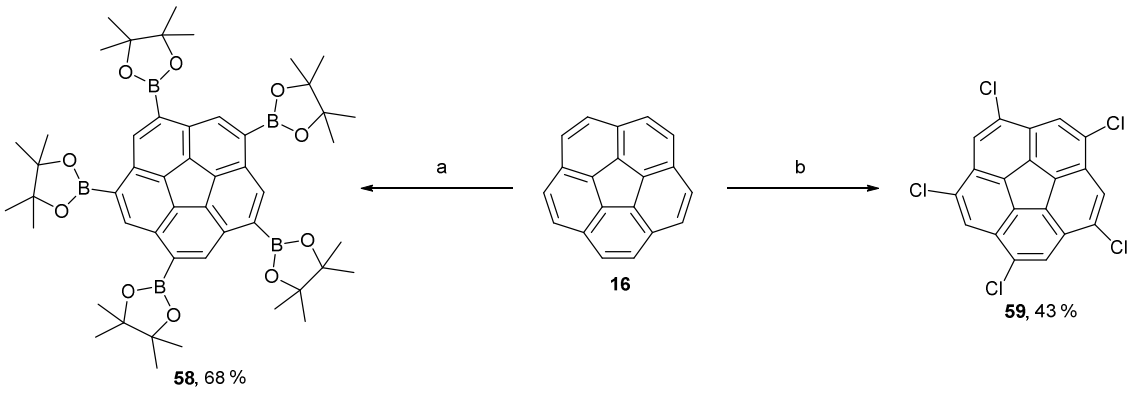

Scheme 2.10.1 Sym-pentasubstituted corannulenes. a) 5.2 eq bis(pinacolato)diboron, 0.4 eq potassium *tert*-butoxide, 0.2 eq (1,5-cyclooctadiene)(methoxy)iridium(I) dimer, 0.4 eq 4,4'-dimethyl-2,2'-bipyridyl, THF, 85 °C, 5 d; b) 12 eq ICl (1M in dichloromethane) -80 °C, 24 h, RT, 48 h.[74,75a]

The *sym*-pentaboronic ester of corannulene **58** is accessible as described by Scott *et al*.[74] by iridium catalysis in a one-step reaction from **16** in 68 % yield and purity after recrystallization from methanol. **58** is an air stable colorless solid and can be used for Suzuki-Miyaura cross-coupling reactions with halocarbon compounds.

Since the boronic ester **58** could be prepared easily in high yield, it was first used as a starting material for pentaferrocenylated corannulenes. Boronic esters or acids as used Suzuki-Miyaura cross-coupling reactions are air stable but less reactive than the sensitive zinc compounds used

for NCC reactions. Only monoiodoferrocene **60** and phenyl substituted **13** were employed due to the weakness of their C-I bond.

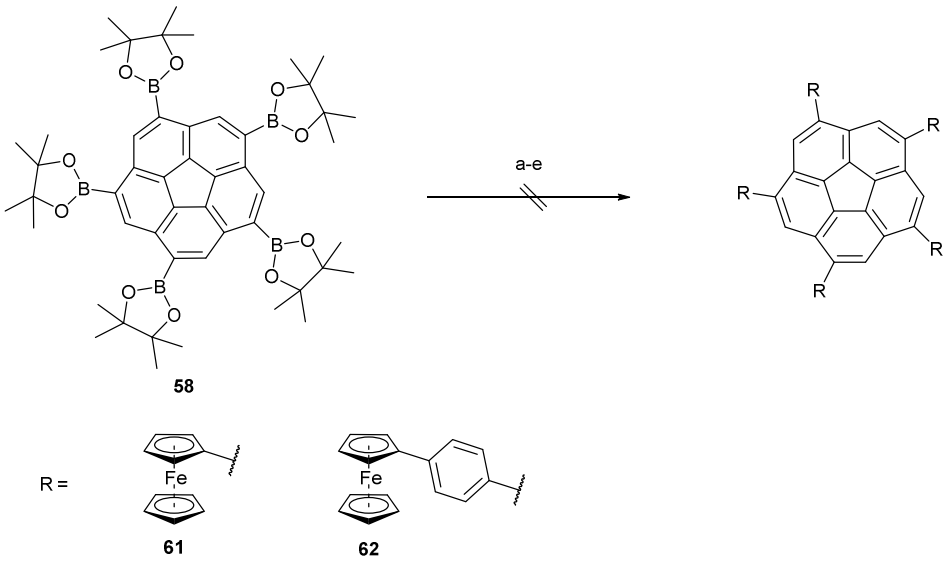

Scheme 2.10.2 Suzuki-Miyaura cross-couplings of **58**. a) 7.5 eq **60**, 12 eq caesium carbonate, 25 mol% tris(dibenzylideneacetone)dipalladium(0), 50 mol% SPhos, THF, 77 °C, 2 d; b) 10 eq **13**, 12,5 eq caesium carbonate, 11 mol% tris(dibenzylideneacetone)dipalladium(0), triphenylphosphine (22 mol%) THF, 95 °C 7 h; c) 10 eq **13**, 12.5 eq caesium carbonate, 22 mol% palladium(II) acetate, 22 mol% 1,1'-bis(diphenylphosphino)ferrocene, THF, 70 °C, 24 h; d) 10 eq **13**, 12.5 eq caesium carbonate, 22 mol% [1,1'-bis(diphenylphosphino)ferrocene]-dichloropalladium(II), THF, 70 °C, 3 d; e) 10 eq **13**, 8.6 eq potassium phosphate, 44 mol% tris(dibenzylideneacetone)dipalladium(0), 88 mol% SPhos, DMF/H_2O, 110 °C, 5 d.

First **60** was used but after two days reaction time **60** was recovered quantitatively under conditions a). It was assumed that due to the steric demand of directly coupled ferrocene no conversion took place and further experiments were run with **13**. The phenyl spacer was expected to exert sterical release on the tightly substituted system. Different catalysts, reported for high yields in Suzuki-Miyaura reactions were screened.[74,76] Under condition b) and c) **13** was recovered and ferrocenylbenzene was obtained. Under condition d) mainly **13** was recovered and less than 5 % of the homocoupling product 4,4'-diferrocenyl-1,1'-biphenyl was obtained. Under the harsher reaction condition e) **13**, ferrocenylbenzene and 4,4'-diferrocenyl-

1,1'-biphenyl were isolated, as well as a small amount red solid which was an inseparable mixture of compounds but none of the desired product could be detected.

These results suggested that ferrocene compounds are not suitable reactants for Suzuki-Miyaura cross-coupling reactions on **58** and chlorinated **59** was used as starting material, which offered the possibility for substitution reactions by NCC reactions. The symmetrical 1,3,5,7,9-pentachlorocorannulene (**59**) was first synthesized by the group of Scott and has shown to be a versatile building block for a variety of pentasubstitued corannulene derivatives.[75,77] In 1999 the group of Siegel demonstrated that though chlorinated aromatics are relatively unreactive compounds, **59** readily undergoes conversion to corresponding alkyl corannulene derivatives.[75b] Impressed by the clean five-fold symmetry and regiochemical control, *sym*-pentaaryl, *sym*-pentaalkynyl corannulenes were prepared by iron(II) catalysis, as well as a variety of other compounds retaining the five-fold symmetry.[64,77-78] For aryl substituents nickel-mediated NCC reactions were shown to work best and offer yields of up to 49 %.[75b] **59** could be conveniently prepared from **16** by addition of iodine monochloride in dichloromethane followed by recrystallization. The white needles contained only very small residues of lower chlorinated corannulene derivatives as determined by MALDI mass spectrometry.

For obtaining a sufficiently soluble product **12** was zincated and used as reactant.

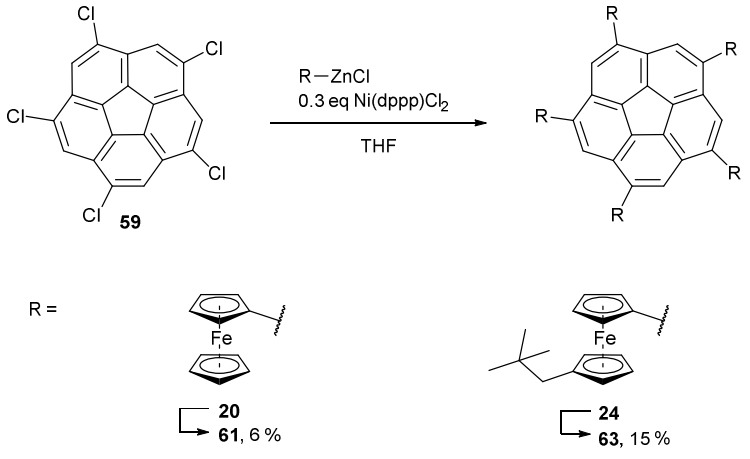

Scheme 2.10.3 Nickel-catalyzed NCC on **59**. **61**: 15 eq **20**, 67 °C, 29 h; **63**: 10 eq **24**, 60 °C for 3 d.

After addition of the nickel(II) catalyst and **59** to the zincated ferrocene **24** upon heating an immediate color change from a light red suspension to a dark red solution was observed and after work-up 15 % of the targeted compound were isolated. The yield was not very high, which might be due to the steric demand of these directly coupled ferrocenes. In addition, calculations showed that the steric demand of five ferrocenyl substituents leads to a very crowded molecule, which could impede the coupling reaction and lead to diminished yields. Still a ferrocenylation grade of 68 % per chlorine atom and a total yield of 15 % for the neopentyl substituted derivative could be achieved, which is surprisingly high for a chlorinated derivative. Following the successful preparation of **63**, **61** could be obtained under similar reaction conditions. The yield of these NCC reactions was strongly dependent on the solubility of the intermediates and the product. Purification of **61** without the solubilizing alkyl chain was exceedingly difficult. First, residual ferrocene was washed out of the product by sonication of the crude material with *n*-hexane and after filtration through a plug of silica gel, a red solid is obtained. MALDI mass measurements showed the pentasubstituted derivative as the main product with hexa- and tetrasubstituted byproducts, which could be removed by careful PTLC on silica gel with *n*-pentane/dichloromethane (1:1). Other fractions still contained small amounts of the product, nevertheless 7 % of pure product could be isolated which corresponds to 58 % of successful substitution *per* coupling position.

The attempt to synthesize additional compounds by the use of **59** were unsuccessful. An attempted cross-coupling reaction with ferrocenylethynylzincchloride or zincated octamethylcompound **6** yielded only traces of less than one percent of the desired product as observed by ESI mass spectrometry. Mainly homocoupling of zinc compounds were observed, further large amounts of the ethynylferrocenes **6** and **28** were recovered. NCC reactions with zincated **28** only yielded traces (about 1%) of the desired symmetrically pentasubstituted compound, observed by MALDI mass spectrometry. Dehalogenation was also observed and the main product was a mixture of different tetrasubstituted compounds, deriving not only from dehalogenation but also incomplete chlorination in the prior reaction.

2.11 Attempts to Synthesize *Per*ferrocenylated Corannulenes

Two different perhalogenated corannulene derivatives are accessible by synthesis, decabromocorannulene (**64a**) and decachlorocorannulene (**65**). Synthesis of decabromocorannulene was described by Scott et al.[79] by electrophilic aromatic substitution of elemental bromine on unsubstituted **16**. After the reaction an insoluble red-brown solid was obtained. Purification by Soxhlet extraction with dichloromethane and recrystallization from diphenyl ether yielded a bright yellow solid. Unlike reported previously, the compound obtained was nonabromocorannulene (**64b**) with a small amount of **64a**, as determined by EI-Mass measurements. Nevertheless, this mixture of products was used to explore the potential coupling reactions in principal, leading to *per*ferrocenylation.

65 could be easily prepared starting from tetrabrominated **50** as described by Scott et al.[80] and showed mainly the desired *per*chlorated product in MALDI mass measurements. Due to the strong C-Cl bond palladium-catalyzed cross-coupling reactions with high yields for chlorinated aromatics are sparse. Especially ten-fold reactions are incredibly challenging. The different reaction conditions explored are depicted in Scheme 2.11.1.[75a,77]

The reaction of **64a/b** with ethynyl compound **24** yielded no desired products. After reaction of **64a/b** with **24** some residual starting material (**12**) was recovered and the homo coupling products 1,4-di(ferrocenyl)buta-1,3-diyne and 1,1'''-bis(neopentyl)biferrocene were obtained in small quantities. Under both reaction conditions it could be observed that the poorly soluble **64a/b** was dissolved under the given conditions. Even a color change of the reaction mixture to red, which was usually only observed for successful NCCs, was observed. But no traces of the desired *per*ferrocenylated compounds could be obtained.

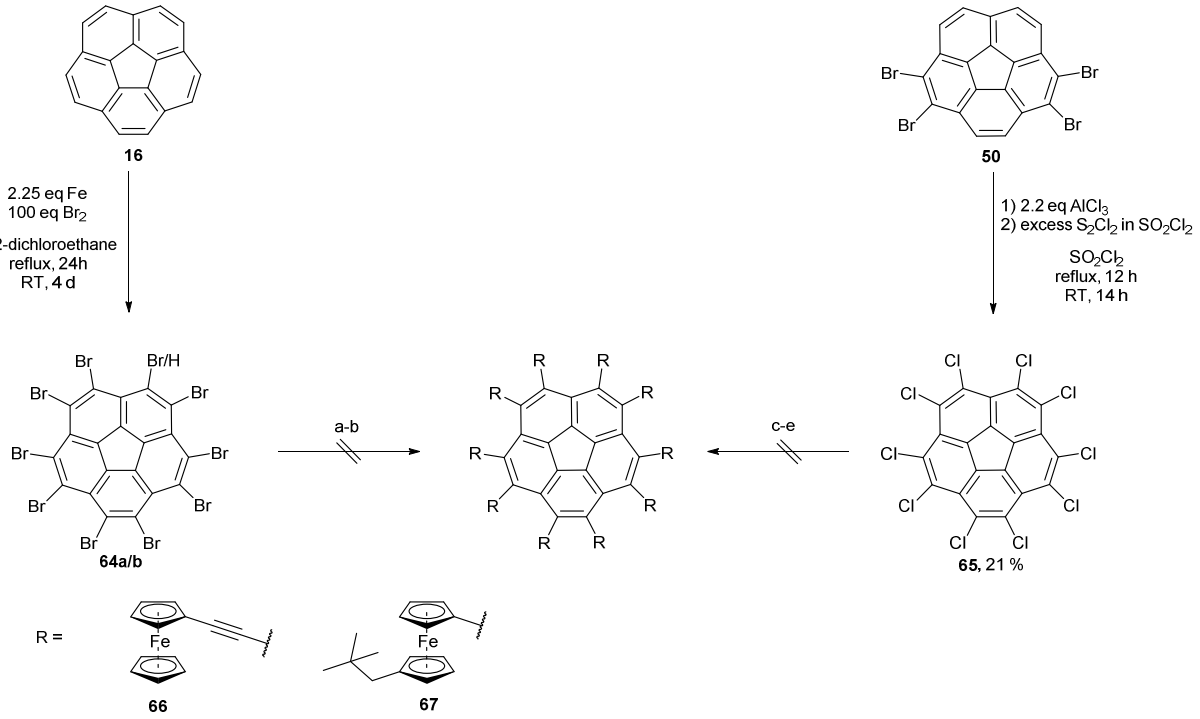

Scheme 2.11.1 Attempted perferrocenylation of **16**. a) 11 eq **28**, 50 mol% tris(dibenzylideneacetone)dipalladium(0), 55 mol% copper(I) iodide, 25 mol% triphenylphosphane, toluene/triethylamine, 80 °C, 3 d; b) 30 eq **24**, 30 mol% palladium(II) acetate, 60 mol% triphenylphosphane, THF, 80 °C, 3 d; c) 30 eq **24**, 0.7 eq dichloro(1,3-bis(diphenylphosphino)propane)nickel, THF, 70 °C, 5 d; d) 20 eq **24**, 2 eq palladium(II) acetate, 2 eq 1,3-bis(2,6-diisopropylphenyl)imidazolium chloride, 2 eq potassium *tert*-butoxide, DME, 87 °C for 2 h then at 80 °C, 4 d; e) 20 eq **24**, 5 mol% tris(dibenzylideneacetone)dipalladium(0), 20 mol% RuPhos, THF, 70 °C, 3 d.

Reactions starting from **65** were run on a small scale of 10 – 20 mg. Though in contrast to 64, 65 was obtained in very high purity. Nevertheless, under reaction condition c) only very small amounts of nonachlorocorannulene reacted to form traces of monoferrocenylated octachlorocorannulene as observed in the ESI-Mass spectrum. Again, mainly the homocoupling product of the ferrocene species was isolated. Reaction conditions d), e) and f) did not show any traces of successful coupling reactions. Large amounts of neopentylferrocene could be isolated and no homocoupling products were observed.

3. NMR

NMR spectra of corannulene derivatives are generally complex and an exact assignment of all signals is often difficult. In order to facilitate and unify the assignment of ^{13}C NMR signals, the resonances are divided into three groups (rim, spoke and hub carbon atoms) according to the convention for corannulene compounds (depicted in Figure 3.1).[81]

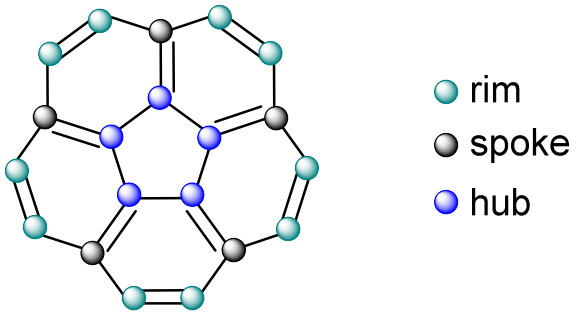

Figure 3.1 Nomenclature of the three groups of carbon atoms in the corannulene molecule.

3.1 Monoferrocenyllated Compounds

Monoferrocenyllated compounds are C_1-symmetric and hence show complex NMR spectra. The ^1H NMR generally shows partially overlapping AB-typ splittings with coupling constants of around ^3J = 8.8 Hz for the rim protons of the corannulene unit in the lower field. The usual set of signals for the ferrocene unit was observed as an AA'BB'-set of signals at around 5.00 for the protons of the substituted cyclopentadienyl ring and a singlet at 4.30 ppm for the unsubstituted cyclopentadienyl ring. The very complex ^{13}C NMR spectra of these compounds shows 20 individual signals for all 20 carbon atoms of the corannulene unit which were assigned to the groups of rim, spoke and hub carbon atoms as described earlier.[81]

Exemplarily, the ^1H NMR spectrum of the neopentylferrocene substituted **25** is depicted in Figure 3.1.1. The resonance of the *ipso*-rim carbon atom experiences the strongest low field shift (139.28 ppm), followed by the hub carbon atoms (136.20 – 134.78 ppm) and the spoke carbon atoms (131.04 – 129.81 ppm). The resonances of the rim atoms can easily be

distinguished by their increased intensity deriving from the Nuclear Overhauser effect (NOE) known for proton substituted carbon atoms in proton decoupled ^{13}C NMR experiments and appear between 127.49 and 124.88 ppm. The signals of the ferrocene unit were found in the higher field at around 70 ppm.

The ^{1}H NMR (Figure 3.3.1) is characterized by partially overlapping AB-type sets of signals. Further four resonances were found for the cyclopentadienyl protons, the neopentyl group gave two singlets at 2.22 ($C\underline{H}_2$) and 0.74 ppm ($C\underline{H}_3$).

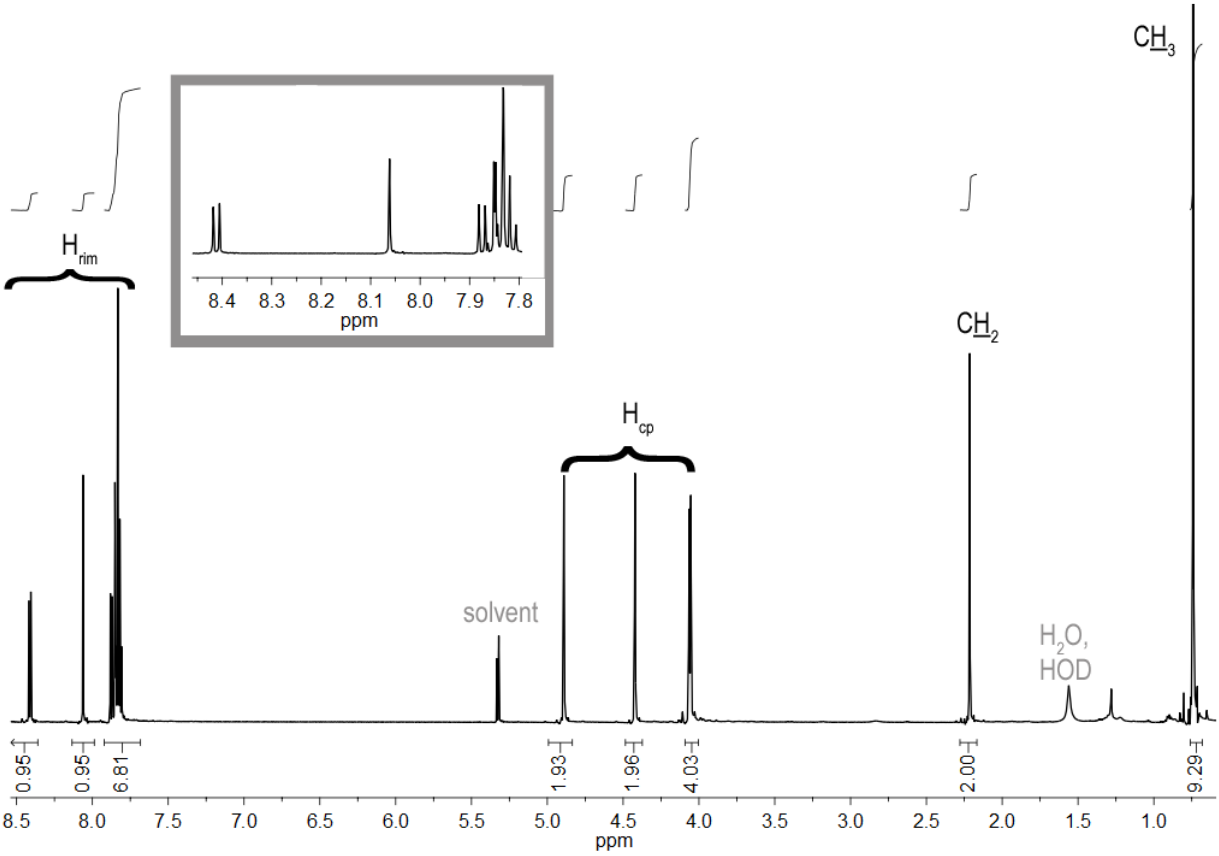

Figure 3.1.1 700 MHz ^{1}H NMR of **25** in CD_2Cl_2. Proton resonances are assigned to the different groups of protons: Rim protons of the corannulene moiety (H_{rim}), protons of the cyclopentadienyl rings of the ferrocene unit (H_{cp}) and protons of the neopentyl substituent ($C\underline{H}_2$, $C\underline{H}_3$). Resonances not belonging to the described compound (here water) are labelled in grey.

The ^{13}C NMR spectrum of **25** shows the distinctive groups of resonances for hub (136.48 – 134.92), spoke (131.55 – 130.39) and rim (128.15 – 124.85 ppm) carbon atoms. Again the *ipso* carbon atom (140.07 ppm) experienced the strongest low field shift and the resonances of the CH_{rim} carbon atoms are intensified by the NOE.

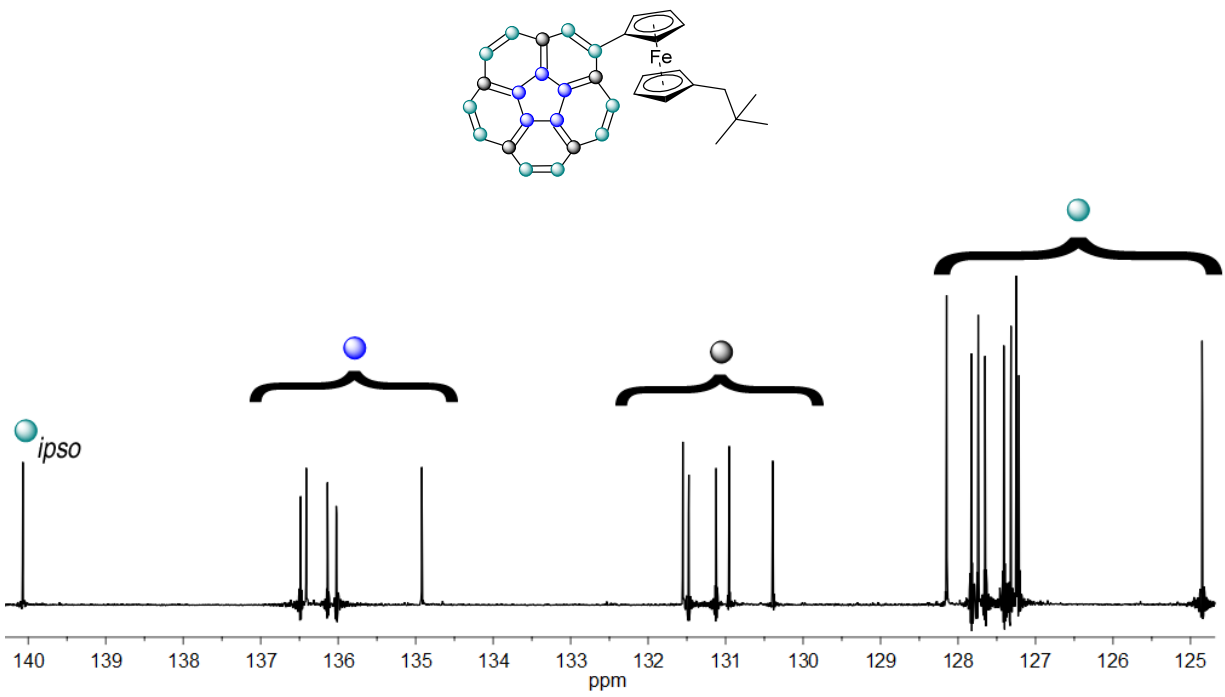

Figure 3.1.2 Section of the 175 MHz ^{13}C NMR spectrum of **25** in CD_2Cl_2 showing the resonances of the corannulene moiety. Signals are assigned to the groups of hub (blue), spoke (dark grey) and rim (turquoise) carbon atoms.

The resonances of the ferrocene moiety can be found in the higher field of the spectrum. The peaks of the *ipso* carbon atoms were found at 87.82 and 85.83 ppm. Three of the CH-signals of the cyclopentadienyl rings (72.50 – 70.34 ppm) are also intensified by the NOE, while one signal at 70.47 ppm is broadened and low in intensity. The resonances of the neopentyl group can be found at 45.01 ($\underline{C}H_2$), 32.06 ($\underline{C}(CH_3)_3$) and 29.59 ppm ($\underline{C}H_3$).

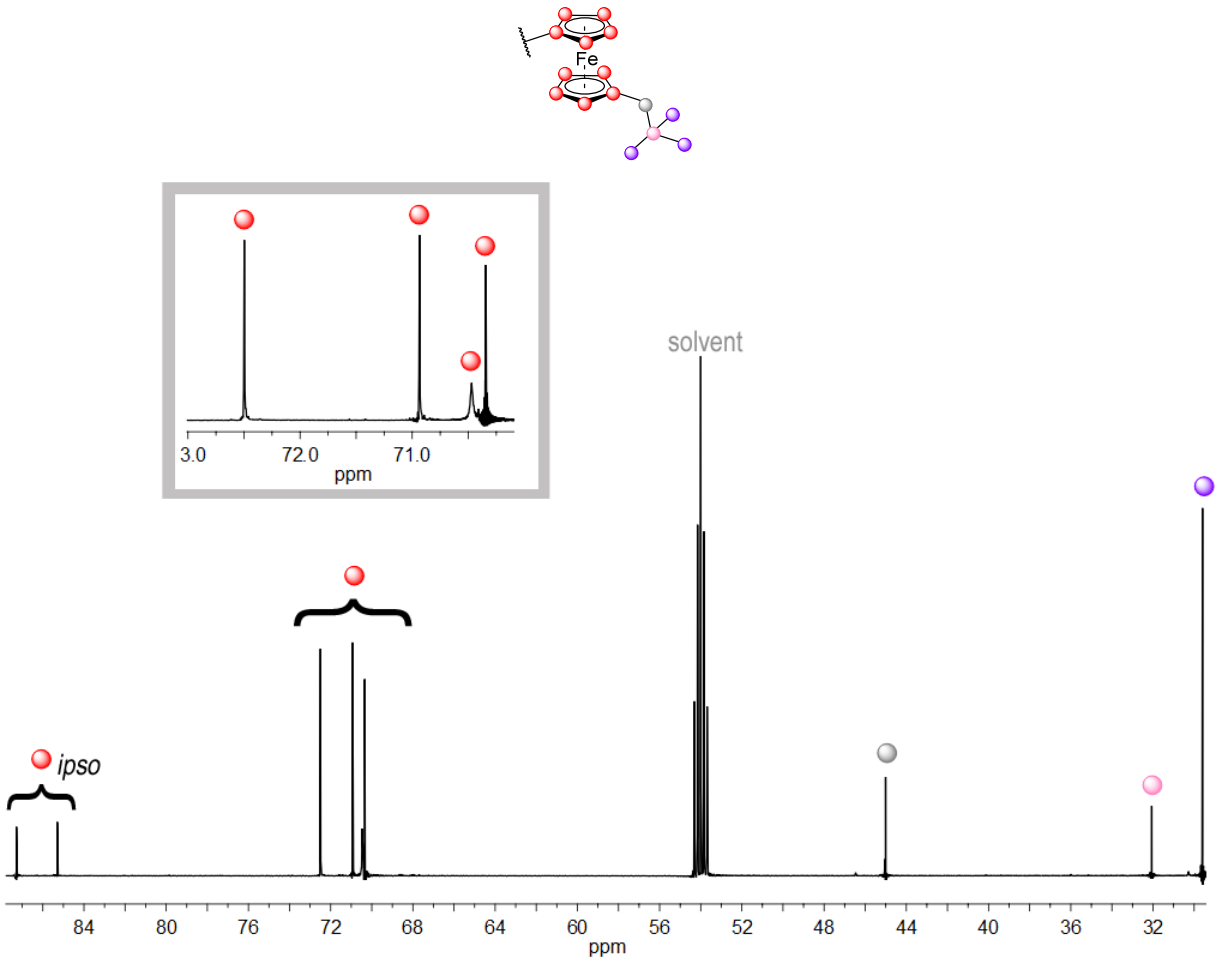

Figure 3.1.3 High field of the **25** 175 MHz ^{13}C NMR in CD_2Cl_2, displaying resonances of the ferrocene moiety.

Other monoferrocenyllated compounds are similar regarding the signals of the ferrocene or corannulene moiety and show no unexpected effects. The ^{1}H and ^{13}NMR spectra of the dicorannulated ferrocene **33**[58] are very similar to the monosubstituted species and will thus not be discussed in detail.

The NMR spectra of the Ugi's Amine compound **41**[72] are a little more complex and due to its sensitivity in solid and solution possess a noisy background. The proton neighboring the ferrocene gives a singlet at 8.40 ppm, the resonances for the other rim protons of the corannulene substituent can be found between 8.06 and 7.82 ppm as partially overlapping AB-type signals. The resonances of the cyclopentadienyl rings are visible between 4.78 and 4.27 ppm, again showing a pseudo-triplet splitting of 2.5 Hz. The CH-proton is split into a quartet at

4.01 ppm with a coupling constant of 6.4 Hz and the methyl groups of the amine resonate at 1.74 ppm and the methyl group at the stereocenter is visible as a singlet at 1.70 ppm.
The ^{13}C NMR is very similar to those of the previously discussed ferrocenylated corannulenes. Additionally, the resonances of the amine's methyl groups can be found at 40.46 ppm and the chiral carbon center resonates at 55.37 ppm.

3.2 Sumanenylferrocene (23)

The also C_1-symmetric **23**[62] shows even more complex NMR spectra which are depicted in Figure 3.2.1 – 3.2.2. Within the ^1H NMR spectrum the resonance of the proton neighboring the ferrocenyl unit is observed as a broadened singlet at 7.33 ppm. At 7.08 ppm the aromatic protons of the sumanene substituent split into an AB-type set of signals with a slightly smaller coupling constant of ^3J = 7.7 Hz. The peaks of the substituted cyclopentadienyl ring, as well as the peaks for three of the benzylic protons of the sumanene moiety can be observed between 4.79 and 4.30 ppm as a slightly broadened and more complex set of peaks that was not possible to evaluate when the compound was measured in $CDCl_3$ (Figure 2.2.1). In CD_2Cl_2, with help of HMQC measurements the peaks could be assigned as depicted in Figure 3.2.2. Resonances of the unsubstituted cyclopentadienyl ring shows four broad signals at 4.78, 4.64, 4.39 and 4.34 ppm. Resonances of benzylic protons show AB-type sets of signals with a coupling constant of ^2J = 19 Hz. At 4.78 ppm a resonance of the substituted cyclopentadienyl ring overlaps with one peak of an AB-resonance of the nuclei of a benzylic proton.

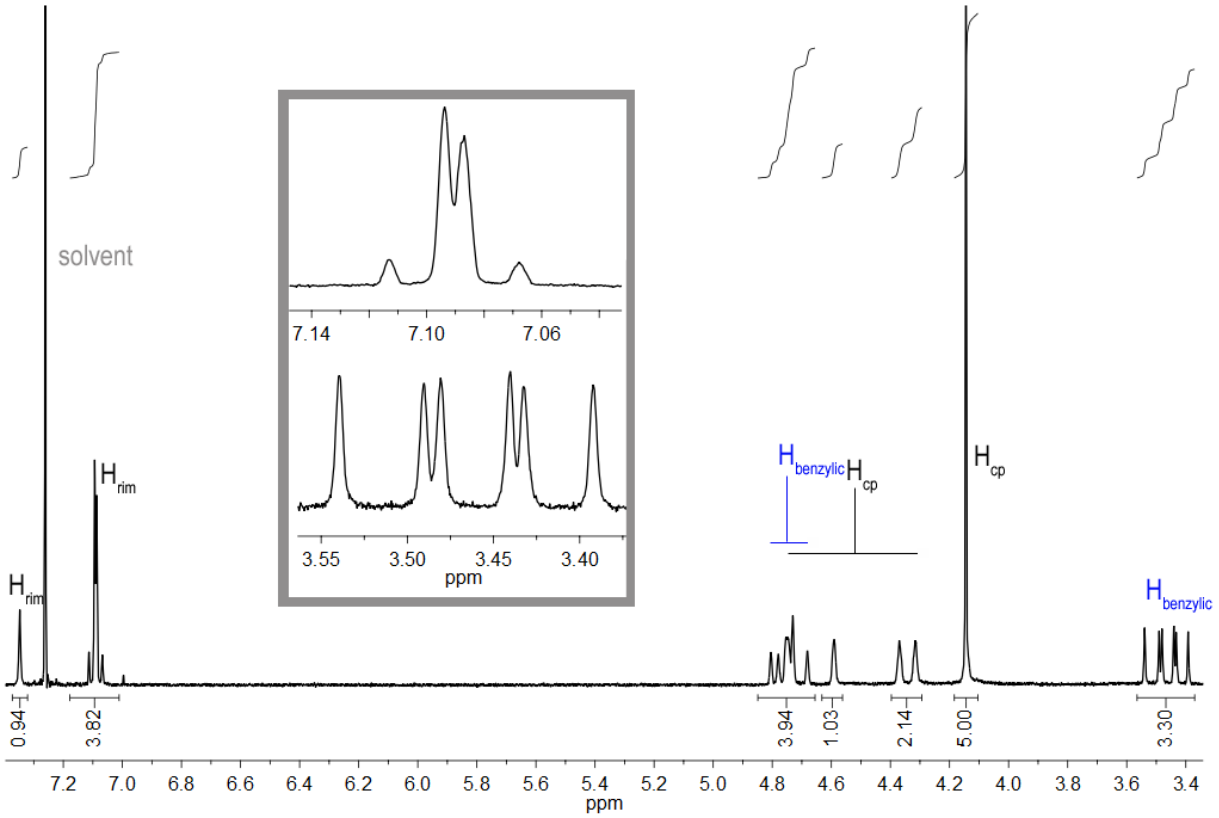

Figure 3.2.1 500 MHz ^{1}H NMR spectrum of **23** in $CDCl_3$.

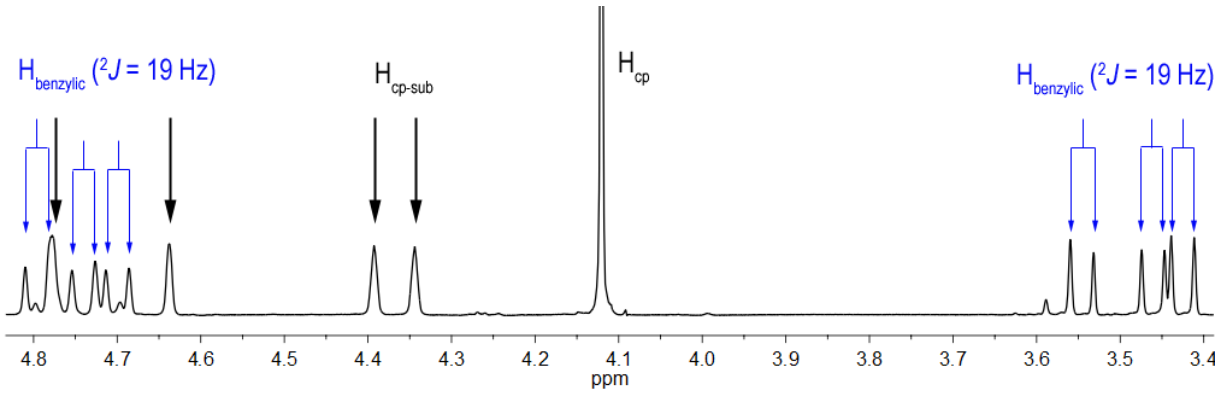

Figure 3.2.2 Splitting of ^{1}H the benzylic and cyclopentadienyl resonances 700 MHz ^{1}H NMR spectrum of **23** in CD_2Cl_2.

The ^{13}C NMR shows 21 signals, one for each carbon atom of the sumanenyl substituent (Figure 3.2.3). The peaks were assigned to hub, flank, rim and benzylic carbon atoms.

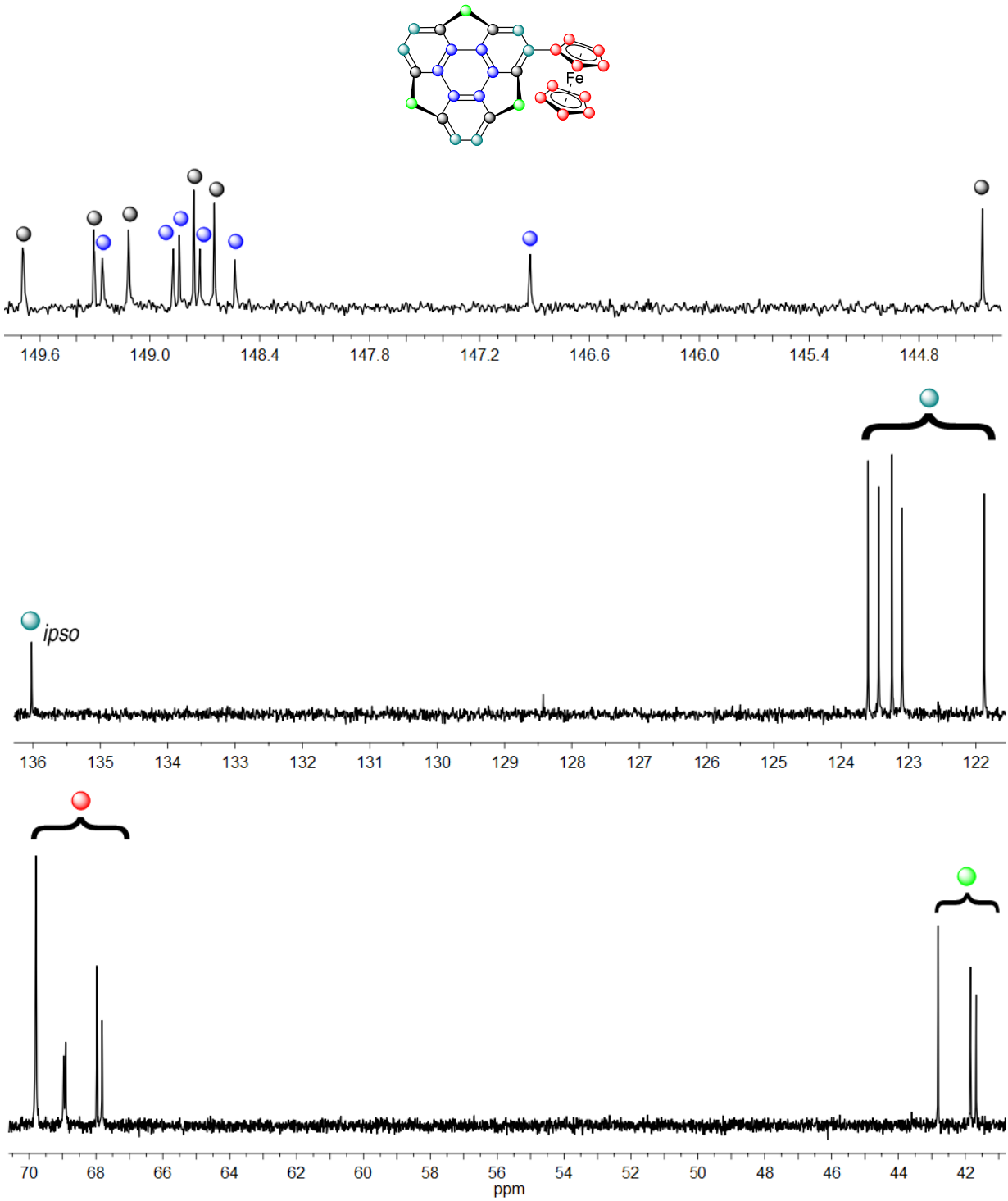

Figure 3.3.2 125 MHz ^{13}C NMR of **23** in $CDCl_3$. Resonances are assigned to hub (blue), spoke (black), rim (turquoise), cyclopentadienyl (red) and benzylic carbon atoms (green).

Other than in **25**, hub and flank atoms were found within the same area of the spectrum (149.53 - 144.29 ppm), but could be distinguished by their intensities.
The *ipso* carbon atom of the sumanene moiety was found at 135.86 ppm and the resonances of the rim carbon atoms were found to be between 123.44 and 121.71 ppm. The peaks of the ferrocene moiety were at 69.64 ppm (unsubstituted cyclopentadienyl ring) and 67.82, 67.66 ppm (substituted cyclopentadienyl ring). The three benzylic carbon atoms were found in the higher field of the spectrum (42.65, 41.68, 41.52 ppm).

Again the spectrum of the disumanulenyl substituted ferrocene **34**[62] is similar, though the ^{1}H-NMR of **34** is difficult to analyze due to the very poor solubility and overlapping broad signals of the ferrocene moiety and the benzylic protons of sumanene. Broadened signals in the ^{1}H NMR suggest a dynamic stereochemistry in solution where the in-plane rotation of the cyclopentadienyl ligand of the ferrocenyl moiety, bowl-inversion and rotation of the bowls occur. A similar phenomenon was extensively studied, for example bisumanenyl by the group of Hirao[82] or bicorannulenyl by the group of Scott.[83]

3.3 1,1'''-Dicorannulenylbiferrocene (39)

The ^{1}H NMR spectrum (Figure 3.3.1) was recorded in deuterated dichloromethane instead of chloroform for NMR measurements, but even then the compound decomposed slowly during measurement causing a noisy spectrum background, probably because of the formation of paramagnetic species.[69] The ^{1}H spectrum of **39** shows 13 very sharp signals suggesting fast rotation and bowl-to-bowl inversion on the NMR time scale. Similar to **25** the rim protons corannulene substituent split into partially overlapping AB-type signals. One half of the AB-set of signals for the two protons neighboring the biferrocene can be observed at 8.22 ppm with a coupling constant of 8.7 Hz. The proton in α-position to the ipso carbon gives a sharp singlet at 7.79 ppm. The signal at 7.8 ppm can also be assigned by HMQC and HMBC measurements. Other resonances of the corannulene rim were observed as a multiplet at 7.86 –

7.73 ppm. The protons of the cyclopentadienyl rings of the biferrocene unit can be observed as an AA'BB' -type set of signals showing a pseudo-triplet splitting between 4.71 and 3.70 ppm.

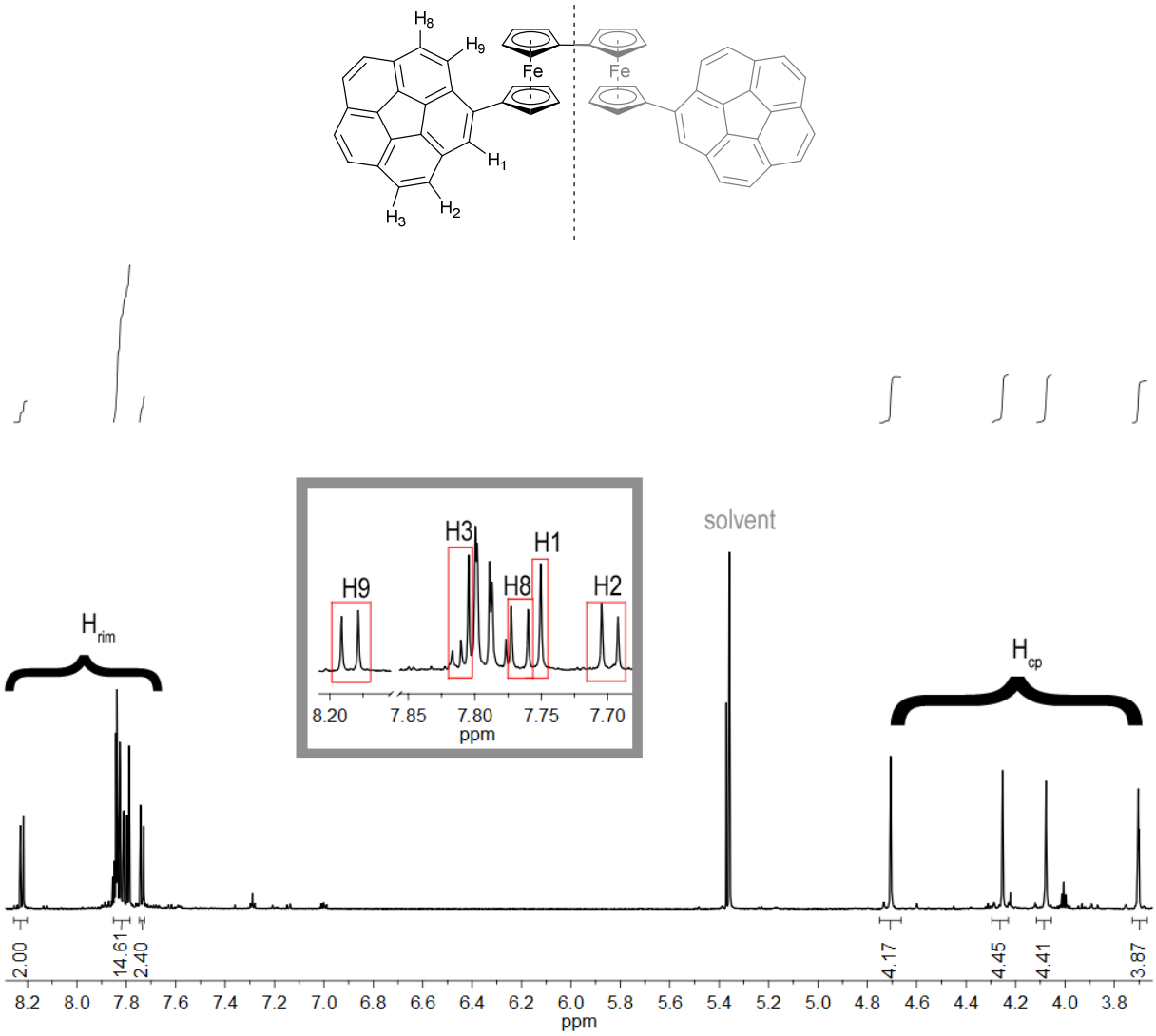

Figure 3.3.1 ^{1}H NMR resonances of the corannulenyl substituent of **39** recorded at 700 MHz in CD_2Cl_2.

The ^{13}C NMR spectrum is very similar to that of **25**. With the help of COSY, HMBC and HMQC measurements some signals could be assigned as depicted in Figure 3.3.2. The *ipso*-carbon atom of the corannulenyl substituent is shifted to higher field of the spectrum. Ultimately, only the resonances of carbon atoms in close proximity to the biferrocene unit could be assigned distinctly.

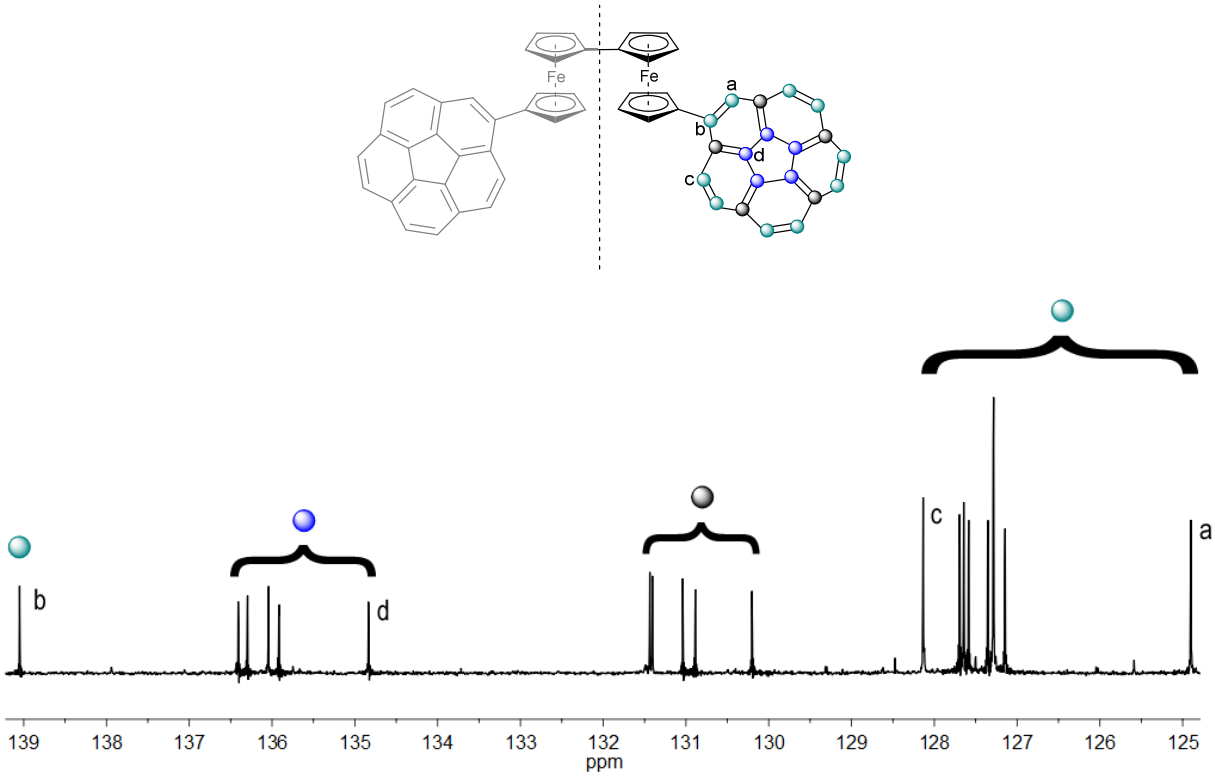

Figure 3.3.2 ^{13}C NMR resonances of the corannulenyl substitutent of **39** recorded at 700 MHz in d2-dichloromethane.

3.4 Diferrocenylated Compounds

Upon symmetrical substitution the NMR spectra of corannulene compounds are getting easier to analyse. The fast bowl-to-bowl in version in solution of the diferrocenylated dimethylcorannulenes leads to a C_s-symmetry.

The ^1H NMR spectra (exemplarily displayed for **46** in Figure 3.4.1) show two sets of signals for the corannulene rim protons. A singlet for the two protons neighbouring the methyl groups and an AB-type set of signals with a coupling constant of ^3J = 8.8 Hz for the other four protons are observed, suggesting bowl inversion and fast rotation of the ferrocene substituents in solution on the NMR timescale. The resonances of the methyl groups can be observed at 3.06 ppm for **46**.

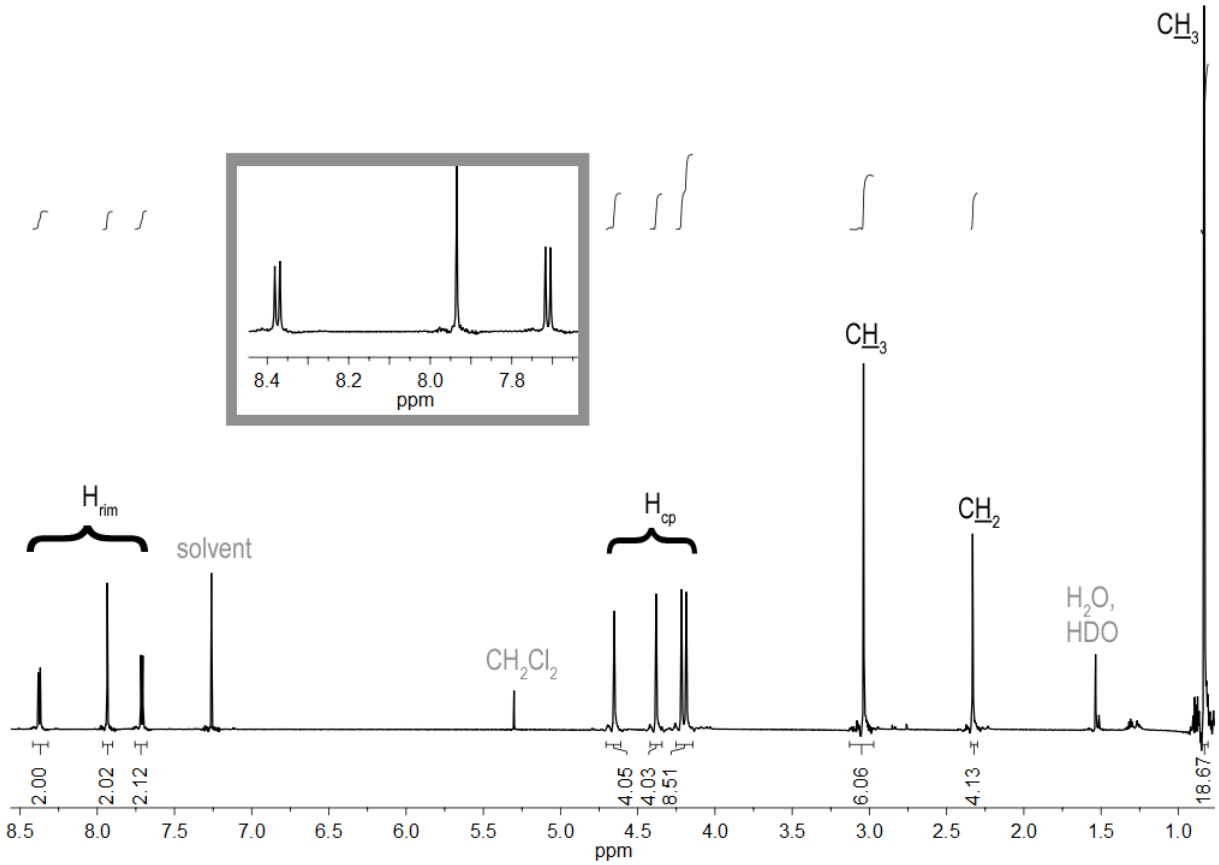

Figure 3.4.1 700 MHz ^{1}H NMR spectrum of **46** in $CDCl_3$.

The ^{13}C NMR is also facilitated due to the C_s-symmetry. Three signals for each, the hub (134.36 – 133.69 ppm), spoke (133.36 – 131.21 ppm) and rim carbon atoms (127.78 – 125.36 ppm) were observed for **46**. The NOE is not as prominent as in the monosubstituted derivative **25**. The ipso carbon nuclei, showing inferior intensity, resonate at 135.43 and 129.47 ppm (see Figure 3.4.2). The ferrocene substituents exhibit similar resonances as described for **25** thus will be not further discussed in this part. The methyl groups are chemically equivalent, resulting in a singlet at 17.08 ppm.

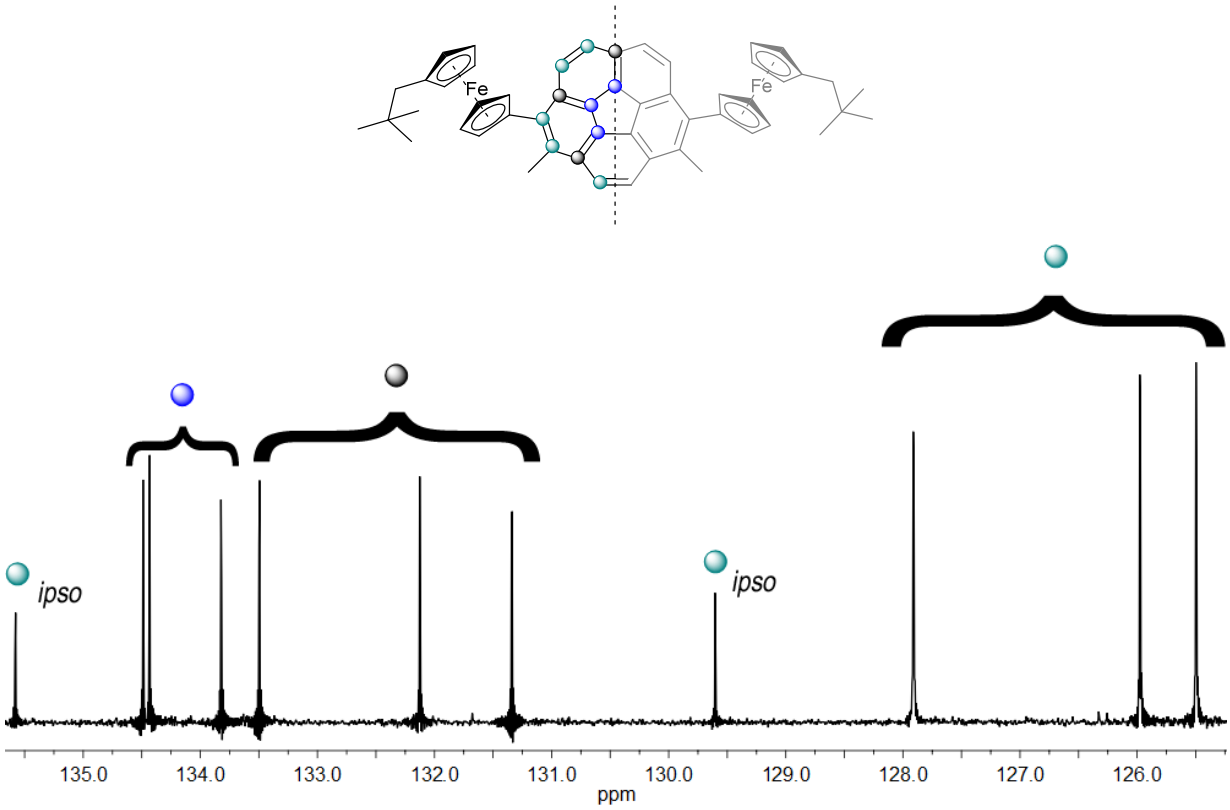

Figure 3.4.2 Resonances of the corannulene moiety of **46** recorded at 175 MHz ^{13}C NMR in $CDCl_3$.

Spectra of **45** and **47** are very similar whereas the spectrum of the bistrifluoromethylated corannulene **48** is slightly different due to the different substitution pattern. This compound also exhibitis a C_s-symmetry in solution. The ^{1}H NMR spectrum showed a singlet at 8.41 ppm and an AB-set of signals with a coupling constant of ^3J = 8.9 Hz. The signals of the ferrocenyl units are similar to those described above. The ^{19}F NMR spectrum consists of a singlet at -50.07 ppm.

In the ^{13}C spectrum the *ipso* carbon connected to the ferrocenyl unit experiences the strongest low field shift (141.42 ppm). Again the hub, spoke and rim carbon nuclei cause the usual separation of the resonances in three distinct chemical shift regions. For the rim and spoke atoms only two signals were observed within the usual shifts of these groups of atoms. The signals for the hub and rim carbon atom between the ferrocenyl unit and the trifluoromethyl group are shifted to the higher field due to their proximity to the electron-withdrawing effect of

the trifluoromethyl groups. The carbon atoms of the trifluoromethyl groups and the corresponding *ipso* carbon atoms are not visible within the spectrum due to their couplings with the fluorine atoms and the consequential loss in intensity.

3.5 Tetraferrocenylated Corannulenes

The tetraferrocenylated corannulene compounds possess C_s-symmetry in solution and also undergo rapid bowl-to-bowl inversion. ^{1}H NMR spectra, as well as ^{13}C NMR spectra, resemble those of the ferrocenylated dimethyl compounds prepared from **44** and are showing similar sets of signals for rim, spoke and hub atoms. Exemplary the ^{1}H NMR spectrum and the ^{13}C NMR spectrum of **52** are presented in Figure 3.5.1 and 3.5.2.

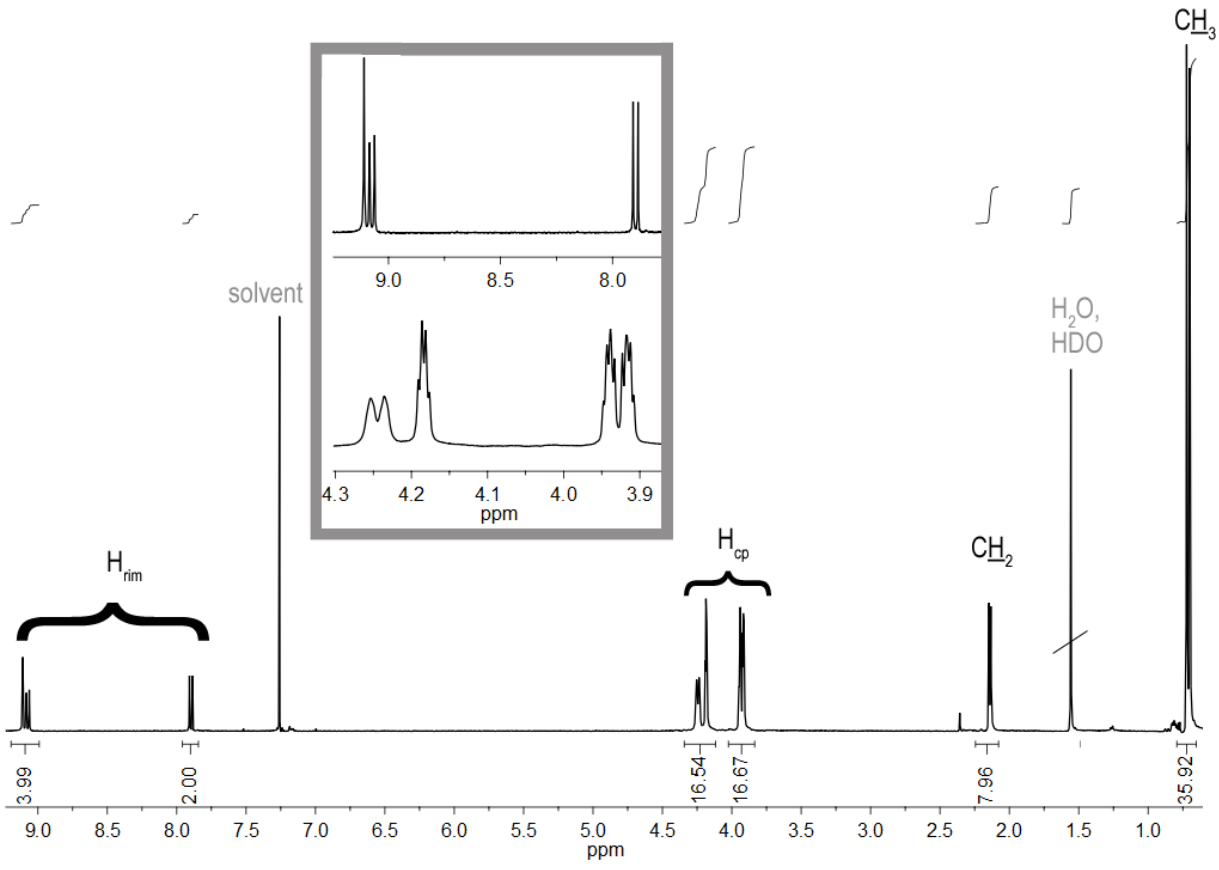

Figure 3.5.1 ^{1}H NMR of **52** recorded at a 400 MHz NMR in $CDCl_3$.

The rim protons of the corannulene moiety give raise to a singlet for the two protons in between the ferrocenyl substituents (9.11 ppm) and AB-type set of signals for the other rim protons at 8.49 ppm with a coupling constant of 8.9 Hz. The ferrocenyl units show a complex set of signals between 4.25 and 3.91 ppm, the doublet-esque signal at 4.23 ppm is broadened and other ferrocene-derived signals show further splittings into *pseudo*-quartets and quintets. Due to the C_S-symmetry in solution respectively pairs of the ferrocenyl substituents show identical resonances in the NMR spectrum. Therefore two singlets for the CH_2-unit of the neopentyl group can be observed at 2.15 and 2.13 ppm and the singlets of the each time 18 methyl groups show singlets at 0.72 and 0.70 ppm.

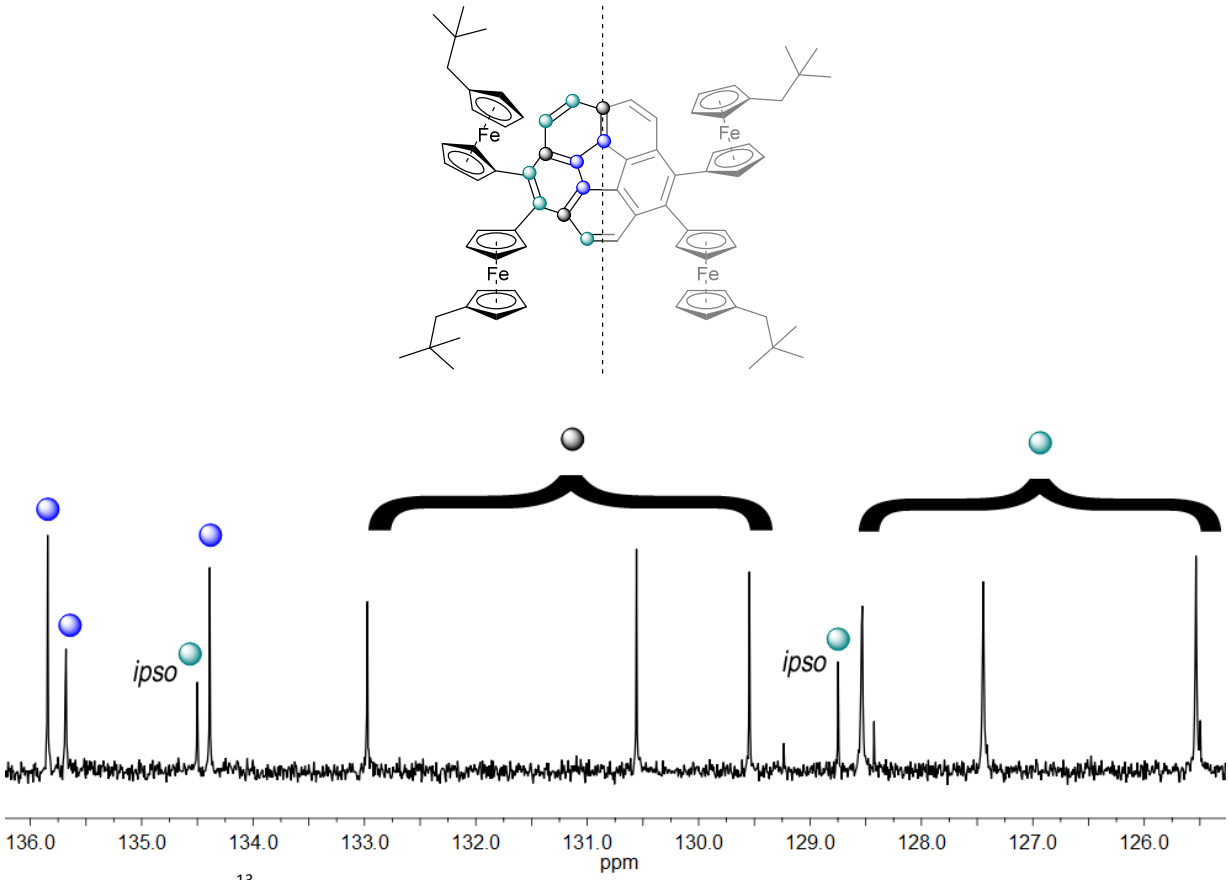

Figure 3.5.2 125 MHz ^{13}C NMR of **52** in $CDCl_3$.

The ^{13}C NMR of **52** exhibits all expected signals for hub spoke and rim atoms, again three for each group. The ipso carbon atoms of the corannulene rim are reduced in intensity. Within this

spectrum the NOE of the aromatic rim carbon atoms are less pronounced than in the atoms described previously. The signals of the ferrocene substituents show similar patterns as previously described at 86.51 – 69.10 (CH cyclopentadienyl, eight signals), 44.88, 44.86 (CH_2), 31.84, 31.82 ($\underline{C}(CH_3)_3$) and 29.45, 29.44 ppm (CH_3) and thus were not displayed graphically.

3.6 Pentaferrocenylated Corannulenes

The fast bowl-to-bowl inversion in solution is still retained for the pentaferrocenylated, C_5-symmetric corannulene derivatives **61** and **63**. In the ^{1}H NMR spectrum only one singlet was observed for all five chemical equivalent on the corannulene rim (Figure 3.6.1).

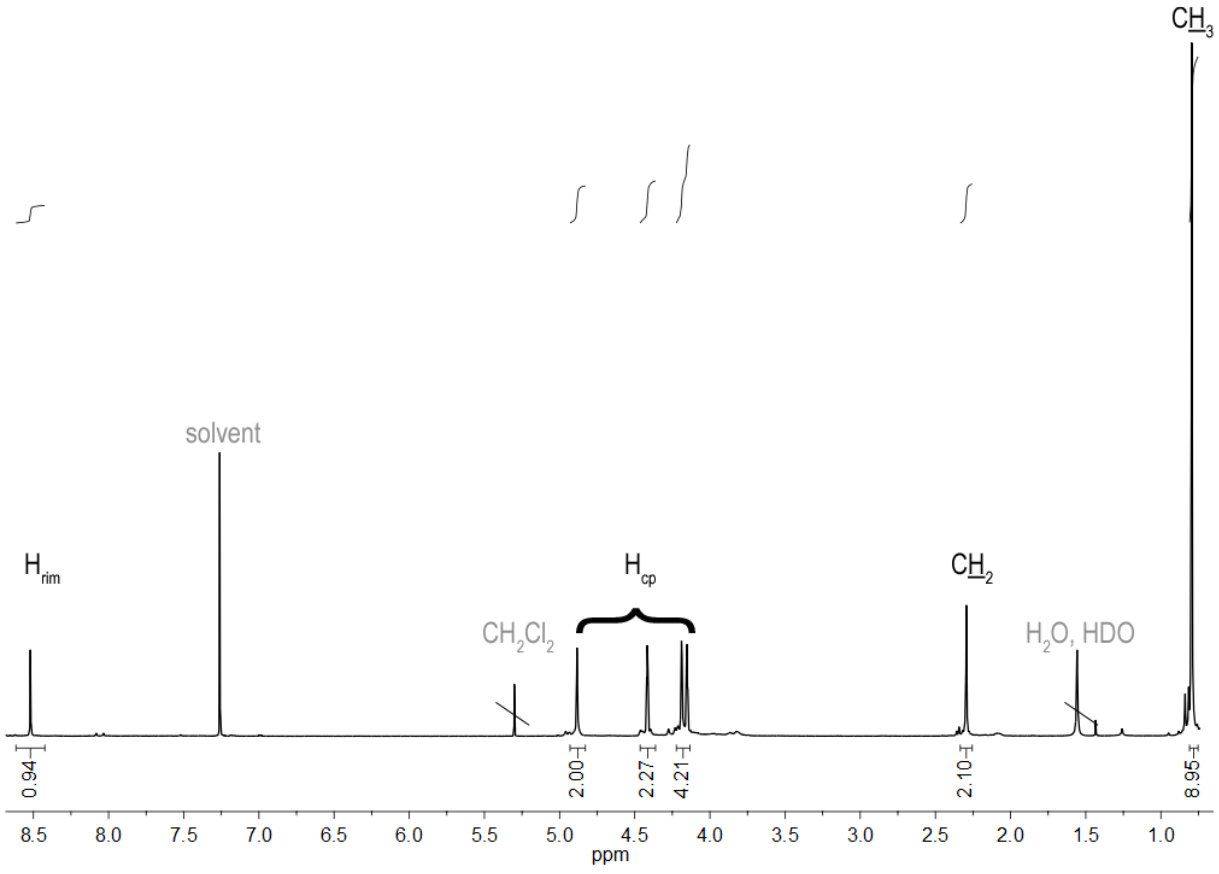

Figure 3.6.1 400 MHz ^{1}H NMR of **63** in $CDCl_3$.

The ferrocenyl group shows the expected signals for mono- and 1,1'-substituted derivatives between 4.00 and 5.00 ppm.

The ^{13}C NMR spectrum of **63** is fairly simple and shows only one signal for each group, the corannulene hub (134.51), spoke (128.90) and rim (125.15 ppm), as well as the *ipso* ^{13}C nuclei at 138.53 ppm according to the five-fold symmetry axis. The chemical shift values of **61** are nearly identical.

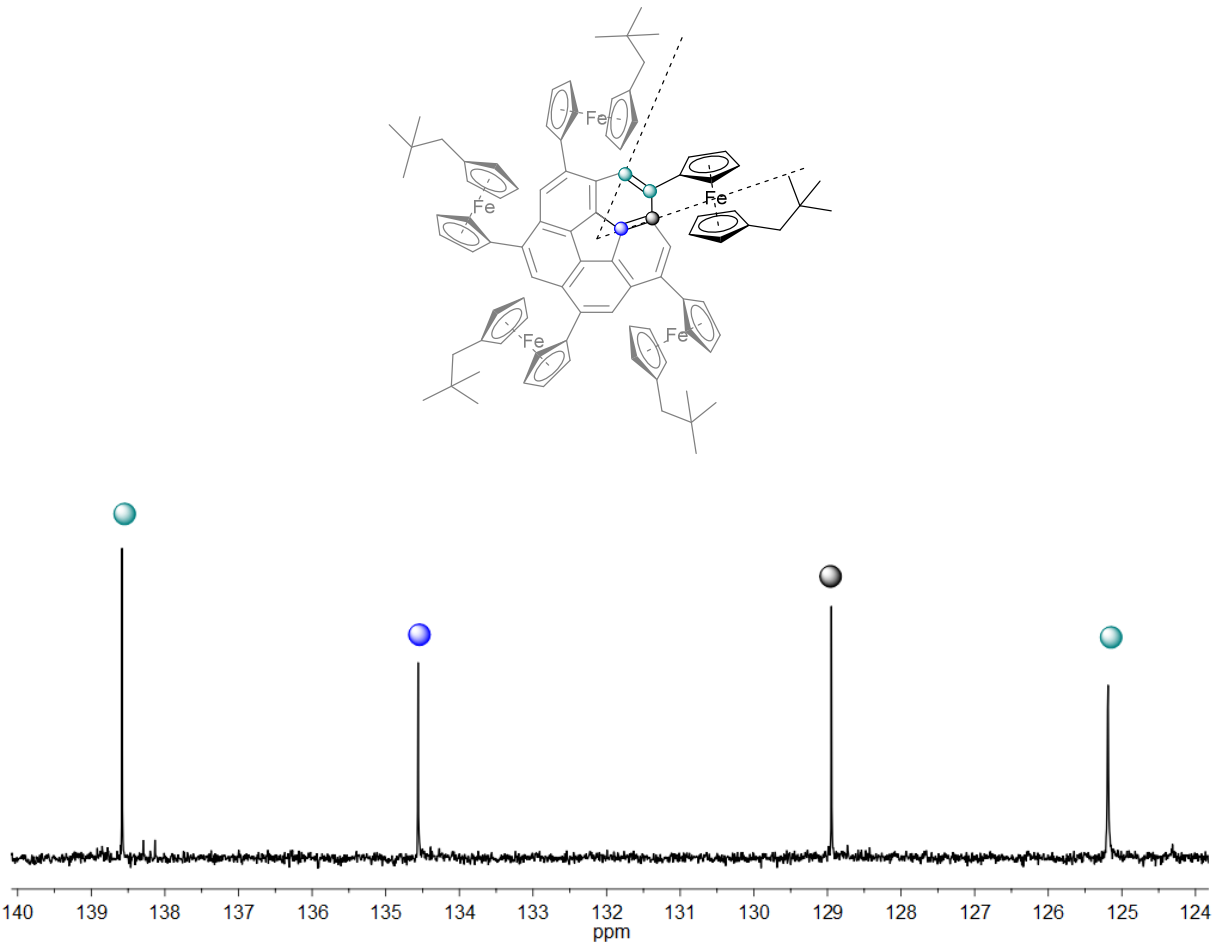

Figure 3.6.2 125 MHz ^{13}C NMR of **63** in $CDCl_3$.

4. Crystallography

In recent years various solid state structures of all kinds of buckybowls were reported.[17,39,84] Single-crystal X-ray analysis offers the direct possibility to obtain an experimental bowl depth for the curved compounds, which is also correlated to the bowl-to-bowl inversion. The stacking motif of buckybowls is highly dependent on the substituents attached and the nature of the buckybowl.[17,58,62] Furthermore several buckybowls were reported with favorable solid-state packings for potential application in organic electronics, such as the columnar stacking of **17** or bis(trifluoromethyl)corannulene.[17c,23,58,85] Therefore it is of great interest to examine the structure in the solid state of the synthesized derivatives, if possible.

4.1 Corannulenylferrocene (22)

22 was crystallized in the form of orange platelets by slow evaporation of a dichloromethane solution. The solid-state structure of **22** was determined by single-crystal X-ray diffraction.[58] It crystallizes in the orthorhombic space group *Fdd*2 with a single molecule forming the asymmetric unit and 16 molecules in one unit cell.

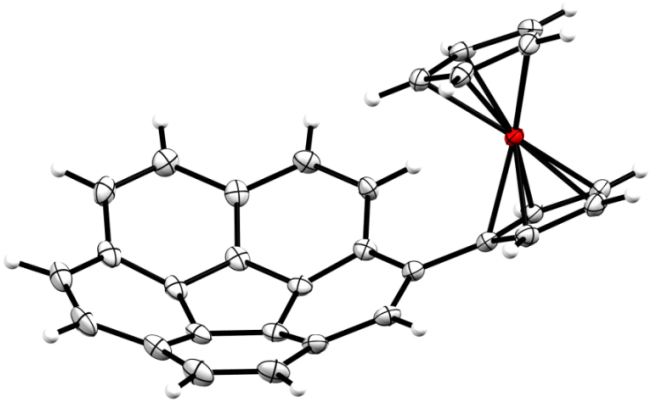

Figure 4.1.1 Single molecule of (*C*)-**22** in Mercury representation, rendered with POV-Ray. Ellipsoids are drawn at 50 % probability. The iron atom is depicted in red, the carbon in light grey and hydrogen atoms in white. The bowl-depth of **22** was found to be 0.864(1) Å.[58]

Table 4.1 Maximum and minimum bond length of **22**.

Bond distances and bowl depth (Å)			
Bond type	**22** (X-ray)	**22** (calc'd)	**16** (X-ray)
Hub bond	1.406(3) – 1.428(3)	1.4130 – 1.4169	1.411(2) – 1.417 (2)
Spoke bond	1.379(3) – 1.387(3)	1.3741 – 1.3774	1.376(2) – 1.381(2)
Flank bond	1.430(3) – 1.468(3)	1.4417 – 1.4622	1.441(2) – 1.450(2)
Rim bond	1.388(4) – 1.404(3)	1.3816 – 1.3898	1.337(2) – 1.387(2)
Cp-rim bond	1.479(3)	1.4772	-
Bowl- depth	0.864(1)	0.861	0.8784(5)[86]

Calculated (wb97xd 6-31g(d,p) for C,H and LANL2DZ for Fe) and experimental bond lengths of **22** in comparison with **16**. Maximum and minimum bond length values of **16** taken from ref. 81 are from two data sets, bowl depth of **16** was taken from ref 86.

All C-C bonds are within the range of common values for corannulene derivatives.[81]

An official stereo descriptor system for the absolute configuration of chiral buckybowls has not yet been established. Two systems for this description are used, the first one is based on the nomenclature of fullerenes and the second was suggested by Scott et al.[87] Here the system

based on fullerene nomenclature was applied.[88] The assignment of a descriptor to the chirality is done by looking at the convex face of a buckybowl and tracing the path of numbering of the carbon atoms starting from the hub carbons. If the path describes a clockwise direction, the configuration is expressed by the descriptor (*C*). In contrast, if the path describes an anticlockwise direction, the descriptor is (*A*). For **22** both enantiomers are possible through the bowl-to-bowl inversion in solution and are found in the solid state structure.

The cyclopentadienyl rings of the ferrocene unit show a nearly perfectly eclipsed conformation (1.91° deviation) and the ferrocene unit is in *endo* conformation towards the open face corannulene bowl.

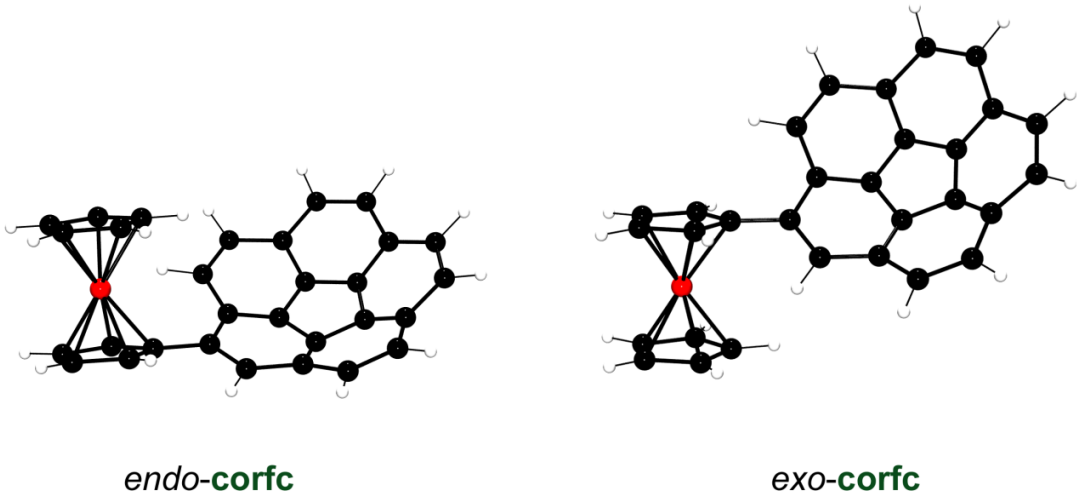

Figure 4.1.2 Calculated **22** bearing the ferrocene unit in *exo* (left) and *endo* (right) conformation using using wb97xd 6-31g(d,p) for C,H and LANL2DZ for Fe.

Energy differences in the gas phase between *endo* and *exo* position of the ferrocene unit were determined by calculations, which resulted in a neglectable difference of 0.1 kcal*mol^{-1} in favor for the *endo* conformation which is also found in the solid state structure.

The substituted cyclopentadienyl ring of the ferrocene unit is about 20.8° (24.70 calculated) out of plane with the attached six-membered ring of the corannulene substituent. The bowl depth of **22** is with 0.864(1) (calc'd: 0.861) Å only slightly flatter compared the experimental bowl-depth of **16** (0.8784(5) Å).[86]

The overall solid-state packing is dominated by CH···π interactions, similar to the one of **16**. These interactions proceed from a corannulene rim hydrogen atom to the convex surface of an adjacent corannulene moiety ranging from 2.8 to 3.2 Å.

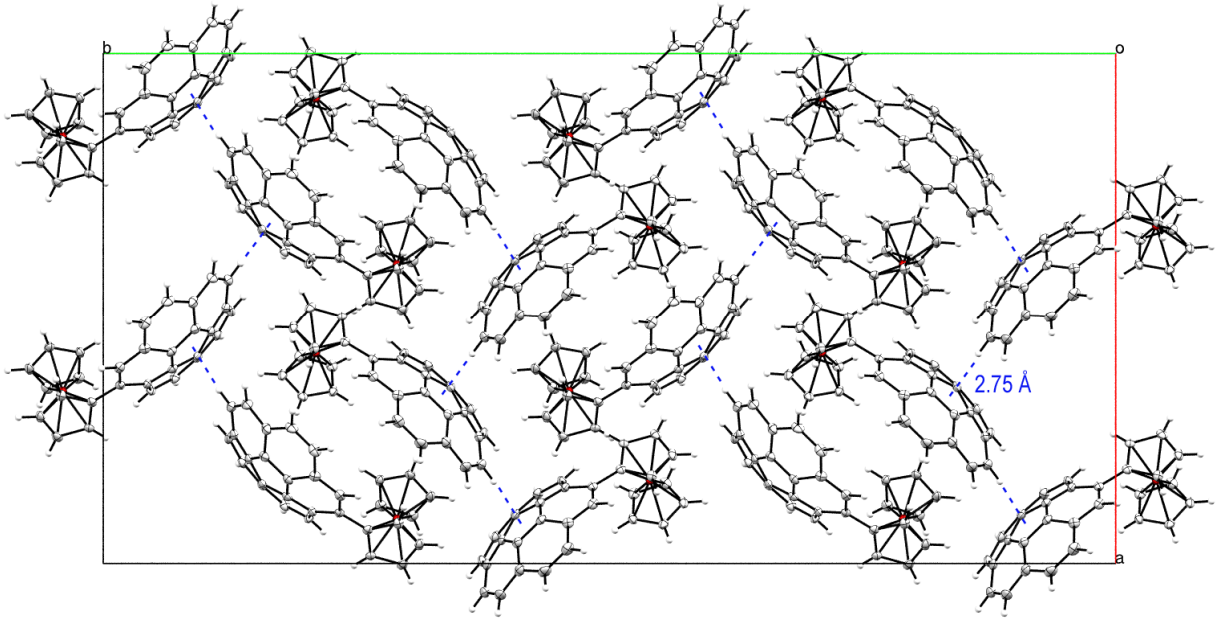

Figure 4.1.2 Solid-state packing structure of **22**. The shortest C–H···π contact of 2.75 Å between a corannulene rim proton and the center of the five-membered ring of an adjacent corannulene unit, was visualized in blue. View along the crystallographic *c* axis.

Weak interactions occur from the corannulene open face bowl towards an oppositely facing cyclopentadienyl ring. The rim region of corannulene possesses a less negative electrostatic potential relative to the hub region and thus facilitates this type of interaction.[86] Every molecule in the orthorhombic unit cell acts as both a donor and an acceptor of at least one C-H···π contact.

4.2 Sumanenylferrocene (23)

23 crystallizes in the monoclinic space group $P2_1/c$ with one molecule in the asymmetric unit and four molecules in the unit cell. Bond lengths similar to those of **17** were observed.[62]

Noteworthy, like observed for **17**, a significant bond alternation was observed in the hub of the central six-membered ring. The bonds connected to six-membered rings are slightly shortened, while the bonds connected to five-membered rings are elongated compared to benzene.

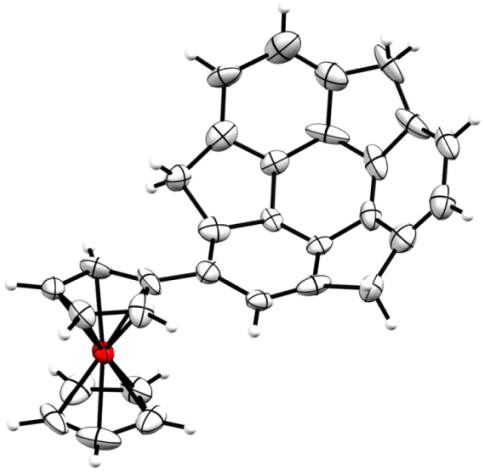

Figure 4.2.1 Single molecule of **23** in Mercury representation, rendered with POV-Ray. Ellipsoids are drawn at 50 % probability. (*C*)-**23** is displayed above.[62]

Table 5.2 Maximum and minimum bond length of **23**, **23** calculated and **17** in comparison.

Bond distances and bowl depth (Å)			
Bond type	**23** (X-ray)	**23** (calc'd)	**17** (X-ray)
Hub bond	1.340(9) – 1.43(1)	1.3790 – 1.4350	1.4830(2) – 1.4292(3)
Spoke bond	1.39(1) – 1.463(8)	1.3937 – 1.3949	1.3954(2) – 1.3956(2)
Flank bond	1.34(1) – 1.415(9)	1.3910 – 1.4004	1.3991(2) – 1.3996(3)
Rim bond	1.460(7) – 1.54(1)	1.4253 – 1.4253	1.4309(2)
Benzylic-bond	1.500(9) – 1.57(1)	1.5465 – 1.5483	1.5472(3) – 1.5482(3)
Cp-rim bond	1.526(9)	1.4748	-
Bowl-depth	1.1563(3) Å	1.1537	1.11

Calculated in (wb97xd 6-31g(d,p) for C,H and LANL2DZ for Fe). Bond length and bowl depth values of **17** are taken from ref 24.

The cyclopentadienyl rings show a deviation of 21.9° from a perfectly eclipsed conformation. In contrast to the corannulenyl compound **22** the attached ferrocene is in *exo* conformation with

respect to the sumanenyl substitutent. Gas-phase calculations predicted an energy difference of 2.5 kcal*mol^{-1} in favor for the *endo* conformation. The difference in energy is very small and crystal packing effects probably account for the formation of the less favored *exo* **23**. The bowl depth of **23** (1.16) increases slightly upon the introduction of the ferrocenyl group to the rim of the molecule (1.11 Å for **17**) as seen from the X-ray data, which is in accordance with the calculated bowl depth of 1.15 Å.

Unsubstituted **17** shows a perfectly columnar solid state packing structure.[23a] The introduction of the bulky ferrocene unit to the sumanene rim changes the structure drastically. A unit cell dominated by intermolecular C–H···π interaction is observed. These include a 3.11 Å contact of the *endo* hydrogen atoms of the benzylic carbons to the center of a six-membered ring above. Also present is an even shorter contact (2.90 Å) of the corresponding *exo* hydrogen atom to a six-membered ring of a molecule pointing downward (convex bowl) and the fairly short contact (2.53 Å) of one hydrogen atom of the ferrocene pointing to the bowl of an adjacent molecule.

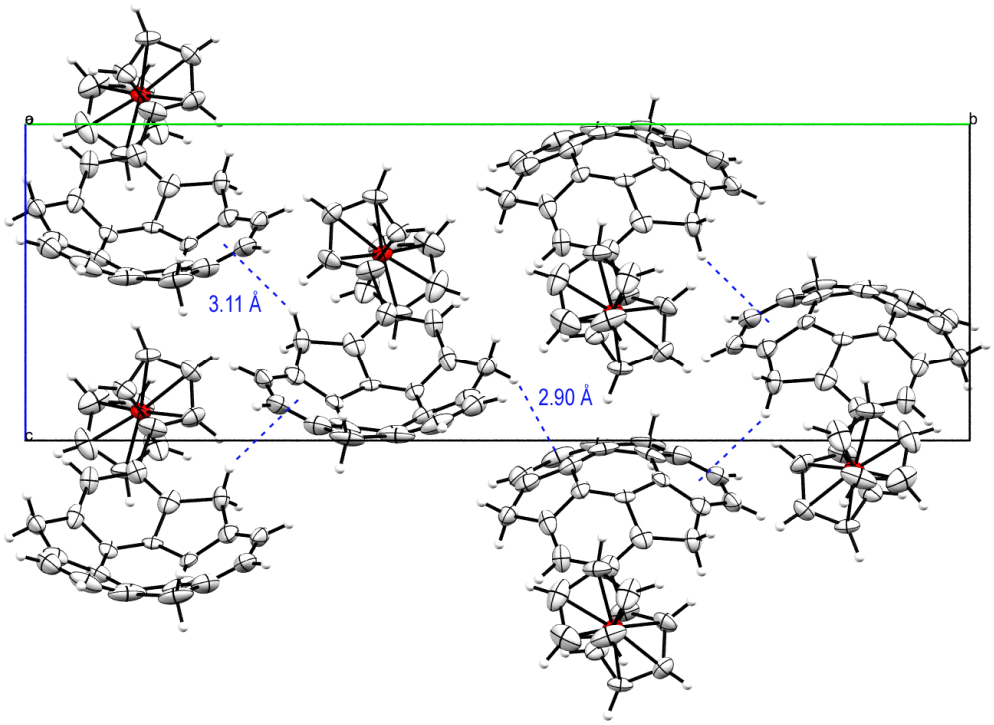

Figure 4.2.2 Solid state packing structure of **23** along the crystallographic *a* axis.

No π-stacking occurs between the molecular bowls. In contrast to the structure of **22** not only C–H···π interactions are present within this structure but an unprecedented staircase-like arrangement is formed between identical enantiomers in the structure by approach of the unsubstituted five-membered cyclopentadienyl ring to the open face of the next buckybowl along the crystallographic *a* axis via π···π interactions (3.70 Å).

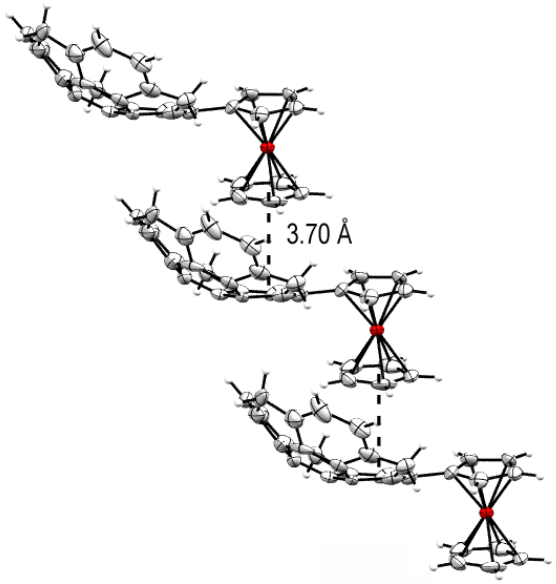

Figure 4.2.3 Staircase-like arrangement of **23**. The shortest π···π contact is depicted in black.

4.3 1-Corannulenyl-4-ferrocenylbenzene (26)

Unlike previously synthesized corannulenylferrocenes **26** is light orange in colour. It crystallizes in the monoclinic space group $P2_1$ with two molecules in the asymmetric unit. Bowl depths of the corannulene moieties of both molecules (0.832 and 0.895 Å) are at an average within the range of unsubsituted **17** (0.87 Å) and in accordance with the calculated bowl-depth, see table 5.2. Interestingly, while on one molecule the ferrocenes is in *exo* position regarding the corannulene bowl, the other ferrocene is in *endo* position. By introduction of the phenyl spacer, the differences in energy between the *endo* and *exo* position are probably neglectable.

The cyclopentadienyl rings of both molecules are only 2.4° and 4.8° distorted from a perfectly eclipsed conformation of the cyclopentadienyl rings within a ferrocenyl unit.

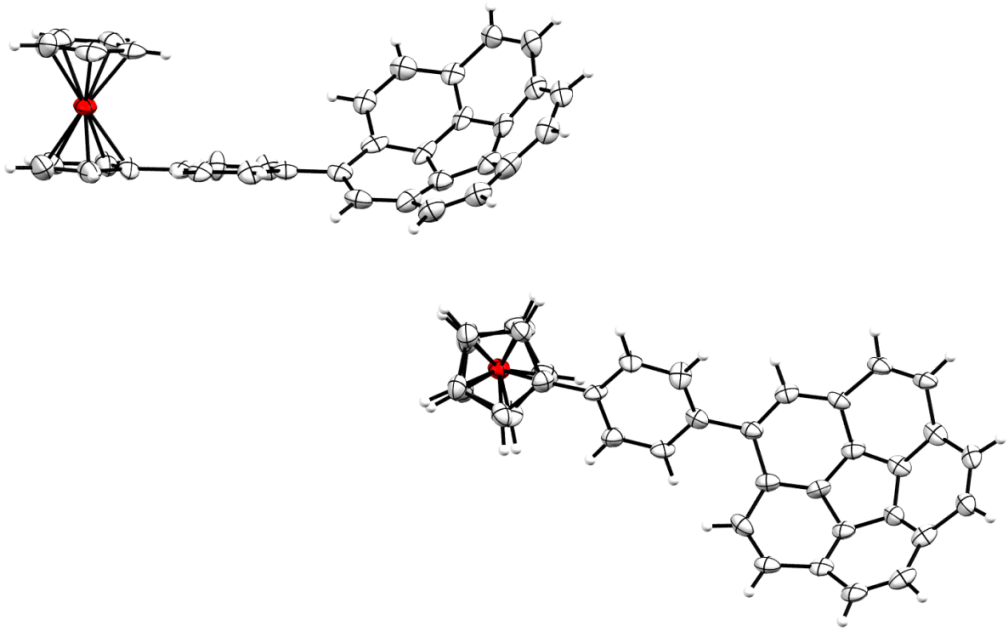

Figure 4.3.1 Asymmetric unit of **26** in Mercury representation, rendered with POV-Ray. Ellipsoids are drawn at 50 % probability. Bowl depths are 0.8951(1) for *endo*-(*C*)-**26** and 0.8322(1) Å for *exo*-(*A*)-**26**.

Table 4.3.1 Maximum and minimum bond length of *endo*- and *exo*-**26**.

Bond distances and bowl depth (Å)			
Bond type	*Endo*-**26**	*Exo*-**26**	*Exo*-**6** calc'd
Hub bond	1.40(1) – 1.43(1)	1.40(1) – 1.42(1)	1.4140 – 1.4159
Spoke bond	1.37(1) – 1.38(1)	1.36(1) – 1.39(1)	1.3758 – 1.3771
Flank bond	1.42(1) – 1.47(1)	1.43(1) – 1.49(1)	1.4428 – 1.4590
Rim bond	1.35(1) – 1.42(1)	1.36(1) – 1.37(1)	1.3816 – 1.3889
Bowl-depth	0.8951(1)	0.8322(1)	0.8747

Comparison of the solid state structure with the calculations (wb97xd 6-31g(d,p) for C,H and LANL2DZ for Fe).

The torsion angle between the phenyl and the cyclopentadienyl ring differs for both molecules. In the upper molecule in Figure 5.3.1 both are nearly perfectly in plane (deviation 2.31°) in the

lower molecule the torsion angle amounts to 29.15° (32.33° calculated). In both molecules the phenyl spacer is not in plane with the connected six-membered ring of the corannulene moiety (upper molecule 31.71°, lower molecule 35.93°, 42.80° calculated) which militates against an extended conjugated π-system reaching from the corannulene moiety to the ferrocene unit. The cyclopentadienyl rings of both ferrocenes are nearly perfectly eclipsed.

The molecular packing of corannulene, as previously shown, for example in the case of corannulenlyferrocene and 1,1'-dicorannulenylferrocene can be greatly influenced through ferrocene substitution.[58,62]

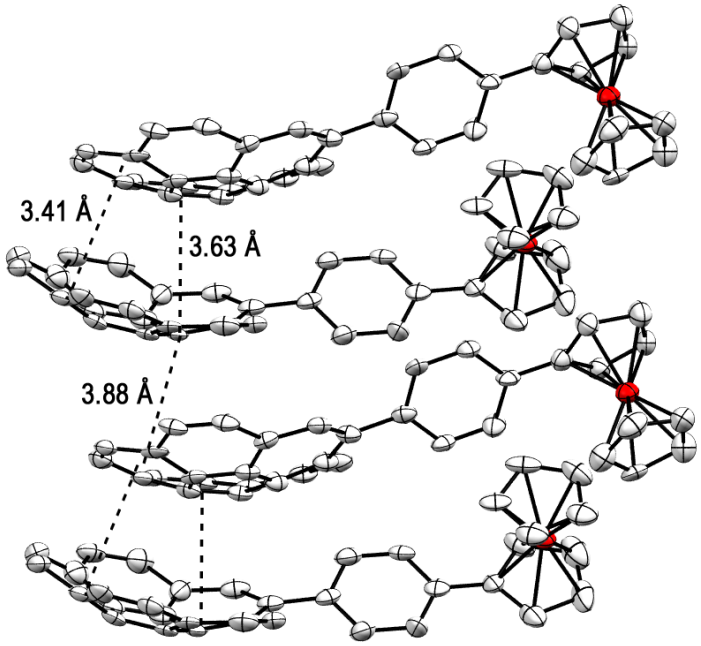

Figure 4.3.2 Packing of **26** along the crystallographic *a* axis.

The structure is dominated by CH···π interactions but is also showing a remotely columnar arrangement with slipped stacking along the crystallographic *b* axis. π···π Interactions with alternating distances of 3.41 and 3.88 Å can be observed within one strand of bowls (centroid-to-centroid distances of two six-membered rings). The strands of molecules interact *via* CH···π contacts. The closest CH···π interactions are: 2.81 Å between a proton of the phenyl spacer and an unsubstituted cyclopentadienyl ring of a neighboring molecule and 2.98 Å between a rim

proton of the corannulene moiety and an unsubstituted cyclopentadienyl ring of a ferrocenyl substituent of an adjacent molecule.

4.4 1,1'-Dicorannulenylferrocene (33)

33 crystallizes as red platelets by slow evaporation of a pentane/dichloromethane/toluene mixture in the orthorhombic space group $Pna2_1$.[58] Due to their thin nature the platelets were submitted to synchrotron measurements. Two molecules are displayed in the asymmetric unit. A deformation of the ferrocene sandwich structure is present in both enantiomers, with a tilt angle between the iron center and the center of the cyclopentadienyl ring averaging to 5.5° (1.2° for the monocorannulenyl compound **22**). The cyclopentadienyl rings are in eclipsed conformation.

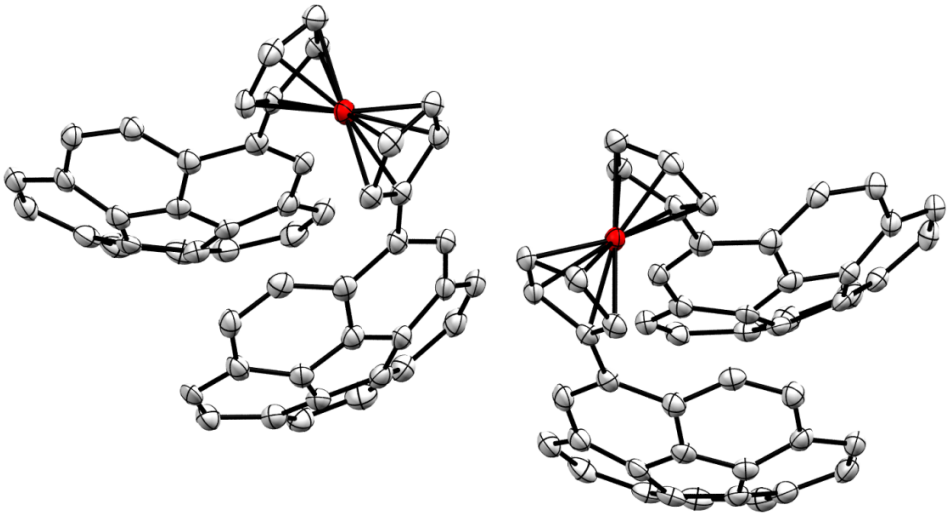

Figure 4.4.1 Asymmetric unit of **33** displayed with Mercury and rendered with POV-Ray. Ellipsoids were drawn at 50 % probability. Hydrogen atoms were omitted for reasons of clarity. (*A,A*)-cor2fc and (*C,C*)-**33** are present in the asymmetric unit.

Both corannulene substituents are arranged on one side of the ferrocene molecule in a convex-concave fashion offset π-stacking of approximately 3.8 Å, where the upper bowl is slightly tilted.

The bowl-depths of the corannulene substituents are in average 0.878 Å (molecule 1 upper bowl 0.899, lower bowl 0.841, molecule 2 upper bowl 0.889, and lower bowl 0.884 Å). It can be observed that the upper bowl is a little deepened in comparison with plain corannulene, while the lower bowl is flattened. The intramolecular bowl-to-bowl distances are 3.58 and 3.60 Å.

The overall solid-state packing structure is best described by: close intermolecular CH···π contacts between the hydrogen atoms of corannulene and a six-membered ring of the bowl of another column of stacked molecules (approx. 2.83 Å to the center of the ring) and intermolecular π-stacking between the double-decker alignments of **33**.

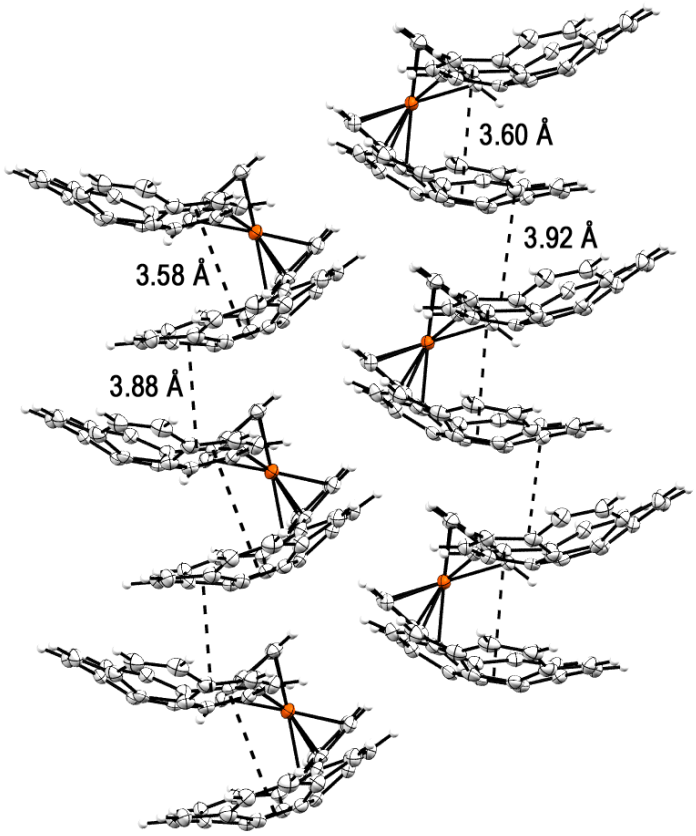

Figure 4.4.1 Metal-organic nano-wire like structure of **33** with intra- and intermolecular π···π contacts.

The two molecules present in the asymmetric unit form π···π contacts with an identical enantiomer along the crystallographic *c*-axis. The different enantiomers are interacting *via* C-H···π contacts with each other. It seems favorable to avoid perfect columnar

stacking to facilitate C-H···π contacts by tilting the bowls. Again, the small differences in the electrostatic potential of the rim guide direction to interaction with the π-basicity of the central five-membered ring. In contrast to other stacked bowl-shaped molecules, neighboring columns show identical bowl directions.[64]

4.5 1,1'-Disumanenylferrocene (34)

34 crystallizes in the monoclinic, centrosymmetric space group $P2_1/n$.[62] The sumanene bowls as well as the cyclopentadienyl rings of the ferrocene moiety are in eclipsed conformation. In the columnar solid-state structure of sumanene itself the sumanene molecules are arranged in an eclipsed fashion where the benzylic positions are above a six-membered ring.

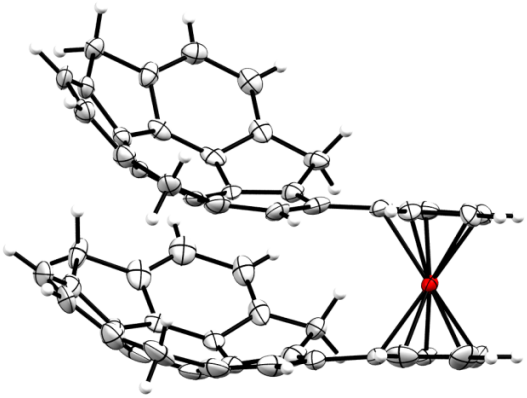

Figure 4.5.1 Single molecule of **34** in Mercury representation. Ellipsoids are drawn in 50% probability. The bowl-depths are 1.1431(0) for the upper and 1.0915(0) Å for the lower bowl.

The tilt angle between the two planes of the cyclopentadienyl rings is 3.9(2)°, which surprisingly does not differ from 3.9(3)° for **23**. Due to the centrosymmetric space group two different enantiomers are present in the unit cell corresponding to (*A*,*A*)-**34** and (*C*,*C*)-**34.** The bowl-depth of the sumanenyl substituents is 1.143 for the upper bowl which is again slightly deepened compared to **17** and 1.091 Å for the lower bowl, which is slightly flatter.

Compared to **23** the solid-state arrangement of **34** drastically changed through the introduction of a second sumanene substituent. Though being a fellow buckybowl and despite the similar structural motif, the crystal packing also differs extensively from the columnar structure of the corresponding corannulene compound **33**. For reasons of clarity and comprehensibility the structure of **34** is best described by two features: the formation of a dimer and the interaction of these groups of dimers with each other.

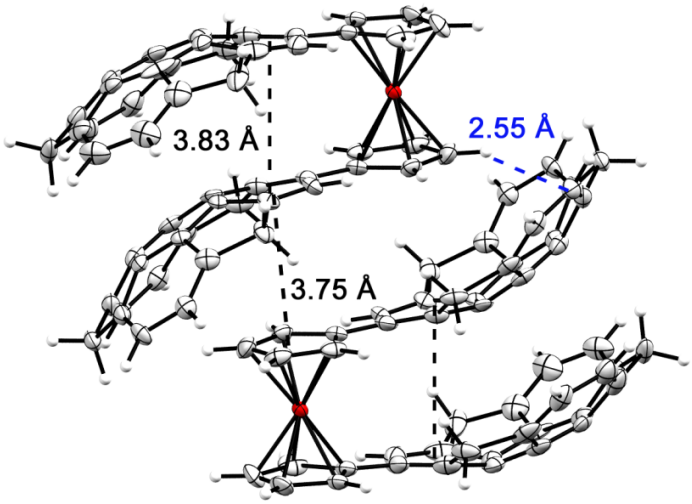

Figure 4.5.2 Orientations of **34** in the solid state, depicted as the formation of a head-to-tail dimer. CH···π contacts are displayed in blue, π···π contacts in black.

Within a dimeric unit (Figure 5.5.2), a head-to-tail alignment is observed where the staggered bowls are hosting the ferrocene unit of its counterpart. This ligand-to-bowl π-stacking occurs at a distance of 3.83 Å and is supported by a short C–H···π contact from the inbound cyclopentadienyl ring of only 2.55 Å to the center of a five-membered ring.

The dimeric units, being perpendicular to each other (Figure 5.5.3), give rise to the possibility of C–H···π interactions from a ferrocene to the outside of a close-by bowl within short distances of up to 2.83 Å. These are considered to be highly favorable interactions due to the negative electrostatic potential at the outside of the molecular bowl.[89]

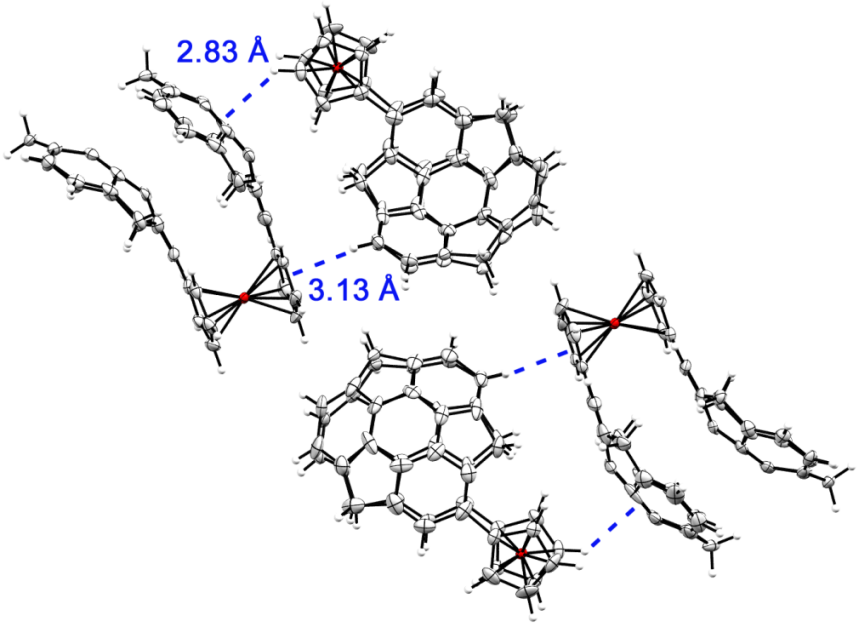

Figure 4.5.2 CH···π contacts within the unit cell of **34**.

4.6 1,2,5,6-Tetrakis(4-ferrocenylphenyl)corannulene (53)

53 crystallizes in the triclinic space group *P*1 from toluene solution by layering with isopropyl alcohol. Two molecules **53** and additionally three toluene solvent molecules form the asymmetric unit. The bowl depths are slightly shallower than the one of unsubstituted **16** (0.837 and 0.793 Å (0.820 Å calculated)), as a result of the steric strain caused by the phenyl groups.[90] All ferrocenyl substituents are in *exo* position to the corannulene bowl. On both molecules the cyclopentadienyl rings are nearly in plane with the phenyl spacer, but not in plane with the attached six-membered rings of the corannulene moieties. So again no considerable dislocation of the π-system can be assumed.

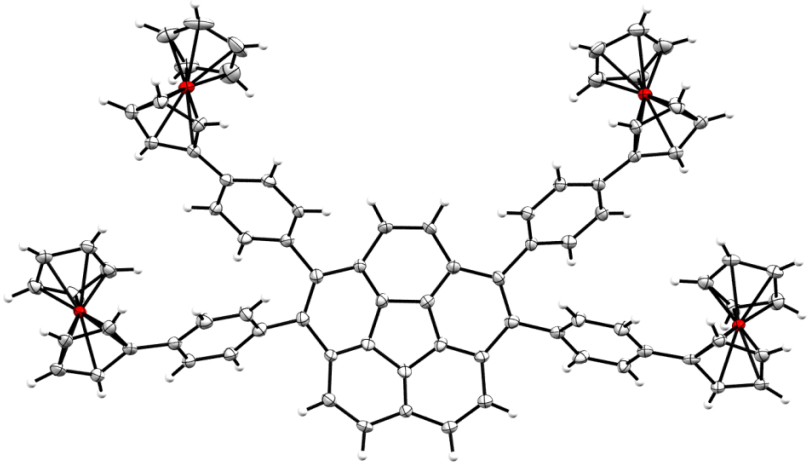

Figure 5.6.1 Single molecule of **53** in Mercury representation rendered with POV-Ray. Ellipsoids are drawn in 50% probability.

Table 4.2 Maximum and minimum bond length of **53** from the X-ray structure in comparison with the calculation.

Bond distances and bowl depth (Å)			
Bond	Molecule a	Molecule b	Calc'd
Hub	1.401(7) – 1.424(7)	1.406(8) – 1.420(7)	1.4161 – 1.4196
Spoke	1.359(8) – 1.384(8)	1.377(7) – 1.396(7)	1.3834 – 1.3861
Flank	1.443(7) – 1.473(7)	1.437(8) – 1.472(7)	1.4512 – 1.4660
Rim	1.381(8) – 1.411(7)	1.370(8) – 1.418(8)	1.3947 – 1.4178
Bowl-depth	0.7931(1)	0.8373(1)	0.8203

Calculations in B3LYP 6-31g.

Two molecules of **53** surround one toluene molecule in a nutshell-like arrangement. The toluene molecule within the cavity is located in a distance of 4.04 and 3.80 Å to a six-membered ring of the corannulene moiety (see Figure 5.6.2). Two additional toluene molecules are located on the outside of this arrangement and are within distance of approximately 3.20 Å to the corannulene rim, located on the same side of one molecular sandwich.

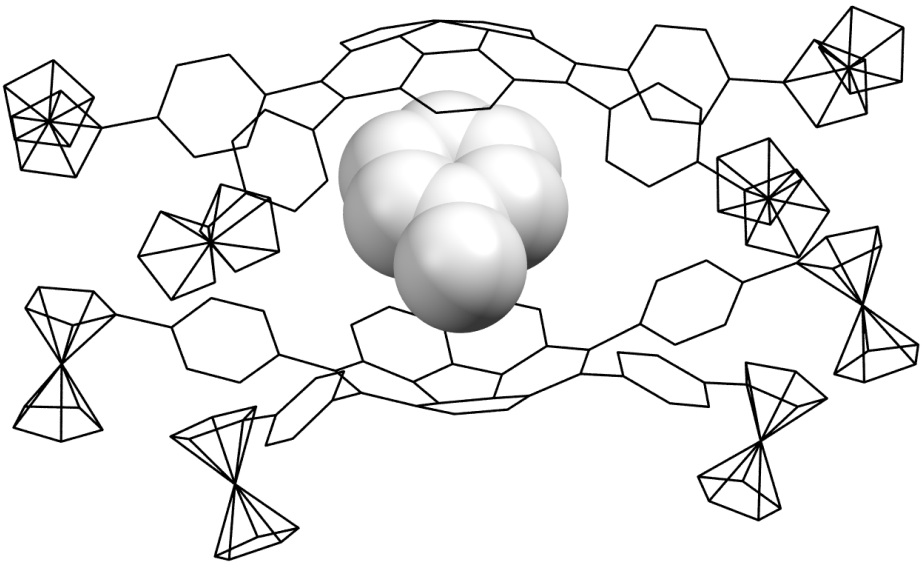

Figure 5.6.2 Mercury representation rendered with POV-Ray of the nutshell-like arrangement of two molecules of **53** surrounding one toluene molecule (spacefilling model). The two outer toluene molecules and protons are omitted for reasons of clarity.

The overall packing motif does not show a columnar array. The “nutshell” motif repeats itself in a slightly shifted packing, along the crystallographic *a* axis. This arrangement is supported by C-H···π contacts of the ferrocene groups between the “nutshell” and CH···π interactions between the phenyl spacer and the outer corannulene bowl of an adjacent dimer. Rim protons of the corannulene bowl also show C-H···π contacts to the centre of the phenyl spacer within the range of 3.04 Å. Along the crystallographic *b* axis the main contact is the CH···π interaction of an outer toluene molecule with the next dimer formation (3.12 Å) along this axis. Along the crystallographic *c* axis, only an overlap of one ferrocene substituent with an adjacent formation can be observed. The CH···π contact of the two unsubstituted cyclopentadienyl rings is 3.13 Å.

5. UV/Vis measurements

All ferrocenylcorannulenes are strongly colored, ranging from purple to orange, depending on the spacer and the ferrocene attached. To quantify these differences in color and thus different optical properties, UV/Vis measurements were conducted. Reference compounds **1** and **16** were measured individually, as depicted in Figure 5.1.

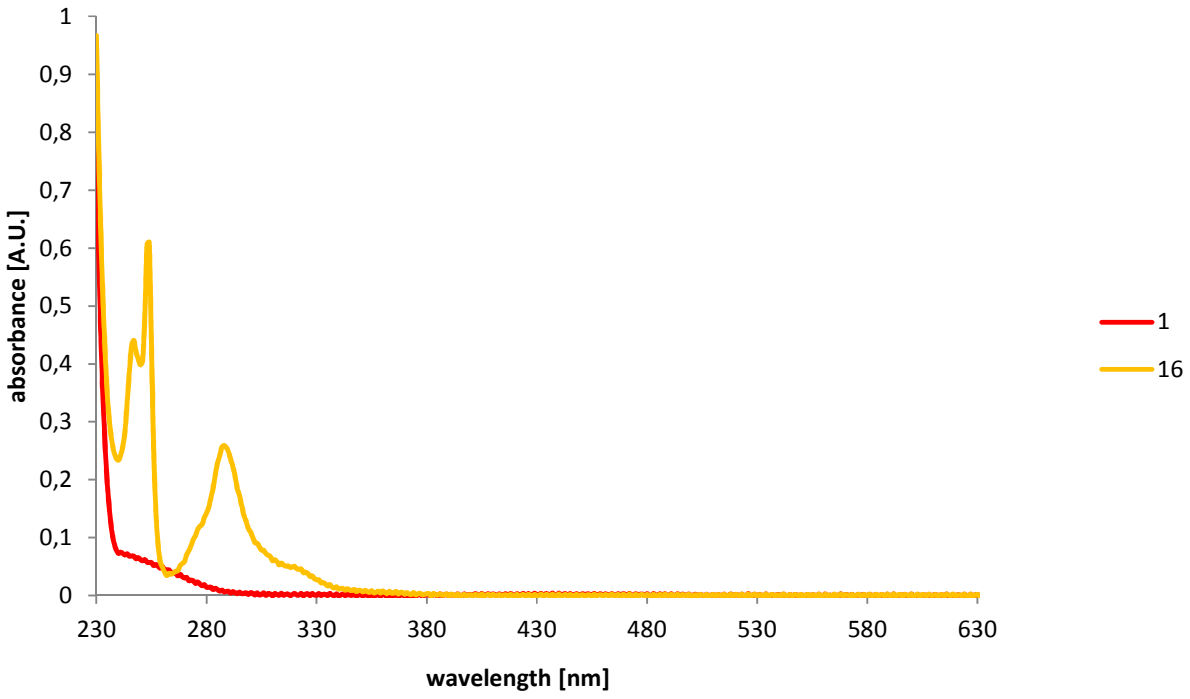

Figure 5.1 UV/Vis spectrum of **1** ($1*10^{-5}$ M) and **16** ($1*10^{-5}$ M) in dichloromethane.

Although **1** possesses a strong color in the solid state, it does not show strong absorbances,[91] the absorbance at 437 nm is very weak in comparison to the absorption maxima of **16**. Thus UV/Vis maxima mainly arise from the corannulene core itself or descend from intramolecular charge transfer (ICT) between the corannulene core and the attached ferrocene moieties.

16 shows absorption maxima at 288 nm with a shoulder starting at approximately 270 nm and further maxima 254 and 247 nm (lit. 320 (shoulder), 288 and 254 nm)[92] origination from π→π* transitions.[64]

To compare the influence of the different spacers and ferrocenes on the electronical properties of the corannulene core UV/Vis measurements of all monobuckybowl substituted ferrocenes (for colors see Figure 5.2) were conducted, depicted in Scheme 5.3. It has to be taken into account that the change of symmetry alone (C_5 to C_1) already influences the electronic structure and thus properties of the corannulene core.

Figure 5.2 UV/Vis samples $1*10^{-5}$ M in dichloromethane. From left to right**: 30** (ethynyloctamethylferrocene), **22** (directly substituted; $2*10^{-5}$ M), **32** (butadienyl), **31** (vinyl), **29** (ethynyl), **41**, **25** (directly substituted, neopentyl compound) and **26** (phenyl).

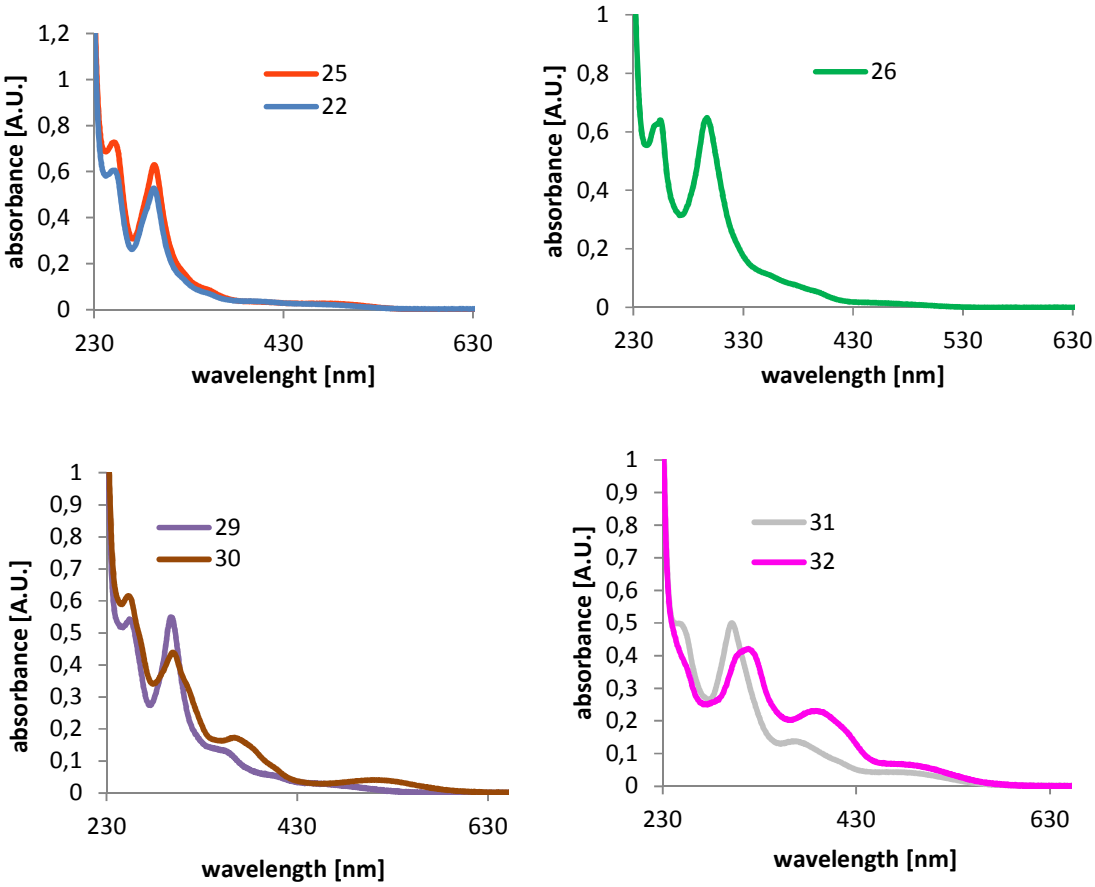

Scheme 5.3 Absorptions of monocorannulenylferrocenes $1*10^{-5}$ M in dichloromethane.

All monosubstituted compounds show strong absorption maxima between 430 and 230 nm, as well as tailing into the visible region of the spectra. The main absorption maxima of **22** (294, 250 nm) and **25** (293, 251), both with a tailing into the visible region, are identical within the range of error, confirming the neglectable influence of the neopentyl group on the electronic structure of the molecule. Shape of both spectra is similar to the spectrum of **16**, though the maxima at higher wavelength experience a bathochromic shift, while the maxima at lower wavelength stay nearly identical. Giving an overview of the different spacers, the bathochromic shift increases in the order of none < phenyl = ethynyl < vinyl < butadienyl.

The larger red shift of butadienyl-bridged **32** can be explained by the extended π-system and the good delocalization as exemplarily shown by the HOMO (Figure 5.4).

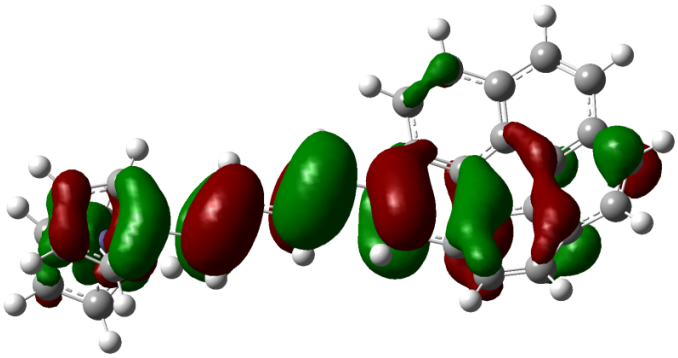

Figure 5.4 Calculated HOMO of **32** using wb97xd 6-31g(d,p) for C,H and LANL2DZ for Fe. Plotted with an isovalue of 0.02.

In comparison the absolute size of other ferrocenylcorannulenes is smaller; thus they possess a smaller π-system. Phenyl-bridged **26** is similar in size but possesses a less favorable molecular geometry (compare the solid state structure of 53 in Chapter **4.6**). The torsion angle between the cyclopentadienyl ring, the phenyl spacer and the connected six-membered ring of the corannulene unit might lead to an inferior overlap of the HOMO orbitals (Figure 5.5).

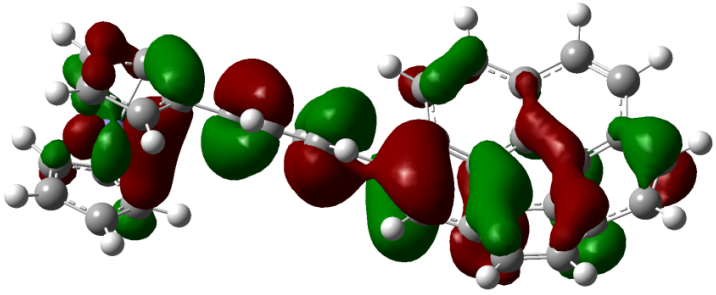

Figure 5.5 Calculated HOMO of **26** using wb97xd 6-31g(d,p) for C,H and LANL2DZ for Fe. Plotted with an isovalue of 0.02, showing the impact of the unfavorable molecular geometry on the HOMO orbital.

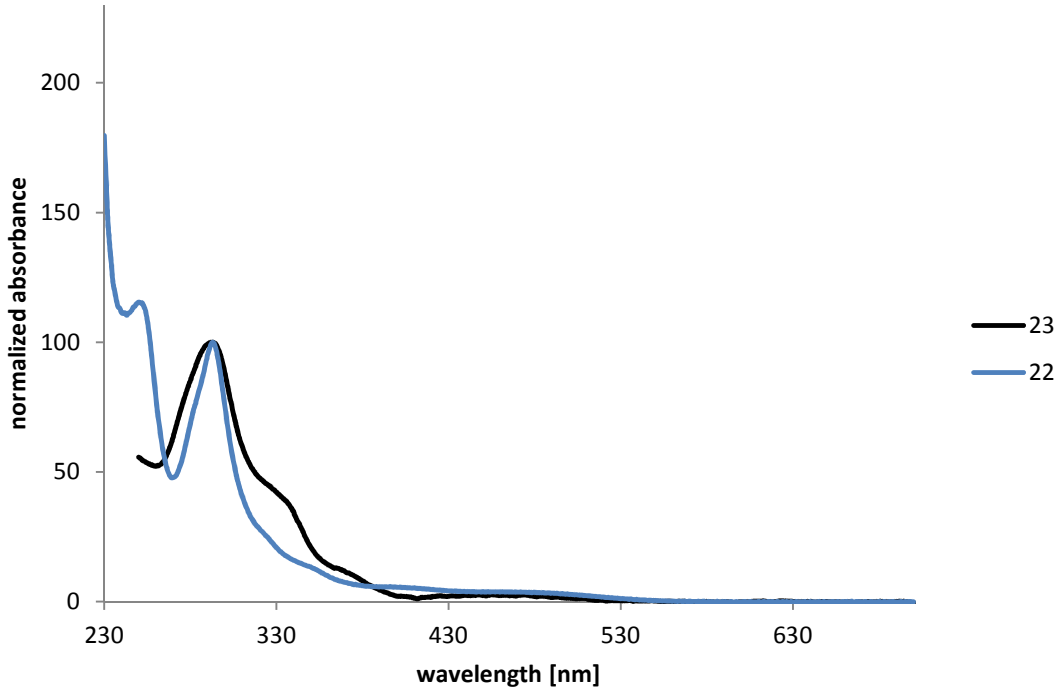

Figure 5.6 Normalized UV/Vis spectrum of **22** and **23** in dichloromethane.

Comparing the electronic spectra of **22** and **23** (294 or 291 nm), no relevant difference of the main absorption maxima could be discovered; only the shape of the maximum is broadened for the sumanene derived compound and shoulders or further absorptions can be found at 368 and 326 nm. The absorption maximum of unsubstituted **17** in dichloromethane was reported to be at 278 nm, thus a clear bathochromic shift can be observed. Weak CT bands can be observed at approximately between 430 and 530 nm for both compounds.

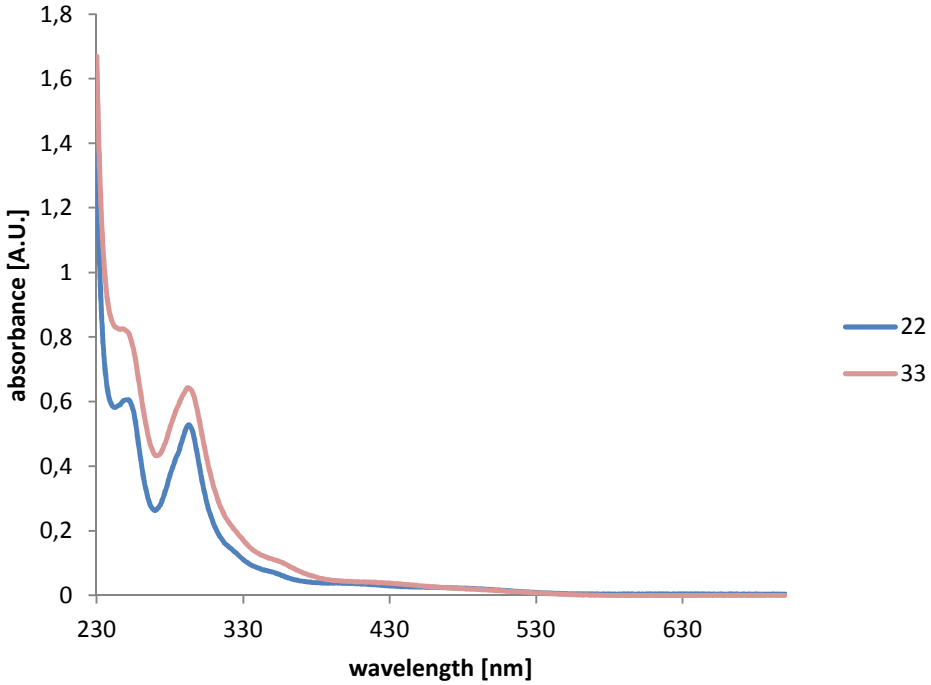

Figure 5.7 Comparison of the UV/Vis spectra of **22** and dicorannulenyl compound **33** $1*10^{-5}$ M in dichloromethane.

The comparison of mono corannulenyl compounds **22** with dicorannulenyl compound **33** shows that the spectra of both compounds show absorptions at nearly identical wavelength. The absorption of **33** is a little higher than the one of **22** which might originate from the larger π-surface.

Assuming that the bowl-to-bowl inversion of buckbowl **16** and its derivatives is frozen on the UV/Vis time scale it was observed by other groups that the amount, as well as the substitution pattern of substituents, influence the electronic spectra of corannulene derivatives. Wu *et al*. examined multiethynyl corannulenes empirically and found that a higher count of substituents leads to longer emission wavelengths.[64] In the publication of their push-pull corannulenes, Diederich *et al*. reported that the exact positioning of substituents, hence the molecular symmetry influences the electronic structure of the resulting corannulene compounds.[93] The soluble neopentylferrocene substituent allowed preparing once, twice, quadruply and quintuply ferrocenylated, soluble corannulenes. The effect of the amount of substituents on the electronic

properties could be examined, whereas the effect of different substitution patterns[17c] could not be examined due to synthetic limitations.

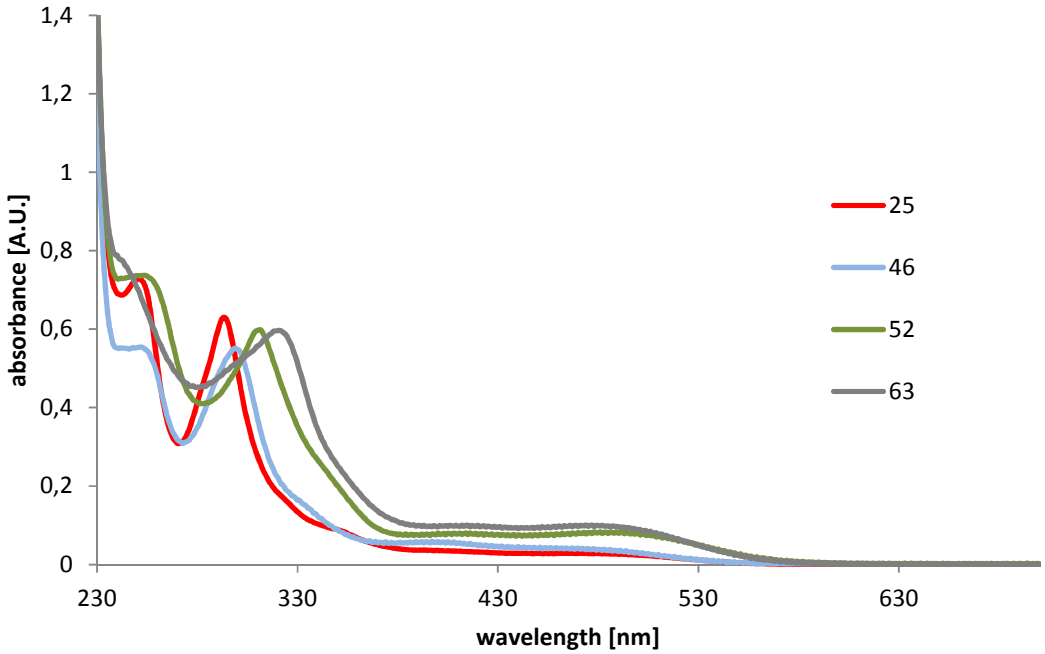

Figure 5.8 UV/Vis spectra of once (**25**), twice (**46**), four times (**52**) and five times neopentylferrocene (**63**) substituted corannulenes, $1*10^{-5}$ M in dichloromethane.

A general trend can be observed, where an increasing grade of ferrocenylation results in a bathochromic shift of the absorption maxima centered at 300 nm ($\pi \rightarrow \pi^*$). The broad absorption maxima at 380 – 550 nm could be assigned to a charge transfer which consequently increases and shows a stronger red-shift with increasing an number of ferrocenyl substituents.

Table 3.1 UV/Vis Absorption maxima of ferrocene buckybowl compounds measured at a concentration of $1*10^{-5}$ in dichloromethane.

Compound	λ_{max} [nm]
1	437 (vw), 288 – 241 (br)
16	318 (br), 288, 254, 247
22	369 – 530 (shoulder), 294, 250
23	467 (br), 368, 326, 291
25	545-380 (br), 351, 293, 251
26	500 – 343 (br), 430 – 331 (shoulder) 297, 254
29	530 – 430 (br), 405, 349, 297, 254
30	515, 365, 299, 253
31	543 – 428 (shoulder), 365, 302, 247
32	487, 384, 311, 249
41	294, 251
33	approx. 449 (br) , 292, 248
46	approx. 472 (br), approx. 401 (br), 299, 248
52	approx. 484 (br), approx. 407 (br), 311, 253
63	approx. 494 (br), approx. 416 (br), 321, 242

6. Electrochemistry

Fullerenes are known to be electrochemically reducible in up to six one-electron-steps (C_{60}^{6-}, C_{70}^{6-}).[94] As mentioned in the introduction the fullerene fragment **16** can be chemically reduced with lithium to the tetraanion.[18b,20-22] Electrochemically **16** undergoes up to three reversible one-electron reduction processes under the right conditions.[22] If the fellow buckybowl **17** is treated with lithium, reduction in its three benzylic positions occurs. The reported CV-spectra of sumanene were measured in DMF where one partially reversible one-electron reduction at -2.60 V and further reductions at very negative potentials were observed. The latter were assigned to follow-up processes (decomposition). Two irreversible one-electron reductions were observed in acetonitrile solution.[25]

1 and most of its derivatives undergo reversible one-electron oxidations in a variety of solvents. The best solvent for stabilizing both, the reduced state as well as the oxidized state of all ferrocenylated corannulenes was found to be anhydrous THF. Under our conditions two reductions were observed for **16** in THF.[58]

6.1 Determination of the Number of Electrons Involved in a Redox Process

6.1.1 Stoichiometric Method

A fast and fairly simple method for determining of the number of electrons participating in an electrode reaction is to add an equimolar amount of an internal standard for which the amount of electrons participating in the electrode reaction is known (e.g. decamethylferrocene) to the analysed sample.[95] The measurement of square wave (SWV) or differential pulse voltammetry (DPV) gives peaks or troughs for the electrode processes. The area of these peaks can be integrated and compared with the internal standard. This method however can only be used if the diffusion coefficient of the compound and standard are expected to be similar.

6.1.2 Baranski Method

This method is based on chronoamperometric measurements and does not require knowledge of diffusion coefficients.[96] The parameters of current against time transients are compared at a microelectrode with a diameter of 60-100 µm and a larger glassy carbon electrode (Ø = 3 mm) in the same solution and under the same conditions. Thus the current is limited by mass transfer and at the micro electrode and the non-linear diffusion is predominant. At the larger electrode the linear diffusion is predominant. In order to calibrate the results for the unknown reaction these measurements are repeated with a standard electrode reaction involving a known number of electrons (e.g. the reaction of decamethylferrocene) at a known concentration.

6.2 Monoferrocenylated Compounds

Investigation of monoferrocenylated buckybowls showed reversible one-electron oxidation waves for the ferrocenyl unit in the anodic region and partially reversible to irreversible reductions at the corannulene unit in the cathodic region.

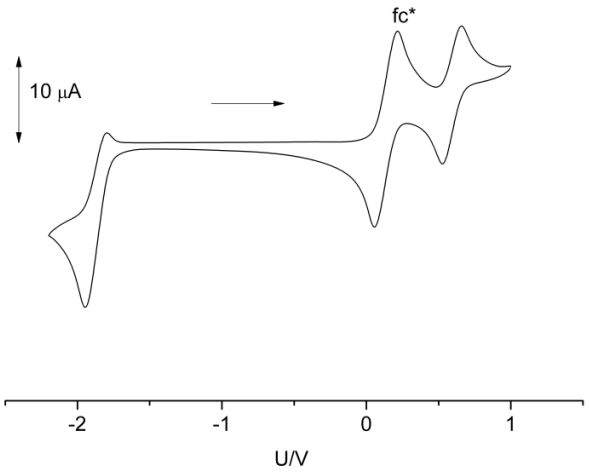

Figure 6.2.1 CV spectrum of **25** in THF with tetra-*n*-butylammonium hexafluorophosphate (0.1M) as conducting salt at a scan rate of 100 mV/s.

The redox potentials of the ferrocenyl units are that different from ferrocene itself. Thus no strong electronical interactions between the ferrocenyl substituent and the corannulene moiety should be assumed. Redox potential of the fereocenyl units of the vinyl and butadienyl bridged compounds **31** and **32**, as well as directly ferrocenylated **25** are shifted to slightly more negative potentials. The same can be observed for **30** but in this case the shift is mainly caused by influence of the eight methylgroups at the ferrocene subunit, which facilitate the oxidation due to their +I effect.

For the reported substituted corannulenes, however in most cases only one reduction was observed and only **32** showed two reduction waves.

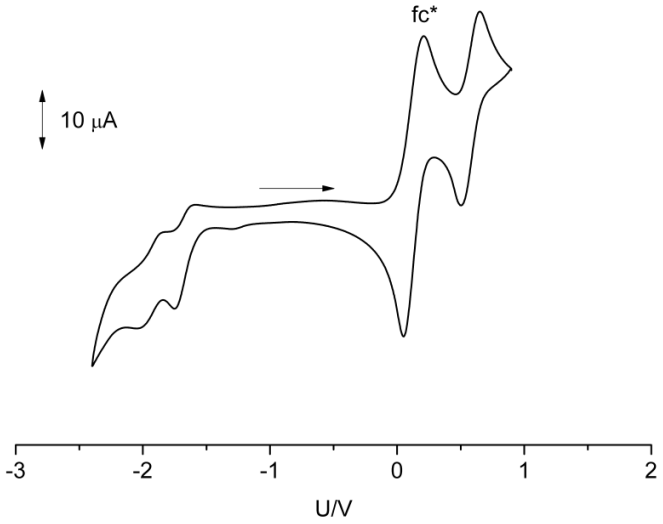

Figure 6.2.2 CV spectrum of **32** in THF with tetra-*n*-butylammonium hexafluorophosphate (0.1M) as conducting salt at a scan rate of 100 mV/s.

The reduction potentials of the corannulene moieties are similar to each other and not very different from the potential of unsubstituted corannulene (-2.47 V). **32** shows with -2.28 V the highest and **25** with -2.48 V the lowest potential for the reduction process, which is in line with the results obtained from the UV measurements, in which the highest grade of charge transfer was observed for the butadienyl bridged **32**.

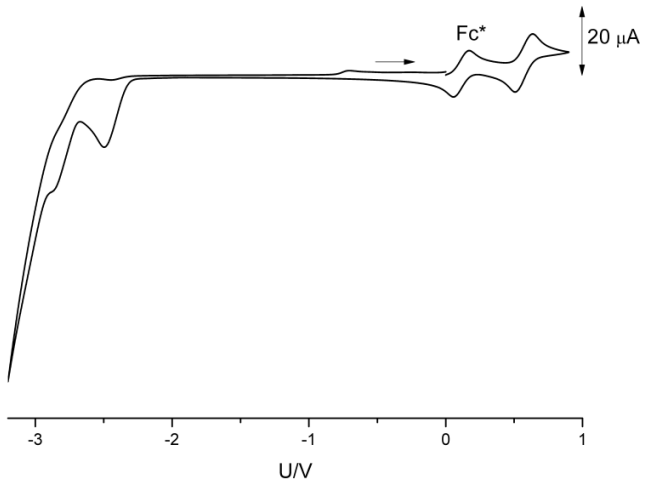

Figure 6.2.3 CV spectrum of **23** in THF with tetra-*n*-butylammonium hexafluorophosphate (0.1M) as conducting salt at a scan rate of 100 mV/s.[62]

The ferrocene substituent of **23** shows the expected reversible one-electron oxidation. For the sumanene unit two irreversible reduction processes were observed at very negative potentials of -3.02 and -3.35 V, close to the lower boundary in which measurement are possible in THF. Thus the ferrocene unit does not stabilize the reduction of the sumanenyl substituent.

Table 6.2.1 Redox potentials and HOMO-LUMO gaps of monoferrocenylated corannulene compounds.

Compound	E^0 Oxidation [V]	E^0 Reduction [V]	HOMO-LUMO gap [V]
22	0.02 0.02 (CH_2Cl_2)	-2.51, -2.99_{irrev} -2.43_{irrev} (CH_2Cl_2)	2.53 2.45
23	-0.03	-3.02_{irrev} -3.35_{irrev}	2.99
25	-0.01	-2.48_{irrev}	2.47
26	0.03	-2.43	2.46
29	0.13	-2.33	2.46
30	-0.25*	-2.30*	2.05
31	-0.02	-2.36_{irrev}	2.34
32	-0.03	-2.28, -2.53	2.25

The E^0 values were measured vs decamethylferrocene and are taken from SWV measurements when possible. The measurements in this work (if not otherwise noted) are referenced against the E^0 of the ferrocene/ferrocenium redox couple for better comparison with literature values. The E^0 of decamethylferrocene/decamethylferrocenium was found to be -0.48 (THF) and -0.56 V (CH_2Cl_2) vs the E^0 of ferrocene/ferrocenium. For all measurements in this table tetra-*n*-butylammonium hexafluorophosphate (0.1M) was used as conducting salt and a scan rate of 100 mV/s was used. If not otherwise mentioned the solvent was THF. Irreversible processes are noted with irrev.(*) **1** was used as internal standard.

6.3 Dicorannulenenylferrocene (33) and Disumanenylferrocene (34)

The reduction waves of **33** (−2.05 V, −2.56 V)[58] indicate that two one-electron steps take place. Since both reduction steps are well separated from each other it can be assumed that one corannulene unit undergoes two reduction steps to the dianion.

THF is apparently not an appropriate environment to stabilize the negatively charged corannulenes; the reduction is shifted further to the cathodic region in comparison to dichloromethane. The redox-potential of the ferrocene unit of the sumanene compound **34** was found to be at -0.05 V.[62] Due to the very low solubility and low stability of this compound,

interpretations with respect to reversibility are not possible. Again irreversible reduction processes at low values of -2.91 and -3.39 V in the cathodic region can be observed.

Table 6.3.1 Redox potentials and HOMO-LUMO gaps of dibuckybowlferrocenes.

Compound	E^0 Oxidation [V]	E^0 Reduction [V]	HOMO-LUMO gap [V]
33	-0.03 0.01 (CH_2Cl_2)	-2.53, -3.04_{irrev} -2.41_{irrev} (CH_2Cl_2)	2.50 2.42
34	-0.05	-2.91_{irrev} -3.39_{irrev}	2.86

The E^0 values were measured *vs.* decamethylferrocene. The measurements in this work (if not otherwise noted) are referenced against the E^0 of the ferrocene/ferrocenium redox couple for better comparison with literature values. The E^0 of decamethylferrocene/decamethylferrocenium was found to be -0.48 (THF) and -0.56 V (CH_2Cl_2) *vs.* the E^0 of ferrocene/ferrocenium. For all measurements in this table tetra-*n*-butylammonium hexafluorophosphate (0.1M) was used as conducting salt and a scan rate of 100 mV/s was used. If not otherwise mentioned the solvent was THF. Irreversible processes are noted with irrev.

6.4 Dicorannulenylbiferrocene (39) and Corannulenylbiferrocene (40)

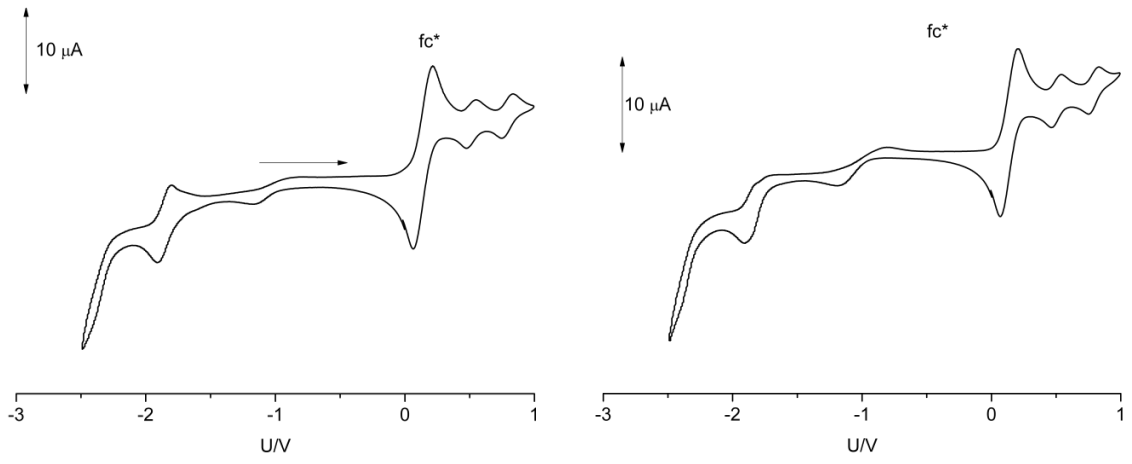

Figure 6.4.1 CV spectra of **39** (left) and **40** (right) in THF with tetra-*n*-butylammonium hexafluorophosphate (0.1M) at scan rate of 50 mV/s. Traces if oxygen are seen in the CV spectrum.

Compounds **39** and **40** showed two reversible one-electron oxidations as already observed for biferrocene itself and other biferrocene compounds.[55,97] For the biferrocene unit of both compounds the redox reactions can be observed at -0.11 and 0.17 V (ΔE = 0.28 V). Calculations of **39** (B3LYP, 6-31G(d,p)) show that the HOMO is located on the biferrocene unit while the LUMO is distributed over both corannulene moieties as in most ferrocenylcorannulenes. Accordingly, the reversible reduction of **39** at -2.48 V includes the reduction of both corannulene moieties but is not resolved. The reduction of **40** shows an irreversible character.

Table 6.4.1. Redox potentials and HOMO-LUMO gaps of biferrocene compounds **39** and **40**.

Compound	E^0 Oxidation [V]	E^0 Reduction [V]	HOMO-LUMO gap [V]
39	0.17, -0.11	-2.48	2.37
40	0.17, -0.11	-2.45_{irrev}	2.56

The E^0 values were measured vs decamethylferrocene. The measurements in this work (if not otherwise noted) are referenced against the E^0 of the ferrocene/ferrocenium redox couple for better comparison with literature values. The E^0 of decamethylferrocene/decamethylferrocenium was found to be -0.48 (THF) and -0.56 V (CH_2Cl_2) vs the E^0 of ferrocene/ferrocenium. For all measurements in this table tetra-*n*-butylammonium hexafluorophosphate (0.1M) was used as conducting salt, THF as a solvent and a scan rate of 100 mV/s was used.

6.5 Diferrocenylated Compounds

Diferrocenylated compounds like directly ferrocenylated **46**, ethynyl compound **47** and bistrifluoromethyl compound **48** offer a unique possibility to directly compare the influence of substituents at the corannulene core in addition to the spacers studied for monoferrocenylated compounds.

All compounds show only one reversible oxidation process for both ferrocenyl substituents, although calculations predict a conjugated HOMO and thus two one-electron oxidations were expected.

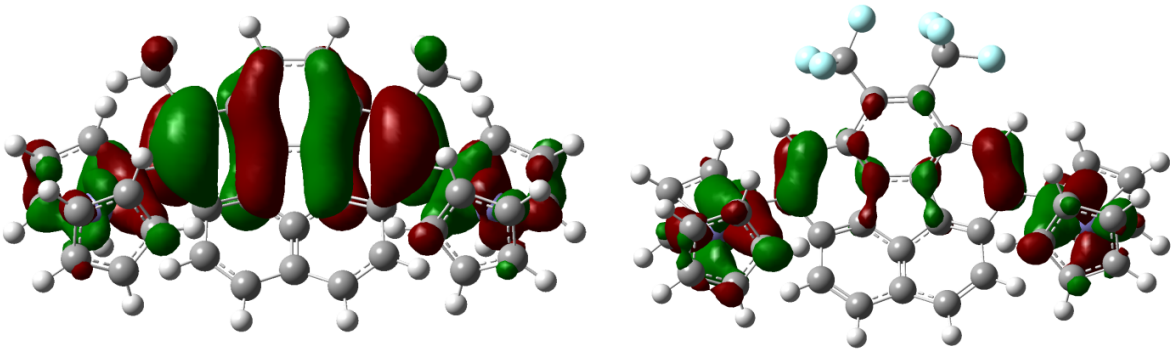

Figure 6.5.1 left side: calculated HOMO of **45** (wB97XD 6-31G*); right side: calculated HOMO of **48** (B3LYP 6-31).

Judging from the CV spectrum of **46** a one-electron reduction is followed by a one-electron oxidation, which is unexpected but not trustworthy due to the irreversibility of the reduction step and the limited solvent range.

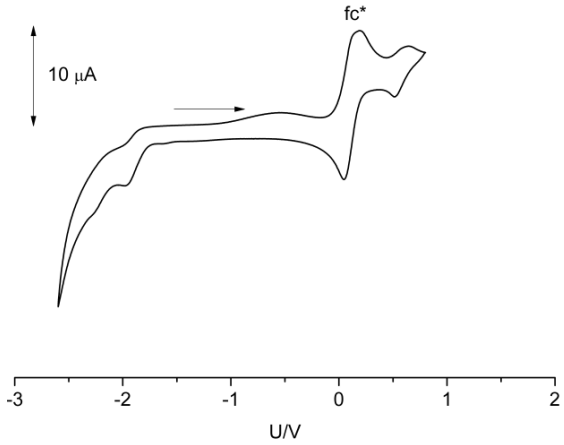

Figure 6.5.2 CV-spectrum of **46** measured in THF with tetra-n-butylammonium hexafluorophosphate as conducting salt at 100 mV/s with internal decamethylferrocene.

Finally, Baranski measurements reveal that one two-electron oxidation occurs. To get further insight into the possible interaction of ferrocene subunits, measurements with BArF were conducted for **48** ($BArF_{(F5)}$; ArF = pentafluorophenyl) and **46** ($BArF_{(CF3)}$; ArF = 3,5-bis(trifluoromethyl)phenyl) but the resulting CV spectra showed no splitting of the oxidation processes, indicating no considerable electronic or electrostatic interactions of both ferrocenes (see Figure 6.5.3 for **48**).[67]

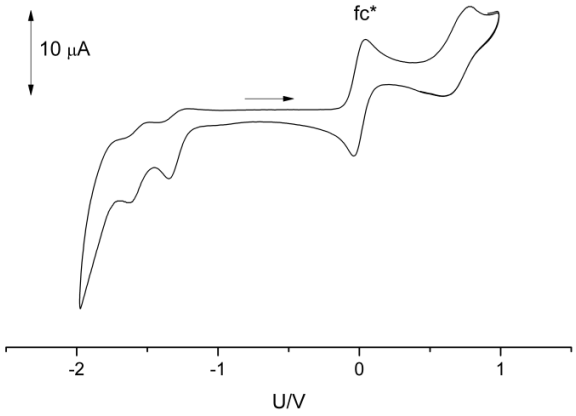

Figure 6.5.3 CV-spectrum of **48** in dichloromethane with $BArF_{(F5)}$ (0.1M) at a scan rate of 100 mV/s.

The reduction at the corannulene moiety is not fully reversible for all three compounds.

While **46** shows again shows almost no changes to **25** or **16**, the reduction of **47** is shifted to less negative potentials compared to the **28** (0.09 V). The electron withdrawing trifluoromethyl groups of **48** facilitate the reduction process on the corannulene unit even more and two reductions could be observed. As a result this compound shows a very small HOMO-LUMO gap of 1.89 V.

Table 6.5.1 Redox potentials and HOMO-LUMO gaps of diferrocenylated corannulenes.

Compound	E^0 Oxidation [V]	E^0 Reduction [V]	HOMO-LUMO gap [V]
46	-0.03 $0.59^{\S}$	-2.48_{irrev}	2.45
47	0.10	-2.25_{irrev}	2.35
48	0.07 (CH_2Cl_2) $0.69^{\#}$	$-1.82_{irrev}(CH_2Cl_2)$, $-2,15(CH_2Cl_2)_{irrev}$ $-1.28^{\#}_{qrev}$, $-1.56^{\#}$	1.89

§: $BArF_{(CF3)}$ (0.1M) in CH_2Cl_2, referenced against E^0 of decamethylferrocene/decamethylferrocenium, #: $BArF_{(F5)}$ (0.1M) in CH_2Cl_2, both referenced against decamethylferrocene.

6.6 Tetraferrocenylated compounds

The tetraferrocenylated corannulene compounds are especially interesting due to their two pairs of ferrocene substituents within close proximity. Generally compounds where the ferrocene substituents are connected *via* spacers to the corannulene moiety show one reversible oxidation wave when measured with tetra-*n*-butylammonium hexafluorophosphate in THF or dichloromethane. The only compounds that show a splitting of the oxidation wave are **51** and **52**. During the CV-measurements of **51** a new problem occurred. While the first oxidation wave as depicted in Figure 6.6.1 shows a reversible character the second oxidation wave shows a severely increased process for the back-reaction of the second oxidation, that increases if several cycles are measured. This can be explained by the very low solubility of the second oxidized species which precipitates on the electrode. When dichloromethane was used as a solvent, the separation of the two processes increased but the solubility problem remained. The reduction of this compound shows a reversible character in THF but is strictly irreversible in dichloromethane. The amount of electrons of the two oxidations steps could not be assigned because the Baranski method requires a good solubility of the analyte.

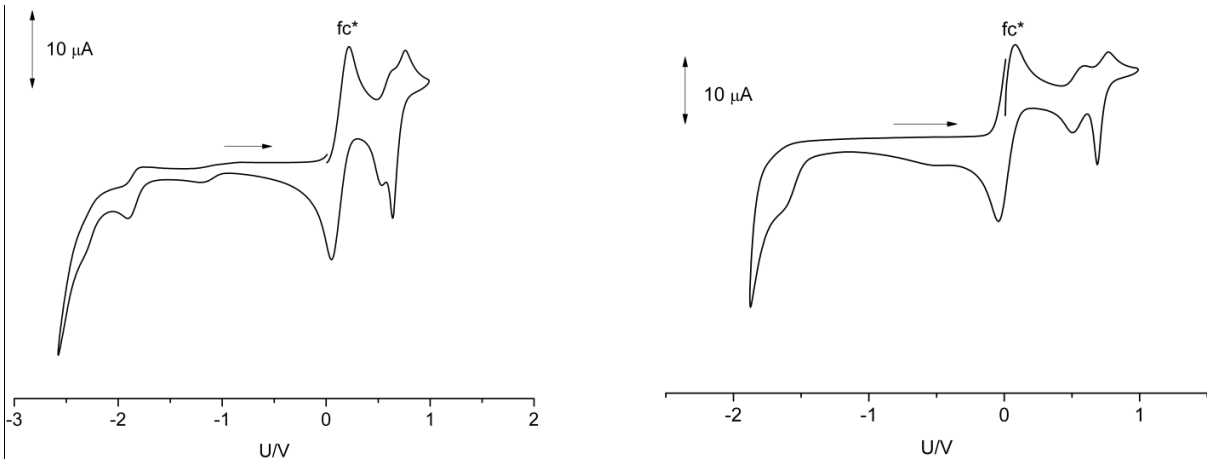

Figure 6.6.1 left: **51** measured in THF, right: **51** measured in dichloromethane. For both compounds the conducting salt was tetra-*n*-butylammonium hexafluorophosphate (0.1M) and a scan rate of 100 mV/s was applied.

The solubility problem was addressed by the introduction of neopentylferrocenes. For **52** two oxidation processes can be observed and both of them show a reversible character without any signs of precipitation.

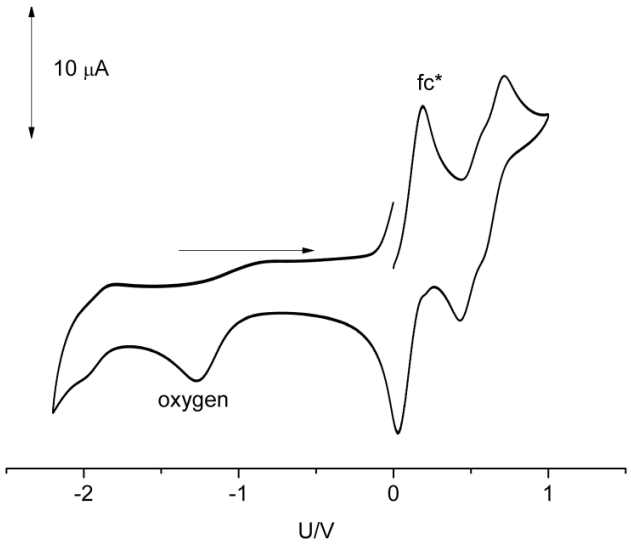

Figure 6.6.2 left: **52** measured in THF with tetra-*n*-butylammonium hexafluorophosphate (0.1M) and a scan rate of 100 mV/s.

The amount of electrons participating in these oxidation processes were determined at first by measurement of a differential pulse voltammogram (dpv) with an equimolar amount of decamethylferrocene in THF (depicted in Figure 6.6.3).

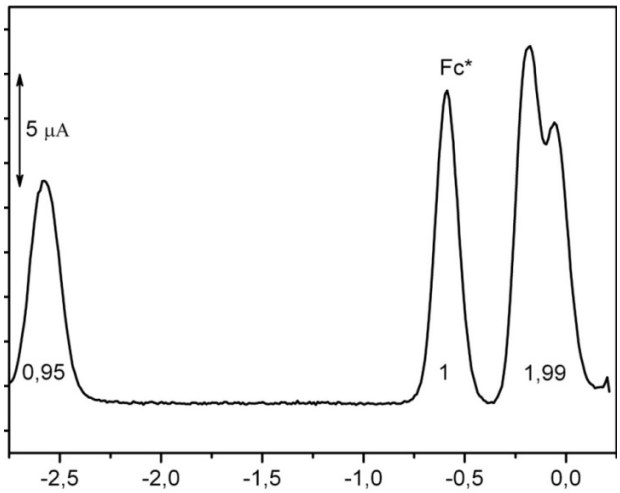

Figure 6.6.3 Differential pulse measurement of **52** in THF with tetra-*n*-butylammonium hexafluorophosphate (0.1M).

Since decamethylferrocene is very different in size, an adulteration due to different diffusion coefficients is possible but Baranski measurements confirm two consequent one-electron processes, although four one-electron processes were expected initially.

Measurements with $BArF_{(CF3)}$ gave satisfying results. For **52** the two redox processes on the ferrocene unit showed a splitting of potentials, initially four well resolved oxidation one-electron processes were observed with a ΔE_{ox} of (0.11, 0.31 and 0.14 V).

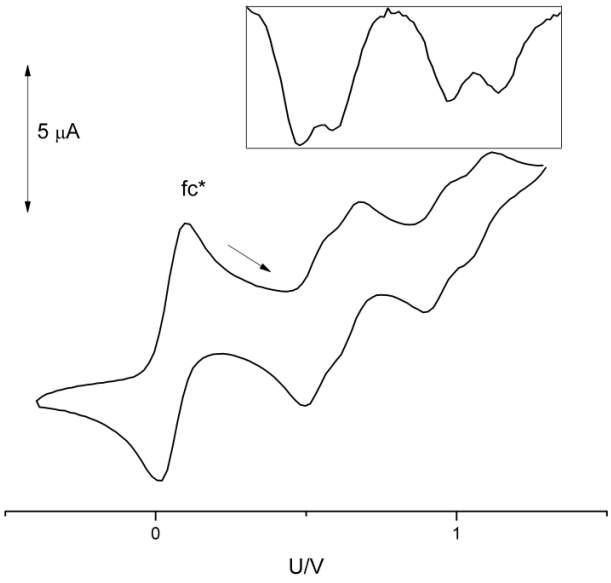

Figure 6.6.4 CV and SWV measurements of **52** in dichloromethane with $BArF_{(CF3)}$ (0.1M) as conducting salt at a scan rate of 100 mV.

The CV measurements of **54** in THF with tetra-*n*-butylammonium hexafluorophosphate reveal one reversible oxidation process at 0.10 V. Again precipitation on the electrode is visible. Further $BArF_{(CF3)}$ measurements were conducted for the alkynyl bridged **54** and if the weaker coordinating conducting salt was used this process splits into two reversible processes, probably deriving from the electrostatic repulsion of two neighbouring ferrocenyl substituents (see Figure 6.6.5).

The same effect can be observed for the octamethylethynyl substituted compound **55**, while for the phenyl-bridged compound **53** only one oxidation process occurs under both conditions.

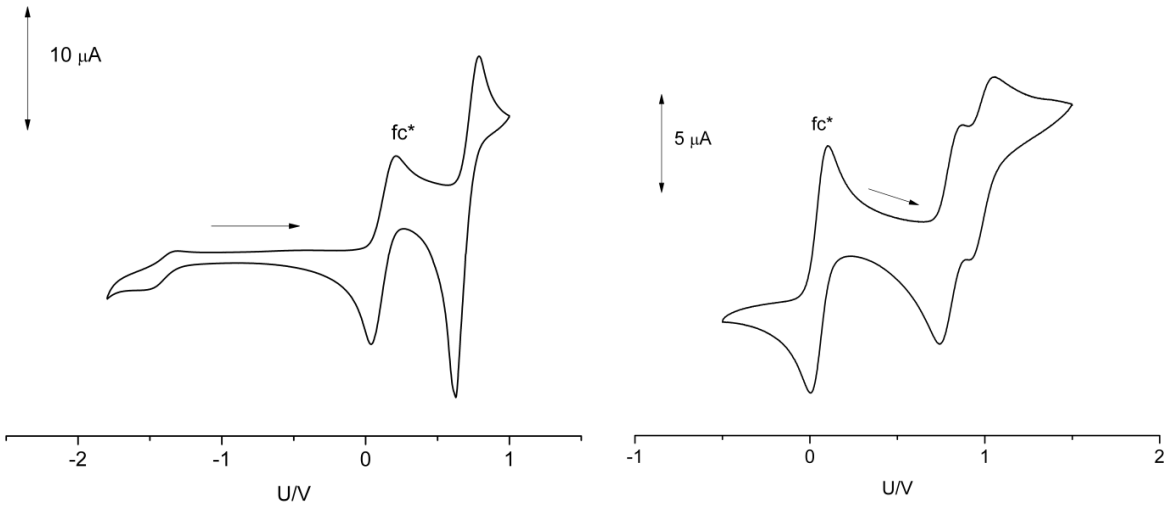

Figure 6.6.5 left side: CV of **54** in THF with tetra-*n*-butylammonium hexafluorophosphate (0.1M) as conducting salt, right side: CV of **54** in dichloromethane with $BArF_{(CF3)}$ (0.1M) as conducting salt, scan rate 100 mV/s.

The reductions differ depending on the spacer or substituent attached. The largest shift (0.49 V *vs*. **16**) of the reduction is observed for **54** whereas reduction of neopentyl compound **52** remains almost unchanged.

The broad range of HOMO-LUMO gaps ranges from 1.8 to 2.7 V, with the lowest gap for the octamethylethynyl compound **55** and the largest for directly ferrocenylated **51**.

Table 6.6.1 Redox potentials and HOMO-LUMO gaps of tetraferrocenylated corannulenes.

Compound	E^0 Oxidation [V]	E^0 Reduction [V]	HOMO-LUMO gap [V]
51	0.09, -0.03 0.15 (CH_2Cl_2), -0.03 (CH_2Cl_2)	-2.45	2.42
52	0.06, -0.07 1.03[§], 0.89[§], 0.58[§], 0.47[§]	-2.48	2.41
53	-0.02	-2.33	2.31
54	0.10 0.93[§], 0.76[§]	-1.98	2.08
55	-0.24 0.43*, 0.25*	-2.07	1.83
56	-0.03	-2.27	2.24

All measurements in THF with tetra-n-butylammonium hexafluorophosphate (0.1M), measured with internal decamethylferrocene but referenced against the E^0 of ferrocene/ferrocenium. §: $BArF_{(CF3)}$ (0.1M) in CH_2Cl_2, referenced against decamethylferrocene, * $BArF_{(CF3)}$ (0.1M) in CH_2Cl_2, referenced against ferrocene

6.7 Pentaferrocenylated corannulene

Pentaferrocenyl **61** could be prepared and isolated in very high purity but the low solubility prohibited any measurements. Neopentyl compound **63** proved again to be more soluble but not sufficiently high enough for Baranski measurements. The observed oxidation process is almost identical to the one of ferrocene. No statement about the amount of electrons can be made for the measurement with tetra-*n*-butylammonium hexafluorophosphate.

Measurements with $BArF_{(CF3)}$ show five one-electron processes with ΔE of approximately 0.1 V. Although the difference in voltage between these five redox processes is not very large, at least three of them show a reversible character. Ultimately, it could be shown that the pentacation and all oxidized intermediates of symmetrically ferrocenylated **63** can be generated (Figure 6.7.1).

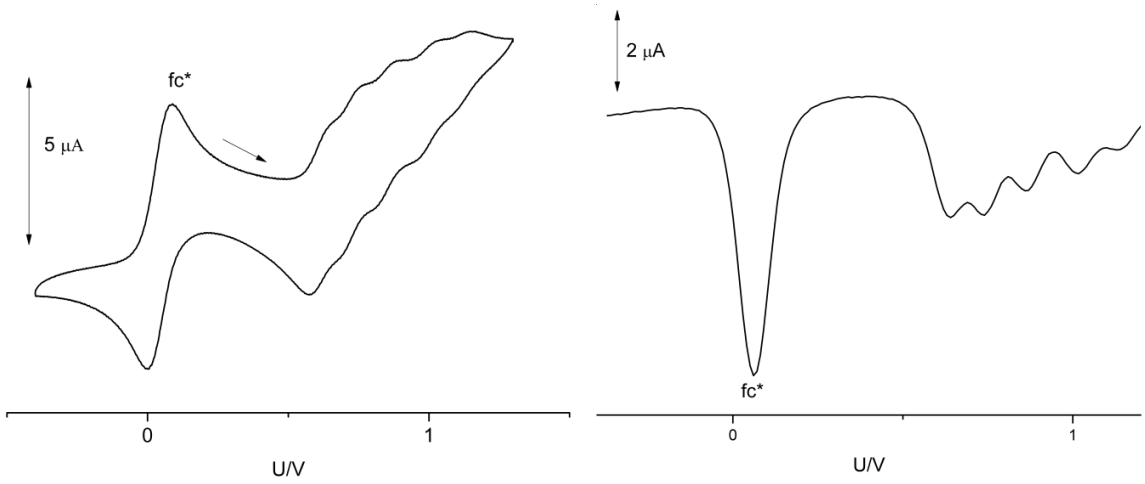

Figure 6.7.1 left side: CV spectrum of **63**, right side: SW spectrum of **63**; both recorded in dichloromethane, with $BArF_{(CF3)}$ (0.1M) as conducting salt. Decamethylferrocene (fc*) was added as internal standard, scan rate 100 mV/s.

Judging from the conducted measurements, where only the use of weakly coordinating anions separates the oxidation processes, no electronic communication between the ferrocene units can be expected. Electrostatic effects that arise from the close proximity of the ferrocenyl substituents probably cause the separation of the redox processes.[31] However some exceptions where intramolecular electronic interactions have only little effect on the CV spectra are known.[35-38]

Compound	E^0 Oxidation [V]	E^0 Reduction [V]	HOMO-LUMO gap [V]
63	-0.01 1.08§, 0.97§, 0.81§, 0.68§, 0.59§	-2.40	2.39

Measurement in THF with tetra-*n*-butylammonium hexafluorophosphate (0.1M), measured with internal decamethylferrocene but referenced against the E^0 of ferrocene/ferrocenium. §: $BArF_{(CF3)}$ (0.1M) in CH_2Cl_2, referenced against E^0 of decamethylferrocene.

It was shown that ferrocenylated buckybowls can be synthesised with a wide range of tunable HOMO-LUMO gaps, oxidation and reduction potentials. Ethynyl spacers facilitate the reduction in a way similar to trifluoromethyl groups attached to the corannulene rim. If no shift of the reduction is desired the ferrocene can be directly connected to the corannulene molecule. The

oxidation can be tuned by choosing different alkyl ferrocenes. With increasing size the kinetic measurements of the electron count becomes very difficult with standard measurement techniques. Weakly coordinating BArF salts cause a splitting of oxidation processes of several tetrasubstituted derivatives and five processes for pentaferrocenylated **63**, the compound with the highest grade of ferrocenylation within this work. By choosing different spacers the oxidation of ferrocenyl substituents can be addressed stepwise (for directly substituted or ethynyl bridged compounds) or concerted for phenyl bridged compounds.

7. Summary

This study aims to investigate interactions of a variety of ferrocenes which are connected to non-planar polycyclic aromatic hydrocarbons. Starting from corannulene ($C_{20}H_{10}$) and sumanene ($C_{21}H_{12}$), corannulenylferrocene and sumanenylferrocene were successfully synthesized by Negishi cross-coupling reactions and their solid-state structures were studied. Corannulenylferrocene shows a structure dominated by C-H···π interactions like corannulene. Sumanenylferrocene does not show the regular columnar stacking structure like pristine sumanene, but a staircases-like "ferrocene-in-bowl" stacking. 1,1'-Dibuckybowlferrocenes of both buckybowls were prepared and are significantly different to their monobuckybowlferrocene counterparts. 1,1'-Dicorannulenylferrocene showed the desirable π-stacking arrangement by unprecedented intra- and intermolecular π-stacking while the corresponding 1,1'-disumanenylferrocene formed a dimeric structure in the solid state. Additional corannulenylferrocenes were prepared from monoiodocorannulene, to illustrate the influence of spacers between ferrocene and the buckybowl corannulene. The ferrocene with spacers were introduced by Negishi coupling, and modified Heck- and Sonogashira-type coupling reactions. 1,6-Dibromo-2,6-dimethylcorannulene reacted correspondingly to yield two types of diferrocenylated corannulenes. It was found that ferrocenes with solubilizing groups are necessary to facilitate the handling. 1,2,5,6-Tetrabromocorannulene was used accordingly to obtain corannulenes bearing four ferrocene substituent at its rim, directly and *via* spacer groups. A single-crystal X-ray analysis of 1,2,5,6-tetra(ferrocenylphenyl)corannulene revealed a nutshell-like arrangement of the corannulene molecules in the crystal, where two bowl encapsulate one solvent molecule. Starting from 1,3,5,7,9-pentachlorocorannulene, corannulenes bearing five ferrocene substituents could be prepared and isolated as well. The highest grade of ferrocenylation was achieved with the preparation of *sym*-pentaferrocenylcorannulene.

All ferrocenylcorannulenes were studied by optical spectroscopy and electrochemistry to elucidate electronical interactions between the ferrocenes and between the ferrocenes and the buckybowl bound to it. It was shown that the spacer units have a distinct influence on the conjugation between the buckybowl and the ferrocene. Weakly coordinating conducting salts showed a splitting in the redox-processes of some multiple ferrocenylated compounds.

Zusammenfassung

Im Rahmen dieser Arbeit wurden die Wechselwirkungen zwischen verschiedenen, substituierten Ferrocenen gebunden an schalenförmigen, aromatischen Kohlenwasserstoffen studiert. Ausgehend von Corannulen ($C_{20}H_{10}$) und Sumanen ($C_{21}H_{12}$) wurden durch Negishi-Kupplungen ferrocenylierte Derivate in guten Ausbeuten hergestellt und teilweise röntgenkristallographisch untersucht. Während das durch C-H···π Interaktionen dominierte Corannulenylferrocen in weiten Teilen der Struktur von Corannulen ähnelte, wurde bei Sumanenylferrocen eine drastische Änderung der Festkörperstruktur beobachtet wobei die ehemals strangförmige Stapelungsstruktur nicht beibehalten wurde. Durch geschickte Reaktionsführung gelang es 1,1‘-bisubstituierte Ferrocenverbindung der gleichen Art zu erhalten und zu studieren. Es stellte sich nach röntgenkristallographischer Untersuchung heraus, dass die 1,1‘-Dicorannulenyl-ferrocenverbindung die wünschenswerte Stapelungsstruktur durch eine bisher einzigartige intra- und intermolekulare π-π Wechselwirkungskaskade bildete. Das korrespondierende Sumanenderivat hingegen zeigte die Ausbildung einer eher dimeren Struktur. Der Einfluss von verbrückenden Einheiten wurde studiert. Dies gelang durch Negishi-Kupplungen und modifizierte Heck- bzw. Sonogashira-Reaktion. Durch Kupplungsreaktionen mit 1,6-Dibrom-2,6-dimethylcorannulen wurden Corannulenderivate mit zwei Ferrocensubstituenten erhalten. Hierbei zeigte sich, dass Ferrocene mit löslichkeitsvermittelnden Gruppen notwendig sind, um die Handhabung zu erleichtern. 1,2,5,6-Tetrabromcorannulen wurde analog genutzt um vier Ferrocensubstituenten direkt und über verbrückende Elemente einzuführen. Die röntgenkristallographische Untersuchung des 1,2,5,6-Tetra(ferrocenylphenyl)corannulen zeigte eine überraschende, nussschalenartige Festkörperstruktur, indem zwei Moleküle ein Lösungsmittelmolekül umschließen. Ausgehend von 1,3,5,7,9-Pentachlorcorannulen gelang es fünffach ferrocenylierte Corannulene darzustellen, zu isolieren und zu charakterisieren.

Alle dargestellten Derivate wurden hinsichtlich ihrer optischen und elektrochemischen Eigenschaften untersucht um eventuelle Kommunikation der Ferrocene untereinander und mit dem gebundenen Corannulen zu beobachten. Hierbei zeigte sich, dass die Spacer einen Einfluss auf die Elektrochemie dieser Verbindungen haben und dass die Verwendung schwach koordinierender Leitsalze zur Aufspaltung der Redoxprozesse führen kann.

8. Experiments

8. 1 General

All experiments were carried out under standard Schlenk conditions, if not otherwise noted, with Argon as inert gas. Air or moisture sensitive materials were stored and handled in in either an argon-filled MBraun glove box model LAB master SP or a nitrogen-filled MBraun glove box model UNIlab 2000.

8.1.1 Chemicals

Tetrahydrofuran was distilled freshly from sodium/benzophenone and further purified by trap-to-trap distillation if used for electrochemical measurements. Diethyl ether was distilled from potassium/benzophenone. 1,2-Dichloroethane and DMF were distilled from phosphorus pentoxide and stored over molecular sieve (3 Å). Dichloromethane for electrochemical measurements, triethylamine and diisopropylamine were distillied from calcium hydride.
Chemicals were purchased from the following companies: ABCR GmbH & Co. KG (dichloromethane for electrochemical use, gold(III) chloride, decamethylferrocene, vinylferrocene, 1,1'-bis(diphenylphosphino) ferrocene, SPhos, tetrakis(triphenylphosphane)-palladium(0)), Alfa Aesar (ferrocene, (R)-*N*,*N*-dimethyl-1-(ferrocenyl)ethylamine, bis(pinacolato)diboron, dichloro[1,3-bis(diphenylphosphino)propane]nickel, anhydrous zinc(II) chloride), Acros (*n*-butyllithium, *sec*-butyllithium and *tert*-butyllithium, tris(dibenzylideneacetone)dipalladium(0)), Chempur (palladium(II) acetate), Fluka Analytical (tetra-*n*-butylammonium hexafluorophosphate (electrochemical grade)), Molecular (*N*-iodosuccinimide), Sigma-Aldrich (ethynylferrocene, RuPhos). TLC analysis was performed using Merck Silica gel 60 F254 and PTLC was conducted using Wako Wakogel B-5F.

Butadienylferrocene (**5**),[47] 1-ethynyl-1',2,2',3,3',4,4',5-octamethylferrocene (**6**),[50] 1,1'-dibromo-ferrocene (**10**),[53] 1-bromo-1'-neopentylferrocene (**12**),[52] 1-iodo-4-ferrocenylbenzene (**13**),[54] 1,1'''-dibromobiferrocene (**15**),[56] corannulene (dibenzo[*ghi,mno*]fluoranthene **16**) and 1,2,5,6-tetrabromocorannulene (1,2,5,6-tetrabromodibenzo[*ghi,mno*]fluoranthene **50**),[13c]

sumanene (4,7-dihydro-1H-tricyclopenta[*def,jkl,pgr*]triophenylene (**17**),[15] 1,2-dibromo-ferrocene **36**),[68] 1,6-dibromo-2,5-dimethylcorannulene (1,6-dibromo-2,5-dimethyldibenzo-[*ghi,mno*]fluoranthene **44**),[64] 1,3,5,7,9-pentakis(4,4,5,5-tetramethyl-1,3,2-dioxaborolan-2-yl)corannulene (1,3,5,7,9-pentakis(4,4,5,5-tetramethyl-1,3,2-dioxaborolan-2-yl) dibenzo-[*ghi,mno*]fluoranthene, **58**)[74] 1,3,5,7,9-pentachlorocorannulene (1,3,5,7,9-pentachlorodibenzo-[*ghi,mno*]fluoranthene **59**),[74] decabromocorannulene (decabromoodibenzo[*ghi,mno*]-fluoranthene **64**),[79] decachlorocorannulene (decachlorodibenzo[*ghi,mno*]fluoranthene **65**),[80] $BArF_{(CF3)}$ (tetra-*n*-butylammonium tetrakis[3,5-bis(trifluoromethyl)phenyl]borate),[98] $BArF_{(F5)}$ (tetra-*n*-butylammonium tetrakis(pentafluorophenyl)-borate)[99] were synthesized according to reported methods.

8.1.2 Instrumentations

Some reactions were carried out using personal parallel chemical reactors (EYELA Chemistationseries) and low-temperature reactors (EYELA PSL series). Gel permeation chromatography (GPC) was performed on JAIGEL 1H and 2H using a JAI Recycling Preparative HPLC LC-908W and chloroform as eluent. TLC (precoated) analysis and PTLC (precoated and self-made) was performed using Merck Silica gel 60 F254 or Wako Wakogel B-5F.

Melting points were determined on a Stanford Research Systems MPA100 or on a Gallenkamp Melting Point Apparatus and are uncorrected. IR spectra were recorded on a Nicolet iS10 MFR FT-IR Sp spectrometer (signals are denoted as following, s (strong), m (middle) and w (weak)). ^{1}H, ^{19}F and ^{13}C NMR spectra were measured on JEOL ECS 400/500 spectrometer or on a Bruker Instruments AVIII 700 at 23 °C. $CDCl_3$ and CD_2Cl_2 were used as solvents and the residual solvent peak was taken as an internal standard (^{1}H NMR: $CDCl_3$ 7.26; ^{13}C NMR: $CDCl_3$ 77.0; CD_2Cl_2 54.00 ppm always proton-decoupled). Spectra were visualized with MestReNova.

High resolution mass spectra (HRMS) were measured on a JEOL JMS-777V or on a MAT CH7A spectrometer using electron impact ionization method (EI). ESI-TOF spectra were measured on an Agilent 6210 ESI-TOF, Agilent Technologies, Santa Clara, CA, USA with a flow rate of 4 µL/min and a spav voltage of 4 kV. The pressure of the desolvatisation gas was 1 bar.

Single-crystal X-ray structure determination was performed on a Bruker-AXS SMART 1000 fitted with a CCD detector. The data set of **26** was collected on a Bruker Kappa ApexII duo. The data set of **33** was collected on a MAR225 (Bruker) CCD image plate detector with synchrotron radiation (λ= 0.9050 Å) on the BL 14.1 beamline at the BESSY storage ring (the laboratory site of the Protein Structure Factory at the Free University of Berlin, Germany).

Data collection, reduction and empirical absorption correction were performed using the SMART, SAINT and SADABS programs.[100] The SHELX program package was used for structure solution and refinement.[101] Mercury 3.1[102] was employed for structure visualization and images were rendered using POVray.[103] Additional supplementary data for each compound is available from the attached CD-ROM in cif-format. Data of already published structures was deposited and can be obtained free of charge from the Cambridge Crystallographic Data Centre *via* www.ccdc.cam.ac.uk/data_request/cif, **22** (869094), **23** (944835), **33** (881577), **34** (94434).

Gaussian09 was used for calculations, images were generated using GaussView 5.0.9[104] and calculated molecules were visualized with Ortep3v2.[105] Calculations were executed by Bernd M. Schmidt.

The single-crystal X-ray crystallographic analysis of **23** was performed on a Rigaku Mercury-CCD. Data were collected and processed by using CrystalClear software (Rigaku).[106]

UV-Vis spectra were measured on a Perkin-Elmer Lambda 9 UV/VIS/NIR spectrometer using Hellma Analytics 111-QS cuvettes. Dichloromethane was used as solvent; with a $1*10^{-5}$ M compound concentration.

Cyclic voltammetry measurements were performed on a MaterialsM 510 (20V/1A) potentiostat, ALS/CH Instruments Electrochemical Analyzer Model 620c or a VersaSTAT 3 Princeton Applied Research potentiostat using a Schlenk measuring cell with three platinum wires as electrodes. A conducting salt concentration of 0.1M was used. Linear Scan voltammetry and chronoamperometric measurements as well as differential pulse voltammetry measurements were performed with a VersaSTAT 4 Princeton Applied Research potentiostat a Classic-Carbon or micro platinum working electrode (WE), a platinium counter electrode (CE) and a silver pseudo-reference electrode (RE). Decamethylferrocene was used as internal standard.

8.2 X-ray Tables

Table 8.2.1 X-ray crystallographic details for the compounds **22**, **23**, **33**, **34**.

Compound reference	**22**	**23**	**33**	**34**
Chemical formula	$C_{30}H_{18}Fe$	$C_{31}H_{20}Fe$	$C_{50}H_{26}Fe$	$C_{52}H_{30}Fe$
Formula Mass	434.29	448.32	682.56	710.61
Crystal system	orthorhombic	monoclinic	orthorhombic	monoclinic
a/Å	22.011(5)	7.624(3)	38.198(8)	15.7594(8)
b/Å	43.742(9)	27.809(8)	23.938(5)	11.2328(5)
c/Å	8.1622(17)	9.570(3)	7.6480(15)	18.3713(9)
α/°	90.00	90.00	90.00	90.00
β/°	90.00	102.692(4)	90.00	105.643(2)
γ/°	90.00	90.00	90.00	90.00
Unit cell volume/ Å^3	7858(3)	1979.4(17)	6993(2)	3131.7(3)
Temperature/K	133(2)	123(2)	100(2)	100(2)
Space group	*Fdd*2	$P2_1/c$	*Pna*2(1)	$P2_1/n$
Z	16	4	8	4
Radiation type	MoKα	MoKα	synchrotron	MoKα
Absorption coefficient, μ/mm^{-1}	0.783	0.780	0.467	0.525
No. of reflections measured	25166	15241	70718	63873
No. of independent reflections	5905	4445	13727	6412
R_{int}	0.0455	0.0377	0.0519	0.0645
Final R_1 values ($I > 2\sigma(I)$)	0.0429	0.0947	0.1001	0.0721
Final $wR(F^2)$ values ($I > 2\sigma(I)$)	0.0925	0.1870	0.2561	0.1677
Final R_1 values (all data)	0.0554	0.1137	0.1130	0.0890
Final $wR(F^2)$ values (all data)	0.0978	0.2094	0.2643	0.1795
Goodness of fit on F^2	1.081	1.127	1.039	1.040

Table 8.2.2 X-ray crystallographic details for the compounds **26** and **53**.

Compound reference	**26**	**53**
Chemical formula	$C_{36}H_{22}Fe$	$(C_{84}H_{58}Fe_4)_2(C_7H_8)_3$
Formula Mass	510.39	1428.90
Crystal system	monoclinic	Triclinic
a/Å	17.617(3)	12.706(3)
b/Å	7.6767(12)	13.142(3)
c/Å	17.983(2)	23.320(6)
α/°	90.00	77.024(6)
β/°	103.483(13)	77.709(6)
γ/°	90.00	64.576(6)
Unit cell volume/ Å^3	510.39	3397.0(16)
Temperature/K	110(2)	120(2)
Space group	*P*2(1)	*P*1
Z	4	2
Radiation type	CuKα	MoKα
Absorption coefficient, μ/mm^{-1}	5.285	0.888
No. of reflections measured	12217	65932
No. of independent reflections	5198	32554
R_{int}	0.1552	0.0459
Final R_1 values ($I > 2\sigma(I)$)	0.0811	0.0568
Final $wR(F^2)$ values ($I > 2\sigma(I)$)	0.1718	0.1324
Final R_1 values (all data)	0.1346	0.0798
Final $wR(F^2)$ values (all data)	0.2012	0.1453
Goodness of fit on F^2	1.035	1.073

8.3 Syntheses

8.3.1 Monoiodocorannulene (18)

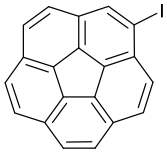

18

Corannulene (**16**) (120.0 mg, 0.48 mmol, 1 eq), *N*-iodosuccinimide (108 mg, 0.48 mmol, 1 eq) and gold(III) chloride (5 mol%) were dissolved in 1,2-dichloroethane (10 mL). The mixture immediately became dark. After stirring for 6 h at RT the reaction mixture was heated to reflux for 48 h. The solvent was removed in vacuum and the crude product was purified by flash column chromatography on silica gel with *n*-pentane/ethyl acetate (20:1) to yield pure **18** (162.3 mg, 90 %), a yellow amorphous powder.

M.p. 163 °C; **^{1}H NMR** (400 MHz, $CDCl_3$): δ = 7.70 (d, ^{3}J = 8.8 Hz, 1 H), 7.75 – 7.84 (m, 6 H), 7.86 (d, ^{3}J = 8.8 Hz, 1 H), 8.32 ppm (s, 1 H); **^{13}C NMR** (101 MHz, $CDCl_3$): δ = 136.44 (1C, CH_{rim}), 135.64 (1C, C_{hub}), 135.53 (1C, C_{hub}), 135.32 (1C, C_{hub}), 135.09 (1C, C_{hub}), 134.97 (1C, C_{hub}), 132.77 (1C, C_{flank}), 132.36 (1C, C_{flank}), 131.00 (1C, C_{flank}), 130.98 (1C, C_{flank}), 130.83 (1C, C_{flank}), 129.90 (1C, CH_{rim}), 128.24 (1C, CH_{rim}), 127.72 (1C, CH_{rim}), 127.64 (1C, CH_{rim}), 127.39 (1C, CH_{rim}), 127.25 (1C, CH_{rim}), 126.99 (1C, CH_{rim}),125.68 (1C, CH_{rim}), 125.68 (1C, CH_{rim}), 96.04 ppm (1C, C-I); **IR**: ν = 2919 (m, shr), 2850 (m, shr), 1601 (w, shr), 1070 (m, shr), 1011 (m, shr), 821 (m, shr), 669 cm^{-1} (m, shr); **EI-MS** (50 °C): *m/z* 375.9752 ($[M]^{+\cdot}$, found), 375.9749 ($[M]^{+\cdot}$, calc'd), 248 ($[M]^{+\cdot}$-HI, 100 %), 124 ($[M\text{-}HI]^{2+}$, 43 %).

8.3.2 Corannulenylferrocene (22)

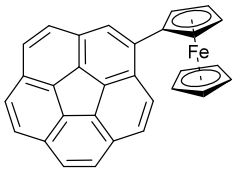

22

In a 100 mL Schlenk tube ferrocene (**1**) (79 mg, 0.43 mmol, 2 eq) and potassium *tert*-butoxide (5 mg, 0.04 mmol, 0.2 eq) were dissolved in THF (2 mL). The orange solution was cooled to -20 °C and *tert*-butyllithium in *n*-hexane (0.34 mL, 1.9M, 3.5 eq) was added dropwise. After addition the reaction was stirred at -30 °C for one hour. A solution of anhydrous zinc(II) chloride (103 mg, 0.75 mmol, 3.5 eq) in THF (1 mL) was added *via* cannula and the solution was stirred for an additional hour at -30 °C, followed by one hour at RT. Palladium(II) acetate (1 mol%), triphenylphosphane (2 mol%) and monoiodocorannulene (**18**) (64 mg, 0.18 mmol, 1 eq) were added in one portion and the reaction mixture was heated at 60 °C for 48 h. After the addition of water (10 mL) the red reaction mixture is transferred to a separation funnel, dichloromethane is added and the organic layer was washed with water (4 x 30 mL). After drying with anhydrous sodium sulfate and removal of the solvent in vacuum the crude product was purified by column chromatography on neutral aluminiumoxide *n*-pentane/toluene (3:1). The product was obtained as a red solid (33 mg, 42 %) from the fourth fraction.

M.p. 216 °C; **^{1}H NMR** (700 MHz, $CDCl_3$): δ = 8.00 (½ AB, ^{3}J = 8.6 Hz, 1H, H_{rim}), 7.77 –7.97 (m, 8H), 5.00 (s, 2H), 4.54 (s, 2H), 4.25 ppm (s, 5H); **^{13}C NMR** (175 MHz, $CDCl_3$): δ = 139.28 (1C, C_{ipso}), 136.20 (1C, C_{hub}), 136.00 (1C, C_{hub}), 135.79 (1C, C_{hub}), 135.67 (1C, C_{hub}), 134.78 (1C, C_{hub}), 131.04 (1C, C_{spoke}), 130.60 (1C, C_{spoke}), 130.59 (1C, C_{spoke}), 130.54 (1C, C_{spoke}), 129.81 (1C, C_{spoke}), 127.49 (1C, CH_{rim}), 127.48 (1C, CH_{rim}), 127.45 (1C, CH_{rim}), 127.32 (1C, CH_{rim}), 127.17 (1C, CH_{rim}), 126.97 (1C, CH_{rim}), 126.93 (1C, CH_{rim}), 126.82 (1C, CH_{rim}), 124.88 (1C, CH_{rim}), 70.56 (5C, C_{cp}), 69.91 (2C, $_{Ccp\text{-}sub}$), 69.66 ppm (2C, $_{Ccp\text{-}sub}$); **IR**: ν = 2956 (m, shr), 2922 (m, shr), 2852 (m, shr), 1902 (w, br), 1771 (w, shr), 1615 (w, shr), 1481 (m, shr), 1454 (m, shr), 1427 (m, shr), 1402 (m, shr), 1386 (w, shr), 1310 (m, shr), 1258 (m, shr), 1140 (w, shr), 1099 (m, shr), 1045 (m, shr), 1029 (m, shr), 995 (m, shr), 950 (w, shr), 826 (s, shr), 787 (s, shr), 762 (m, shr), 695 (m, shr), 654 (m, shr), 561 (m, shr), 582 cm^{-1} (m, shr); **EI-MS** (50 °C): *m/z* 434.0737 ($[M]^{+\cdot}$, found), 434.0758 ($[M]^{+\cdot}$, calc'd), 311 (37 %, $[C_{25}H_{11}]^{+\cdot}$), 121 (14 %, $[C_5H_5Fe]^{+}$), 56 (8 %, Fe^{+}), 217 (5 %, $[M]^{2+}$).

8.3.3 Sumanenylferrocene (23)

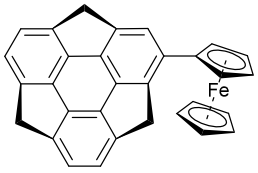

23

In a 20 mL Schlenk tube ferrocene (**1**) (43 mg, 0.23 mmol, 4 eq) and potassium *tert*-butoxide (3 mg, 0.02 mmol, 0.4 eq) were dissolved in 2 mL anhydrous THF. After cooling to -40 °C *tert*-butyllithium (0.2 mL, 1.3M in *n*-hexane, 5 eq) was added dropwise and formation of a red precipitate was observed. After 1 h at the same temperature anhydrous zinc(II) chloride (52 mg, 0.38 mmol, 7 eq) dissolved in 2 mL dry THF was added dropwise. The orange solution was stirred for another 30 min at -40 °C and then for 30 min at RT. The solution was transferred to a 20 mL chemstation tube containing monoiodosumanene (**19**) (22 mg, 0.06 mmol, 1 eq), palladium(II) acetate (3 mol%) and triphenylphosphane (6 mol%) under argon. The reddish solution was heated at 70 °C for 3 d in a chemstation. Afterwards the red-brown solution was transferred to a flask and the solvent was removed. PTLC on silica gel with *n*-hexane/dichloromethane (1:1) yielded 11 mg of an orange solid (third fraction). Final purification using a recycling GPC (with chloroform as eluting solvent) yielded the orange **23** (10 mg, 38%). Crystals suitable for X-ray analysis were grown by slow evaporation of a dichloromethane solution.

M.p. 219 °C (decomposition); **^{1}H-NMR** (500 MHz, $CDCl_3$): δ = 7.33 (s, 1H, H_{rim}), 7.10 - 7.06 (AB, ^{3}J = 7.7 Hz, 4H, H_{rim}), 4.79 - 4.70 (m, 3H, $H_{benzylic}$), 4.73 (s, 1H, $H_{cp\text{-}sub}$), 4.58 (s, 1H, H_{cp}), 4.35 (s, 1H, $H_{cp\text{-}sub}$), 4.30 (s, 1H, $H_{cp\text{-}sub}$), 4.13 (s, 5H, $H_{cp\text{-}sub}$), 3.53 - 3.38 ppm (m, 3H, $H_{benzylic}$); **^{1}H-NMR** (500 MHz, CD_2Cl_2): δ = 7.43 (s, 1H, H_{rim}), 7.12 - 7.09 (m, 4H, H_{rim}), 4.78 (s, 1H, $H_{cp\text{-}sub}$), 4.74 (1/2 AB, ^{2}J = 19.0 Hz, 1H), 4.74 (1/2 AB, ^{2}J = 19.0 Hz, 1H), 4.70 (1/2 AB, ^{2}J = 19.0 Hz, 1H), 4.64 (s, 1H, H_{rim}), 4.39 (s, 1H, H_{rim}), 4.34 (s, 1H, H_{rim}), 3.55 (1/2 AB, ^{2}J = 19.0 Hz, 1H), 3.46 (1/2 AB, ^{2}J = 19.0 Hz, 1H), 3.43 ppm (1/2 AB, ^{2}J = 19.0 Hz, 1H); **^{13}C-NMR** (125 MHz, $CDCl_3$): δ = 135.86 (1C, $C_{ipso\text{-}sum}$), 123.44 (1C, CH_{arom}), 123.28 (1C, CH_{arom}), 123.09 (1C, CH_{arom}), 122.94 (1C, CH_{arom}), 121.71 (1C, CH_{arom}), 149.53 (1C, C_{flank}), 149.15 (1C, C_{flank}), 149.10 (1C, C_{hub}), 149.00 (1C, C_{flank}), 148.71 (1C, C_{hub}), 148.67 (1C, C_{hub}), 148.60 (1C, C_{flank}), 168.57 (1C, C_{hub}), 148.49 (1C, C_{flank}), 148.37 (1C, C_{hub}), 146.76 (1C, C_{hub}), 144.29 (1C, C_{flank}), 85.50 (1C, $C_{ipso\text{-}cp}$), 69.64 (5C, C_{cp}), 67.82 (2C, $C_{cp\text{-}sub}$), 67.66 (2C, $C_{cp\text{-}sub}$), 42.65 (1C, $\underline{C}H_2$), 41.68 (1C, $\underline{C}H_2$), 41.52 ppm (1C, $\underline{C}H_2$);). **FT-IR:** ν = 3094 (w, shr),

3040 (w, shr), 2897 (w, shr), 2424 (w, shr), 2244 (w, shr), 1720 (w, shr), 1633 (w, shr), 1563 (w, shr), 1489 (w, shr), 1452 (w, shr), 1395 (m, shr), 1377 (w, shr), 1343 (w, shr), 1260 (w, shr), 1260 (w, shr), 1229 (w, shr), 1179 (w, shr), 1149 (w, shr), 1075 (w, shr), 1032 (m, shr), 998 (m, shr), 921 (w, shr), 902 (m, shr), 826 (m, shr), 807 (w, shr), 783 (s, shr), 755 (vw, shr), 730 (m, shr), 682 (w, shr), 664 (w, shr), 644 (w, shr), 609 (m, shr), 590 (vw, shr), 559 (vw, shr), 535 cm^{-1} (vw, shr); **EI-MS:** m/z = 448.0926 (100 %, $[M]^{+\cdot}$, found), 448.0914 (calc'd), 326 (14 %, $[cp\text{-}C_{21}H_{11}]^{+\cdot}$), 224 (8 %, $[M]^{2+}$).

8.3.4 1-Corannulenyl-1'-neopentylferrocene (25)

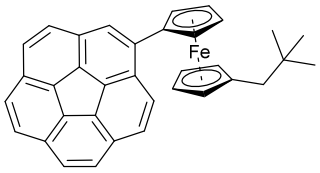

25

1-Bromo-1'-neopentylferrocene (**12**) (83 mg, 0.25 mmol, 1.6 eq) was dissolved in THF (2 mL) and cooled to -30 °C. *n*-Butyllithium (0.11 mL, 2.5M in *n*-hexane, 1.8 eq) was added dropwise. After stirring for 30 min at -30 °C anhydrous zinc(II) chloride (100 mg, 0.74 mmol, 3 eq) was added in one batch and stirring at -30 °C was continued for 30 min. The reaction mixture was warmed to RT and stirred for further 30 min. Monoiodocorannulene (**18**) (56 mg, 0.15 mmol, 1 eq), palladium(II) acetate (3 mol%) and triphenylphosphane (6 mol%) were added in one batch and the red reaction mixture was stirred at 80 °C for 17 h. The solvent was removed and the residue was purified by column chromatography on silica gel with *n*-pentane/dichloromethane (40:1) including 1 % triethyl-amine. The product was obtained as a deep red solid 44 mg (57 %) from the fourth fraction.

M.p. 61 °C; **^{1}H-NMR** (700 MHz; CD_2Cl_2): δ = 8.15 (AB, ^{3}J = 8.8 Hz, 2H, H_{rim}), 8.06 (s, 1H, H_{rim}), 7.88-7.81 (m, 6H, H_{rim}), 4.89 (s, 2H, H_{cp}), 4.42 (s, 2H, H_{cp}), 4.07 (s, 2H, H_{cp}), 4.06 (s, 2H, H_{cp}), 2.22 (s, 2H, C$\underline{H}_2$), 0.74 ppm (s, 9H, C$\underline{H}_3$); **^{13}C-NMR** (175 MHz, CD_2Cl_2): δ = 140.07 (1C, C_{ipso}), 136.48 (1C, C_{hub}), 136.41 (1C, C_{hub}), 136.14 (1C, C_{hub}), 136.02 (1C, C_{hub}), 134.92 (1C, C_{hub}), 131.55 (1C, C_{spoke}), 131.48 (1C, C_{spoke}), 131.12 (1C, C_{spoke}), 130.95 (1C, C_{spoke}), 130.39 (1C, C_{spoke}), 128.15 (1C, CH_{rim}), 127.83 (1C, CH_{rim}), 127.74 (1C, CH_{rim}), 127.65 (1C, CH_{rim}), 127.41 (1C, CH_{rim}), 127.32 (1C, CH_{rim}), 127.25 (1C, CH_{rim}), 127.22 (1C, CH_{rim}), 124.85 (1C, CH_{rim}), 87.82 (1C, C_{cp}), 85.30 (1C, C_{cp}), 72.50 (2C, C_{cp}), 70.93 (2C, C_{cp}), 70.47 (2C, C_{cp}), 70.34 (2C, C_{cp}), 45.01 (1C, $\underline{C}H_2$), 32.06 (1C, $\underline{C}(CH_3)_3$), 29.59 ppm (3C, $\underline{C}H_3$); **FT-IR:** ν = 3081 (w, br), 3027 (w, br), 2946 (m, shr), 2946 (m, shr), 2861 (m, shr), 1896 (w, br), 1617 (w, br), 1474 (m, shr), 1463 (m, shr), 1433 (w, shr), 1407 (w, shr), 1390 (m, shr), 1361 (m, shr), 1229 (m, shr), 1199 (w, shr), 1132 (w, shr), 1084 (w, shr), 1042 (m, shr), 1025 (m, shr), 953 (w, shr), 907 (m, shr), 872 (m, shr), 825 (s, shr), 749 (s, shr), 698 (m, shr), 666 (m, shr), 655 (m, shr), 643 (m, shr), 613 (w, shr), 583 (m, shr), 563 (m, shr), 541 cm^{-1} (m, shr); **ESI-MS:** m/z = 540.1570 (M^+, found), 504.1540 (M^+, calc'd).

8.3.5 1-Corannulenyl-1'-(ferrocenyl)benzene (26)

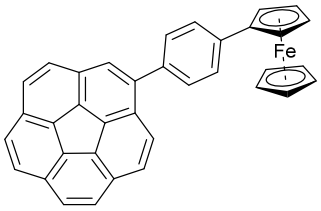

26

1-Iodo-4-ferrocenylbenzene (**13**) (163 mg 0.42 mmol, 2 eq) was dissolved in THF (2 mL) and cooled to -20 °C. *n*-Butyllithium (0.2 ml, 2.5M in *n*-hexane, 2.4 eq) was added dropwise and the reactions mixture was stirred at -20 °C for 30 min. Anhydrous zinc(II) chloride (100 mg, 0.73 mmol, 3.5 eq) was added in one batch and stirring at -20 °C was continued for 30 min. After stirring at RT for 30 min palladium(II) acetate (1 mol%), triphenylphosphane (2 mol%) and monoiodocorannulene (**18**) (80 mg, 0.21 mmol, 1 eq) were added and the orange reaction mixture was stirred at 60 °C for 48 h. Water (20 mL) and dichloromethane (20 mL) were added. The organic layer was separated, washed with water (4 x 30 ml) and dried with sodium sulfate. Column chromatography on silica gel using *n*-pentane/dichloromethane (4:1) as solvent yielded **26** (61 mg, 56 %) as an orange solid. Crystals were grown by evaporation of a dichloromethane/ethanol solution.

M.p. 223 °C (decomposition); **^{1}H NMR** (700 MHz, $CDCl_3$): δ = 7.95 (s, 1H, H_{rim}), 7.92 (d, ^{3}J = 8.8 Hz, 1H), 7.90 – 7.81 (m, 7H), 7.76 (d, ^{3}J = 7.8 Hz, 2H), 7.69 (d, ^{3}J = 7.8 Hz, 2H), 4.78 (s, 2H), 4.42 (s, 2H), 4.17 ppm (s, 5H); **^{13}C NMR** (176 MHz, $CDCl_3$): δ = 141.74 (1C, $C_{ipso\ ph\text{-}cor}$), 139.06 (1C, $C_{ipso\ ph\text{-}fc}$), 137.26 (1C, $C_{ipso\ cor\text{-}ph}$), 136.42 (1C, C_{hub}), 136.24 (1C, C_{hub}), 135.90 (1C, C_{hub}), 135.49 (1C, C_{hub}), 135.28 (1C, C_{hub}), 131.00 (1C, C_{spoke}), 130.95 (1C, C_{spoke}), 130.90 (1C, C_{spoke}), 130.71 (1C, C_{spoke}), 130.01 (1C, C_{ph}), 129.75 (1C, CH_{rim}), 127.39 (1C, CH_{rim}), 127.39 (1C, CH_{rim}), 127.27 (1C, CH_{rim}), 127.13 (1C, CH_{rim}), 127.04 (1C, CH_{rim}), 126.97 (1C, CH_{rim}), 126.95 (1C, CH_{rim}), 126.49 (s, C_{ph}), 125.41 (1C, CH_{rim}), 85.00 (s, $C_{cp\text{-}ipso}$), 69.74 (1C, C_{cp}), 69.16 ppm (1C, C_{cp}), 66.68 ppm (s, C_{cp}); **FT-IR:** ν = 3027 (w, shr), 2923 (w, shr), 1607 (w, shr), 1526 (w, shr), 1409 (m, shr), 1312 (m, shr), 1260 (m, shr), 1103 (m, shr), 1084 (m, shr), 1018 (m, shr), 1000 (m, shr), 888 (m, shr), 826 (s, shr), 807 (m, shr), 693 (m, shr), 663 (m, shr), 624 (m, shr), 572 (m, shr), 546 cm^{-1} (m, shr); **ESI-MS:** m/z = 510.1071 ($[M]^+$, found), 510.1071 ($[M]^+$, calc'd).

8.3.6 Ferrocenylethynylcorannulene (29)

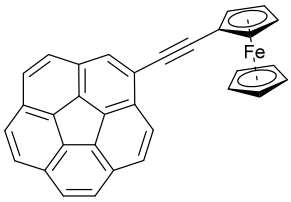

29

Monoiodocorannulene (**18**) (73 mg, 0.27 mmol, 1 eq), potassium *tert*-butoxide (65 mg, 0.53 mmol, 2 eq), ethynylferrocene (**28**) (67 mg, 0.32 mmol, 1.2 eq) and 1 mol% tris(dibenzylideneacetone)dipalladium(0) were dissolved in anhydrous THF (1.7 mL) and heated for 4 h at 80 °C (a colour change from orange to dark red was observed after several min.). The reaction mixture was cooled to RT, dichloromethane (20 mL) was added and the red solution was washed with water (3 x 20 mL). After drying with sodium sulfate, filtration and evaporation of the solvent, a red oil was obtained. Column chromatography with cyclohexane on silica gel afforded the pure compound the red solid **29** (73 mg, 72 %) as the fourth fraction.

M.p. 208-211 °C; **^{1}H-NMR** (400 MHz; $CDCl_3$): δ = 7.99 (AB, ^{3}J = 8.7 Hz, 2H, H_{rim}), 7.97 (s, 1H, H_{rim}), 7.83-7.75 (m, 6H H_{rim}), 4.70 (s, 2H, $H_{cp\text{-}sub}$), 4.38 (s, 2H, $H_{cp\text{-}sub}$), 4.36 ppm (s, 5H, H_{cp}); **^{13}C-NMR** (175 MHz, $CDCl_3$): δ = 136.31 (1C, C_{hub}), 135.97 (1C, C_{hub}), 135.92 (1C, C_{hub}), 135.42 (1C, C_{hub}), 135.17 (1C, C_{hub}), 131.28 (1C, C_{spoke}), 131.21 (1C, C_{spoke}), 131.18 (1C, C_{spoke}), 131.12 (1C, C_{spoke}), 130.75 (1C, C_{spoke}), 130.52 (1C, CH_{rim}), 127.65 (1C, CH_{rim}), 127.56 (1C, CH_{rim}), 127.50 (1C, CH_{rim}), 127.38 (1C, CH_{rim}), 127.27 (1C, CH_{rim}), 127.26 (1C, CH_{rim}), 126.79 (1C, CH_{rim}), 126.30 (1C, CH_{rim}), 122.38 (1C, $C_{cor\text{-}ipso}$), 92.79 (1C, C_{ethyn}), 84.31 (1C, C_{ethyn}), 72.18 (2C, C_{cp}), 70.80 (5C, C_{cp}), 69.86 ppm (2C, C_{cp}); **FT-IR:** ν = 3092 (w, shr), 3027 (w, br), 2921 (mid, shr), 2850 (w, shr), 2207 (mid, shr), 1621 (w, shr), 1480 (w, shr), 1428 (w, shr), 1408 (mid, shr), 1261 (w, shr), 1104 (m, shr), 1047 (m, shr), 999 (m, shr), 923 (m, shr), 879 (s, shr), 819 (s, shr), 762 (m, shr), 688 (m, shr), 637 (m, shr), 626 (m, shr), 566 cm^{-1} (m, shr); **EI-MS (170 °C):** m/z = 458.0738 ($[M]^{+\cdot}$, found), 458.0759 ($[M]^{+\cdot}$, calc'd), 337 ($[M]^{+\cdot}$-C_5H_5Fe, 24 %), 250 ($[M]^{+\cdot}$-$C_{12}H_9Fe$, 31 %) 124 ($[M]^{+\cdot}$-$C_{12}H_9Fe$].

8.3.7 1-Corannulenylethyny-1',2,2',3,3',4,4',5-octamethylferrocene (30)

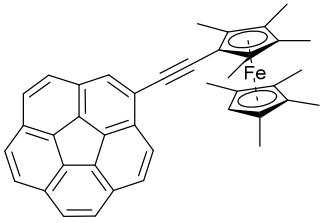

30

Monoiodocorannulene (**18**) (57 mg, 0.15 mmol, 1 eq), potassium *tert*-butoxide (66 mg, 0.54 mmol, 3.6 eq) and tris(dibenzylideneacetone)dipalladium(0) (3.5 mol%) were dissolved in DMF (2 mL) and water was added (0.4 mL). After degassing three times 1-ethynyl-1',2,2',3,3',4,4',5-octamethylferrocene (**6**) (97 mg, 0.30 mmol, 2 eq) was added. The yellow slurry was heated to 80 °C while turning from yellow to red, finally to purple and was stirred at that temperature for 5 h. The solvent was removed and the residue was subjected to column chromatography on basic alumina (activity level 1) with *n*-pentane/toluene (10:1) as solvent. The product was obtained as a dark purple solid (40 mg, 47 %).

M.p. the compound appears nearly black in solid state, no melting point could be observed up to 300 °C; **^{1}H-NMR** (400 MHz; $CDCl_3$): δ = 7.99 (s, 1H, H_{rim}), 7.95 (AB, ^{3}J = 8.8 Hz, 2H, H_{rim}), 7.46-7.39 (m, 4H, H_{rim}), 7.35 (AB, ^{3}J = 8.8 Hz, 2H, H_{rim}), 3.26 (s, 1H, H_{cp}), 2.07 (s, 6H, $C\underline{H}_3$), 1.73 (s, 6H, $C\underline{H}_3$), 1.67 (s, 6H, $C\underline{H}_3$), 1.66 ppm (s, 6H, $C\underline{H}_3$); **^{13}C-NMR** (175 MHz, C_6D_6): δ = 136.63 (1C, C_{hub}), 136.44 (1C, C_{hub}), 136.30 (1C, C_{hub}), 135.94 (1C, C_{hub}), 135.20 (1C, C_{hub}), 131.59 (1C, C_{spoke}), 131.47 (1C, C_{spoke}), 131.42 (1C, C_{spoke}), 131.28 (1C, C_{spoke}), 129.95 (1C, C_{spoke}), 129.33 (1C, $C_{cor\ ipso}$), 128.35 (1C, CH_{rim}), 127.99 (1C, CH_{rim}), 127.66 (1C, CH_{rim}), 127.53 (1C, CH_{rim}), 127.42 (1C, CH_{rim}), 127.29 (1C, CH_{rim}), 126.93 (1C, CH_{rim}), 126.50 (1C, CH_{rim}), 123.89 (1C, C), 93.88 (1C, C_{ethyn}), 88.87 (1C, C_{ethyn}), 82.61 (2C, C_{cp}) 82.60 (2C, C_{cp}), 81.54 (2C, C_{cp}), 81.29 (1C, C_{cp}), 72.18 (2C, C_{cp}), 65.49 (1C, C_{cp}), 11.21 (2C, $\underline{C}H_3$), 11.15 (2C, $\underline{C}H_3$), 10.21 (2C, $\underline{C}H_3$), 9.27 ppm (2C, $\underline{C}H_3$); **FT-IR:** ν = 3033 (w, br), 2962 (w, shr), 2941 (w, shr), 2896 (m, br), 2851 (w, shr), 2188 (m, shr), 1497 (w, shr), 1421 (w, shr), 1374 (m, shr), 1367 (m, shr), 1323 (m, shr), 1260 (w, shr), 1240 (w, shr), 1221 (m, shr), 1129 (w, shr), 1106 (w, shr), 1028 (m, shr), 951 (m, shr), 872 (m, shr), 831 (s, shr), 815 (m, shr), 751 (m, shr), 685 (m, shr), 652 (m, shr), 627 (m, shr), 618 (m, shr), 595 (m, shr), 587 (m, shr), 556, 536 cm^{-1} (m, shr); **ESI-MS:** m/z = 570.1988 ($[M]^+$, found), 570.2010 ($[M]^+$, calc'd).

8.3.8 (*E*)-1-(2-Ferrocenyl)ethenyl)corannulene (31)

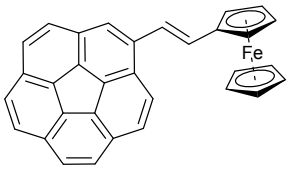

31

Monoiodocorannulene (**18**) (92 mg, 0.24 mmol, 1 eq), vinylferrocene (**2**) (34 mg, 0.26 mmol, 1.1 eq), palladium(II) acetate (10 mol%), potassium acetate (36 mg, 0.37 mmol, 1.5 eq) and tetra-*n*-butylammonium bromide (47 mg, 0.24 mmol, 1 eq) were dissolved in anhydrous DMF (2.8 mL). After degassing three times the reaction mixture was heated for 15 h at 80 °C. After cooling to RT, dichloromethane (20 mL) was added and the dark red solution was washed with water (3 x 100 mL). Drying with sodium sulfate, filtration and evaporation of the solvent and PTLC on silica gel with *n*-pentane/dichloromethane (3:1) afforded **31** (40 mg, 60 %) as a red solid from the third fraction.

M.p. 199.5 °C; **^{1}H NMR (700 MHz; CD_2Cl_2):** δ = 8.04 (AB, ^{3}J = 8.8 Hz, 2H, H_{rim}), 7.88-7.81 (m, 7H, H_{rim}), 7.39-7.32 (AB, ^{3}J = 16 Hz, 2H, H_{vinyl}), 4.63 (s, 2H, $H_{cp\text{-}sub}$), 4.39 (s, 2H, $H_{cp\text{-}sub}$), 4.23 ppm (s, 5H, H_{cp}); **^{13}C-NMR (175 MHz, CD_2Cl_2):** δ = 138.90 (1C, C_{ipso}), 136.71 (1C, C_{hub}), 136.56 (1C, C_{hub}), 136.21 (1C, C_{hub}), 136.13 (1C, C_{hub}), 132.45 (1C, CH_{vinyl}), 131.93 (1C, C_{spoke}), 131.68 (1C, C_{spoke}), 131.40 (1C, C_{spoke}), 131.21 (1C, C_{spoke}), 129.63 (1C, C_{spoke}), 127.94 (1C, CH_{rim}), 127.85 (1C, CH_{rim}), 127.72 (1C, CH_{rim}), 127.59 (1C, CH_{rim}), 127.44 (1C, CH_{rim}), 127.34 (1C, CH_{rim}), 126.36 (1C, CH_{rim}), 124.06 (1C, CH_{rim}), 123.42 (1C, CH_{rim}), 83.99 (1C, $C_{cp\text{-}ipso}$), 70.08 (2C, C_{cp}), 69.95 (5C, C_{cp}), 67.79 (2C, C_{cp}); FT-IR: ν =3085 (w, br), 3030 (m, shr), 2847 (m, shr), 1891 (w, shr), 1723 (m, shr), 1610 (m, shr), 1459 (m, shr), 1409 (m, shr), 1310 (m, shr), 1267 (m, shr), 1246 (m, shr), 1778 (m, shr), 1135 (m, shr), 1043 (m, shr), 1027 (m, shr), 995 (m, shr), 812 (s, shr), 742 (s, shr), 682 (m, shr), 557 cm^{-1} (m, shr); EI-MS (170 °C): m/z = 460.0894 (100 %, $[M]^{+\cdot}$,found), 460.0914 (calc'd), 337 (71 %), 395 (15 %, $[M]^{+\cdot}$-C_5H_5), 121 (10 %, $[CpFe]^{+}$), 56 (4 %, Fe^{+}).

8.3.9 1-((1*E*,3*E*)-4-(Ferrocenyl)buta-1,3-dienyl)corannulene (32)

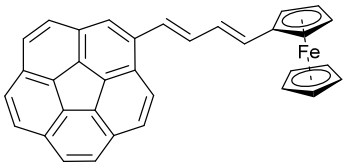

32

Monoiodocorannulene (**18**) (67 mg, 0.18 mmol, 1 eq), butadienyl ferrocene (**5**) (47 mg, 0.20 mmol, 1.1 eq), potassium acetate (44 mg, 0.45 mmol, 2.5 eq), tetra-*n*-butylammonium bromide (57 mg, 0.18 mmol, 1 eq) and palladium(II) acetate (5 mol%) were dissolved in DMF (3 mL). After degassing three times, the dark red solution is stirred at 80 °C for 24 h. After cooling to RT dichloromethane (10 mL) was added and the organic layer was washed with water (3 x 10 mL). After drying over sodium sulfate, filtration and evaporation of the solvent, column chromatography on silica gel with *n*-pentane/ethyl acetate (20:1) afforded a red solid. Purification by preparative TLC on alumina (type T) with *n*-pentane/toluene (1:1) yielded **32** (53 mg, 70 %) from the third fraction.

M.p. 207.8 °C; **^{1}H NMR** (700 MHz; CD_2Cl_2): δ = 7.99 (AB, ^{3}J = 8.7 Hz, 2H, H_{rim}), 7.85-7.77 (m, 7H, H_{rim}), 7.29-7.16 (m, 2H, $H_{butadienyl}$), 6.73-6.59 (m, 2H, $H_{butadienyl}$), 4.51 (s, 2H, $H_{cp\text{-}sub}$), 4.36 (s, 2H, $H_{cp\text{-}sub}$), 4.20 ppm (s, 5H, H_{cp}); **^{13}C-NMR** (175 MHz, CD_2Cl_2): δ = 138.07 (1C, C_{ipso}), 136.42 (1C, C_{hub}), 136.15 (1C, C_{hub}), 135.87 (1C, C_{hub}), 135.76 (1C, C_{hub}), 135.74 (1C, C_{hub}), 133.74 (1C, $CH_{butadiene}$), 132.94 (1C, $CH_{butadiene}$), 131.24 (1C, C_{spoke}), 131.12 (1C, C_{spoke}), 130.88 (1C, C_{spoke}), 130.75 (1C, C_{spoke}), 129.18 (1C, C_{spoke}), 127.89 (1C, CH_{rim}), 127.89 (1C, CH_{rim}), 127.64 (1C, CH_{rim}), 127.49 (1C, CH_{rim}), 127.48 (1C, CH_{rim}), 127.40 (1C, CH_{rim}), 127.40 (1C, CH_{rim}), 127.25 (1C, CH_{rim}), 127.16 (1C, CH_{rim}), 127.01 (1C, CH_{rim}), 126.89 (1C, CH_{rim}), 125.81 (1C, $CH_{butadiene}$), 123.50 (1C, $CH_{butadiene}$), 83.59 (1C, $C_{cp\text{-}ipso}$), 69.71 (C_{cp}), 69.64 (C_{cp}), 67.22 ppm (C_{cp}); **FT-IR:** ν = 3039 (w, br), 3023 (mid, shr), 2956 (w, shr), 2922 (m, shr), 2849 (m, shr), 1897 (w, br), 1606 (m, shr), 1429 (m, shr), 1409 (m, shr), 1323 (w, shr), 1305 (w, shr), 1260 (m, shr), 1235 (m, shr), 1221 (m, shr), 1133 (m, shr), 1104 (s, shr), 1022 (s, shr), 927 (m, shr), 879 (m, shr), 864 (m, shr), 814 (s, shr), 783 (m, shr), 735 (m, shr), 681 (m, shr), 618 (m, shr), 563 cm^{-1} (m, shr); **EI-MS (200 °C):** m/z = 186 (100 %, $[C_{10}H_{10}Fe]^{+\cdot}$), 486.1055 (63 %, $[M]^{+\cdot}$, found), 486.1071 (calc'd), 363 (30 %, $[M]^{+\cdot}$-2H), 121 (12 %, $CpFe^{+}$), 300 (9 %, $[M]^{+\cdot}$-Fc), 421 (6 %, $[M]^{+\cdot}$-Cp), 56 (4 %, Fe^{+}).

8.3.10 1,1'-Dicorannulenylferrocene (33)

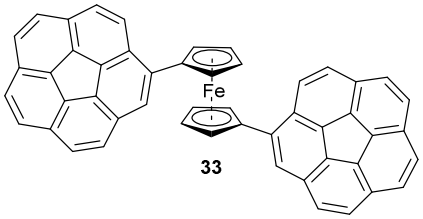

33

In a 25 mL Schlenk tube a solution of 1,1'-dibromoferrocene (**10**) (50 mg, 0.15 mmol, 1 eq) in THF (2 mL), degassed and after cooling to -70 °C *n*-butyllithium in *n*-hexane (0.18 mL, 2.5M, 3 eq) was added dropwise. After stirring for 1 h at RT and then cooling to -30 °C, dry zinc(II) chloride (70 mg, 0.51 mmol, 3.5 eq) was added in one portion. The mixture was stirred at RT for 1 h. Upon addition of monoiodocorannunene (**18**) (121 mg, 0.32 mmol, 2.2 eq), palladium(II) acetate (2.5 mol%) and triphenylphosphane (5 mol%) the orange mixture underwent a color changed to deep red and was stirred for 12 h at 70 °C. The reaction mixture was transferred to a separation funnel using dichloromethane (20 mL) and washed with water (4 x 100 mL). After drying with anhydrous sodium sulfate and filtration the crude product was purified by column chromatography on silica gel with *n*-pentane/dichloromethane (3:1). **33** was obtained as red solid (40 mg, 40 %).

M.p. 237 °C (decomposition); **^{1}H NMR** (700 MHz, CD_2Cl_2): δ = 8.16 (d, ^{3}J = 8.7 Hz, 2H, H_{rim}), 8.10 (s, 2H, H_{rim}), 7.66-7.37 (m, 12H, H_{rim}), 7.26 (d, ^{3}J = 8.5 Hz, 2H, H_{rim}), 5.03-4.58 ppm (m, 8H, H_{cp}); **^{13}C NMR** (176 MHz, CD_2Cl_2): δ = 137.13 (2C, C_{ipso}), 136.05 (2C, C_{hub}), 135.54 (2C, C_{hub}), 135.45 (2C, C_{hub}), 135.31 (2C, C_{hub}), 134.15 (2C, C_{hub}), 130.62 (2C, C_{spoke}), 130.53 (2C, C_{spoke}), 130.30 (2C, C_{spoke}), 130.23 (2C, C_{spoke}), 129.60 (2C, C_{spoke}), 127.51 (2C, CH_{rim}), 127.45 (2C, CH_{rim}), 127.44 (2C, CH_{rim}), 127.31 (2C, CH_{rim}), 127.09 (2C, CH_{rim}), 127.05 (2C, CH_{rim}), 126.99 (2C, CH_{rim}), 126.60 (2C, CH_{rim}), 125.10 (2C, CH_{rim}), 71.37 (4C, $C_{cp\text{-}sub}$), 71.12 (4C, $C_{cp\text{-}sub}$), 63.34 ppm (2C, $C_{cp\text{-}ipso}$); **IR**: ν = 2918 (m, shr), 2853 (m, shr), 1892 (vw, shr), 1723 (m, shr), 1620 (w, shr), 1513 (m, shr), 1462 (m, shr), 1313 (m, shr), 1258 (m, shr), 1138 (m, shr), 1020 (m, shr), 863 (m, shr), 814 (s, shr), 739 (m, shr), 690 (m, shr), 659 (m, shr), 538 (s, shr) cm^{-1}; **EI-MS** (250 °C): m/z = 682.1364 ($[M]^{+\cdot}$, found), 682.1385 ($[M]^{+\cdot}$, calc'd), 313 (35 %, $[C_{25}H_{13}]^{+\cdot}$), 341 (17 %, $[M]^{2+}$).

8.3.11 1,1'-Disumanenylferrocene (34)

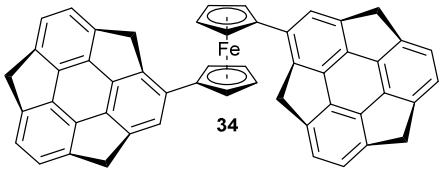

34

1,1'-Dibromoferrocene (**10**) (18 mg, 51.3 µmol, 1 eq) was dissolved in THF (0.5 mL). The orange solution was cooled to -30 °C. *n*-Butyllithium (0.1 mL, 2.5M in *n*-hexane, 2.5 eq) was added, orange precipitate appeared and stirring at -30 °C was continued for 30 min. After stirring for 15 min at RT the precipitate dissolved and the red solution was again cooled to -30 °C. Anhydrous zinc(II) chloride (21 mg, 0.15 mmol, 3 eq) was added at once. After stirring at -30 °C for 30 min and at RT for 30 min, palladium(II) acetate (5 mol%) and triphenylphosphane (10 mol%) were added. Monoiodosumanene (**19**) (44 mg, 0.11 mmol, 2.2 eq) was dissolved in 1 mL dry THF and added *via* syringe. The Schlenk tube was sealed and heated in an oil bath for 24 h at 70 °C. Afterwards the solvent was removed; column chromatography on silica gel was conducted with *n*-pentane/dichloromethane (3:1) as eluting solvents which yielded the red **34** (4 mg, 11%) as the last (fifth) fraction. Crystals suitable for X-ray analysis were grown from a 1:1 mixture of chloroform and dichloromethane by slow evaporation.

M.p. 158 °C (decomposition); **^{1}H-NMR** (400 MHz, $CDCl_3$): δ = 7.07 (d, ^{3}J = 6.3 Hz, 1H, H_{rim}), 7.03 - 6.84 (m, 3H, H_{rim}), 6.79 (d, ^{3}J = 6.6 Hz, 1H), 5.29 - 4.84 (br, 3H), 4.78 – 4.59 (br, 1H), 4.59 (d, 2*J* = 19.3 Hz, 1H), 4.51 (d, ^{2}J = 19.3 Hz, 1H), 4.31 – 4.11 (br, m, 1H), 3.67 – 3.44 (br, 1H), 3.22 (d, 2*J* = 19.4 Hz, 1H), 3.10 ppm (d, ^{2}J = 19.3 Hz, 1H). **^{13}C-NMR** (175 MHz, CD_2Cl_2): δ = 149.25 (2C, C_{flank}), 149.07 (2C, C_{flank}), 148.72 (2C, C_{hub}), 148.63 (2C, C_{hub}), 148.58 (2C, C_{hub}), 148.49 (2C, C_{hub}), 148.38 (2C, C_{flank}), 148.29 (2C, C_{flank}), 148.23 (2C, C_{flank}), 148.15 (2C, C_{flank}), 148.05 (2C, C_{hub}), 123.76 (2C, CH_{rim}), 123.62 (2C, CH_{rim}), 123.52 (2C, CH_{rim}), 123.23 (2C, br, CH_{rim}), 122.98 (2C, br, CH_{rim}), 71.28 (4C, $C_{cp\text{-}sub}$), 68.30 (4, $C_{cp\text{-}sub}$), 42.20 (2C, $\underline{C}H_2$), 41.69 (2C, $\underline{C}H_2$), 41.66 ppm (2C, $\underline{C}H_2$). Due to the very low solubility of **34** the signals for both *ipso*-carbons and one hub carbon could not be assigned. **FT-IR:** ν = 3098 (w, br), 3044 (vw, br), 2921 (m, shr), 2853 (w, shr), 2360 (w, br), 2246 (vw, br), 1862 (vw, br), 1725 (w, br), 1637 (w, shr), 1572 (w, br), 1492 (vw, shr), 1455 (w, br), 1395 (w, shr), 1379 (w, shr), 1346 (vw, shr), 1261 (w, shr), 1232 (vw, shr), 1208 (vw, shr), 1181

(w, shr), 1152 (vw, shr), 1109 (vw, shr), 1080 (w, shr), 1036 (w, shr), 1000 (w, shr), 966 (vw, shr), 922 (w, shr), 904 (w, shr), 828 (vw, shr), 786 (m, shr), 756 (vw, shr), 731 (m, shr), 683 (vw, shr), 665 (vw, shr), 646 (vw, shr), 610 cm^{-1} (m, shr); **EI-MS:** m/z = 710.1705 (100 %, $[M]^{+\cdot}$, found), 710.1697 (calc'd), 326 (15 %, $[cp\text{-}C_{21}H_{11}]^{+\cdot}$).

8.3.12 Attempts to Synthesize 1,2-Dicorannulenylferrocene (35)

NCC-approaches: 1,2-Dibromoferrocene (32 mg, 0.09 mmol, 1 eq) was dissolved in THF (1.5 mL). This solution was cooled to **(a)** -70 °C, **(b)** -30 °C, **(c)** -78 °C and **(a,b)** *n*-butyllithium or **(c)** tert-butyllithium (0.11 mL, 2.5 M, 3 eq) was added dropwise. The reaction mixture was allowed to warm to RT and was stirred for 1 h. After cooling to -30 °C anhydrous zinc(II) chloride (44 mg, 0.32 mmol, 3.5 eq) was added and the orange mixture was stirred for 30 min at -30 °C and 15 min at RT. Monoiodocorannulene (76 mg, 0.20 mmol, 2.2 eq), palladium(II) acetate (2.5 mol%) and triphenylphosphane (5 mol%) was added and the reaction mixture was stirred at 70 °C for 17 h. The solvent was removed and column chromatography on silica gel with *n*-pentane/dichloromethane (3:1) and 1 % triethylamine was conducted.

(a) The first fraction contained a mixture of corannulene (^{1}H NMR (400 MHz, $CDCl_3$): δ = 7.81 (s, 10 H)) and monoiodocorannulene (**18**). The second fraction afforded a complex ^{1}H NMR spectrum. EI-Mass measurements were conducted: **EI-MS:** m/z = 512 (100 %, $[C_{30}H_{17}BrFe]^{+\cdot}$), 434 (77 %, $[C_3H_{18}Fe]^{+\cdot}$), 375 (73 %, $[C_{20}H_9I]^{+\cdot}$), 212 (5 %, $[C_5H_5Fe]^+$).

(b) The first fraction contained corannulene (**16**), monoiodocorannulene (**18**) and 1,2-dibromoferrocene (**10**) (^{1}H NMR (400 MHz, $CDCl_3$): δ = 4.44 (s, 2H, $H_{cp\text{-}sub}$), 4.25 (s, 5H, H_{cp}), 4.11 ppm (s, 1H, $H_{cp\text{-}sub}$)). The second and third fraction contained corannulene, monoiodoferrocene and ferrocene and traces of 1-bromo-2-corannulenylferrocene (**37**). (**^{1}H NMR** (400 MHz, $CDCl_3$): δ = 8.42 (s, 1H, H_{rim}), 7.92 – 7.75 (m, 8H, H_{rim}), 4.74 (s, 2H, $H_{cp\text{-}sub}$), 4.68 (s, 1H, $H_{cp\text{-}sub}$), 4.41 ppm (s, 5H, H_{cp}).)

The second and third fraction were combined and PTLC on silica gel with *n*-pentane/dichloromethane (3:1) was conducted. The first fraction contained pure corannulene. The other fractions contained monoiodocorannulene (**18**) and the monosubstituted derivative (**37**) Recrystallization from *n*-hexane gave 5 mg monoidocorannunlene and a mixture of corannulenylferrocene and 1-bromo-2-corannulenylferrocene (**37**).

(c) All fractions contained only corannulene (**16**), monoiodocorannulene (**18**) and ferrocene (**1**).

Suzuki approaches: 1,2-Dibromoferrocene (**36**) (15 mg, 0.04 mmol, 1 eq), 2-(corannulenyl)-4,4,5,5-tetramethyl-1,3,2-dioxaborolane (35 mg, 0.09 mmol, 2.2 eq), palladium(II) acetate (8 mg, 0.037 mmol, 0.8 eq), 1,1'-bis(diphenylphosphino)ferrocene (21 mg, 0.037 mmol, 0.8 eq) and sodium carbonate (13 mg, 0.13 mmol, 3 eq) were dissolved in a degassed THF/water mixture (3:1, 2 mL) and stirred at 80 °C for 40 h. The solvent was removed and the crude solid was filtrated through silica gel with dichloromethane. For analysis ^{1}H NMR and EI-MS were measured.

The ^{1}H NMR showed clear peaks for ferrocene and 1,2-dibromoferrocene (**36**) traces of aromatic signals were observed between 7.90 - 7.70 ppm. **EI-MS** (30 °C): m/z =128 (100 %), 344 (35 %, $[C_{10}H_8Br_2Fe]^{+\cdot}$), 264 (21 %, $[C_{10}H_9BrFe]^{+\cdot}$).

1,2-Dibromoferrocene (**36**) (15 mg, 0.04 mmol, 1 eq), 2-(corannulenyl)-4,4,5,5-tetramethyl-1,3,2-dioxaborolane (35 mg, 0.09 mmol, 2.2 eq), palladium(II) acetate (3 mol%) SPhos (3 mol%), potassium phosphate (13 mg, 0.12 mmol, 3 eq) were dissolved in a THF/water mixture (10:1, 1.1 mL). The mixture was stirred at 80 °C for 6 d. The solvent was removed and the crude solid was filtrated through silica gel with dichloromethane.

The ^{1}H NMR showed a mixture of ferrocene (**1**) and 1,2-dibromoferrocene (**36**) **^{1}H NMR** (400 MHz, $CDCl_3$): δ = 4.44 (s, 2H, $H_{cp\text{-}sub}$), 4.25 (s, 5H, H_{cp}), 4.11 ppm (s, 1H, $H_{cp\text{-}sub}$).

8.3.13 Attempted Synthesis of 1-Bromo-2-corannulenylferrocene (37)

1,2-Dibromoferrocene (34 mg, 0.10 mmol, 1 eq) was dissolved in THF (1.5 mL). *n*-Butyllithium (0.05 mL, 2.5M, 1.2 eq) was added dropwise at -70 °C. The reaction mixture was stirred at RT for 1 h, then cooled to -30 °C. Anhydrous zinc(II) chloride (27 mg, 0.20 mmol, 2 eq) was added and the orange solution was stirred for 30 min at -30 °C and 30 min at RT. Monoiodocorannulene (**18**) (37 mg, 0.10, 1 eq), palladium(II) acetate (2.5 mol%) and triphenylphosphane (5 mol%) were added and the reaction mixture was heated at 70 °C for 16 h. The solvent was removed and column chromatography on silica gel with *n*-pentane/dichloromethane (3:1) was conducted.

The first fraction contained corannulene and monoiodocorannulene (**18**). The second fraction contained a mixture of corannulenylferrocene (**22**) and 1-bromo-2-corannulenylferrocene (**37**) which could not be separated.

1-Bromo-2-corannulenylferrocene (**37**): ^{1}**H NMR** (400 MHz, $CDCl_3$): δ = 8.42 (s, 1H, H_{rim}), 7.92 – 7.75 (m, 8H, H_{rim}), 4.74 (s, 2H, $H_{cp\text{-}sub}$), 4.68 (s, 1H, $H_{cp\text{-}sub}$), 4.41 ppm (s, 5H, H_{cp}).

8.3.14 1,1‘’‘-Dicorannulenylbiferrocene (39) and Biferrocenylcorannulene (40)

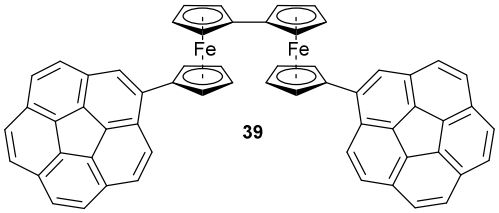

39

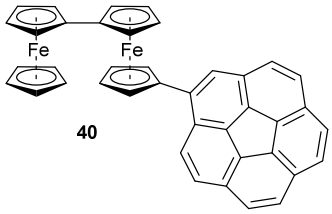

40

In a 10 mL Schlenk tube 1,1‘’‘-dibromobiferrocene (**15**) (45 mg, 0.08 mmol, 1 eq) was dissolved in THF (2.5 mL) and cooled to -70 °C. *n*-Butyllithium (0.10 mL, 2.5M in *n*-hexane, 3 eq) was added. The resulting red slurry was stirred for 1 h at RT, then cooled to -30 °C and anhydrous zinc(II) chloride (40 mg, 0.29 mmol, 3.5 eq) was added and the reaction mixture was stirred at -30 °C for 30 min and at RT for 30 min. Monoiodocorannulene (**18**) (121 mg, 0.32 mmol, 2.2 eq), palladium(II) acetate (5 mol%) and triphenylphosphane (10 mol%) were added and the mixture was stirred at 65 °C for 18 h. The red solution was evaporated on silica gel. Purification by column chromatography with *n*-pentane/dichloromethane (3:1) yielded **40** (7 mg, 13 %) as the second fraction. **39** (20 mg, 28 %) was isolated from the third fraction.

39: M.p. 230 °C (decomposition); **^{1}H NMR** (700 MHz, CD_2Cl_2): δ = 8.22 (d, ^{3}J = 8.7 Hz, 1H, H_{rim}), 7.85 (d, ^{3}J = 8.6 Hz, 1H, H_{rim}), 7.85 - 7.79 (m, 8H, H_{rim}), 7.80 (d, ^{3}J = 8.8 Hz, 1H, H_{rim}), 7.79 (s, 1H, H_{rim}), 7.74 (d, ^{3}J = 8.6 Hz, 1H, H_{rim}), 4.71 (s, 1H, H_{cp}), 4.25 (s, 1H, H_{cp}), 4.08 (s, 1H, H_{cp}), 3.70 ppm (s, 1H, H_{cp}); **^{13}C NMR** (176 MHz, CD_2Cl_2): δ = 138.46 (2C, $C_{ipso\text{-cor-fc}}$), 135.82 (2C, C_{hub}), 135.71 (2C, C_{hub}), 135.46 (2C, C_{hub}), 135.33 (2C, C_{hub}), 134.25 (2C, C_{hub}), 130.85 (2C, C_{spoke}), 130.82 (2C, C_{spoke}), 130.45 (2C, C_{spoke}), 130.30 (2C, C_{spoke}), 129.61 (2C, C_{spoke}), 127.55 (2C, CH_{rim}), 127.11 (2C, CH_{rim}), 127.06 (2C, CH_{rim}), 127.00 (2C, CH_{rim}), 126.76 (2C, CH_{rim}), 126.70 (2C, CH_{rim}), 126.70 (2C, CH_{rim}), 126.56 (2C, CH_{rim}), 124.31 (2C, CH_{rim}), 85.00 (2C, $C_{cp\text{-}ipso}$), 83.97 (2C, $C_{cp\text{-}ipso(fc\text{-}fc)}$), 70.44 (4C, C_{cp}), 70.19 (4C, C_{cp}), 69.18 (4C, C_{cp}), 68.11 ppm (4C, C_{cp}); **FT-IR**: ν = 2954 (m, shr), 2920 (s, shr), 2851 (m, shr), 1737 (m, shr), 1607 (m, shr), 1461 (m, shr), 1427 (m, shr), 1407 (m, shr), 1378 (m, shr), 1260 (m, shr), 1107 (w, shr), 1023 (m, shr), 956 (m, shr), 823 (s, shr), 733 (m, shr), 698 cm^{-1} (m, shr); **EI-MS** (280 °C): m/z = 682 (100 %, $[C_{45}H_{30}Fe_2]^{+\cdot}$), 313 (76 %, $[C_{25}H_{13}]^{+\cdot}$), 368 (39 %,

$[C_{20}H_{16}Fe_2]^{+\cdot}$), 618 (23 %, $[C_{34}H_{21}Fe]^{+\cdot}$), 618 (15 %, $[C_{39}H_{18}Fe_2]^{+\cdot}$), 433 (13 %, $[M]^{2+}$), 866.1326 (11 %, $[M]^{+\cdot}$, found), 866.1363 ($[M]^{+\cdot}$, calc'd) 185 (7 %, $[C_{10}H_9Fe]^{+\cdot}$).

40: M.p. 80 °C; **^{1}H NMR** (700 MHz, CD_2Cl_2): δ = 8.33 (d, ^3J = 8.8 Hz, 1H, H_{rim}), 7.93 – 7.84 (m, 7H, H_{rim}), 7.79 (d, ^3J = 8.6 Hz, 1H, H_{rim}), 4.82 – 4.80 (m, 2H, $H_{cp\text{-}sub}$), 4.40 - 4.38 (m, 2H, $H_{cp\text{-}sub}$), 4.38 - 4.36 (m, 2H, $H_{cp\text{-}sub}$), 4.24 – 4.22 (m, 2H, $H_{cp\text{-}sub}$), 4.22 – 4.20 (m, 2H, $H_{cp\text{-}sub}$), 3.91 (s, 5H, H_{cp}), 3.85 - 3.83 ppm (m, 2H, $H_{cp\text{-}sub}$); **^{13}C NMR** (176 MHz, CD_2Cl_2): δ = 138.70 (1C, $C_{\textit{ipso}}$), 135.87 (1C, C_{hub}), 135.76 (1C, C_{hub}), 135.51 (1C, C_{hub}), 135.37 (1C, C_{hub}), 134.31 (1C, C_{hub}), 130.90 (1C, C_{spoke}), 130.86 (1C, C_{spoke}), 130.51 (1C, C_{spoke}), 130.34 (1C, C_{spoke}), 129.71 (1C, C_{spoke}), 127.58 (1C, CH_{rim}), 127.14 (1C, CH_{rim}), 127.09 (1C, CH_{rim}), 127.03 (1C, CH_{rim}), 126.80 (1C, CH_{rim}), 126.75 (1C, CH_{rim}), 126.72 (1C, CH_{rim}), 126.60 (1C, CH_{rim}), 124.47 (1C, CH_{rim}), 85.60 (1C, $C_{cp\text{-}\textit{ipso}}$), 85.12 (1C, $C_{cp\text{-}\textit{ipso}}$), 70.62 (C, C_{cp}), 70.40 (C, C_{cp}), 69.55 (C, C_{cp}), 69.03 (C, C_{cp}), 68.08 (C, C_{cp}), 67.49 (C, C_{cp}), 66.43 ppm (C, C_{cp}); **FT-IR**: ν = 2954 (m, shr), 2921 (s, shr), 2851 (m, shr), 1658 (m, shr), 1631 (m, shr), 1464 (m, shr), 1425 (m, shr), 1409 (m, shr), 1378 (m, shr), 1261 (m, shr), 1107 (m, shr), 1026 (m, shr), 999 (m, shr), 951 (m, shr), 813 (s, shr), 698 cm^{-1} (m, shr); **EI-MS** (280 °C): m/z = 618.0763 (100 %, $[M]^{+\cdot}$, found), 618.0733 ($[M]^{+\cdot}$, calc'd), 249 (16 %, $[C_{20}H_{19}]^{+\cdot}$), 370 (13 %, $[C_{20}H_{18}Fe_2]^{+\cdot}$), 309 (12 %, $[M]^{2+}$), 185 (7 %, $[C_{10}H_9Fe]^{+\cdot}$).

8.3.15 (*R*)-(+)-N,N-Dimethyl-1-ferrocenylethylaminecorannulen (41)

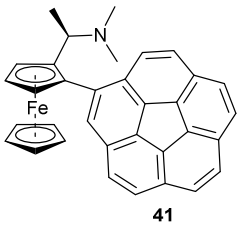

41

Ugi's Amin (**42**) (84 µL, 0.4 mmol, 1 eq) was dissolved in THF (3 mL) and cooled to -78 °C. *Sec*-butyllithium (0.46 ml, 1.3M, 0.6 mmol, 1.5 eq) was added dropwise, the reaction mixture was slowly warmed to RT and then stirred for 1 h. After cooling to -30 °C anhydrous zinc(II) chloride (100 mg, 0.73 mmol, 1.8 eq) was added. The mixture was allowed to warm to RT and stirred for 1 h. Palladium(II) acetate (1 mol%), triphenylphosphane (2 mol%) and monoiododcorannulene (**18**) (100 mg, 0.27 mmol, 0.7 eq) were added and the reaction mixture was stirred at 60 °C for 48 h. The reaction was quenched by addition of water (10 mL). Dichloromethane (30 mL) was added; the organic layer was washed with water (4 x 50 mL), and then dried with sodium sulfate. The crude material was purified by column chromatography on silica gel with a solvent mixture of *n*-pentane/diethyl ether/triethylamine (50:50:3) followed by *n*-pentane/dichoromethane/ triethylamine (50:50:3). The product was obtained as an orange solid (36 mg, 26 %), which was stored at -30 °C but still showed decomposition after several months, resulting in an orange oil.

M.p. 90-92°C; **^{1}H NMR (700 MHz, CD_2Cl_2):** δ= 8.40 (s, 1H, H_{rim}), 8.06 (d, ^{3}J = 8.8 Hz, 1H, H_{rim}), 7.94 – 7.82 (m, 7H, H_{rim}), 4.78 (s, 1H, $H_{cp\text{-}sub}$), 4.55 (t, *J* = 2.5 Hz, 1H, $H_{cp\text{-}sub}$), 4.46 (s, 1H, $H_{cp\text{-}sub}$), 4.27 (s, 5H, H_{cp}), 4.01 (q, ^{3}J = 6.4 Hz, 1H, C<u>H</u>), 1.74 (s, 6H, NC<u>H</u>3), 1.70 (d, ^{3}J = 6.8 Hz, 3H, C<u>H</u>3) ppm; **^{13}C NMR (176 MHz, CD_2Cl_2):** δ = 138.37 (1C, C_{ipso}), 135.94 (1C, C_{hub}), 135.49 (1C, C_{hub}), 135.37 (1C, C_{hub}), 135.16 (1C, C_{hub}), 134.33 (1C, C_{hub}), 131.00 (1C, C_{spoke}), 130.86 (1C, C_{spoke}), 130.64 (1C, C_{spoke}), 130.52 (1C, C_{spoke}), 130.42 (1C, C_{spoke}), 128.85 (1C, CH_{rim}), 127.23 (1C, CH_{rim}), 127.19 (1C, CH_{rim}), 127.08 (1C, CH_{rim}), 127.07 (1C, CH_{rim}), 126.88 (1C, CH_{rim}), 126.86 (1C, CH_{rim}), 126.81 (1C, CH_{rim}), 126.51 (1C, CH_{rim}), 70.49 (C_{cp}), 70.43 (C_{cp}), 68.57 (C_{cp}) 67.40 (C_{cp}), 67.14 (C_{cp}), 55.37 (1C, <u>C</u>H), 40.46 (2C, N<u>C</u>H3), 17.12 (1C, <u>C</u>H3) ppm; **FT-IR:** ν = 3383, 3092, 3034, 2958, 2918, 2848, 2808, 276, 1735, 1625, 1454, 1430, 1365, 1259, 1103, 1072, 1038, 996, 821, 699, 663, 546 cm^{-1}; **EI-MS:** m/z = 505.15526 (100 %, $[M]^{+\cdot}$, found), 505.14929 (calc'd) , 460.1 (-HN(CH3)2).

8.3.16 1,6-Diferrocenyl-2,5-dimethylcorannulene (45)

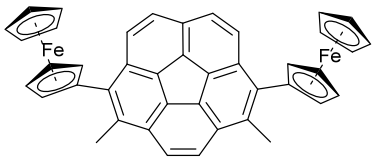

45

Ferrocene (**1**) (170 mg, 0.92 mmol, 4 eq) and potassium *tert*-butoxide (10 mg, 0.09 mmol, 0.4 eq) were dissolved in THF (10 mL). The solution was cooled to -30 °C and *n*-butyllithium (0.6 mL, 2.5M in *n*-hexane, 4.4 eq) was added dropwise. Stirring at -30 °C was continued for 20 min. Anhydrous zinc(II) chloride (187 mg, 1.37 mmol, 6 eq) was added. The bright orange solution was stirred at -30 °C for 30 min and at RT for 30 min. 1,6-Dibromo-2,5-dimethylcorannulene (**44**) (100 mg, 0.23 mmol, 1 eq), palladium(II) acetate (4 mol%) and triphenylphosphane (8 mol%) were added at once and the reaction mixture was stirred at 70 °C for 18 h. The solvent was removed and the resulting solid was purified by column chromatography on silica gel with *n*-pentane/dichloromethane (5:1) and 1% triethylamine as solvent. After a second column chromatography on silica gel using *n*-pentane/dichloromethane (2:1) and 1% triethylamine as solvent, **45** (10 mg, 7 %) was obtained as an analytically pure orange solid.

M.p. darkens above 170.4 °C; **^{1}H-NMR** (400 MHz, $CDCl_3$): δ = 8.02 (AB, ^{3}J = 8.9 Hz, 4H, H_{rim}), 7.92 (s, 2H, H_{rim}), 4.70 (s, 4H, $H_{cp\text{-}sub}$), 4.48 (s, 4H, $H_{cp\text{-}sub}$), 4.31 (s, 10H, H_{cp}), 3.01 ppm (s, 6H, $C\underline{H}_3$); **^{13}C-NMR** (175 MHz, $CDCl_3$): δ = 135.55 (2C, C_{ispo}), 134.14 (2C, C_{hub}), 134.41 (1C, C_{hub}), 133.75 (2C, C_{hub}), 131.89 (C_{spoke}), 131.81 (2C, C_{hub}), 129.46 (2C, C_{hub}), 129.46 (2C, C_{ispo}), 126.27 (2C, CH_{rim}), 125.91 (2C, CH_{rim}), 125.39 (2C, CH_{rim}), 85.13 (2C, $C_{cp\ ipso}$), 72.26 (4C, C_{cp}), 69.91 (10C, C_{cp}), 67.97 (4C, C_{Cp}), 17.02 ppm (6C, CH_3); **FT-IR:** ν = 2923 (m, br), 1446 (w, shr), 1406 (w, shr), 1379 (w, shr), 1379 (w, shr), 1344 (w, shr), 1323 (w, shr), 1301 (vw, shr), 1259 (w, shr), 1198 (w, shr), 1104 (m, shr), 1028 (m, shr), 996 (m, shr), 904 (w, shr), 869 (w, shr), 809 (m, shr), 785 (m, shr), 731 (w, shr), 713 (w, shr), 680 (w, shr), 600 (w, shr), 582 cm^{-1} (w, shr); **ESI-MS:** m/z = 646.1094 ($[M]^+$, found), 646.1064 ($[M]^+$, calc'd).

8.3.17 1,6-Di(1'-neopentylferrocene)-2,5-dimethylcorannulene (46)

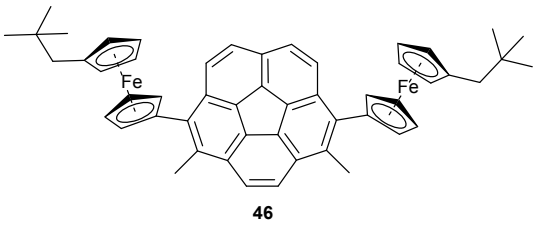

46

1-Bromo-1'-neopentylferrocene (**12**) (111 mg, 0.33 mmol, 4 eq) was dissolved in THF (3 mL) and cooled to -30 °C. *n*-Butyllithium (0.15 mL, 2.5M in *n*-hexane, 4.4 eq) was added dropwise. After stirring for 30 min at -30 °C, anhydrous zinc(II) chloride (68 mg, 0.50 mmol, 6 eq) was added and stirring was continued at -30 °C for 30 min at -30 °C and 30 min at RT. 2,5-Dimethylcorannulene (**44**) (36 mg, 0.08 mmol, 1 eq), palladium(II) acetate (2 mol%) and triphenylphosphane (4 mol%) were added at once and the reaction mixture was stirred at 65 °C for 19 h. After removal of the solvent, column chromatography on silica gel with *n*-pentane/dichloromethane (3:1) and 1% triethylamine afforded of the red **46** (49 mg, 75 %).

M.p. 55.2 - 56.5°C; **^{1}H-NMR** (700 MHz; $CDCl_3$): δ = 8.07 (AB, ^{3}J = 8.8 MHz, 4H, H_{rim}), 7.96 (s, 2H, H_{rim}), 4.68 (s, 2H, $H_{cp\text{-}sub}$), 4.40 (s, 4H, $H_{cp\text{-}sub}$), 4.24 (s, 2H, $H_{cp\text{-}sub}$), 4.21 (s, 2H, $H_{cp\text{-}sub}$), 3.06 (s, 6H, $C\underline{H}_3$), 2.35 (s, 4H, $C\underline{H}_2$), 0.85 ppm (s, 18H, $C\underline{H}_3$); ^{13}C-NMR (175 MHz, $CDCl_3$): δ = 135.45 (2C, C_{ispo}), 134.36 (2C, C_{hub}), 134.30 (2C, C_{hub}), 133.69 (1C, C_{hub}), 133.36 (2C, C_{spoke}), 131.99 (2C, C_{spoke}), 131.21 (1C, C_{spoke}), 129.47 (2C, C_{ipso}), 127.78 (2C, CH_{rim}), 125.84 (2C, CH_{rim}), 125.36 (2C, CH_{rim}), 86.28 (2C, $C_{cp\text{-}ipso}$), 84.84 (2C, $C_{cp\text{-}ipso}$), 72.76 (4C, C_{cp}), 71.68 (4C, C_{cp}), 70.15 (4C, C_{cp}), 69.43 (4C, C_{cp}), 44.84 (2C, $\underline{C}H_2$), 31.83 (2C, $\underline{C}(CH_3)_3$), 29.40 (6C, $C(\underline{C}H_3)_3$), 17.08 ppm (6C, $\underline{C}H_3$); **FT-IR:** ν = 3083 (w, br), 2947 (m, shr), 2904 (m, shr), 2863 (m, shr), 1620 (w, br), 1463 (m, shr), 1390 (m, shr), 1328 (w, shr), 1262 (w, shr), 1361 (m, shr), 1328 (w, shr), 1262 (m, shr), 1236 (m, shr), 1201 (w, shr) 1147 (w, shr), 1094 (w, shr), 1026 (m, shr), 822 (s, shr), 807 (s, shr), 794 (s, shr), 735 (s, shr), 705 (s, shr), 668 (m, shr), 585 (m, shr), 540 cm^{-1} (m, shr); **ESI-MS:** 786.2624 ($[M]^+$, found), 786.2611 ($[M]^+$, calc'd).

8.3.18 1,6-Bis(ethynylferrocenyl)-2,5-dimethylcorannunlene (47)

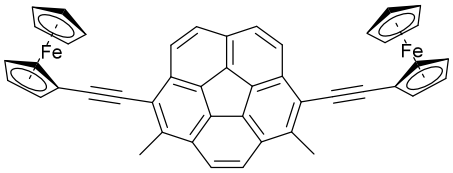

47

1,6-Dibromo-2,5-dimethylcorannulene (**44**) (30 mg, 0.07 mmol, 1 eq) dissolved in toluene (3 mL) and triethylamine (1.5 mL) in a 25 mL Schlenk flask. After degassing ethynylferrocene (**28**) (44 mg, 0.21 mmol, 3 eq), palladium(II) acetate (5 mol%), triphenylphosphane (10 mol%) and copper(I) iodide (11 mol%) were added. The reaction mixture was stirred for 24 h at 70 °C. The solvent was removed under vacuum and the residual red-brown solid was purified chromatographically on silica gel with *n*-pentane/dichloromethane (3:1) with 1 % triethylamine added. **47** was obtained as an orange solid (6 mg, 12 %).

M.p. 282 °C (decomposition); **^{1}H NMR** (700 MHz, $CDCl_3$): δ = 8.02 (s, 2H, H_{rim}), 7.92 (s, 2H, H_{rim}), 7.84 (s, 2H, H_{rim}), 4.67 (s, 4H, $H_{cp\text{-}sub}$), 4.34 (s, 4H, $H_{cp\text{-}sub}$), 4.32 (s, 10H, H_{cp}), 2.98 ppm (s, 6H); **^{13}C NMR** (175 MHz, $CDCl_3$): δ = 139.26 (2C, $C_{ipso\text{-}cor}$), 135.81 (C, C_{hub}), 134.24 (C, C_{hub}), 134.12 (C, C_{hub}), 131.67 (C, C_{spoke}), 130.52 (C, C_{spoke}), 127.54 (C, C_{spoke}), 126.10 (2C, CH_{rim}), 125.09 (2C, CH_{rim}), 120.25 (2C, $C_{ipso\text{-}cor}$), 97.53 (2C, $C_{ethynyl}$), 83.07 (2C, $C_{ethynyl}$), 80.77 (2C, $C_{ipso\text{-}cp}$), 71.71 (C, C_{cp}), 70.24 (C, C_{cp}), 69.25 (C, C_{cp}), 29.67 (2C, $\underline{C}H_3$) ppm; **FT-IR**: ν = 2916 (s, shr), 2848 (s, shr), 2203 (w, shr), 1737 (m, shr), 1593 (m, shr), 1466 (m, shr), 1410 (m, shr), 1373 (m, shr), 1240 (m, shr), 1105 (m, shr), 1023 (m, shr), 1003 (m, shr), 913 (m, shr), 875 (m, shr), 825 (s, shr), 792 (s, shr), 718 (s, shr), 691 (m, shr), 585 (m ,shr), 529 cm^{-1} (s, shr); **ESI-MS:** m/z = 694.1063 ($[M]^+$,found), 694.1046 ($[M]^+$, calc'd).

8.3.19 1,2-Bis(trifluoromethyl)-4,9-diferrocenylcorannulene (48)

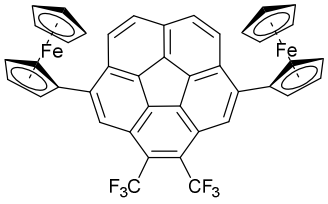

48

Ferrocene (**1**) (215 mg, 1.16 mmol, 5 eq) and potassium *tert*-butoxide (13 mg, 0.17 mmol, 0.5 eq) were combined in a 25 mL Schlenk tube and dissolved in THF (2 mL). The mixture was cooled to -80 °C and *tert*-butyllithium (0.84 mL, 1.6M in *n*-hexane, 7.5 eq) was added dropwise. After stirring for 1 h at -30 °C, anhydrous zinc(II) chloride (284 mg, 2.08 mmol, 9 eq) was added to the yellow suspension and stirring at -30 °C was continued for 1 h at -30 °C and one 1 h at RT. 4,9-Dibromo-1,2-bis(trifluoromethyl)corannulene (**49**) (126 mg, 0.23 mmol, 1 eq), palladium(II) acetate (4 mol%) and triphenylphosphane (8 mol%) were added and the reaction mixture was stirred at 60 °C for 24 h. The reaction was quenched by dilution with dichloromethane and poured on water. The organic layer was washed with water (4 x 100 mL). After drying with sodium sulfate and filtration, the product was purified by column chromatography on silica gel with *n*-pentane/dichloromethane (5:1). The product, (14 mg, 8 %) of a deep red solid, was obtained in the second fraction.

M.p. 162 °C (decomposition); **^{1}H NMR** (400 MHz, $CDCl_3$): δ = 8.41 (s, 2H, H_{rim}), 8.17 (AB, ^{3}J = 8.9 Hz, 4H, H_{rim}), 4.92 – 4.53 (m, 8H, $H_{cp\text{-}subst}$), 4.20 ppm (s, 10 H, H_{cp}); **^{13}C NMR** (176 MHz, $CDCl_3$): δ = 141.42 (2C, $C_{ipso\text{-}cor}$), 136.20 (1C, C_{hub}), 134.66 (2C, C_{hub}), 134.22 (2C, C_{hub}), 130.55 (2C, C_{spoke}), 130.35 (1C, C_{spoke}), 128.43 (2C, CH_{rim}), 127.64 (2C, CH_{rim}), 125.13 (2C, C_{spoke}), 124.57 (2C, CH_{rim}), 70.73 (4C, $C_{cp\text{-}sub}$), 70.20 (4C, $C_{cp\text{-}sub}$), 67.97 (2C, $C_{ipso\text{-}cp}$), 65.84 ppm (10C, C_{cp}); The *ipso* carbon atom where the trifluoromethylgroups, as well as the carbon atom of the trifluoromethylgroups could not be observed. **^{19}F NMR** (376 MHz, $CDCl_3$): δ = -50.07 ppm (s, 6F, CF_3); **FT-IR:** ν = 2921 (s, shr), 2851 (m, shr), 1737 (w, shr), 1704 (w, shr), 1626 (w, br), 1462 (w, shr), 1416 (w, shr), 1300 (m, shr), 1264 (s, shr), 1228 (m, shr), 1125 (s, shr), 1067 (m, shr), 1031 (m, shr), 1000 (m, shr), 906 (m, shr), 806 (s, shr), 729 (m, shr), 646 (w, shr), 567 (w, shr) cm^{-1}; **EI-MS (250 °C):** m/z = 745.0498 (100 %, $[M]^{+\cdot}$, found), 754.0483 ($[M]^{+\cdot}$, calc'd), 377 (21 %, $[M]^{2+}$), 614 (11 %, $[C_{40}H_{22}Fe_2]^{+\cdot}$), 250 (5 %, $[C_{20}H_{10}]^{+\cdot}$), 376(4 %, $[C_{30}H_{16}]^{+\cdot}$), 434 (4 %, $[C_{30}H_{18}Fe]^{+\cdot}$).

8.3.20 1,2,5,6-Tetra(ferrocenyl)corannulene (51)

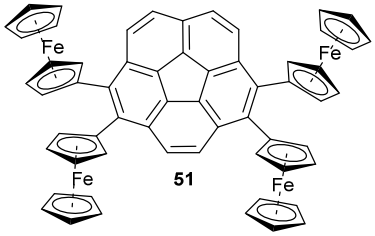

51

Ferrocene (**1**) (265 mg, 1.42 mmol, 8 eq) and potassium *tert*-butoxide (16 mg, 0.14 mmol, 0.8 eq) were dissolved in THF (4 mL). After cooling to -30 °C and *tert*-butyllithium (1.12 mL in *n*-hexane, 2.34 mmol, 12 eq) was added dropwise. After stirring for 1 h at the same temperature anhydrous zinc(II) chloride (340 mg, 2.49 mmol, 14 eq) was added. The orange reaction mixture was stirred for further 30 min at -30 °C and 30 min at RT. Palladium(II) acetate (4 mol%), triphenylphosphane (8 mol%) and 1,2,5,6-tetrabromocorannulene (**50**) (100 mg, 0.19 mmol, 1 eq) were added and the reaction mixture was stirred at 60 °C for 48 h. After adding water (2 mL) the reaction mixture was extracted with dichloromethane (20 mL), the organic layer was washed with water (3 x 50 mL), dried with anhydrous sodium sulfate, filtrated and the solvent was removed under vacuum. After column chromatography on silica gel with *n*-pentane/dichloromethane (2:1) as an eluent the red product was obtained in the second fraction. After removal of the solvent a red amorphous solid was obtained (108 mg, 57%).

M.p. 253.7 °C (decomposition); **^{1}H NMR** (700 MHz; CD_2Cl_2): δ = 9.12 (s, 2H, H_{rim}), 8.48 (AB, ^{3}J = 8.9 Hz, 4H, H_{rim}), 4.30 (br s, 20H, H_{cp}), 4.04 (s, 8H, $H_{cp\text{-}sub}$), 4.00 ppm (s, 8H, $H_{cp\text{-}sub}$); **^{13}C NMR** (175 MHz, $CDCl_3$): δ = 136.39 (2C, C_{ipso}), 136.06 (2C, C_{ipso}), 134.64 (1C, C_{hub}), 134.45 (2C, C_{hub}), 133.53 (2C, C_{hub}), 130.93 (2C, C_{spoke}), 129.88 (2C, C_{spoke}), 129.31 (1C, C_{spoke}), 128.64 (2C, CH_{rim}), 128.09 (2C, CH_{rim}), 126.12 (2C, CH_{rim}), 87.40 (2C, $C_{cp\text{-}ipso}$), 86.75 (2C, $C_{cp\text{-}ipso}$), 73.42 (4C, $C_{cp\text{-}sub}$), 73.34 (4C, $C_{cp\text{-}sub}$), 70.40 (10C, C_{cp}), 70.37 (10C, C_{cp}), 68.12 (4C, $C_{cp\text{-}sub}$), 68.10 ppm (4C, $C_{cp\text{-}sub}$); **FT-IR:** ν = 3039 (m, shr), 2960 (m, shr), 2849 (m, shr), 1732 (m, br), 1680 (w, br), 1619 (m, shr), 1436 (m, shr), 1409 (m, shr), 1380 (w, shr), 1328 (m, shr), 1298 (m, shr), 1258 (m, shr), 1221 (w, shr), 1104 (m, shr), 1027 (s, shr), 1000 (s, shr), 873 (m, shr), 812 (s, shr), 799 (s, shr), 733 (s, shr), 701 (s, shr), 672 (m, shr), 640 (m, shr), 582 cm_{-1} (m, shr); **EI-MS (300 °C):** m/z = 732 (100 %, $[C_{45}H_{24}Fe_3]^{+\cdot}$), 986 (82 %, $[M]^{+\cdot}$), 614 (71 %, $[C_{40}H_{22}Fe_2]^{+}$), 558 (52 %, $[C_{40}H_{17}Fe_2]^{+\cdot}$), 186 (40 %,

$[C_{10}H_{10}Fe]^+$), 367 (10 %, $[C_{45}H_{24}Fe_3]^{2+}$); **ESI-MS:** m/z = 986.0678 ($[M]^+$, found), 986.0684 ($[M]^+$, calc'd).

8.3.21 1,2,5,6-Tetra(1'-neopentylferrocenyl)corannulene (52)

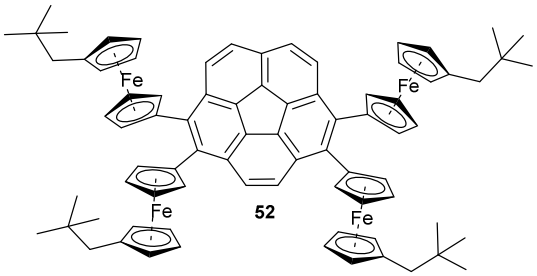

n-Butyllithium (0.63 mL, 2.5M in *n*-hexane, 8.8 eq) was added dropwise to a solution of 1-bromo-1'-neopentylferrocene (**12**) (477 mg, 1.42 mmol, 8 eq) in THF (5.7 mL). The reaction mixture was stirred at -30 °C for 30 min. Anhydrous zinc(II) chloride (340 mg, 2.49 mmol, 14 eq) was added and stirring was continued for 30 min at -30 °C and for 30 min at RT. 1,2,5,6-Tetrabromocorannulene (**50**) (100 mg, 0.18 mmol, 1 eq), palladium(II) acetate (4 mol%) and triphenylphosphane (8 mol%) were added and the reaction mixture was stirred at 62 °C for 48 h. The solvent was removed under vacuum. Purification by column chromatography on silica gel with *n*-pentane/dichloromethane (10:1) including 1 % triethylamine as eluent, yielded **52** (87 mg, 38 %) as a red solid from the last (fourth) fraction as a red solid.

M.p. 131.5 °C; **^{1}H NMR** (400 MHz; $CDCl_3$): δ = 9.11 (s, 2H, H_{rim}), 8.49 (AB, ^{3}J = 8.9 Hz, 4H, H_{rim}), 4.25 - 4.24 (br m, 8H, $H_{cp\text{-}sub}$), 4.19 - 4.18 (m, 8H, $H_{cp\text{-}sub}$), 3.95 - 3.91 (m, 16H, $H_{cp\text{-}sub}$), 2.15 (s, 4H, $C\underline{H}_2$), 2.13 (s, 4H, $C\underline{H}_2$), 0.72 (s, 18H, $C\underline{H}_3$), 0.70 ppm (s, 18H, $C\underline{H}_3$); **^{13}C-NMR** (175 MHz, $CDCl_3$): δ = 135.79 (2C, C_{hub}), 135.62 (2C, C_{hub}), 134.45 (2C, C_{ispo}), 134.34 (1C, C_{hub}), 132.93 (2C, C_{spoke}), 130.51 (2C, C_{spoke}), 129.49 (1C, C_{spoke}), 128.70 (2C, C_{ispo}), 128.49 (2C, CH_{rim}), 127.40 (2C, CH_{rim}), 125.49 (2C, CH_{rim}), 86.51 (2C, $C_{cp\text{-}ipso}$), 86.30 (2C, $C_{cp\text{-}ipso}$), 86.09 (2C, $C_{cp\text{-}ipso}$), 86.01 (2C, $C_{cp\text{-}ipso}$), 73.36 (4C, C_{cp}), 73.35 (4C, C_{cp}), 71.61 (4C, C_{cp}), 71.58 (4C, C_{cp}), 70.60 (4C, C_{cp}), 70.50 (4C, C_{cp}), 69.20 (4C, C_{cp}), 69.10 (4C, C_{cp}), 44.88 (2C, $\underline{C}H_2$), 44.86 (2C, $\underline{C}H_2$), 31.84 (2C, $\underline{C}(CH_3)_3$), 31.82 (2C, $\underline{C}(CH_3)_3$), 29.45 (6C, $\underline{C}H_3$), 29.44 ppm (6C, $\underline{C}H_3$); **FT-IR:** ν = 3085 (w, br), 2947 (m, shr), 2904 (m, shr), 2862 (w, shr), 1464 (m, shr), 1389 (w, shr), 1361 (m, shr), 1328 (w, shr), 1234 (m, shr), 1159 (m, shr), 1026 (m, shr), 904 (m, shr), 818 (s, shr), 729 (s, shr), 645 (m, shr), 586 cm^{-1} (m, shr); **ESI-MS:** m/z = 1266.3900 ($[M]^+$ found), 1266.3814 ($[M]^+$ calc'd).

8.3.22 1,2,5,6-Tetra(4-ferrocenylphenyl)corannulene (53)

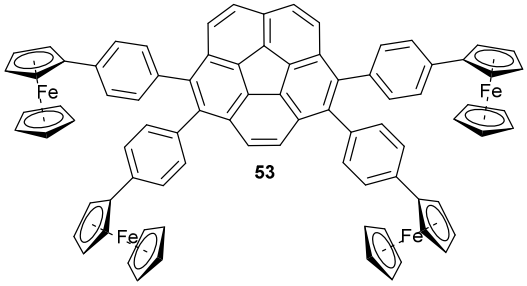

53

1-Iodo-4-(ferrocenyl)benzene (**13**) (274 mg, 0.71 mmol, 8 eq) was dissolved in THF (5.7 mL). After cooling to -20 °C *n*-butyllithium (0.31 mL, 2.5M in *n*-hexane, 8.8 eq) was added dropwise and stirring at -20 °C was continued for further 20 min. Anhydrous zinc(II) chloride (169 mg, 1.24 mmol, 14 eq) was added, stirring was continued for 30 min at -20 °C and for 30 min at RT. 1,2,5,6-Tetrabromocorannulene (**50**) (50 mg, 0.09 mmol, 1 eq), palladium(II) acetate (4 mol%) and triphenylphosphane (8 mol%) were added and the reaction mixture was heated at 70 °C for 24 h. The solvent was removed and column chromatography on silica gel with *n*-pentane/dichloromethane (2:1) afforded of the orange **53** (33 mg, 28 %) within the last (third) fraction.

M.p. darkens above 196.7 °C; **^{1}H-NMR** (700 MHz; CD_2Cl_2): δ = 7.82 (AB, ^{3}J = 8.7 Hz, 4H, H_{rim}), 7.73 (s, 2H, H_{rim}), 7.47-7.44 (m, 8H, H_{phenyl}), 7.27-7.24 (m, 8H, H_{phenyl}), 4.67 (s, 4H, $H_{cp\text{-}sub}$), 4.66 (s, 4H, $H_{cp\text{-}sub}$), 4.32 (s, 4H, $H_{cp\text{-}sub}$), 4.30 (s, 4H, $H_{cp\text{-}sub}$), 4.04 (s, 10H, H_{cp}), 4.02 ppm (s, 10H, H_{cp}); **^{13}C-NMR** (175 MHz, CD_2Cl_2): 139.51 (C_{hub}), 139.29 (C_{hub}), 138.42 (2C, $C_{ph\text{-}ipso}$), 138.39 (2C, $C_{ph\text{-}ipso}$), 135.84 (1C, C_{spoke}), 135.49 (2C, C_{spoke}), 134.67 (2C, C_{spoke}), 132.31 (4C, CH_{ph}), 132.28 (4C, CH_{ph}), 131.27 (2C, CH_{rim}), 130.93 (2C, CH_{rim}), 130.74 (2C, CH_{rim}), 127.85 (2C, CH_{rim}), 127.75 (2C, CH_{rim}), 125.66 (8C, CH_{ph}), 85.18 (2C, $C_{cp\text{-}ipso}$), 85.15 (2C, $C_{cp\text{-}ipso}$), 70.35 (10C, C_{cp}), 70.33 (10C, C_{cp}), 69.70 (4C, C_{cp}), 69.69 (4C, C_{cp}), 66.99 (4C, C_{cp}), 66.97 ppm (4C, C_{cp}); **FT-IR:** ν = 3088 (w, br), 3026 (w, br), 2921 (m, shr), 2850 (m, shr), 1607 (m, shr), 1526 (m, shr), 1455 (m, shr), 1387 (w, shr), 1353 (w, br), 1280 (m, shr), 1186 (w, shr), 1105 (m, shr), 1082 (w, shr), 1054 (w, shr), 1000 (m, shr), 906 (w, shr), 886 (m, shr), 727 (s, shr), 755 (m, shr), 650 (m, shr), 600 (m, shr) cm^{-1}; **ESI-MS:** 1290.1994 ($[M]^+$, found), 1290.1936 ($[M]^+$, calc'd).

8.3.23 1,2,5,6-Tetra(ferrocenylethynyl)corannulene (54)

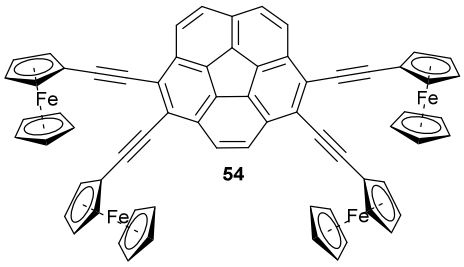

54

1,2,5,6-Tetrabromocorannulene (**50**) (100 mg, 0.19 mmol, 1.0 eq), ethynylferrocene (**28**) (163 mg, 0.78 mmol, 4.4 eq), copper(I) iodide (8 mg, 0.04 mmol, 0.2 eq), palladium (II) acetate (10 mol%) and triphenylphosphane (20 mol%) were dissolved in a mixture of toluene (10 mL) and triethylamine (5 mL). The brown solution was degassed three times and the stirred at 70 °C for 20 h. The redbrown reaction mixture was transferred to a separation funnel with dichloromethane (20 mL) washed with water (3 x 100 mL) and brine (1 x 50 mL). The organic layer was dried with anhydrous sodium sulfate, filtrated and the solvent was removed. Column chromatography on silica gel was conducted with *n*-pentane/dichloromethane (2:1). The product was obtained in the last fraction as a deep red solid (81 mg, 42 %).

M.p. 225.0 °C; **^{1}H NMR** (700 MHz; CD_2Cl_2): δ = 8.12 (s, 2H, H_{rim}), 7.97 (AB, ^{3}J = 8.7 Hz, 4H, H_{rim}), 4.73 (s, 8H, $C_{cp\text{-}sub}$), 4.37 (s, 8H, $C_{cp\text{-}sub}$) 4.32 ppm (s, 20H, C_{cp}); **^{13}C NMR** (175 MHz, $CDCl_3$): δ = 135.75 (1C, C_{hub}) 134.82 (2C, C_{hub}), 134.07 (2C, C_{hub}), 131.54 (1C, C_{spoke}), 131.48 (2C, C_{spoke}), 131.33 (2C, C_{spoke}), 128.01 (2C, CH_{rim}), 129.94 (2C, CH_{rim}), 126.58 (2C, CH_{rim}), 124.89 (2C, C_{ipso}), 124.72 (2C, C_{ipso}), 98.57 (2C, $C_{ethynyl}$), 98.42 (2C, $C_{ethynyl}$), 84.11 (2C, $C_{ethynyl}$), 84.01 (2C, $C_{ethynyl}$), 72.01 (8C, $C_{cp\text{-}sub}$), 70.45 (20C, C_{cp}), 69.52 (8C, $C_{cp\text{-}sub}$), 65.33 ppm (4C, $C_{cp\text{-}ipso}$); **FT-IR:** ν = 3087 (w, shr), 3048 (w, shr), 2953 (w, shr), 2924 (m, shr), 2847 (w, shr), 2250 (w, shr), 2187 (m, shr), 773 (w, shr), 1628 (m, br), 1470 (m, shr), 1405 (m, shr), 1386 (m, shr), 1341 (m, shr), 1260 (m, shr), 1199 (m, shr), 1185 (m, shr), 1102 (m, shr), 1045 (m, shr), 1025 (m, shr), 998 (s, shr), 948 (w, shr), 905 (m, shr), 810 (s, shr), 726 (s, shr), 674 (m, shr), 647 (m, shr), 600 (m, shr), 579 cm^{-1} (mid, shr); **ESI-MS:** m/z = 1082.0611 ($[M]^+$, found), 1082.0684 ($[M]^+$, calc'd).

8.3.24 1,2,5,6-Tetra(1',2,2',3,3'4,4',5-octamethylferroceneyl)corannulene (55)

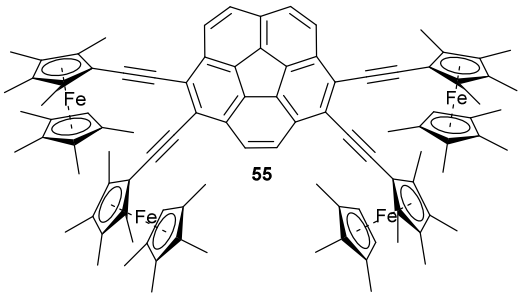

1,2,5,6-Tetrabromocorannulene (**50**) (70 mg, 0.12 mmol, 1 eq), 1-ethynyl-1',2,2',3,3',4,4',5-octamethyl-ferrocene (**6**) (175 mg, 0.54 mmol, 4.4 eq), palladium(II) acetate (5 mol%) and triphenylphosphane (10 mol%) and copper(I) iodide (5 mol%) were dissolved in diisopropylamine (1.2 mL). The slurry was degassed three times and heated to 80 °C turning from brown to a purple solution which was stirred at that temperature for 56 h. After removal of the solvent the dark purple solid was subjected to column chromatography on basic alumina (activity level 1) using *n*-pentane/toluene (3:1) as solvents, resulting in **55** (72 mg, 40 %).

M.p. the compound is black in solid, no melting point could be observed up to 300 °C; **^{1}H-NMR** (400 MHz; $CDCl_3$): δ = 8.60 (s, 2H, H_{rim}), 8.01 (AB, ^{3}J = 8.8 Hz, 4H, H_{rim}), 3.34 (s, 4H, H_{cp}), 2.31 (s, 12H, $C\underline{H}_3$), 2.10 (s, 12H, $C\underline{H}_3$), 1.78 (s, 12H, $C\underline{H}_3$), 1.17 (s, 12H, $C\underline{H}_3$), 1.69 ppm (s, 12H, $C\underline{H}_3$); **^{13}C-NMR** (175 MHz, C_6D_6): δ = 137.90 (1C, C_{hub}), 136.42 (1C, C_{ipso}), 135.24 15 (2C, C_{hub}), 134.55 (2C, C_{hub}), 132.38 (2C, C_{spoke}), 132.21 (2C, C_{spoke}), 131.58 (1C, C_{spoke}), 128.57 (2C, C_{rim}), 127.38 (2C, C_{rim}), 126.74 (2C, C_{rim}), 125.67 (2C, C_{rim}), 125.56 (2C, C_{rim}), 99.60 (2C, $C_{ethynyl}$), 99.37 (2C, $C_{ethynyl}$), 88.89 (2C, $C_{ethynyl}$), 88.62 (2C, $C_{ethynyl}$), 82.81 (C, C_{cp}), 82.78 (C, C_{cp}), 81.51 (C, C_{cp}), 81.46 (C, C_{cp}), 81.39 (C, C_{cp}),81.36 (C, C_{cp}), 81.09 (C, C_{cp}), 81.05 (C, C_{cp}), 66.38 (C, C_{cp}), 66.28 (C, C_{cp}), 11.54 (2C, $\underline{C}H_3$), 11.50 (2C, $\underline{C}H_3$), 11.33 (2C, $\underline{C}H_3$), 11.31 (2C, $\underline{C}H_3$), 10.22 (2C, $\underline{C}H_3$), 10.20 (2C, $\underline{C}H_3$), 9.43 (2C, $\underline{C}H_3$), 9.40 ppm (2C, $\underline{C}H_3$); **FT-IR:** 3056 (w, shr), 2964 (m, shr), 2942 (m, shr), 2899 (s, shr), 2854 (m, shr), 2176 (s, shr), 1611 (w, shr), 1444 (m, shr), 1373 (s, shr), 1328 (s, str), 1261 (w, shr), 1083 (w, shr), 970 (w, shr), 822 (m, shr), 728 (m, shr), 651 (w, shr), 571 cm^{-1} (w, shr); **ESI-MS:** m/z = 1531.5724 ($[M]^+$, found), 1531.5770 ($[M]^+$, calc'd), 765.7833 ($[M]^{2+}$, found), 765.7885 ($[M]^{2+}$, calc'd).

8.3.25 1,2,5,6-Tetrakis((*E*)-2-(ferrocenyl)ethenyl)corannulene (56)

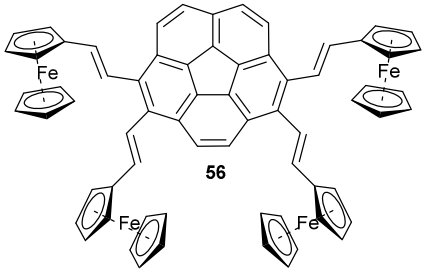

1,2,5,6-Tetrabromocorannulene (**50**) (100 mg, 0.18 mmol, 1 eq), vinylferrocene (**31**) (170 mg, 0.80 mmol, 4.5 eq), potassium carbonate (1.11 g, 8 mmol, 45 eq), tetra-*n*-butylammonium bromide (1.03 g, 3.20 mmol, 18 eq) and palladium(II) acetate (10 mol%) were suspended in DMF (16 mL) and degassed three times. The brown slurry was stirred at 80 °C for 48 h. Again vinylferrocene (170 mg, 0.80 mmol, 4.5 eq) and palladium(II) acetate (10 mol%) were added and stirring at 80 °C was continued for 24 h. After cooling to RT dichloromethane (50 mL) was added and the organic phase was washed with water (4 x 150 mL) and dried with sodium sulfate. Column chromatography on silica gel with *n*-pentane/dichloromethane (2:1) resulted in 62 mg of a red amorphous solid, which was again purified by column chromatography on neutral alumina with *n*-pentane/toluene (1:1) yielding **56** as a bright red solid (17 mg, 9 %).

M.p. 246 °C (decomposition); **^{1}H-NMR** (400 MHz; $CDCl_3$): δ = 8.14 (s, 2H, H_{rim}), 8.00 (AB, ^{3}J = 8.9 Hz, 4H, H_{rim}), 7.35-7.14 (m, 8H, H_{vinyl}), 4.65 (s, 8H, $H_{cp\text{-}sub}$), 4.39 (s, 8H, $H_{cp\text{-}sub}$), 4.27 (s, 10 H, H_{cp}), 4.26 ppm (s, 10H, H_{cp}); **^{13}C-NMR** (175 MHz, $CDCl_3$): δ = 135.74 (1C, C_{hub}), 134.82 (2C, C_{hub}), 134.07 (2C, C_{hub}), 131.54 (1C, C_{spoke}), 131.48 (2C, C_{spoke}), 131.33 (2C, C_{spoke}), 128.01 (2C, C_{rim}), 126.94 (2C, C_{rim}), 126.57 (2C, C_{rim}), 124.89 (2C, C_{rim}), 124.72 (2C, C_{rim}), 98.56 (2C, C_{vinyl}), 98.42 (2C, C_{vinyl}), 84.11 (2C, C_{vinyl}),, 84.01 (2C, C_{vinyl}), 72.01 (4C, C_{cp}), 70.46 (20C, C_{vinyl}), 69.52 (4C, C_{vinyl}), 65.33 ppm (2C, $C_{cp\ ispo}$); **FT-IR:** ν = 3091 (m, br), 3035 (w, shr), 2919 (m, shr), 2849 (m, shr), 2919 (s, shr), 2849 (m, shr), 2191 (m, shr), 1728 (m, shr), 1680 (w, shr), 1613 (m, shr), 1511 (w, br), 1461 (m, shr), 1409 (m, shr), 1375 (m, shr), 1260 (m, shr), 1239 (m, shr), 1183 (w, shr), 1104 (m, shr), 1043 (m, shr), 1027 (m, shr), 1002 (m, shr), 997 (m, shr), 927 (m, shr), 878 (w, shr), 810 (s, shr),726 (m, shr), 695 (m, shr), 656 (m, shr), 629 (w, shr), 593 cm^{-1} (m, shr); **ESI-MS:** m/z = 1090.1385 ($[M]^+$, found), 1090.1310 ($[M]^+$, calc'd).

8.3.26 Attempts to synthesize 1,2,5,6-Tetrakis((*R*)-(+)-*N*,*N*-Dimethyl-1-ferrocenylethylamin)-corannulene (57)

1) 100 mg-scale reactions:

Ugi's amine (**42**) (273 mg, 1.06 mmol, 6 eq) in THF (5 mL) was cooled to -78 °C, *sec*-butyllithium (1.11 ml, 1.3M, 1.56 mmol, 1.5 eq) was added dropwise. The reaction mixture was allowed to warm to RT and was stirred for 1 h. After cooling to -30 °C anhydrous zinc(II) chloride (265 mg, 1.94 mmol, 1.94 eq) was added. The solution was again stirred at RT for 1 h. 1,2,5,6-Tetrabromocorannulene (100 mg, 0.18 mmol, 1 eq) and the catalyst system **(a)** triphenylphosphane (1 mol%), palladium(II) acetate (2 mol%) or **(b)** 1,3-bis(2,6-diisopropylphenyl)imidazolium chloride (1.41 mg, 0.02 mmol, 0.1 eq), palladium(II) acetate (10 mol%) were added.

2) 4 mg-scale reactions:

A stock solution of the zincated species **43** was prepared under the same reaction conditions described above with ugi's amine (273 mg, 1.06 mmol, 6 eq), sec-butyllithium (0.11 mL, 1.4M, 8.8 eq), zinc(II) chloride (265 mg, 1.94 mmol, 11 eq) in THF (5 mL).

To 1 mL of this solution 1,2,5,6-tetrabromocorannulene (**50**) (4 mg, 6 µmol, 0.67 Äq) and the catalyst system was added: **(c)** tris(dibenzylideneacetone)dipalladium(0) (2 mol%), **(d)** tris-(dibenzylideneacetone)dipalladium(0) (2 mol%), XPhos (4 mol%), **(e)** tris(dibenzylideneacetone)-dipalladium(0) (2 mol%), SPhos (4 mol%), **(f)** tris(dibenzylideneacetone)dipalladium(0) (2 mol%), 1,1'-Bis(diphenylphosphino)ferrocene (4 mol%), **(g)** dichloro[1,3-bis(diphenylphosphino)-propane]nickel (30 mol%). The reaction mixtures were stirred for 48 h at 60 °C, the quenched with water and extracted with dichloromethane (4 x 5 mL) and dried with sodium sulfate. The resulting solutions were checked with TLC after evaporation of the solvent the crude product was analysed *via* ^{1}H NMR.

No conversion to the desired product was observed and only starting materials were recovered.

8.3.27 First Attempts to Synthesize *sym*-Pentaferrocenylated Corannulenes

Starting from 58

(a) 58 (20 mg, 0.03 mmol, 1 eq), caesium carbonate (15 mg, 0.05 mmol, 2 eq), monoiodoferrocene (**60**) (53 mg, 0.17 mmol, 7.5 eq), tris(dibenzylideneacetone)dipalladium(0) (25 mol%) and SPhos (50 mol%) were dissolved in THF (2.4 mL) and stirred at 77 °C for 2 d. Filtration through silica gel with *n*-pentane recovered most parts of the monoiodoferrocene (**60**) (16 mg), eluation with dichloromethane gave small amounts of a red solid (2 mg) that did not contain the desired product.

58 (88 mg, 0.02 mmol, 10 eq), 1-iodo-2-ferrocenylbenzene (**13**) (88 mg, 0.28 mmol, 10 eq), caesium carbonate (92 mg, 0.28 mmol, 12.5 eq) and **(b)** tris(dibenzylideneacetone)dipalladium(0) (11 mol%) and triphenylphosphane (22 mol%) were added. This mixture was stirred at 95 °C for 7 h. No reaction took place. **(c)** palladium(II) acetate (22 mol%) and 1,1'-bis(diphenylphosphanyl)ferrocene (22 mol%). The reaction was stirred at 70°C for 24 h. Water (2 mL) and sodium carbonate (12 mg, 0.14 mmol, 5 eq) were added, followed by dichloromethane and the organic layer was separated. PTLC on silica gel with *n*-pentane/dichloromethane (1:1) afforded 1-iodo-2-ferrocenylbenzene (**13**) and ferrocenylbenzene.

58 (10 mg, 0.01 mmol, 1 eq) and 1-iodo-2-ferrocenylbenzene (**13**) (38 mg, 0.12 mmol, 10 eq) were added **(d)** caesium carbonate (46 mg, 0.14 mmol, 12.5 eq), [1,1'-bis(diphenylphosphino)ferrocene]dichloropalladium(II) (22 mol%) and THF (1 mL) and stirred at 70 °C for 3 d. Only 1-iodo-2-ferrocenylbenzene (**13**) and 4,4'-diferrocenyl-1,1'-biphenyl[107] were identified from the crude ^{1}H NMR and TLC. **(e)** Potassium carbonate (21 mg, 0.10 mmol, 8.6 eq), tris(dibenzylideneacetone)dipalladium(0) (44 mol%) and SPhos (88 mol%) and degassed DMF/water (10:1) (1 mL). The reaction mixture was heated for 5 d at 110 °C. The reaction mixture was added dichloromethane (20 mL) and the organic layer was washed with water (3 x 20 mL). Column chromatography on silica gel with *n*-pentane/dichloromethane afforded 4 mg of a mixture of 1-iodo-2-ferrocenylbenzene (**13**) and ferrocenylbenzene and 2 mg 4,4'-diferrocenyl-

1,1'-biphenyl[107] and 6 mg of red solid that did not show the desired product in the ESI-mass spectrum.

Unsuccessful reactions starting from 1,3,5,7,9-Pentachlorocorannulene (59)

Ethynylferrocene (**28**) (248 mg, 1.18 mmol, 10 eq) was dissolved in THF (3 mL) and cooled to -78 °C. *n*-Butyllithium (0.48 mL, 1M in *n*-hexane, 10.3 eq) was added dropwise and the reaction mixture was allowed to warm up to RT and was stirred for 30 min, then cooled to -30 °C. Anhydrous zinc(II) chloride (225 mg, 1.65 mmol, 14 eq) was added and the reaction mixture was stirred for 1 h at RT. **(a)** Dichloro[1,3-bis(diphenylphosphino)propane]nickel (13 mg, 0.04 mmol, 0.34 mg) and 1,3,5,7,9-pentachlorocorannulene (**59**) (50 mg, 0.12 mmol, 1 eq) was added. Upon heating to 70 °C the mixture turned from an orange suspension to a dark orange solution and was stirred for 24 h at this temperature. Dichloromethane (20 mL) were added and the organic layer was washed with water (3 x 20 mL). For a better separation of layers 10% HCl_{aq} was added. A red solution with insoluble red solid was obtained. The solid was filtered off, washed with dichloromethane and subjected to MALDI mass measurements (92 mg). The soluble part of the product was subjected to column chromatography on silica gel. Elution with *n*-pentane afforded ethynylferrocene (**28**), *n*-pentane/dichloromethane (10:1) afforded 1,4-diferrocenylbuta-1,3-diyne,[108] other fractions were not identifyable by NMR and were added to the solid for MALDI measurements. **(b)** Palladium(II) acetate (26 mg, 0.12 mmol, 1 eq) and 1,3-bis(2,6-diisopropylphenyl)imidazolium chloride (50 mg, 0.12 mmol, 1 eq) were added. The closed Schlenk tube was heated at 110 °C for 2 h then at 80 °C for 6 d. The reaction mixture was filtrated through celite. After column chromatography on silica gel with *n*-pentane/dichloromethane ethynylferrocene (**28**) was recovered. No desired product could be detected.

(c) At -78 °C *n*-butyllithium (0.36 mL, 1M in *n*-hexane) was added dropwise to a solution of 1-ethynyl-1',2,2',3,3'4,4',5-octamethylferrocene (**6**) (286 mg, 0.89 mmol, 7.5 eq) in THF (3 mL). After stirring for 30 min at -78 °C and 30 min at RT, anhydrous zinc(II) chloride (164 mg, 1.20 mmol, 10 eq) was added at -78 °C. After stirring for another 20 min at RT dichloro[1,3-bis(diphenylphosphino)propane]nickel (22 mg, 0.04 mmol, 0.34 eq) and 1,3,5,7,9-

pentachlorocornnulene (50 mg, 0.12 mmol, 1 eq) were added. The reaction mixture was stirred at 70 °C for 5 d. The solvent was removed and column chromatography on silica gel with *n*-pentane/toluene (7:2) with 1 % triethylamine was conducted. **6** and the homocoupling product of the ferrocene were isolated. No desired compound was detected.

(d) To a solution of 1-zincio-4-phenylferrocene (**27**) (1.18 mmol, 10 eq) in THF (5 mL) 1,3,5,7,9-pentachlorocorannulene (**59**) (50 mg, 0.12 mmol, 1 eq) and dichloro[1,3-bis(diphenylphosphino)propane]nickel (22 mg, 0.04 mmol, 0.34 eq) were added. The reaction mixture was heated at 70 °C for 3 d. After removal of the solvent column chromatography on silica gel with *n*-pentane/dichloromethane (2:1) and 1 % triethylamine, 41 mg of 4,4'-diferrocenyl-1,1'-biphenyl[107] and no desired product were obtained.

8.3.28 1,3,5,7,9-Pentaferrocenylcorannulene (61)

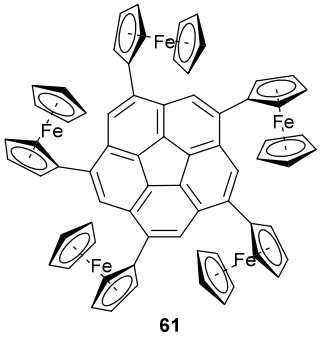

61

Ferrocene (**1**) (264 mg, 1.42 mmol, 15 eq) and potassium *tert*-butoxide (16 mg, 0.14 mmol, 1.5 eq) were dissolved in THF (2 mL). The red solution was cooled to -30 °C and tert-butyllithium (0.87 mL, 1.6M in *n*-pentane, 15 eq) were added dropwise. While stirring at the same temperature for 1 h a red precipitation was observed. Anhydrous zinc(II) chloride (258 mg, 1.89 mmol, 20 eq) in THF (3 mL) were added. After stirring at -30 °C for 30 min and RT for 30 min 1,3,5,7,9-pentachlorocorannulene (**59**) (40 mg, 0.09 mmol, 1 eq) and dichloro[1,3-bis(diphenylphosphino)propane]nickel (17 mg, 0.03 mmol, 0.3 eq) were added and the reaction mixture was stirred at 67 °C for 29 h. The reaction mixture was transferred to a 50 mL one neck flask. The solvent was removed and the red solid residue was sonicated with *n*-hexane (3 x 20 mL). The remaining residue was filtrated through silica gel with *n*-hexane, to remove unpolar residues then *n*-hexane/dichlormethane (1:1). Finally preparative TLC on silica gel with *n*-pentane/dichloromethane (1:1) afforded 4.5 mg (6 %) of the analytically pure product.

M.p. 194.4 °C, ; **^{1}H-NMR (700 MHz, $CDCl_3$):** δ = 8.57 (s, 5H, H_{rim}), 4.99 (s, 10H, $H_{cp\text{-}sub}$), 4.56 (s, 10H, $H_{cp\text{-}sub}$), 4.32 ppm (s, 50H, H_{cp}); **^{13}C-NMR (125MHz, $CDCl_3$):** δ = 138.31 (5C, C_{cor}), 134.44 (5C, C_{cor}), 128.64 (5C, C_{cor}), 125.07 (5C, C_{cor}), 86.08 (5C, $C_{cp\text{-}ipso}$), 70.00 (25C, C_{cp}), 69.45 (10C, $C_{cp\text{-}sub}$), 69.16 ppm (25C, $C_{cp\text{-}sub}$); **FT-IR:** ν = 3090 (m, br), 2919 (m, shr), 2850 (m, shr), 2244 (w, br), 1731 (m, shr), 1612 (w, shr), 1479 (m, shr), 1462 (m, shr), 1412 (m, shr), 1378 (w, shr), 1251 (m, shr), 1163 (w, shr), 1106 (m, shr), 1051 (m, shr), 1024 (m, shr), 1000 (m, shr), 956 (w, shr), 905 (m, shr), 863 (w, shr), 814 (s, shr), 726 (s, shr), 448 cm^{-1} (mid, shr);

MALDI-MS of compound (**61**).

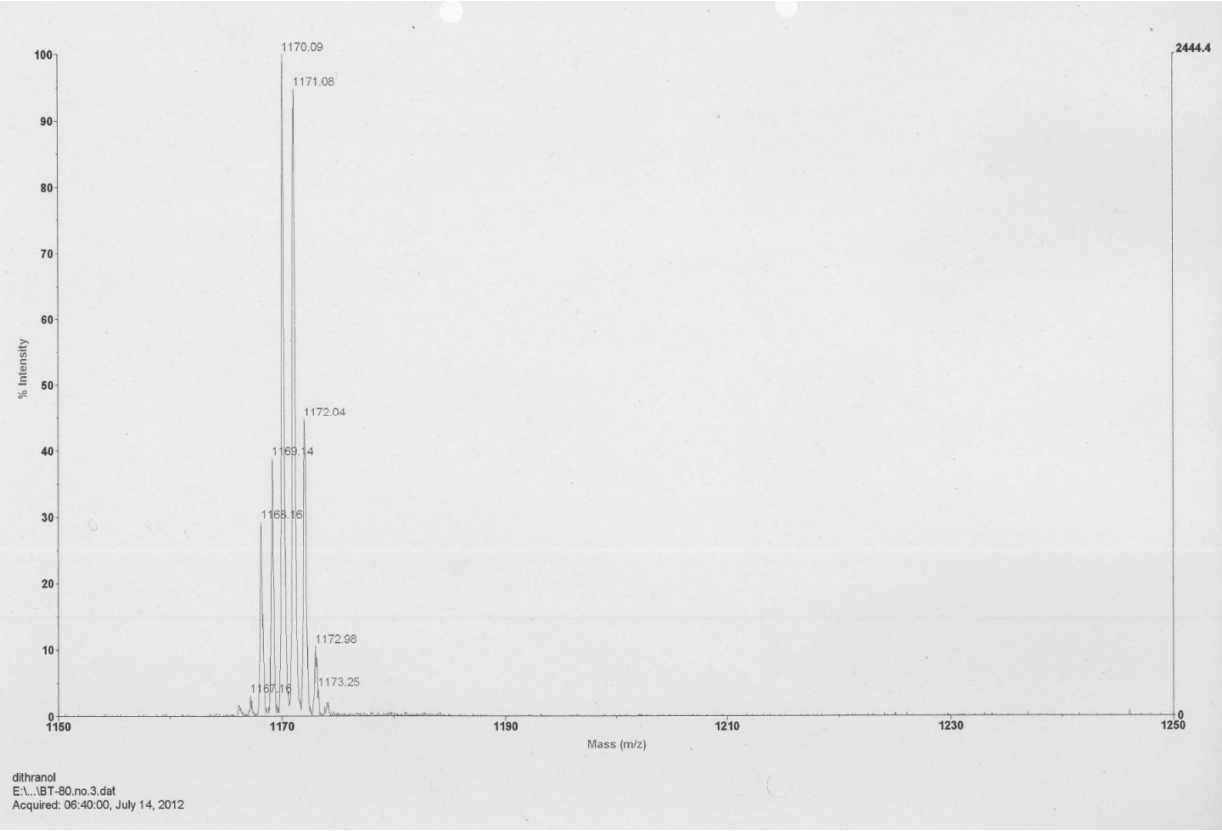

Predicted (http://www.sisweb.com/mstools/isotope.htm):

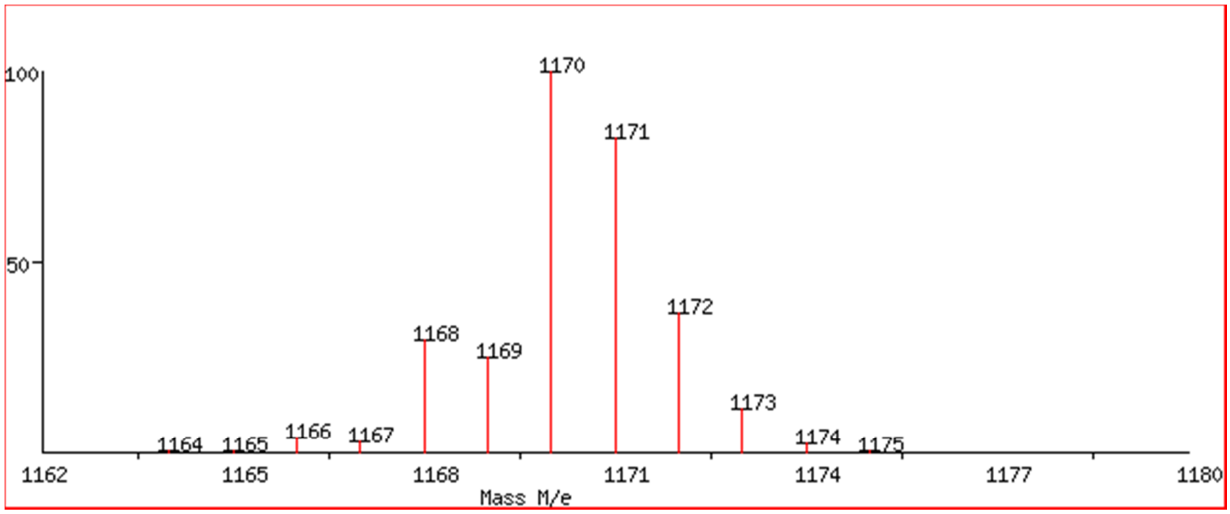

8.3.29 1,3,5,7,9-Penta(1'-neopentylferrocenyl)corannulene (63)

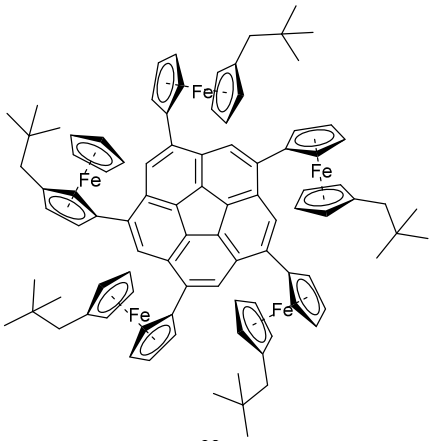

63

1-Bromo-1'-(neopentyl)ferrocene (**12**) (317 mg, 0.95 mmol, 10 eq) was dissolved in THF (2 mL). After cooling to -30 °C *n*-butyllithium (0.46 mL, 2.5M in *n*-pentane, 12 eq) was added dropwise and the red suspension was stirred for 30 min at -30 °C. After addition of anhydrous zinc(II) chloride (194 mg, 1.42 mmol, 15 eq) in THF (2 mL) was added and stirring at -30 °C was continued for 1 h at -30 °C and 1 h at RT. 1,3,5,7,9-Pentachlorocorannulene (**59**) (40 mg, 0.09 mmol, 1 eq) and dichloro[1,3-bis(diphenylphosphino)propane]-nickel (17 mg, 0.03 mmol, 0.3 eq) were added and the reaction mixture was stirred at 60 °C for 3 d. The solvent was removed and preparative TLC on silica gel with *n*-hexane/dichloromethane (3:1) afforded 22 mg (15 %) of the desired product as a red solid.

M.p. 137.1 °C; **^{1}H-NMR (500 MHz, $CDCl_3$):** δ = 8.51 (s, 5H, H_{rim}), 4.87-4.86 (m, 10 H, $H_{cp\text{-}sub}$), 4.41-4.40 (m, 10H, $H_{cp\text{-}sub}$), 4.18-4.16 (m, 10 H, $H_{cp\text{-}sub}$), 4.15-4.14 (m, 10 H, $H_{cp\text{-}sub}$), 2.26 (s, 10 H, $C\underline{H}_2$), 0.78 ppm (s, 45 H, $C\underline{H}_3$); **^{13}C-NMR (125 MHz, $CDCl_3$):** δ = 138.53 (5C, C_{cor}), 134.51 (5C, C_{cor}), 128.90 (5C, C_{cor}), 125.15 (5C, C_{cor}), 86.85 (5C, $C_{cp\ ipso}$), 86.10 (5C, $C_{cp\ ipso}$), 72.03 (10C, C_{cp}), 70.30 (10C, C_{cp}), 70.08 (10C, C_{cp}), 70.06 (10C, C_{cp}), 44.90 (5C, CH_2), 31.94 (5C, $\underline{C}(CH_3)_3$), 29.52 ppm (15C, CH_3); **FT-IR:** ν = 3086 (w, br), 2948 (m, shr), 2948 (m, shr), 2863 (m, shr), 1627 (w, br), 1464 (m, shr), 1309 (m, shr), 1361 (m, shr), 1330 (w, shr), 1235 (m, shr), 1160 (w, shr), 1141 (m, shr), 1027 (m, shr), 941 (m, shr), 877 (m, shr), 817 (s, shr), 754 (m, shr), 633 (w, shr), 614 cm^{-1} (w, shr); ESI-MS: m/z = 1521.4606 ($[M]^+$, found), 1521.4604 ($[M]^+$,calc'd).

8.3.30 Attempts to synthesize Perferrocenylated Corannulenes

a) A mixture of nona- and decabromoferrocene (**64a/b**) (100 mg) was added ethynylferrocene (**28**) (225 mg, 1.07 mmol, 11 eq), copper(I) iodide (10 mg, 0.05 mmol, 0.6 eq), tris(dibenzylideneacetone)dipalladium(0) (25 mol%), triphenylphosphane (50 mol%) triethylamine (7 mL) and toluene (14 mL). The reaction mixture was heated at 80 °C for 3 d. The solvent was removed and PTLC on silica gel with *n*-pentane/dichloromethane (1:1) was conducted. No product was obtained.

b) A mixture of nona- and decabromoferrocene (**64a/b**) (10 mg), 1-zincio-1'-neopentylferrocene (**24**) (0.29 mmol, 30 eq), palladium(II) acetate (30 mol%) and triphenylphosphane (60 mol%) were heated at 80 °C for 3 d. The solvent was removed in vacuum. Flash column chromatography with *n*-pentane to remove starting material, then dichloromethane yielded a red solid which was analysed by ESI-mass spectronomy. No desired product was detected.

c) Decachlorocorannulene (**65**) (20 mg, 0.03 mmol, 1 eq) and dichloro[1,3-bis-(diphenylphosphino)propane]nickel (13 mg, 0.02 mmol, 0.7 eq) were added to freshly prepared 1-zincio-1'-neopentylferrocene (**24**) (1.01 mmol, 30 eq) in THF (5 mL). The reaction mixture was refluxed for 5 d. The solvent was removed and column chromatography on silica gel with *n*-pentane/dichloromethane (4:1) and 1% triethylamine was conducted. No product was obtained.

d) Decachlorocorannulene (**65**) (50 mg, 0.08 mmol 1 eq), palladium(II) acetate (200 mol%) and 1,3-bis(2,6-diisopropylphenyl)imidazolium chloride (200 mol%) were added 1-neopentyl-1'-(zincchloride)ferrocene (**24**) (1.18 mmol, 20 eq) in DME (4 mL). The reaction mixture was heated to 87 °C for 2 h then at 80 °C for 4 d. After filtration of the crude mixture through celite and removal of the residual ferrocene starting material by column chromatography with *n*-pentane/dichloromethane (3:1). No desired product was obtained.

e) Decachlorocorannulene (**65**) (10 mg, 0.02 mmol, 1 eq), tris(dibenzylideneacetone)-dipalladium(0) (5 mol%) and RuPhos (20 mol%) were added to freshly prepared 1-zincio-1'-neopentylferrocene (**24**) (1.01 mmol, 30 eq) in THF (2.5 mL). The reaction mixture was refluxed for 3 d. After removal of the solvent column chromatography on silica gel with *n*-

pentane/dichloromethane (3:1) and 1 % triethylamine gave a purple solid. The first, orange fraction still showed three spots upon TLC. PTLC with *n*-pentane was conducted. No desired product was obtained.

9. Abbreviations

br	broad
n-BuLi	*n*-butyllithium
t-BuLi	tertiary butyllithium
cat.	catalytic amount, catalyst
CV	cyclic voltammetry
d	doublet
DME	1,2-dimethoxyethan
DMF	*N*,*N*-dimethylformamide
Dppf	1,1'-bis(diphenylphosphino)ferrocene
DPV	Differential Pulse Voltammetry
EI	Electron Impact
eq	equivalents
ESI	Electrospray Ionization
fc	ferrocene, (bis(η^5-cyclopentadienyl)iron)
fc*	decamethylferrocene, (bis(η^5-pentametylcyclopentadienyl)iron)
IR	infrared spectroscopy
HOMO	highest occupied molecular orbital
LUMO	lowest unoccupied molecular orbital
m	medium (IR), multiplett (NMR)
M^+	molecular ion
MALDI	Matrix Assisted Laser Desorption Ionization
MS	Mass Spectrometry
MePhos	2-dicyclohexylphosphino-2'-methylbiphenyl
m.p.	melting point
NCC	Negishi *CC*-cross-coupling
NMR	Nuclear Magnetic Resonance (Spectroscopy)

PAH	polycyclic aromatic hydrocarbons
ppm	parts per million
q	quartet
RT	room temperature
RuPhos	2-dicyclohexylphosphino-2’,6’-diisopropoxybiphenyl
s	strong (IR), singlet (NMR)
shr	sharp
SWV	Square Wave Voltammetry
SPhos	2-dicyclohexylphosphino-2',6'-dimethoxybiphenyl
TEA	triethylamine
THF	tetrahydrofuran
TMEDA	*N,N,N,N*-tetramethylethylenediamine
TOF	time-of-flight
Ugi’s amine	(R)-(+)-*N,N*-dimethyl-1-ferrocenylethylamine
vw	very weak
w	weak
XPhos	2-dicyclohexylphosphino-2’,4’,6’-triisopropylbiphenyl

10. References

[1] a) A. Sygula, *Eur. J. Org. Chem.* **2011**, *76*, 1611-1625; b) Y.-T. Wu, J. S. Siegel, *Chem. Rev.* **2006**, *106*, 4843-4867; c) V. M. Tsefrikas, L. T. Scott, *Chem. Rev.* **2006**, *106*, 4868-4884.

[2] a) L. T. Scott, M. M. Hashemi, M. S. Bratcher, *J. Am. Chem. Soc.* **1992**, *114*, 1920-1921; b) T. J. Seiders, K. K. Baldridge, G. H. Grube, J. S. Siegel, *J. Am. Chem. Soc.* **2001**, *123*, 517-525.

[3] a) T.-C. Wu, H.-J. Hsin, M.-Y. Kuo, C.-H. Li, Y.-T. Wu, *J. Am. Chem. Soc.* **2011**, *133*, 16319-16321; b) T.-C. Wu, M.-K. Chen, Y.-W. Lee, M.-Y. Kuo, Y.-T. Wu, *Angew. Chem. Int. Ed.* **2013**, *52*, 1289-1293.

[4] W. E. Barth, R. G. Lawton, *J. Am. Chem. Soc.* **1966**, *88*, 380-381.

[5] L. T. Scott, E. A. Jackson, Q. Zhang, B. D. Steinberg, M. Bancu, B. Li, *J. Am. Chem. Soc.* **2011**, *134*, 107-110.

[6] H. W. Kroto, J. R. Heath, S. C. O'Brien, R. F. Curl, R. E. Smalley, *Nature* **1985**, *318*, 162-163.

[7] R. G. Lawton, W. E. Barth, *J. Am. Chem. Soc.* **1971**, *93*, 1730-1745.

[8] L. T. Scott, M. M. Hashemi, D. T. Meyer, H. B. Warren, *J. Am. Chem. Soc.* **1991**, *113*, 7082-7084.

[9] E. J. Corey, P. L. Fuchs, *Tetrahedron Lett.* **1972**, *13*, 3769-3772.

[10] L. T. Scott, P.-C. Cheng, M. M. Hashemi, M. S. Bratcher, D. T. Meyer, H. B. Warren, *J. Am. Chem. Soc.* **1997**, *119*, 10963-10968.

[11] a) P. W. Rabideau, A. H. Abdourazak, H. E. Folsom, Z. Marcinow, A. Sygula, R. Sygula, *J. Am. Chem. Soc.* **1994**, *116*, 7891-7892; b) A. Sygula, P. W. Rabideau, *J. Am. Chem. Soc.* **1999**, *121*, 7800-7803; c) A. Sygula, P. W. Rabideau, *J. Am. Chem. Soc.* **2000**, *122*, 6323-6324.

[12] A. Sygula, G. Xu, Z. Marcinow, P. W. Rabideau, *Tetrahedron* **2001**, *57*, 3637-3644.

[13] a) A. Borchardt, A. Fuchicello, K. V. Kilway, K. K. Baldridge, J. S. Siegel, *J. Am. Chem. Soc.* **1992**, *114*, 1921-1923; b) T. J. Seiders, E. L. Elliott, G. H. Grube, J. S. Siegel, *J. Am. Chem.*

Soc. **1999**, *121*, 7804-7813; c) A. M. Butterfield, B. Gilomen, J. S. Siegel, *Org. Process Res. Dev.* **2012**, *16*, 664-676.

[14] G. Mehta, S. R. Shahk, K. Ravikumarc, *J. Chem. Soc., Chem. Commun.* **1993**, 1006-1008.

[15] H. Sakurai, T. Daiko, T. Hirao, *Science* **2003**, *301*, 1878.

[16] J. C. Hanson, C. E. Nordman, *Acta Cryst. B* **1976**, *32*, 1147-1153.

[17] a) B. M. Schmidt, B. Topolinski, P. Roesch, D. Lentz, *Chem. Commun.* **2012**, *48*, 6520-6522; b) B. M. Schmidt , B. Topolinski , M. Yamada , S. Higashibayashi, M. Shionoya, H. Sakurai, D. Lentz, *Chem. Eur. J.* **2013**, *19*, 13872-13880; c) B. M. Schmidt, S. Seki, B. Topolinski, K. Ohkubo, S. Fukuzumi, H. Sakurai, D. Lentz, *Angew. Chem. Int. Ed.* **2012**, *51*, 11385-11388. d) H. A. Wegner, L. T. Scott, A. d. Meijere, *J. Org. Chem*. **2003**, *68*, 883-887.

[18] a) A. Ayalon, M. Rabinovitz, P.-C. Cheng, L. T. Scott, *Angew. Chem. Int. Ed. in Engl.* **1992**, *31*, 1636-1637; b) A. Weitz, E. Shabtai, M. Rabinovitz, M. S. Bratcher, C. C. McComas, M. D. Best, L. T. Scott, *Chem. Eur. J.* **1998**, *4*, 234-239; c) M. Baumgarten, L. Gherghel, M. Wagner, A. Weitz, M. Rabinovitz, P.-C. Cheng, L. T. Scott, *J. Am. Chem. Soc.* **1995**, *117*, 6254-6257; d) I. Aprahamian, D. V. Preda, M. Bancu, A. P. Belanger, T. Sheradsky, L. T. Scott, M. Rabinovitz, *J. Org. Chem.* **2005**, *71*, 290-298. Organolithium reagents undergo addition to corannulene: e) A. Sygula, R. Sygula, F. R. Fronczek, P. W. Rabideau*, J. Org. Chem.* **2002**, *67*, 6487-6492.

[19] R. Benshafrut, E. Shabtai, M. Rabinovitz, Lawrence T. Scott, *Eur. J. Org. Chem.* **2000**, *65*, 1091-1106.

[20] A. Ayalon, A. Sygula, P.-C. Cheng, M. Rabinovitz, P. W. Rabideau, L. T. Scott, *Science* **1994**, *265*, 1065-1067.

[21] A. V. Zabula, A. S. Filatov, S. N. Spisak, A. Y. Rogachev, M. A. Petrukhina, *Science* **2011**, *333*, 1008-1011.

[22] C. Bruno, R. Benassi, A. Passalacqua, F. Paolucci, C. Fontanesi, M. Marcaccio, E. A. Jackson, L. T. Scott, *J. Phys. Chem. B* **2009**, *113*, 1954-1962.

[23] a) H. Sakurai, T. Daiko, H. Sakane, T. Amaya, T. Hirao, *J. Am. Chem. Soc.* **2005**, *127*, 11580-11581; b) T. Amaya, H. Sakane, T. Nakata, T. Hirao, *Pure Appl. Chem.* **2010**, *82*, 969-978.

[24] S. Mebs, M. Weber, P. Luger, B. M. Schmidt, H. Sakurai, S. Higashibayashi, S. Onogi, D. Lentz, *Org. Biomol. Chem.* **2012**, *10*, 2218-2222.

[25] P. Zanello, S. Fedi, F. F. de Biani, G. Giorgi, T. Amaya, H. Sakane, T. Hirao, *Dalton Trans.* **2009**, 9192-9197.

[26] T. J. Kealy, P. L. Pauson, *Nature* **1951**, *168*, 1039-1040.

[27] a) R. Gómez Arrayás, J. Adrio, J. C. Carretero, *Angew. Chem. Int. Ed.* **2006**, *45*, 7674-7715; b) A. Togni, T. Hayashi, *Ferrocenes. Homogeneous Catalysis. Organic Synthesis. Materials Science. VCH: Weinheim* **1995**; c) R. C. J. Atkinson, V. C. Gibson, N. J. Long, *Chem. Soc. Rev.* **2004**, *33*, 313-328.

[28] a) J. Quirante, F. Dubar, A. González, C. Lopez, M. Cascante, R. Cortés, I. Forfar, B. Pradines, C. Biot, *J. Organomet. Chem.* **2011**, *696*, 1011-1017; b) C. Ornelas, *New J. Chem.* **2011**, *35*, 1973-1985.

[29] a) R. Afrasiabi, H.-B. Kraatz, *Chem. Eur. J.* **2013**, *19*, 17296-17300; b) S. Nlate, J. Ruiz, J.-C. Blais, D. Astruc, *Chem. Commun.* **2000**, 417-418; c) N. M. Khashab, A. Trabolsi, Y. A. Lau, M. W. Ambrogio, D. C. Friedman, H. A. Khatib, J. I. Zink, J. F. Stoddart, *Eur. J. Org. Chem.* **2009**, *2009*, 1669-1673.

[30] a) V. Mamane, A. Gref, O. Riant, *New J. Chem.* **2004**, *28*, 585-594; b) R. Horikoshi, T. Mochida, *Eur. J. Inorg. Chem.* **2010**, *2010*, 5355-5371.

[31] A. K. Diallo, C. Absalon, J. Ruiz, D. Astruc, *J. Am. Chem. Soc.* **2011**, *133*, 629-641.

[32] Y. Yu, A. D. Bond, P. W. Leonard, U. J. Lorenz, T. V. Timofeeva, K. P. C. Vollhardt, G. D. Whitener, A. A. Yakovenko, *Chem. Commun.* **2006**, 2572-2574.

[33] A. K. Diallo, J.-C. Daran, F. Varret, J. Ruiz, D. Astruc, *Angew. Chem. Int. Ed.* **2009**, *121*, 3187-3191.

[34] R. J. LeSuer, W. E. Geiger, *Angew. Chem. Int. Ed.* **2000**, *39*, 248-250.

[35] a) A. Hildebrandt, U. Pfaff, H. Lang, in *Rev. Inorg. Chem., Vol. 31*, **2011**, 111-141; b) A. Hildebrandt, H. Lang, *Organometallics* **2013**, *32*, 5640-5653.

[36] a) A. Hildebrandt, T. Rüffer, E. Erasmus, J. C. Swarts, H. Lang, *Organometallics* **2010**, *29*, 4900-4905; b) J. M. Speck, R. Claus, A. Hildebrandt, T. Rüffer, E. Erasmus, L. van As, J. C.

Swarts, H. Lang, *Organometallics* **2012**, *31*, 6373-6380; c) A. Hildebrandt, D. Schaarschmidt, R. Claus, H. Lang, *Inorg. Chem.* **2011**, *50*, 10623-10632.

[37] A. Hildebrandt, H. Lang, *Dalton Trans.* **2011**, *40*, 11831-11837.

[38] D. Miesel, A. Hildebrandt, M. Korb, P. J. Low, H. Lang, *Organometallics* **2013**, *32*, 2993-3002.

[39] a) H. Sakane, T. Amaya, T. Moriuchi, T. Hirao, *Angew. Chem. Int. Ed.* **2009**, *48*, 1640-1643; b) T. Hirao, T. Amaya, T. Moriuchi, M. Hifumi, Y. Takahashi, I. Nowik, R. H. Herber, *J. Organomet. Chem.* **2011**, *696*, 3895-3899; c) M. Okumura, Y. Nakanishi, K. Kinoshita, S. Yamada, Y. Kitagawa, T. Kawakami, S. Yamanaka, T. Amaya, T. Hirao, *Int. J. Quant. Chem.* **2013**, *113*, 437-442.

[40] T. Amaya, H. Sakane, T. Hirao, *Angew. Chem. Int. Ed.* **2007**, *46*, 8376-8379.

[41] P. A. Vecchi, C. M. Alvarez, A. Ellern, R. J. Angelici, A. Sygula, R. Sygula, P. W. Rabideau, *Angew. Chem. Int. Ed.* **2004**, *43*, 4497-4500.

[42] P. A. Vecchi, C. M. Alvarez, A. Ellern, R. J. Angelici, A. Sygula, R. Sygula, P. W. Rabideau, *Organometallics* **2005**, *24*, 4543-4552.

[43] M. A. Petrukhina, Y. Sevryugina, A. Y. Rogachev, E. A. Jackson, L. T. Scott, *Organometallics* **2006**, *25*, 5492-5495.

[44] B. Zhu, A. Ellern, A. Sygula, R. Sygula, R. J. Angelici, *Organometallics* **2007**, *26*, 1721-1728.

[45] a) E. L. Elliott, G. A. Hernandez, A. Linden, J. S. Siegel, *Org. Biomol. Chem.* **2005**, *3*, 407-413; b) H. B. Lee, P. R. Sharp, *Organometallics* **2005**, *24*, 4875-4877; c) H. Choi, C. Kim, K.-M. Park, J. Kim, Y. Kang, J. Ko, *J. Organomet. Chem.* **2009**, *694*, 3529-3532; d) R. Maag, B. H. Northrop, A. Butterfield, A. Linden, O. Zerbe, Y. M. Lee, K.-W. Chi, P. J. Stang, J. S. Siegel, *Org. Biomol. Chem.* **2009**, *7*, 4881-4885; e) M. Yamada, S. Tashiro, R. Miyake, M. Shionoya, *Dalton Trans.* **2013**, *42*, 3300-3303.

[46] T. Amaya, W-Z. Wang, H. Sakane, T. Moriuchi, T. Hirao, *Angew. Chem. Int. Ed*. **2010**, *49*, 403-406.

[47] S. Jong, Patent TWI233930(B), **2005**.

[48] A. K. Diallo, J. Ruiz, D. Astruc, *Chem. Eur. J.* **2013**, *19*, 8913-8921.

[49] K. L. Cunningham, D. R. McMillin, *Polyhedron*, **1996**, *15*, 1673-1675.

[50] Reactions were run analogous to a) J. Polin, H. Schottenberger, *Org. Synth., Coll.,* **1998***, 9, 411;* **1996***,73, 262.* For one-pot synthesis and spectral data see: b) P. Jutzi, B. Kleinebekel, *J. Organomet. Chem*. **1997**, *545-546*, 573-576.

[51] M. Roemer, D. Heinrich, Y. K. Kang, Y. K. Chung, D. Lentz, *Organometallics* **2012**, *31*, 1500-1510.

[52] T. Mochida, K. Takazawa, H. Matsui, M. Takahashi, M. Takeda, M. Sato, Y. Nishio, K. Kajita, H. Mori, *Inorg. Chem.* **2005**, *44*, 8628-8641.

[53] M. S. Inkpen, S. Du, M. Driver, T. Albrecht, N. J. Long, *Dalton Trans*. **2013**, *42*, 2813-2816.

[54] A. Ambroise, R. W. Wagner, P. D. Rao, J. A. Riggs, P. Hascoat, J. R. Diers, J. Seth, R. K. Lammi, D. F. Bocian, D. Holten, J. S. Lindsey, *Chem. Mater.* **2001**, *13*, 1023-1034.

[55] Y. Wang, A. Rapakousiou, G. Chastanet, L. Salmon, J. Ruiz, D. Astruc, *Organometallics* **2013**, *32*, 6136-6146.

[56] T.-Y. Dong, C.-K. Chang, S.-H. Lee, L.-L. Lai, M. Y.-N. Chiang, K.-J. Lin, *Organometallics* **1997**, *16*, 5816-5825.

[57] a) D. Qiu, F. Mo, Z. Zheng, Y. Zhang and J. Wang, *Org. Lett.* **2010**, *12*, 5474-5477; b) F. Mo, J. M. Yan, D. Qiu, F. Li and Y. Zhang, *Angew. Chem. Int. Ed.* **2010**, *122*, 2072-2076.

[58] B. Topolinski, B. M. Schmidt, M. Kathan, S. I. Troyanov, D. Lentz, *Chem. Commun*. **2012**, *48*, 6298-6300.

[59] B. B. Shrestha, S. Karanjit, G. Panda, S. Higashibayashi, H. Sakurai, *Chem. Lett.* **2013**, *42*, 386-388.

[60] M. Schlosser, *Pure & Appl. Chem*. **1998**, *60*, 1627-1634.

[61] B. Topolinski, Master Thesis, FU-Berlin, **2011**.

[62] B. Topolinski, B. M. Schmidt, S. Higashibayashi, H. Sakurai, D. Lentz, *Dalton Trans.* **2013**, *42*, 13809-13812.

[63] S. Schwagerius, Research Internship, FU-Berlin, **2013**.

[64] Y.-T. Wu, D. Bandera, R. Maag, A. Linden, K. K. Baldridge, J. S. Siegel, *J. Am. Chem. Soc.* **2008**, *130*, 10729-10739.

[65] C.-M. Lui, B.-H. Chen, W.-Y. Lui, X.-L. Wu, Y.-X. Ma*, J. Organomet. Chem.* **2000**, *598*, 348-352.

[66] R. Knapp, M. Rehahn, *J. Organomet. Chem*. **1993**, *452*, 235-240.

[67] M. Kathan, Bachelor Thesis, FU-Berlin, **2011**.

[68] K. Sünkel, S. Bernhartzeder, *J. Organomet. Chem*. **2011**, *696*, 1536-1540.

[69] M. Kathan, Research Internship, FU-Berlin, **2012**.

[70] a) G. W. Gokel, I. K. Ugi, *J. Chem. Educ.* **1972**, *49*, 294; b) A. Gieren, C. P. Kaerlein, T. Hübner, R. Herrmann, F. Siglmüller, I. Ugi, *Tetrahedron* **1986**, *42*, 427-434.

[71] a) F. P. Camponovo, PhD Thesis, No. 18199, ETH Zürich, **2009**; b) J. F. Buergler, A. Togni, *Organometallics* **2011**, *30*, 4742-4750, c) J. F. Buergler, K. Niedermann, A. Togni, *Chem. Eur. J.* **2012**, *18*, 632-640.

[72] A. Senf, Research Internship, FU-Berlin, **2012**.

[73] S. Czarnecki, Bachelor Thesis, FU-Berlin, **2013**.

[74] M. N. Eliseeva, L. T. Scott, *J. Am. Chem. Soc.* **2012**, *134*, 15169-15172.

[75] a) S. Mizyed, P. E. Georghiou, M. Bancu, A. K. Rai, P. Cheng, L. T. Scott, *J. Am. Chem. Soc*. **2001**, *123*, 12770–12774; b) G. H. Grube, E. L. Elliott, R. J. Steffens, C. S. Jones, K. K. Baldridge, J. S. Siegel, *Org. Lett.* **2003**, *5*, 713-716; c) J. Siegel, private communication, **2013.**

[76] R. Martin, S. L. Buchwald, *Acc. Chem. Res*. **2008**, *41*, 1461-1473.

[77] T. Hayama, K. K. Baldridge, Y.-T. Wu, A. Linden, J. S. Siegel, *J. Am. Chem. Soc.* **2008**, *130*, 1583-1591.

[78] M. Mattarella, J. S. Siegel, *Org. Biomol. Chem*. **2012**, *10*, 5799-5802.

[79] a) H. Prinzbach, A. Weiler, P. Landenberger, F. Wahl, J. Wörth, L. T. Scott, N. Gellmont, D. Olevano, B. v. Issendorff, *Nature* **2000**, *407*, 60-63; b) H. Prinzbach, F. Wahl, A. Weiler, P. Landenberger, J. Wörth, L. T. Scott, M. Gellmont, D. Olevano, F. Sommer, B. v. Issendorff, *Chem. Eur. J.* **2006**, *12*, 6268-6280.

[80] a) S. Samdal, L. Hedberg, K. Hedberg, A. D. Richardson, M. Bancu, L. T. Scott, *J. Phys. Chem. A* **2003,** *107,* 411-417, b) J. M. Quimby, PhD Thesis, Boston College, **2011**.

[81] M. A. Petrukhina, K. W. Andreini, J. Mack, L. T. Scott, *J. Org. Chem.*, **2005**, *70*, 5713-5716.

[82] T. Amaya, K. Kobayashi, T. Hirao, *Asian J. Org. Chem*. **2013**, *2*, 642-645.

[83] D. Eisenberg, A. S. Filatov, E. A. Jackson, M. Rabinovitz, M. A. Petrukhina, L. T. Scott, R. Shenhar, *J. Org. Chem.* **2008**, *73*, 6073-6078.

[84] a) A. S. Filatov, M. A. Petrukhina, *Coord. Chem. Rev.* **2010**, *254*, 2234-2246; b) A. S. Filatov, L. T. Scott, M. A. Petrukhina, *Cryst. Growth Des.* **2010**, *10*, 4607-4621;

[85] I. V. Kuvychko, S. N. Spisak, Y.-S. Chen, A. A. Popov, M. A. Petrukhina, S. H. Strauss, O. V. Boltalina, *Angew. Chem. Int. Ed*. **2012**, *51*, 4939-4942.

[86] S. Grabowsky, M. Weber, Y.-S. Chen, D. Lentz, B. M. Schmidt, M. Hesse, P. Luger, *Z. Naturforsch.* **2010**, *65b*, 452-460.

[87] M. A. Petrukhina, K. W. Andreini, L. Peng, L. T. Scott, *Angew. Chem. Int. Ed.* **2004**, *43*, 5477-5481.

[88] a) C. Thilgen, F. Diederich, *Chem. Rev*. **2006**, *106*, 5049-5135; b) for further explanation and sumanene examples see: b) S. Higashibayashi, R. Tsuruoka, Y. Soujanya, U. Purushotham, G. N. Sastry, S. Seki, T. Ishikawa, S. Toyota, H. Sakurai, *Bull. Chem. Soc. Jpn*. **2012**, *85*, 450-467.

[89] M. Nishio, *Cryst. Eng. Comm*. **2004**, 6, 130-158.

[90] Q. Zhang, K. Kawasumi, Y. Segawa, K. Itami, L. T. Scott, *J. Am. Chem. Soc*. **2012**, *134*, 15664-15667.

[91] a) in ethanol: A. A. O. Sarhan, M. S. Ibrahim, M. M. Kamal, K. Mitobe, T. Izumi, *Monatesh. Chem*. **2009**, *140*, 315-323; in *n*-hexane: Jolly, William L. *The Synthesis and Characterization of Inorganic Compounds.* Prentice-Hall, Inc: Englewood Cliffs, NJ. **1970**. 4-5, 407, 484-487.

[92] J. Mack, P. Vogel, D. Jones, N, Kaval, A. Sutton, *Org. Biomol. Chem*. **2007**, *5*, 2448-2452; b) G. Roullé, C. Jäger, M. Steglich, F. Huisken, T. Henning, G. Theumer, I. Bauer, H.-J. Knölker, *Chem. Phys. Chem*. **2008**, *9*, 2085-2091.

[93] Y.-L. Wu, M. C. Stuparu, C. Boudon, J.-P. Gisselbrecht, W. B. Schweizer, K. K. Baldridge, J. S. Siegel, F. Diederich*, J. Org. Chem*. **2012**, *77*, 11014-11026.

[94] G. Diao, L. Li, Z. Zhang, *Talanta*, **1996**, *43*, 1633-1637.

[95] D. Siebler, C. Försterm T. Gasi, K. Heinze, *Chem. Commun*. **2010**, *46*, 4490-4492.

[96] A. S. Baranski, W. R. Fawcett, C. M. Gilbert, *Anal. Chem*. **1985**, *57*, 166-170.

[97] W. H. Morrison, D. N. Hendrickson, *Inorg. Chem*. **1975**, *14*, 2331-2346.

[98] R. J. LeSuer, W. E. Geiger, *Angew. Chem. Int. Ed.* **2000**, *39*, 248-250.

[99] a) M. Hitoshi, K. Ikuyo, Y. Nakano, patent EP19970308447 19971023, **1998**; b) H. Golf, Research Internship, FU-Berlin, **2009**.

[100] SADBS: Area-Detector Absorption Correction; Siemens Industrial Automation, INC.: Madison, WI, **1996**.

[101] A. Thorn. G. M. Sheldrick, *Acta Cryst. Sec. A* **2008**, *64*, C221.

[102] Mercury CDS 2.0 – New features for the Visualization and Investigation of Crystal Structures C. F. Macrae, I. J. Bruno, J. A. Chrisholm, P. R. Edgington, P. McCabe, E. Pidcock, L. Rodriguez-Monge, R. Taylor, J. van de Streek, P. A. Wood, *J. Appl. Cryst*. **2008**, *41*, 466-470.

[103] Persistence of Vision Pty. Ltd. http://povray.org

[104] Gaussian 09, Revision A.02, M. J. Frisch, G. W. Trucks, H. B. Schlegel, G. E. Scuseria, M. A. Robb, J. R. Cheeseman, G. Scalmani, V. Barone, B. Mennucci, G. A. Petersson, H. Nakatsuji, M. Caricato, X. Li, H. P. Hratchian, A. F. Izmaylov, J. Bloino, G. Zheng, J. L. Sonnenberg, M. Hada, M. Ehara, K. Toyota, R. Fukuda, J. Hasegawa, M. Ishida, T. Nakajima, Y. Honda, O. Kitao, H. Nakai, T. Vreven, J. A. Montgomery, Jr., J. E. Peralta, F. Ogliaro, M. Bearpark, J. J. Heyd, E. Brothers, K. N. Kudin, V. N. Staroverov, R. Kobayashi, J. Normand, K. Raghavachari, A. Rendell, J. C. Burant, S. S. Iyengar, J. Tomasi, M. Cossi, N. Rega, J. M. Millam, M. Klene, J. E. Knox, J. B. Cross, V. Bakken, C. Adamo, J. Jaramillo, R. Gomperts, R. E. Stratmann, O. Yazyev, A. J. Austin, R. Cammi, C. Pomelli, J. W. Ochterski, R. L. Martin, K. Morokuma, V. G. Zakrzewski, G. A. Voth, P. Salvador, J. J. Dannenberg, S. Dapprich, A. D. Daniels, Ö. Farkas, J. B. Foresman, J. V. Ortiz, J. Cioslowski, and D. J. Fox, Gaussian, Inc., Wallingford CT, 2009.

[105] L. Farrugia, *J. Appl. Crystallogr*. **1997**, *30*, 565.

[106] CystalClear: Crystal Structure Analysis Package, Rigaku and Rigaku/MSC, The Woodlands, TX77381, USA, 2007.

[107] Y.-C. Lin, W.-T. Chen, J. Tai, D. Su, S.-Y. Huang, I. Lin, J.-L. Lin, M. M. Lee. M. F. Chiou, Y.-H. Lui, K.-S. Kwan, Y.-L. Chen, H.-Y. Chen, *Inorg. Chem.* **2009**, *48*, 1857–1870.

[107] N. Duffy, J. McAdam, C. Nervi, D. Osella, M. Ravera, B. Robinson, J. Simpson, *Inorg. Chim. Act.* **1996**, *247*, 99-104.